TEAR AND SKIN PHOSPHOLIPIDS; ANALYSIS AND HYDROGEL ANALOGUES

DARREN CAMPBELL

Doctor of Philosophy

ASTON UNIVERSITY

September 2007

THESIS ABSTRACT

Aston University

TEAR AND SKIN PHOSPHOLIPIDS; ANALYSIS AND HYDROGEL ANALOGUES

DARREN CAMPBELL

Doctor of Philosophy September 2007

This thesis is concerned with the analysis of phospholipids in the tear film and with the synthesis of phospholipid analogous hydrogels. The work consists of two areas. The first area is the study of the phospholipids in the tear film, their nature and fate. The use of liquid chromatography mass spectrometry determined that the concentration of phospholipids in the tear film was less than previous thought.

The analysis of the tear film phospholipids continued with thin layer chromatography. This showed the presence of diacylgylcerides (DAGs) in the tear film at relatively high concentrations. The activity of an enzyme, phospholipase C was found in the tear film. It was hypothesised that the low concentration of phospholipids and high concentrations of DAG in the tear film was due to the action of this enzyme.

The second area of study was the synthesis of phospholipid analogous materials for use in ocular and dermal applications. For ocular applications the synthesis involved the use of the monomer N,N-dimethyl-N-(2-acryloylethyl)-N-(3-sulfopropyl) ammonium betaine (SPDA) in combination with 2-hydroxyethyl methacrylate (HEMA). Charge-balanced membranes were also synthesised using potentially anionic monomers in conjugation with cationic monomers in stoichiometrically equivalent ratios also with HEMA as a comonomer. Membranes of SPDA copolymers and charge-balanced copolymers proved to have some properties suitable for ocular applications.

The dermal materials consisted of one family of partially hydrated hydrogels synthesised from SPDA in combination with ionic monomers: sodium 2-(acrylamido)-2-methyl propane sulfonate and acrylic acid-bis-(3-sulfopropyl)-ester, potassium salt. A second family of partially hydrated hydrogels were also synthesised from N-vinyl pyrrolidone in combination with the same ionic monomers. Both of the partially hydrated hydrogels synthesised proved to have some properties suitable for use as adhesives for the skin.

Keywords: Tear film, phospholipids, hydrogels

DECLARATION

This thesis describes the work carried out between October 2003 and September 2007 in the Biomaterials Research Unit at Aston University under the supervision of Professor Brian J. Tighe.

I declare that the work presented in this thesis is, to the best of my knowledge, original, except as acknowledged in the text and has not been submitted, either in full or in part for a degree at any other university.

Note: Some of the diagrams present in the thesis are direct copies (sometimes with minor changes to improve presentation) of those found in the mentioned references.

Darren Campbell

September 2007

DEDICATION

This thesis is dedicated to

my loving, supportive and inspirational wife Andrea
and my children Jade and Patrick

ACKNOWLEDGEMENTS

I would like to thank my supervisor Brian Tighe whose help and guidance was unwavering throughout both the research and writing of this thesis. Without his help this work could not have been completed. I would also like to thank him for always being so enthusiastic about my ideas. I should also mention his anecdotes are second to none and always make me laugh. I am also grateful for the opportunity to have participated in many conferences around the world.

Aisling Mann who was always helpful around the lab, there to answer my questions and give me advice. Of course we also shared many a scoop, "Sláinte Ais"

Valerie Franklin for generally "sorting stuff out"

Raminder Bahia and Anisa Mahomed for always being a great help and source of information and also Anisa for a great guided tour of Lisbon, "Obrigado" Anisa

I would also like thank all the members of the Biomaterials Research Unit

all my friends

my family for all their help and love
especially Andrea without whom this would not have been possible

The project was conducted on an Engineering and Physical Sciences Research Council studentship, with additional funding from First Water by provision of a CASE award. I am grateful to both organisations for their support.

Contents

Title page 1
Thesis abstract 2
Declaration 4
Dedication 5
Acknowledgement 6
Contents 7
List of figures 11
List of tables 16

CHAPTER 1 - INTRODUCTION 17

1.1 Hydrogels **18**
1.1.1 Introduction to hydrogels 18
1.1.2 Neutral, ionic and ampholyte hydrogels 19
1.1.3 Equilibrium Water Content (EWC) 22
1.1.4 The Nature of Water in Hydrogels 23
1.1.5 Applications of Hydrogels 24

1.2 Lipids **28**
1.2.1 Introduction to lipids 28
1.2.2 Lipid Classes 29
1.2.3 Phospholipids 31
1.2.4 The variety of molecular weight (M_r) associated with complex lipids 34

1.3 The Ocular Environment **35**
1.3.1 Anatomy of the eye 35
1.3.2 The Cornea, Conjunctiva and Eyelids 35
1.3.3 The Tear Film [17, 18] 36
1.3.4 The Layers of the Tear Film [17] 37
1.3.5 Lacrimal Functional Unit 38
1.3.6 Composition of the tear film 39
1.3.7 Composition of lipids in meibomian gland secretions (MGS) 41
1.3.8 Lipids in the tear film 45
1.3.9 Interactions of Ocular Lipids 46

1.4 The Skin (the Dermal Environment) **46**
1.4.1 Anatomy of the skin 47
1.4.2 Epidermal Lipids 48
1.4.3 Composition of Epidermal Skin Lipids 48
1.4.4 Sebaceous Lipids (Sebum) 49
1.4.5 Composition of Sebum 49
1.4.6 Oily skin and pressure sensitive adhesives (PSAs) 50
1.4.7 Interactions of Skin Lipids 51

2 CHAPTER 2 – METHODS AND MATERIALS 52

2.1 Reagents **53**

2.2 Collection of tear samples **59**

2.3 Extraction of lipids from the tear film samples **60**
2.3.1 Methanol chloroform 60
2.3.2 Methanol 61
2.3.3 Modified Bligh and Dyer 61

2.4 Chromatography **62**
2.4.1 High Performance Liquid Chromatography (HPLC) 62
2.4.2 Thin Layer Chromatograhy (TLC) 64
2.4.3 TLC method 64
2.4.4 Mobile phases used in TLC 64
2.4.5 Stains used in TLC 64

2.5 Counter Immunoelectrophoresis (CIE) **65**
2.5.1 Agarose/PEG8000 gels for the CIE analysis 65
2.5.2 Coomassie Brilliant Blue stain 66

2.6 Mass Spectrometry (MS) **66**
2.6.1 Introduction to MS 66
2.6.2 MS Sample Inlet 66
2.6.3 MS Parameters 67

2.7 Liquid Chromatography Mass Spectrometry (LCMS) **68**
2.7.1 LCMS System employed 68
2.7.2 Nature of data from MS - Total Ion Chromatogram (TIC), Extracted Ion Chromatogram (EIC) and Compound Mass Spectra (CMS) 68

2.8 Partially hydrated hydrogels (gel) synthesis **71**

2.9 Fully hydrated hydrogels (membrane) synthesis **71**

2.10 Equilibrium water content (EWC) **73**

2.11 Youngs modulus (ε) **73**

2.12 Oxygen permeability (Dk) **74**

2.13 Coefficient of friction (μ) **76**

2.14 The 90° perpendicular peel test **77**

2.15 Contact angle **78**
2.15.1 Initial (instant) measurement 79
2.15.2 Kinetic Measurements 80

2.16 Rheology **80**

2.17 Statistical analysis **81**

3 CHAPTER 3 - LIPID ANALYSIS OF THE TEAR FILM 1 82

3.1 Introduction to lipid analysis of the tear film 1 ..... **83**

3.2 High Performance Liquid Chromatography (HPLC) method development for tear film lipid analysis **84**
3.2.1 Introduction to HPLC Method Development 84
3.2.2 HPLC Method Development 85
3.2.3 Non polar lipid tear film Method Development 86
3.2.4 Polar lipid tear film Method Development 87
3.2.5 Summary of tear film lipid HPLC analysis 88

3.3 Mass Spectrometry (MS) detection in tear film lipids analysis: Direct infusion of non polar lipids **89**
3.3.1 Introduction to MS 89
3.3.2 Lipid MS: Direct Infusion of non polar lipids 90

3.3.3 Lipid MS: fragmentation of phospholipids 92

3.4 LCMS Method Development for tear film lipids analysis 95
3.4.1 Introduction to LCMS Method Development 95
3.4.2 LCMS Method Development 95
3.4.3 Non polar Tear Film LCMS Method Development 95
3.4.4 Polar Tear Film LCMS Method Development 96
3.4.5 Tear film lipid samples analysed with LCMS 98
3.4.6 Extracted Ion Chromatograms (EIC) of tear film samples 101
3.4.7 Common Contaminants in ESI MS 102
3.4.8 Summary of tear film lipid LCMS analysis 102

3.5 Conclusions 102

4 CHAPTER 4 - LIPID ANALYSIS OF THE TEAR FILM 2 106

4.1 Introduction to lipid analysis of the tear film 2 107

4.2 Thin Layer Chromatography (TLC) for tear film lipid analysis 108
4.2.1 Introduction to TLC 108
4.2.2 TLC of polar tear film lipids 109
4.2.3 Dittmer's solution for detection of polar lipids in TLC 111
4.2.4 TLC of non polar tear film lipids 113
4.2.5 Summary of tear film lipids TLC analysis 115

4.3 Detection of Phospholipase C (PLC) in the tear film 115
4.3.1 Detection of PLC in the tear film: Introduction 115
4.3.2 Detection of PLC in the tear film: Counter Immunoelectrophoresis (CIE) for tear film PLC analysis 116
4.3.3 Detection of PLC in the tear film: Phosphatidylcholine-Specific Phospholipase C Assay for tear film PLC analysis 119
4.3.4 Detection of PLC in the tear film: Summary 122

4.4 Conclussions 123

5 CHAPTER 5 – ZWITTERIONIC AND CHARGE-BALANCED HYDROGELS 128

5.1 Introduction to zwitterionic and charge-balanced hydrogels 129

5.2 Synthesis of charge-balanced copolymer membranes 132
5.2.1 Introduction to synthesis of charge-balanced copolymer membranes 132
5.2.2 Cationic monomers selected for charge-balanced copolymer membranes 133
5.2.3 Sterilisation of monomers for charge-balanced membranes 134
5.2.4 Compositions for charge-balanced copolymer membranes 136
5.2.5 Polymerisation of charge-balanced copolymer membranes 137
5.2.6 Sterilisation of charge-balance copolymer membranes 138

5.3 Synthesis of N,N-dimethyl-N-(2-acryloylethyl)-N-(3-sulfopropyl) ammonium betaine (SPDA) copolymer membranes 138
5.3.1 Introduction to synthesis of SPDA copolymer membranes 138
5.3.2 Sterilisation of zwitterionic monomers 139
5.3.3 Compositions for SPDA copolymer membranes 140
5.3.4 Polymerisation of SPDA copolymer membranes 142
5.3.5 Sterilisation of SPDA copolymer membranes 142
5.3.6 NMR of SPDA monomer 143

5.4 Properties of charge-balanced copolymer and N,N-dimethyl-N-(2-acryloylethyl)-N-(3-sulfopropyl) ammonium betaine (SPDA) copolymer membranes 146
5.4.1 Equilibrium water content (EWC) of copolymer membranes 146

5.4.2 Mechanical properties of copolymer membranes 152
5.4.3 Surface free energy (γ) of copolymer membranes 158
5.4.4 Oxygen permeability (Dk) of SPDA membranes 163
5.4.5 Optical transmittance of SPDA membranes 165
5.4.6 Coefficient of friction (μ) of SPDA membranes 166

5.5 Conclusions 169

6 CHAPTER 6 – HYDROGEL SKIN ADHESIVES AND LIPID INTERACTION 172

6.1 Introduction to hydrogel skin adhesives and lipid interaction 173

6.2 N-vinyl pyrrolidone (NVP) copolymer pressure skin adhesives (PSA) 174
6.2.1 Introduction to NVP copolymer PSA 174
6.2.2 Composition of NVP copolymer gels 175
6.2.3 Polymerisation of NVP copolymer gels 178
6.2.4 Peel strengths of NVP copolymer gels 179
6.2.5 Surface free energy (γ) of NVP copolymer gels 185
6.2.6 Rheology of NVP copolymer gels 191

6.3 N,N-dimethyl-N-(2-acryloylethyl)-N-(3-sulfopropyl) ammonium betaine (SPDA) copolymer pressure skin adhesives (PSA) 195
6.3.1 Introduction to SPDA copolymer PSA 195
6.3.2 Composition of SPDA copolymer gels 196
6.3.3 Polymerisation of SPDA gels 198
6.3.4 Peel strength of SPDA copolymer gels 198
6.3.5 Surface free energy (γ) of SPDA copolymer gels 200
6.3.6 Rheology of SPDA copolymer gels 205

6.4 Conclusions 207

7 CHAPTER 7 – DISCUSSION AND FURTHER WORK 209

7.1 Introduction 210

7.2 Summary of the analytical studies 210

7.3 Summary of the synthetic work 215
7.3.1 Zwitterionic and charge-balanced hydrogel membranes 215
7.3.2 Hydrogel skin adhesives 221

8 REFERENCES 230

APPENDICES 240

8.1 Appendix I - Adhesion 241

8.2 Appendix II– Rheology and Viscoelastic materials 244

8.3 Appendix III - Chromatography 252

8.4 Appendix IV - Liquid Chromatography Mass Spectrometry (LCMS) 257

8.5 Appendix V – Ion Trap Mass Spectrometer 265

8.6 Appendix VI – Contact angle 268

List of figures

		page
Figure 1	The structure of some common neutral monomers used for synthesis of hydrogels	20
Figure 2	The structure of some common anionic monomers used for synthesis of hydrogels	20
Figure 3	The structure of some common cationic monomers used for synthesis of hydrogels	21
Figure 4	The structure of some zwitterionic monomers used for synthesis of hydrogels	21
Figure 5	The nature of water in hydrogels	23
Figure 6	Phase diagram revealing the properties from monomer, glycerol and water compositions (w/w)	27
Figure 7	Generic structure of a phospholipid	32
Figure 8	The major classifications of phospholipids	33
Figure 9	Cross section of the tear film	37
Figure 10	The lacrimal functional unit	39
Figure 11	Diagram of the eye and meibomian gland	40
Figure 12	Minimum (blue), maximum (red) and average (yellow) lipid percentage compositions for meibomian secretion	42
Figure 13	Chart showing the percentage of normal meibomian secretions	44
Figure 14	Cross-section of human skin	47
Figure 15	Variation of skin lipids with differentiation	48
Figure 16	Composition of lipids in sebum prior to and after lipase action	50
Figure 17	The structures of crosslinkers, initiators and monomers	55
Figure 18	The structures of monomers used in membrane synthesis	56
Figure 19	The structures of monomers used in gel synthesis	57
Figure 20	Glass capillary collection method	59
Figure 21	Ophthalmic sponges	60
Figure 22	The Agilent 1100 Series LC	63
Figure 23	Kd Sceintific Model 100 Series Syringe Pump	67
Figure 24	Agilent 1100 Series LC/MSD	68
Figure 25	An example of a Total Ion Chromatogram (TIC)	69
Figure 26	An example of a mass spectrum	69
Figure 27	An example of a Extracted Ion chromatogram (EIC)	70
Figure 28	An example of a TIC with a section showing the data to be extracted	70
Figure 29	An example of the CMS of specified data	70
Figure 30	Diagram of a membrane mould	72
Figure 31	Schematic representation of a nanobiotribometer	76
Figure 32	A schematic of a typical coefficient of friction vs distance trace	77
Figure 33	A diagrammatic representation of the 90 Degree Peel Test	78

Figure 34	A diagrammatic representation of the GBX Goniometer.	79
Figure 35	Correct loading of parallel plate measuring system (Bohlin Instruments	81
Figure 36	Absorbance versus wavelength for solvents	89
Figure 37	Compound Mass Spectrum (CMS) of the Direct Infusion of cholesterol	91
Figure 38	Compound Mass Spectrum (CMS) of the Direct Infusion of cholesterol myristate	91
Figure 39	Compound Mass Spectrum (CMS) of the Direct Infusion of cholesterol palmitate	91
Figure 40	Compound mass spectra (CMS) of dilauroylphosphotadiylcholine (DLPC)	93
Figure 41	Total Ion chromatogram (TIC) of phospholipid species	97
Figure 42	Intensity of Peak Vs Concentration of sample	98
Figure 43	Total Ion Chromatograms (TIC) of samples	100
Figure 44	MALDI-TOF mass spectra of the tear total chloroform extractables	104
Figure 45	Structure of a sphingomyelin (SM)	105
Figure 46	Structure of a phosphatidylcholine (PC)	105
Figure 47	Iodine stained silica plate from polar phase TLC	110
Figure 48	Dittmers sprayed silica plate from polar phase TLC	112
Figure 49	Iodine stained silica plate from non polar phase TLC	114
Figure 50	Principle of counter immunoelectrophoresis (CIE)	117
Figure 51	The results of counter immunoelectrophoresis (CIE)	118
Figure 52	10-acetyl-3,7-dihydrophenoxazine (Amplex red reagent)	119
Figure 53	Reaction scheme for the conversion of phosphatidylcholine to resorufin	120
Figure 54	Standard curve for the detection of activity of phospholipase C	121
Figure 55	TLC plate of human tear lipids	124
Figure 56	Cleavage specificities of phospholipases	125
Figure 57	The structure of 2-methacryloyloxyethylphosphorylcholine (MPC)	130
Figure 58	Sulfobetanisation reaction scheme	131
Figure 59	The structure of N,N-dimetyl-N-(2-acryloylethyl)-N-(3-sulfopropyl) ammonium betaine (SPDA)	131
Figure 60	General structure of cationic monomers 1	133
Figure 61	General structure of cationic monomers 2	134
Figure 62	The structure of 2-acrylamido-2-methylpropane sulfonic acid (AMPS)	134
Figure 63	The structure of 2-hydroxyethyl methacrylate (HEMA)	137
Figure 64	Structures of zwitterionic monomers subjected to gamma (γ) ray irradiation	140

Figure 65	1H NMR of N,N-dimethyl-N-(2-acryloylethyl)-N-(3-sulfopropyl) ammonium betaine (SPDA) before gamma ray irradiation	143
Figure 66	1H NMR of N,N-dimethyl-N-(2-acryloylethyl)-N-(3-sulfopropyl) ammonium betaine (SPDA) after gamma ray irradiation	144
Figure 67	Possible degradation of N,N-dimethyl-N-(2-acryloylethyl)-N-(3-sulfopropyl) ammonium betaine (SPDA)	145
Figure 68	Equilibrium water content (EWC) of charge-balanced membranes	147
Figure 69	Comparison of 2-(dimethylamino) ethyl methacrylate (DMA EMA) and 3-(dimethylamino) propyl methacrylamide (DMA PMA)	148
Figure 70	Equilibrium water content (EWC) of SPDA membranes	149
Figure 71	EWC vs % SPDA and % NVP comonomer in a HEMA copolymers	150
Figure 72	Comparison of the EWC of ionic comonomer and SPDA comonomer in HEMA copolymer	151
Figure 73	Youngs modulus (ε) of charge-balanced membranes	153
Figure 74	Tensile strength (Ts) and elongation to break (Eb) of charge-balanced membranes	154
Figure 75	The correlation between EWC and mechanical properties of the DMAEMA:AMPS copolymer membrane	155
Figure 76	The correlation between EWC and mechanical properties of the DMAPMA:AMPS copolymer membrane	155
Figure 77	Youngs modulus (ε) of SPDA membranes	156
Figure 78	Tensile strength (Ts) and elongation to break (Eb) of SPDA membranes	157
Figure 79	The correlation between EWC and mechanical properties of the SPDA copolymer membrane	157
Figure 80	Surface free energy of polyampholyte membranes	159
Figure 81	Surface free energy of SPDA membranes	161
Figure 82	The correlation between EWC and surface free energies of the SPDA, DMAEMA:AMPS and DMAPMA copolymer membrane	163
Figure 83	Coefficient of friction (μ) of SPDA membranes	167
Figure 84	The structure of N-vinyl pyrrolidone (NVP)	175
Figure 85	The structure of poly(N-vinyl pyrrolidone) using WebLab	177
Figure 86	Monomer composition for SPA, AMP and NVP gels	178

Figure 87	The structure of acrylic acid bis-(3-sulfopropyl)-ester potassium salt (SPA), 2-acrylamido-2-methyl propane sulfonic acid sodium salt (AMPS) and N-vinyl pyrrolidone (NVP)	179
Figure 88	The structure of Irgacure 184 and Ebacryl 11	179
Figure 89	Peel strengths of SPA, AMPS and NVP copolymer gels	180
Figure 90	Proposed hydrogen bonding between AMPS and SPA	182
Figure 91	Proposed hydrogen bonding between AMPS and NVP	183
Figure 92	Initial surface free energy of SPA:AMPS:NVP gels	186
Figure 93	Final surface free energy of SPA:AMPS:NVP gels	187
Figure 94	Initial surface free energy of AMPS:NVP gels	189
Figure 95	Final surface free energy of AMPS:NVP gels	190
Figure 96	Sample graph of an oscillatory frequency sweep of a gel	192
Figure 97	Elastic modulus (G'), viscous modulus (G'') and tan delta (G''/G') at 1Hz for control and SPA:AMPS:NVP gels.	193
Figure 98	Elastic modulus (G'), viscous modulus (G'') and tan delta (G''/G') at 10Hz for control and SPA:AMPS:NVP gels.	194
Figure 99	Intercalation of phosphatidylcholine and phosphatidylethanolamine with N,N-dimethyl-N-(2-acryloylethyl)-N-(3-sulfopropyl) ammonium betaine (SPDA)	196
Figure 100	Monomers composition in SPDA, AMPS and SPA gels	197
Figure 101	Peel strengths of SPDA, AMPS and SPA gels	198
Figure 102	Initial surface free energy of SPDA:AMPS:SPA gels	201
Figure 103	Final surface free energy of SPDA:AMPS:SPA gels	201
Figure 104	Initial surface free energy of SPDA:SPA gels	202
Figure 105	Final surface free energy of SPDA:SPA gels	203
Figure 106	Initial surface free energy of SPDA:AMPS gels	203
Figure 107	Final surface free energy of SPDA:AMPS gels	204
Figure 108	Example graph of an oscillatory frequency sweep of an SPDA containing gel	205
Figure 109	Elastic modulus (G'), viscous modulus (G'') and tan delta (G''/G') at 1Hz	206

Figure 110	Elastic modulus (G'), viscous modulus (G") and tan delta (G"/G') at 10Hz for control and SPDA:AMPS:NVP gels	206
Figure 111	Examples of types of forces: (a) Tensile force. (b) Compressive force. (c) Shear force.	245
Figure 112	Shear strain	246
Figure 113	A Maxwell element and a Voigt element	248
Figure 114	Viscous and Elastic Responses to an Applied Strain	249
Figure 115	Components of an Isocratic Liquid Chromatography System	254
Figure 116	Thin Layer Chromatography (TLC)	256
Figure 117	Different ionisation sources and their applicability with regard to sample polarity and molecular weight.	258
Figure 118	Overview of a differentially pumped API source coupled to a mass spectrometer	259
Figure 119	The Electrospay Ionisation Interface Chamber	260
Figure 120	Nebulisation or droplet formation	261
Figure 121	Taylor Cone production	262
Figure 122	Desolvation process of ESI	262
Figure 123	Evapouration process of ESI	263
Figure 124	Ion trap accumulation and ejection of ions	265
Figure 125	Figure showing how the ions are accumulated	266
Figure 126	Examples of contact angle measurement	268

List of tables

		page
Table 1	Classification of hydrogels	18
Table 2	Sub Classes of Lipids	29
Table 3	Molecular weights of phosphatidylcholines with different fatty acid chains	34
Table 4	Average, normalized, minimum and maximum lipid percentage compositions for meibomian secretion	42
Table 5	Phospholipids in rabbit meibomian gland secretions	45
Table 6	Crosslinkers and initiators	53
Table 7	Monomers used in the synthesis of membranes	54
Table 8	Monomers used in the synthesis of gels	54
Table 9	Other reagents and materials	58
Table 10	Dynamic range of optimum flow rates for columns of different internal diameter	63
Table 11	Non polar samples injected	86
Table 12	Polar samples injected	88
Table 13	Samples Directly Infused	90
Table 14	MS peaks and molecular weight (Mr) of samples	92
Table 15	MSn of dilauroylphosphotadiylcholine (DLPC)	93
Table 16	MSn of dilauroylphosphotadiylethanolamine (DLPE)	94
Table 17	MS peaks and molecular weight (Mr) of samples	96
Table 18	PC mix solutions	97
Table 19	Tear samples for Thin Layer Chromatography	109
Table 20	Standards Rf values for THIN Layer Chromatography of polar lipids	110
Table 21	Sample Rf values. LPC is lysophospholipids and PA is phosphatidic acid	111
Table 22	Volume of lipid	113
Table 23	Standard Rf values for non polar TLC	115
Table 24	PLC activity in the tear film	122
Table 25	PLC activity in the tear film using second calibration curve	122
Table 26	Aroma of cationic monomers before and after gamma (γ) ray irradiation	135
Table 27	Composition of charge-balanced (polyampholyte) membranes	137
Table 28	N,N-dimethyl-N-(2-acryloylethyl)-N-(3-sulfopropyl) ammonium betaine (SPDA) containing membranes	141
Table 29	Peaks of interest in the 1H NMR specturm of N,N-dimethyl-N-(2-acryloylethyl)-N-(3-sulfopropyl) ammonium betaine (SPDA) proir to gamma ray irradiation	145
Table 30	Theoretical Dk from literature	164
Table 31	Transmission of light across SPDA membranes	166
Table 32	Polar and dispersive components for water and diiodomethane	269

Chapter 1 - Introduction

"May we meet, as we part, with a tear"
Lord Byron, *The tear*

1.1 Hydrogels

1.1.1 Introduction to hydrogels

Hydrogels can be defined as water swollen hydrophilic polymeric networks. These materials have the ability to be swollen by and to imbibe water (or other suitable solvents) while preserving their three-dimensional structure at physiological pH, temperature and ionic strength [1]. This definition includes a wide variety of materials of both biological and synthetic origin [2]. While hydrogels are not a novel idea it was not until Wichterle and Lim [3] introduced 2-hydroxyethyl methacrylate and suggested that hydrogels would make biologically compatible polymers that widespread interest was sparked.

Hydrogels can be classified in variety of ways [2, 4, 5] and some examples are according to the source, the components, the nature of the crosslinks, the nature of pendant groups, its responsiveness or degradability (Table 1).

Table 1. Classification of hydrogels

Classification	Contents
Source	Natural Synthetic Combination
Component	Polymer Copolymer Interpenetrating network
Crosslink	Physical Chemical
Nature of pendant groups	Non ionic Ionic Amphoyltic
Responsiveness	Non responsive Responsive • pH, temperature, electric field, light, etc
Degradability	Degradable Non degradable

One of the most common and perhaps useful classifications is that of the crosslinks. The three-dimensional structures of hydrogels are networks of polymer chains that can be held together by physical or chemical bonds. Physically bonded hydrogels are held together by molecular entanglements, ionic forces and secondary forces (hydrogen and van der Waals bonds) which are (relatively) reversible bonds. Chemically bonded hydrogels are held together by covalent bonds crosslinking the polymer chains thus making them more stable than physically bonded hydrogels and therefore relatively non-reversible.

Chemically bound synthetic hydrogels are used for applications in this thesis. These are normally polymers or copolymers of hydrophilic monomers. Examples of the hydrophilic monomers used in the polymerisation of such hydrogels are shown in section 1.2.1. The hydrophilicity is due to the presence of hydrophilic gorups, such as the hydroxyl, carboxyl and amide. These polymers are known to perform well in biomaterial applications.

The chemical bonds are formed in hydrogels can created by various techniques, for example chemical crosslinking, irradiation crosslinking, physical interaction and free radical polymerisation. The free radical polymerisation method is the most preferred and was used in this work with thermal or photo-induced initiation.

1.1.2 Neutral, ionic and ampholyte hydrogels

Neutral or non ionic hydrogels are those which are synthesied from monomers have no charge bearing groups in their structure. Examples of these are acrylamides, alkyl methacrylates, vinyl lactams (such as N-vinyl pyrrolidone), and hydrophobic acrylics such as vinyl acetate (Figure 1).

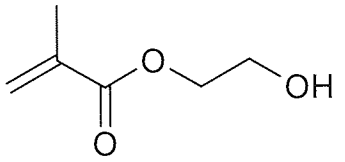

2-hydroethyl methacrylate (HEMA)

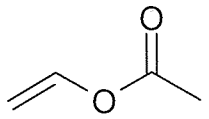

vinyl acetate (VA)

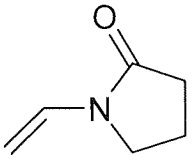

N-vinyl pyyrolidone

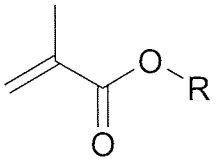

alkyl methacrylate

Figure 1. The structure of some common neutral monomers used for synthesis of hydrogels

Ionic hydrogels are synthesised from monomers which posses charge bearing groups in their structure. These monomers can be cationic or anionic with the resulting hydrogel being negatively or positively charged. Examples of anionic monomers are 3-sulfopropyl ester acrylate (SPA), 2-acrylamido-2-methyl propane sulfonic acid sodium salt (NaAMPS), acrylic acid and its derivatives, and sodium styrene sulfonate (Figure 2).

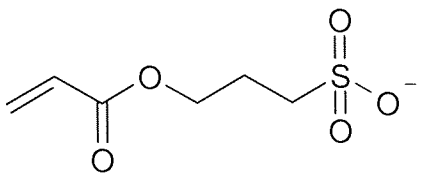

3-sulfopropyl ester acrylate (SPA)

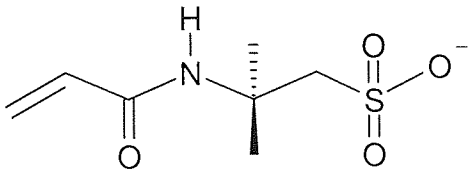

2-acrylamido 2,2-methyl propane sulfonic acid sodium salt (NaAMPS)

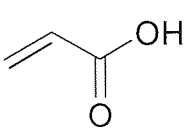

acrylic acid

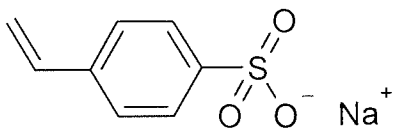

sodium styrene sulphonate

Figure 2. The structure of some common anionic monomers used for synthesis of hydrogels

Examples of cationic monomers are aminoethyl methacrylate derivatives (such as 2-(dimethylamino) ethyl acrylate) and 4-Vinyl pyridine (Figure 3).

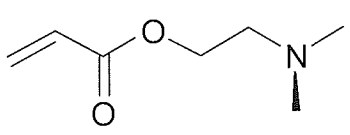

2-(dimethylamino) ethyl acrylate

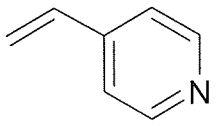

4-vinyl pyridine

Figure 3. The structure of some common cationic monomers used for synthesis of hydrogels

Ampholyte hydrogels contain both positive and negative charges. They are synthesised from cationic and anionic monomers with the resulting charge depending on the amount of each incorporated. A special case of ampholyte monomers are the zwitterions which are molecules that contain both the positive and negative charges. Examples of ampholyte monomers include N,N-dimethyl-N-(2-acryloylethyl)-N-(3-sulfopropyl) ammonium betaine (SPDA), 2-methacryloyloxyethylphosphorylcholine (MPC) and 1-(3-sulfopropyl)-2-vinylpyridinium (SPV) (Figure 4).

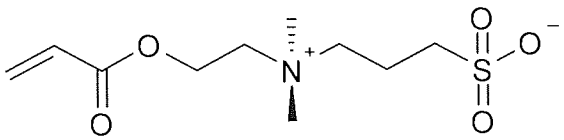

N,N-dimethyl-N-(2-acryloylethyl)-N-(3-sulfopropyl) ammonium betaine (SPDA)

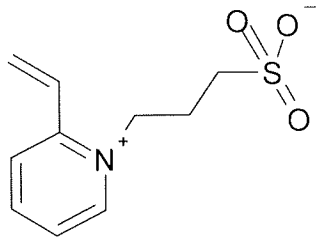

1-(3-sulfopropyl)-2-vinylpyridinium (SPV)

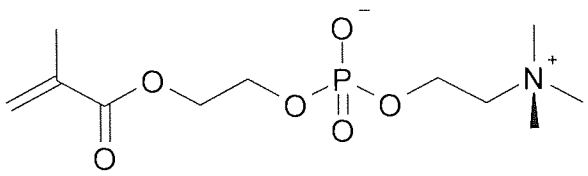

2-methacryloyloxyethylphosphorylcholine (MPC)

Figure 4. The structure of some zwitterionic monomers used for synthesis of hydrogels

1.1.3 Equilibrium Water Content (EWC)

If a hydrogel is allowed to swell with water then it will reach equilibrium. This is the equilibrium water content (EWC) of the hydrogel. EWC can be found using equation 1:

$$\mathbf{EWC(\%)} = \frac{\mathbf{weight\ of\ water\ in\ hydrogel}}{\mathbf{Total\ weight\ of\ hydrated\ hydrogel}} \times \mathbf{100} \qquad \text{Equation 1}$$

If at equilibrium a polymer embibes water of its own dry weight then it would have a EWC of 50%. EWC can be determined by bringing a hydrogel to its water equilibrium by soaking in water and then dehydrating, weighing prior to and after dehydration provides the masses to be used in the equation above. This is the basis of the gravimetric method [6].

The hydrogel swells to accommodate the water in the chain network while maintaining the bonds that hold it together. This sets up conflicting forces of osmotic drive versus "bonding force" retraction and the amount of water imbibed reaches equilibrium when these forces are balanced. The degree of swelling is dependent on a range of factors the most influential of which are the nature of monomers used, the nature and concentration of bonds formed, the pH and the tonicity of the polymer. Imbibed water can swell a hydrogel from a lower arbitrary limit of 10-20% up to 1000's of times its dry weight depending on the factors [2].

The EWC is perhaps the most important property of a hydrogel as it impinges on so many other properties of the material. The water held within the polymer substrate gives the hydrogels their properties. The water in a hydrogel acts as a plasticizer or an internal lubricant allowing chains to rotate and conferring flexibility. It also acts as a transport medium for dissolved species such as oxygen and water-soluble metabolites. The water also operates as a "bridge" between the surface of natural and synthetic systems. It can behave as a lubricant to reduce the friction at the interface.

1.1.4 The Nature of Water in Hydrogels

There is a widely accepted theory that proposes that water in hydrogels is in dynamic equilibrium between two states known as bound and free water, or non-freezing and freezing water. When water is first absorbed it interacts with the hydrogels hydrophobic and hydrophilic regions forming secondary bonds and this is known as *bound water (non-freezing)*. After this initial period water continues to be driven by osmosis into the hydrogel but does not interact with the hydrogel, this is known as *free water (freezing)*. There is also an intermediate state between the bound and free water. These states of water are shown in Figure 5 [7].

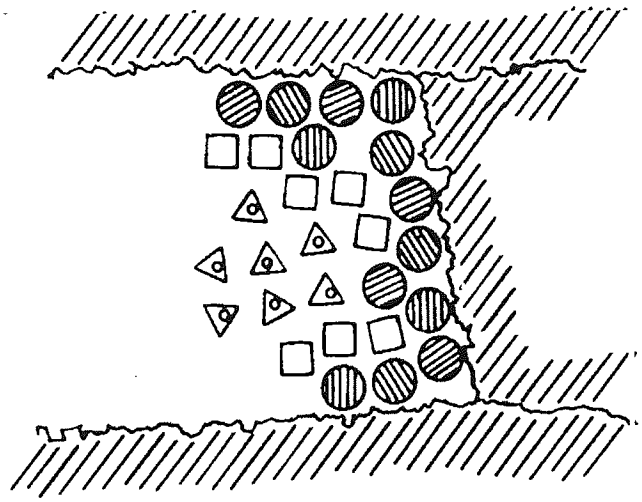

The different types of water in hydrogels. ⊘ = bound water, △ = free water; □ = intermediate water.

Figure 5. The nature of water in hydrogels [7]

Three methods are common for deteriming the amounts of free and bound water. These are small molecular probes, dynamic scanning calorimetry and nuclear magnetic resonance.

1.1.5 Applications of Hydrogels

Hydrogels have been used for applications in agricultural as water storage granules, in the food industry as thickeners and in analytical techniques such as electrophoresis and chromatography. It is their use as biomaterial where they find many applications.

1.1.5.1 Hydrogels as Biomaterials

A definition for a biomaterial is *a material that is natural and/or synthetic in origin which is designed to interact with the organism (or a part of it) in order to control, support, modify or improve some of its function or properties*. To do this the material must be biocompatible and while there is no such thing as a universally biocompatible material but there are degrees of biocompatibility. A device that is biocompatible is harder to define but one definition is

"a device that performs in the environment in which it is placed, with an appropriate host response"

Hydrogels fall within this definition and are employed as biomaterials. Applications of hydrogels as biomaterials include blood contact devices, ocular environmental uses (contact lenses, intraocular lenses, scheral buckling and keratoprothesis), implanted materials (synthetic articular cartilages, soft tissue prosthesis, bone and hard tissue prosthesis, composites and coatings), wound dressings (natural hydrogels, synthetic hydrogels, hydrocolloids) and pressure sensitive adhesives (transdermal drug delivery systems, wound dressings and biosensors). An overview of biomaterial applications and relevant patent literature can be found by Corkhill et. al. [6]. It is the contact lens and pressure sensitive adhesive (skin adhesive patch) applications that are of interest in this thesis.

1.1.5.2 Contact lenses

Hydrogel contact lenses are directly attributable to the work of Wichterle and Lim [3]. Not only did they introduce the concept of soft contact lenses utilising the properties of HEMA but also developed the spin casting method of production. Bausch & Lomb licensed Wichterle's patent and went on to commercialise the first soft contact lens in 1972. The other major contact lens manufacturers introduced there own soft contact lens materials, Johnson & Johnson with their daily disposable HEMA-based 1-Day Acuvue contact lens in 1987 and Ciba Vision's release of poly(vinyl alcohol) Dailies in 1997.

However throughout the 80's it became apparent that the oxygen permeability (Dk) of these soft contact lens was not suitable for overnight use, as exemplified by the work of Holden and Mertz [8] and more recently Harvitt and Bonanno [9]. The drive for higher Dk led to the use of silicone hydrogels. These are a different family of hydrogels that are based around the use of silicone in the place of carbon in the backbone of the polymer. Silicone hydrogels have found commercial applications as contact lenses with the introduction Bausch & Lomb's PureVision and Ciba Vision's Focus Night&Day in 1999. More recently this was followed by Johnson & Johnson's Acuvue Advance and Acuvue Oasys, Ciba Vision's with O2Optix and Coopervision's Biofinity.

1.1.5.3 Pressure-sensitive adhesives (PSAs)

A PSA can be defined as a material that adheres to a substrate with low pressure and leaves no residual adhesion upon removal [10]. Johnson and Johnson first introduced PSAs in 1899 in the form of a tape with adhesive attached and recent applications include wound dressings, sensor application and transdermal drug delivery devices.

A PSA must possess the thermodynamic and kinetic requirements of adhesion (see Appendix I – Adhesion) in order to adhere to skin. PSAs have been successfully produced from materials such as polyisobutylenes, polyacrylics and polysilicones. It was thought that materials with a greater degree of hydrophilicity could be used to enhance adhesion to skin. This led to the use of hydrogels that provide a higher degree of

hydrophilicity due to the nature of polymers used. The enhanced adhesion is thought be due to hydrogen bonding between the hydrophilic PSA and the skin.

Hydrogel PSAs are formulated to be partially hydrated and are therefore below their EWC. This partial hydration of the hydrogels leads to the PSAs with an appetite for the uptake of water, which has the consequence of aiding adhesion due to the removal of any interfacial water. However the partially hydrated hydrogels state of hydrogel pressure sensitive adhesives leaves them with the ability to absorb enough water to destroy their ability as pressure sensitive adhesives. Imbibed water can swell them prolifically and their mechanical strength diminishes as they expand until they become unusable.

Previous research in this laboratory by Flemming described hydrogel PSAs synthesised from 2-acrylamido-2-methyl propane sulfonic acid sodium salt (AMPS) and acrylic acid bis-(3-sulfopropyl)-ester potassium salt (SPA) monomers which made PSAs suitable for application as skin adhesives [11].

The three key components of hydrogel PSAs are an unsaturated water soluble monomer, water and a humectant/plasticiser. Glycerol is a typical humectant/plasticizer used in PSA formulations. Flemming [11] has defined the upper and lower limits of the these three key components of hydrogel PSAs for the production of cohesive, adhesive hydrogels gels. Flemming's work used AMPS as the monomer and glycerol as the humectant to produce a series of hydrogel membranes with differing ratios AMPS, water and glycerol. The characteristics of these membranes are shown in Figure 6.

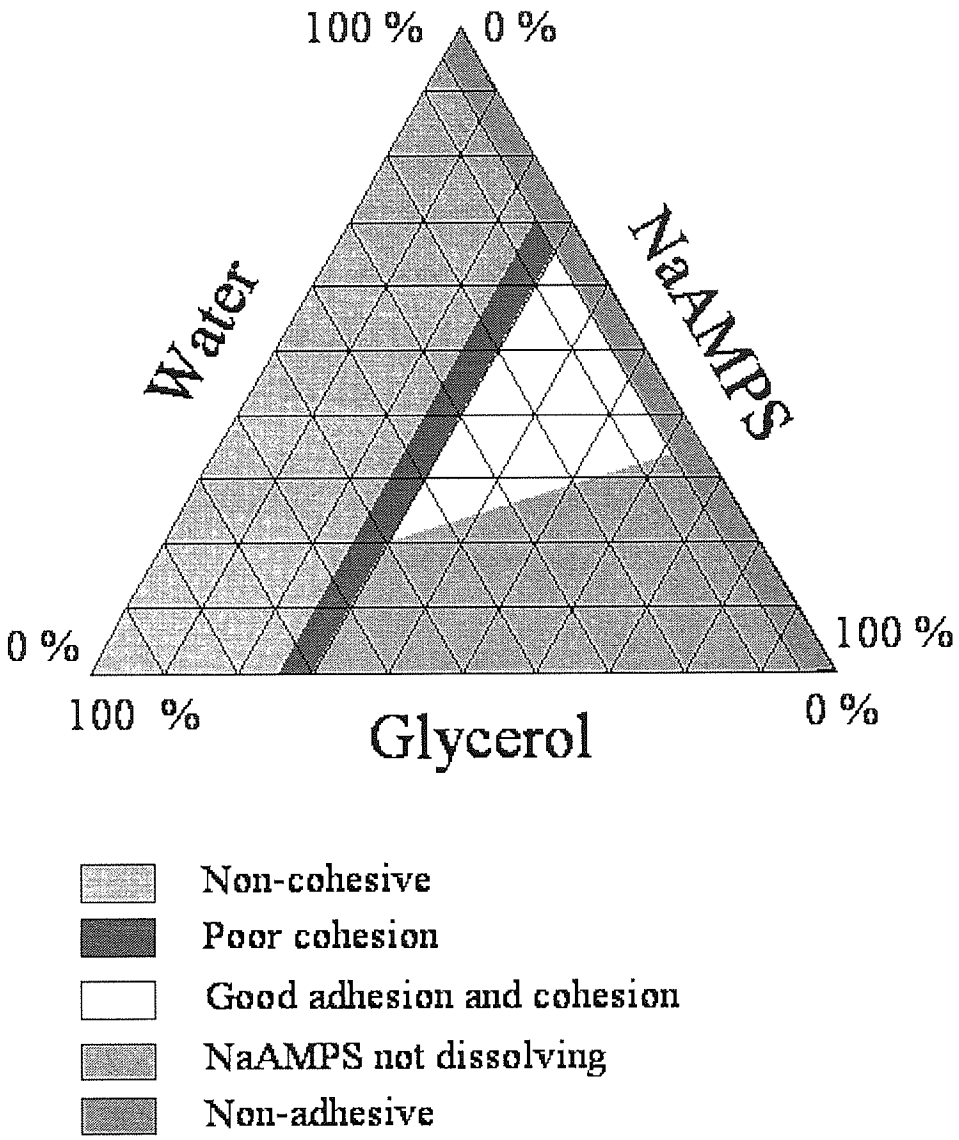

Figure 6. Phase diagram revealing the properties from monomer, glycerol and water compositions (w/w) [11]

These compositions can then be used as a basis for the design of new hydrogel PSAs. A composition from within the white area of this triangle denotes those hydrogels with good adhesive and cohesive properties; this composition was chosen as a starting point for the PSAs in this thesis. Details of the chosen starting point composition are 40% monomer(s), 30% water and 30% glycerol. Cartwright continued Flemming's work using these and other ionic monomers and found that a ratio of 6:4 AMPS:SPA provided PSAs with improved adhesion while still remaining cohesive and clear [12].

1.2 Lipids

1.2.1 Introduction to lipids

Lipid is a term often used to describe compounds that can be grouped together according to their solubility, i.e insolubility in water and soluble in non polar solvents such as benzene, chloroform and hexane. There is no widely accepted definition for lipids and Christie [13] has sought to rectify this by defining lipids as:

"fatty acids and their derivatives, and substances related biosynthetically or functionally to these compounds"

Lipids are hydrophobic and in an aqueous or polar environment will aggregate however some lipids also have a hydrophilic component and are amphipathic; these types of lipids are habitually found in membranes. Lipids are classified on the chemistry and chemical property of the compound. Classifications include fatty acids, n-acylglycerols, phospholipids, isoprenoids, esters, eicosanoids and glycolipids [14] and are detailed in Section 1.2.2.

Lipids can be divided into two sub divisions: firstly those that contain ester linkages and can be hydrolysed such as waxes and fats and secondly those which do not contain ester linkages such as steroids [15]. Christie [13] also has sub definitions of simple and complex lipids where simple lipids produce at most two primary products per mole from hydrolysis and complex lipids produce three or more primary products per mole from hydrolysis. Simple and complex lipids are sometimes referred to as neutral and polar respectively (Table 2).

Table 2. Sub Classes of Lipids

Simple	Complex
neutral	polar
two primary hydrolysis products	three or more primary hydrolysis products

1.2.1.1 Simple lipids

The simple (neutral) lipids include the subclasses of free fatty acids, triacylglycerols (triacylglycerides), diacylglycerols, 2-mono-sn-glycerols, sterols, sterol esters and waxes.

1.2.1.2 Complex lipids

The complex (polar) lipids include the subclasses of glycerophospholipids (phospholipids), glycoglycerolipids, sphingolipids and glycosphingolipids.

1.2.2 Lipid Classes

1.2.2.1 Free Fatty acids

Fatty acids consist of chains of 3 to 30 carbon atoms with a carboxylic acid group at one chain end. The individual characteristics of the fatty acids are determined by the chain length and degree of unsaturation. The longer the carbon chain of the fatty acid the higher the melting point and the more hydrophobic the fatty acid. The more double bonds the lower the melting and the more fluidity [14].

Free fatty acids are synthesized in nature via condensation of malonyl coenzyme A units by an ester synthase complex. They usually contain even numbers of carbon atoms in straight chains and may be saturated or unsaturated and may contain substituent groups [13]. About 40 fatty acids occur naturally with palmitic acid (C_{16}) and stearic acid (C_{18}) being the most abundant saturated types, oleic acid and linoleic acid (both C_{18}) are the most abundant unsaturated types [15].

1.2.2.2 n-acylglycerols

n-acylglycerols consist of a glycerol backbone with fatty acids esterified. The fatty acids can differ in chain length and saturation to each other. n-acylglycerols can be triacyl, diacyl or 2-mono acyl depending on the number of fatty acids attached to the glycerol backbone [13].

Triacylglycerols (triacylglycerides or triglycerols) consist of three fatty acids esterfified to a glycerol backbone. In nature they are synthesized by enzymes and the asymmetry is created about the C-2 carbon of the glycerol backbone therefore enantiomeric forms exist. Sterospecific nomenclature has been developed to describe these forms so that a Ficher projection of a natural L-gylcerol derivative the second hydroxyl group is shown to the left of the C-2 and the carbon above this is the C-1 carbon atom and that below is the C-3. A prefix of "sn" indicates that the compound is has defined stereochemistry.

Diacylglycerols (or diglycerides) consist of two fatty acids per glycerol moiety and have various isomeric forms. 2-mono acylglycerols have the fatty acid in the C-2 position which can undergo acyl migration rapidly at room temperature.

1.2.2.3 Sterols

Sterols are a family of polycylic compounds [13] of which cholesterol (cholest-5-en-3β-ol) is the most abundant member, other examples include 7-dehydrocholesterol and lathosterol. They are amphipathic lipids synthetised naturally from acetyl-coenzyme A. In essence they consist of a tetracyclic structure with an iso-octyl side chain at carbon 17. The four rings (A, B, C, D) have trans ring junctions and the side chain and two metyhyl groups (C-18 ad C-19) are at an angle to the rings above the plane with β stereochemistry There is adouble bond between carbons 5 and 6. The overall molecule is quite flat. The hydroxyl group on the A ring is polar. The rest of the aliphatic chain is non-polar.

1.2.2.4 Waxes

Waxes are esters of long chain carboxylic acids and long chain alcohols. The carboxylic acid usually has an even number of carbon atoms from 16 to 36 while the alcohol has an even number of carbon atoms from 24 to 36.

1.2.2.5 Esters

Similar to waxes an ester can be formed by esterification of a fatty acid to a hydroxyl group attached to a ring compound, for example cholesterol can be esterified with a fatty acid to form a cholesterol ester.

1.2.2.6 Phospholipids (glycerophospholipids)

These are similar to triacylglycerols in that they have two fatty acids esterified to a glycerol backbone but the C-3 has a phosphate ester with one of four types of polar head groups attached; namely ethanolamine, choline, serine or inistol. The degree of saturation and the chain length of the fatty acids can differ so there are a great variety of phospholipids. The phospholipids are detailed in Section 1.2.3.

1.2.2.7 Isoprenoids, Eicosanoids and glycolipids (glycoglycerolipids)

Isoprenoids are cyclic lipids formed from eicosanoid acids which are twenty carbon chains. This class includes prostaglandins, thromboxanes and leukotrines. Eicosanoids are any product derived from arachidonic acid. Eicosanoids include prostaglandins, thromboxanes, and leukotrienes. The eicosanoids can collectively mediate almost every aspect of the inflammatory response Glycolipids are 1,2-diacyl-sn-glycerols with a glycosidic linkage at the C3 joining carbohydrate moiety.

1.2.3 Phospholipids

As much of this thesis deals with phospholipids a more detailed explanation of this class is given. Phospholipids are composed of a glycerol backbone with a phosphate group esterified at the sn3 position and two fatty acids chains esterified at the sn1 and sn2 positions. A further group (the head group) is found attached to the phosphate moiety. The generic structure of phospholipids is shown in Figure 7.

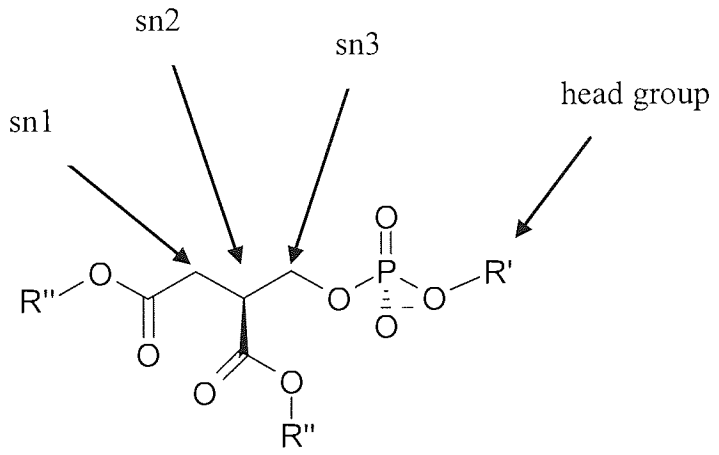

Figure 7. Generic structure of a phospholipid. The sn1, sn2 and sn3 show the positions on the glycerol backbone of the fatty acids and the phosphate group respectively. R' is a head group and R'' are fatty acid groups.

The headgroup establishes the way in which phospholipids are classified. The major classifications of phospholipids are shown in Figure 8 and are: phosphatidylcholine (PC), phosphatidylethanolamine (PE), phosphatidylserine (PS), phosphatidylinositol (PI), phosphatidylglycerol (PG) and diphosphatidylglycerol (DPG).

Another important and common lipid is sphingomyelein which is a glycolipid or more specifically a glycosphingolipids. Sphingomyelein is structurally similar to the phospholipids and consists of a ceramide with a phosphatidylcholine in position sn1 (Figure 8).

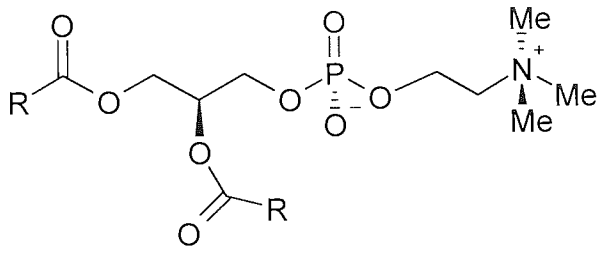

phosphatidylcholine (PC)

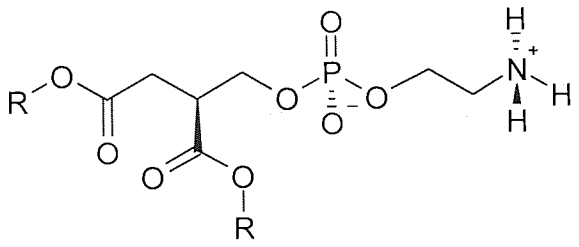

phosphatidylethanolamine (PE)

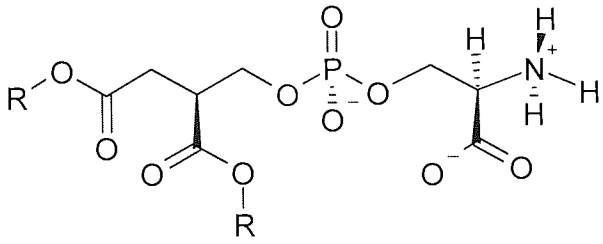

phosphatidylserine (PS)

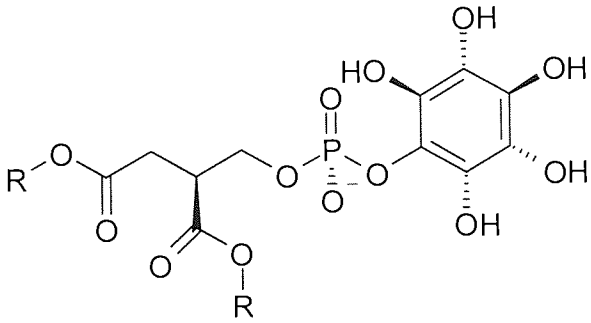

phosphatidylinositol (PI)

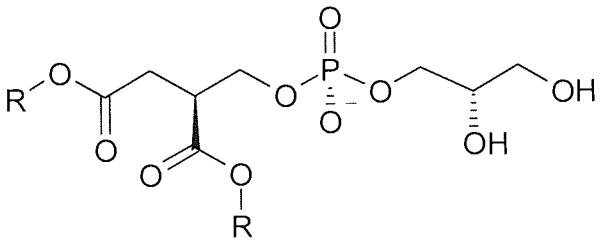

phosphatidylglycerol (PG)

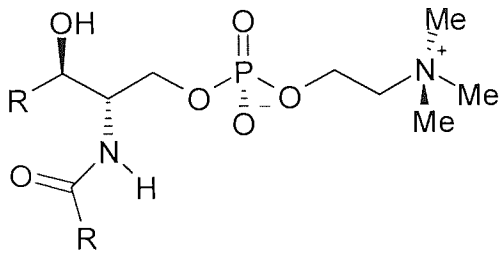

sphingomyelein (SM)

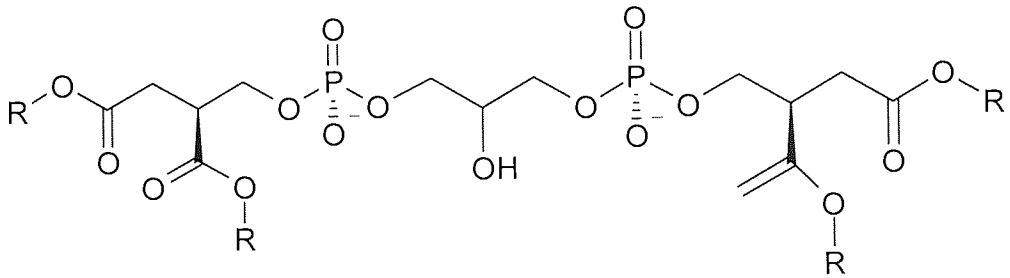

diphosphatidylglycerol (DPG)

Figure 8. The major classifications of phospholipids are phosphatidylcholine (PC), phosphatidylethanolamine (PE), phosphatidylserine (PS), phosphatidylinositol (PI), phosphatidylglycerol (PG), sphingomyelein (SM) and diphosphatidylglycerol (DPG)

1.2.4 The variety of molecular weight (M_r) associated with complex lipids

The two fatty acids groups present in phospholipids can lead to a great variety of molecular weights of phospholpids. If we consider phosphatidylcholine which has a glycerol backbone with its two fatty acids and phosphate polar head group as a model complex lipid.

The fatty acid groups of phosphatidylcholines differ from one species to another and so the M_r of each species will also differ. Table 3 shows a variety of phosphatidylcholines which have fatty acid chain groups with lengths of between 12 and 24 carbons. These are the most common type of fatty acid chain length in organic species. Some entries in the table have the same M_r even though they have different fatty acid chains, for example 20,20-phosphatidylcholine and 18,22-phosphatidylcholine both have a M_r of 846.25g/mol.

Table 3. Molecular weights of phosphatidylcholines with different fatty acid chains. FA is fatty acids carbon chain length and the number entries are the theoretical molecular weights of the species. For example the first entry is 12, 12 phosphatidylcholines (dilauroylphosphatidylcholines or DLPC) and its Mr is 621.828g/mol.

FA	12:0	14:0	16:0	18:0	20:0	22:0	23:0	24:0
12:0	621.828							
14:0	649.881	677.934						
16:0	677.934	705.987	734.04					
18:0	705.987	734.04	762.093	790.146				
20:0	734.04	762.093	790.146	818.199	846.252			
22:0	762.094	790.147	818.2	846.253	874.306	902.36		
23:0	776.12	804.173	832.226	860.279	888.332	916.386	930.412	
24:0	790.146	818.199	846.252	874.305	902.358	930.412	944.438	958.464

The differences in M_r continue with the unsaturation of fatty acid chains. For example the 20, 20-phosphatidylcholine and a 20:1, 20-phosphatidylcholine would have M_r's of

846.25g/mol and 842.25g/mol respectively. So we see from the different fatty acids and their degree of unsaturation there can be a great variety of M_r's of phosphaticylcholines alone and this diversity is seen throughout the complex lipids.

1.3 The Ocular Environment

1.3.1 Anatomy of the eye

When discussing contact lenses in relation to the eye one must consider the anterior of the ocular system which includes the cornea, conjunctiva, tear film and eyelids as all interact with the lens.

1.3.2 The Cornea, Conjunctiva and Eyelids

The cornea is the transparent, dome-shaped window covering the front of the eye. It provides 66% of the refractive power of the ocular system. There are no blood vessels in the cornea and it is extremely sensitive being richly populated with nerves endings. The adult cornea is only about 0.5 millimeters thick and is comprised of 5 layers: the epithelium, Bowman's membrane, stroma, Descemet's membrane and the endothelium.

The conjunctiva is the thin, transparent tissue that covers the outer surface of the eye beginning at the outer edge of the cornea, it covers the sclera and lines the interior the eyelids. It is nourished by tiny blood vessels that are nearly invisible to the naked eye and secretes oils and mucous which helps to moisten and lubricate the ocular surface. The eyelids are significant in contact lens wear [16].The eyelids are involved in the control of the flow and spreading of tears therefore any interaction with their function will impact upon the ocular surface.

Contact lenses cover the cornea to adjust the refraction of light to improve vision and are separated from the cornea only by a thin pre corneal tear film. Contact lenses interact with the conjunctiva and eyelids when the eyelids close during blinking and if worn when the eye is closed at night. During blinking contact lenses may block the meibomian

glands which are located on the leading edges of the eyelids. Contact lenses are intimately involved with the cornea, conjunctiva and eyelids due to their function.

1.3.3 The Tear Film [17, 18]

The ocular surface represents the interface between the eyes and the outer world; it must guarantee the quality of refractive surface to ensure sharp vision and react quickly to resist injury and protect the ocular structure. It is continually challenged by the shearing forces of blinking, air currents, low humidity and foreign bodies. It is for these reasons that the system is in a dynamic state and it is the tear film that is the most dynamic component of this structure.

Tears cleanse and lubricate the surface of the eye along with providing nourishment and immune protection. The tear film is linked to the epithelial cells via the glycocalyx which is a mucin layer embedded in the epithelial cells of the cornea and schelera. Immaturity or damage to the epithelium results in the absence of the glycocalyx and poor adhesion of tear film. The tear film is thought to be spread over the ocular surface by the action of the eyelids. The applied shear force of the eyelids would be damaging to the epithelial cells without the presence of the tear film.

The volume of the tear film has been determined to be approximately 6 to 7 μl [19] in a layered of phase like film, with estimates of thickness ranging from 3 μm to 35 μm [20, 21]. The tear film can be thought to be composed of three layers which are the lipid, aqueous and mucin, although the aqueous and mucin can be thought of as a continuous layer with a mucin gradient (Figure 9 [17]). There evidence to show mixing of lipid into the aqueous.

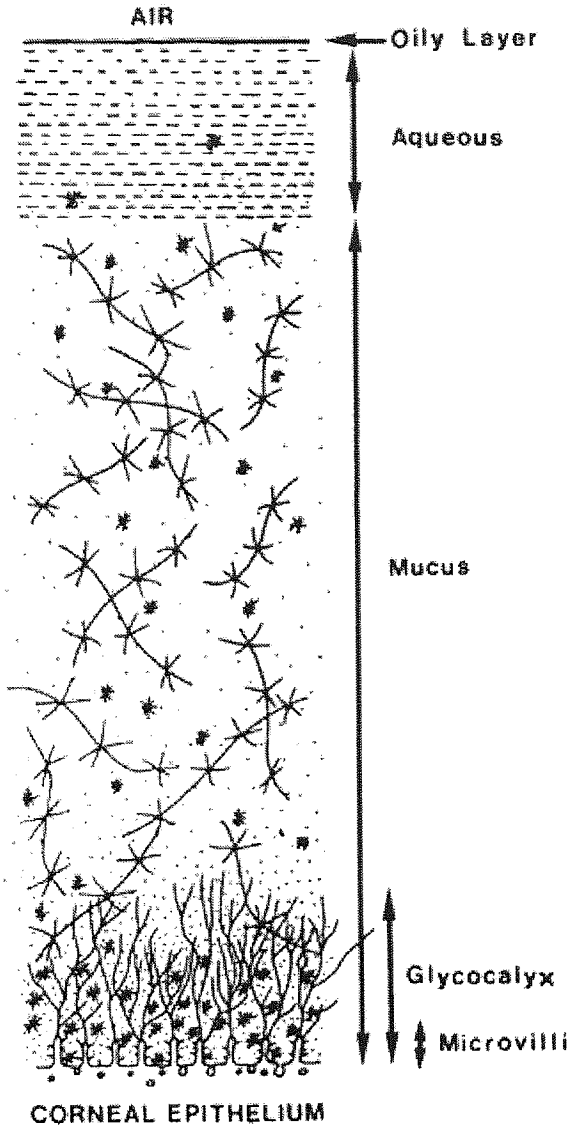

Figure 9. Cross section of the tear film [17]

1.3.4 The Layers of the Tear Film [17]

1.3.4.1 The Lipid layer

The meibomian glands are the main provider of the lipid layer. The functions of lipids in the lid margin are to maintain the lid skin in a hydrophobic state and prevent tear overspill, to resist contamination by sebum and to prevent tears from macerating the skin. The functions of lipids in the precorneal tear film are to spread over the aqueous layer increasing stability, thicken and retard evaporation of the aqueous phase, to supply a

smooth optical surface for the cornea, to act as a barrier against foreign particles, to act as an anti-microbial agent and to seal the lid margin during prolonged closure .

1.3.4.2 The Aqueous layer

The main and accessory lacrimal glands provide the aqueous layer. This layer is quantitatively the most important and provides a route for the delivery of oxygen and removal of epithelial debris. It is also a pathway for many other species.

1.3.4.3 The Mucin layer

The Goblet cells are the main provider of the mucin layer. The mucin layer maintains the glycoocalyx of the ocular surface, providing a hydrophilic surface of the otherwise hydrophilic epithelial cells. The mucin layer also provides the viscoelastic nature of the tear film allowing changes in the shear forces applied to it by the eyelids to be absorbed. Tear lipocalins also play a part in this viscoelastic behaviour.

1.3.5 Lacrimal Functional Unit

The tear film, lacrimal glands, meibomian glands, goblet cells, epithelium (of cornea and conjunctiva) and the eyelids act as a functional unit [22, 23] which operate in anatomical unity and share feedback mechanisms that result in a simultaneous reaction to a single stimulus. This physiologically harmony is sometimes known as the *lacrimal functional unit* and is shown in Figure 10.

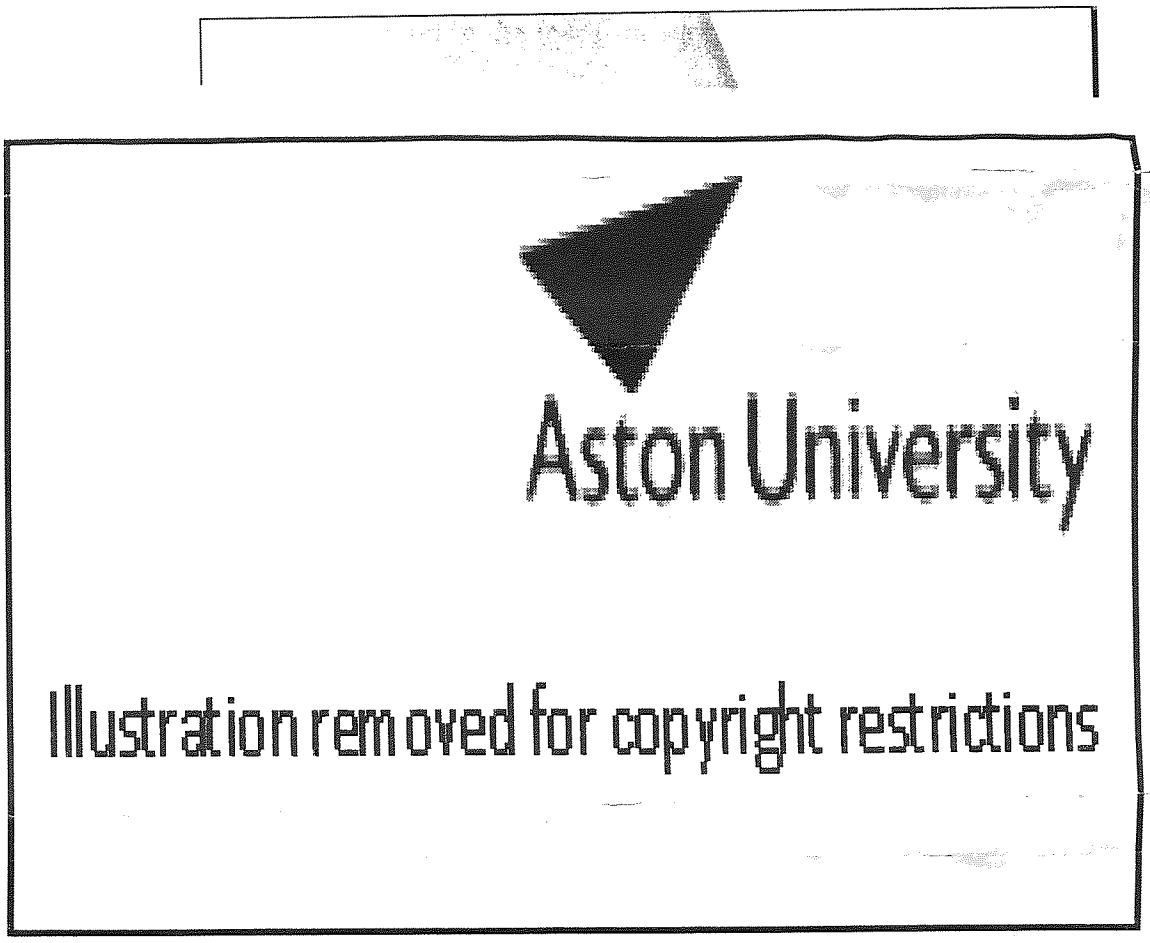

Figure 10. The lacrimal functional unit (Peter Mallen)

1.3.6 Composition of the tear film

Tears are comprised of a complex solution containing water, enzymes, proteins, immunoglobulins, lipids, metabolites and epithelial cells. As the tear film is highly dynamic definition of the exact composition at a point in time is difficult as the content will vary according to the situation.

1.3.6.1 Composition of the aqueous and mucin layer

The aqueous layer of the tear fluid is supplied mainly by the lacrimal glands. The indigenously tear-specific proteins population includes lipocalin, lactoferrin and lysozyme [24, 25]. These proteins are secreted by the lacrimal, Kraus and Wolfring

glands. Some proteins found in the tear film such as albumin and IgG are plasma derived [26, 27]. The number of proteins found in the tear film in the literature ranges from 60 to 491 [28-30] and this number will continue to grow as techniques become more sophisticated. Concentration values quoted for individual proteins in tears vary in the literature partly due to the different sensitivities and requirements of analysis. The mucins are large heavily glycosylated glycoproteins which can be found in the aqueous layer of the tear film; these are prodecued by the goblet cells of the conjunctiva. Another form of ocular mucins is the membrane-associated types which are tethered to the ocular surface and are produced from the epithelium itself.

1.3.6.2 Composition of the lipid layer

The lipid layer is predominately supplied by the meibomian glands. These are holocine and as such secrete the whole contents of the cells onto the surface of the eyelid. The secretion is delivered from the glands to the eyelid surface edges continuously but the action of blinking increases delivery via a pumping mechanism [31]. The meibomian glands are distributed along the edges of the upper and lower eyelids (Figure 11 [32]) shows the anatomy of a meibomian gland in relation to the tear film.

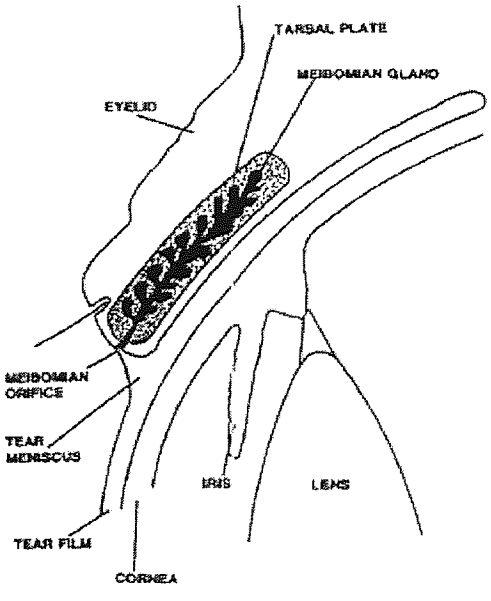

Figure 11. Diagram of the eye and meibomian gland [32]

1.3.7 Composition of lipids in meibomian gland secretions (MGS)

The lipid layer can be divided into two areas for discussion of composition, the polar and the non polar. The polar lipids, especially the phospholipids are of particular interest as they are interfacial lipids forming a bridge between the hydrophobic non polar lipids and the hydrophilic aqueous layer.

The MGS has been studied and Baron and Blough's [33] reported that bovine non polar lipids composed about 97% of the secretion with polar lipids composing the other 3%. In comparison Nicolaides [34] studied human secretions and his work suggested similar composition to that reported by Baron and Blough. The exceptions were that hydrocarbons and diesters were present at 7.5% and 7.7% respectively and the polar lipids were at much higher concentrations at 13.3%.

Stuchell et al [35] also studied human secretions and their analysis showed non polar lipids constituting 44% of the total composition but a composition of free fatty acids of 19% as compared to less than 3% previously reported in the earlier publication. McCulley and Shine [36] summarised their analysis work on human MGS over a thirty year period; they report the composition to be approximately 90% non polar lipids with the polar lipids comprising 8%.

In a comprehensive Tiffany [37] report indicated that compositions which varied with individual subjects and therefore reported ranges for lipid composition. The ranges were 26-38% for hydrocarbons, 13-23% for wax esters, 8-34% for sterol esters, 11-43% for triglycerols, 0-24% for free fatty acids and 0.5% of polar lipids.

The diversity of the literature values for lipid composition is obvious if these figures are presented in Table 4 and Figure 12 [33-37]. The average lipid percentage compositions for meibomian gland secretions from selected authors are hydrocarbons at 10.3%, wax esters at 42.8%, sterol esters at 24.7%, triglycerols at 12.9%, diesters at 2.4%, free sterols at 1.3%, free fatty acids at 9.2% and polar lipids (phospholipids) lipids at 6.1%.

Table 4. Average, normalized, minimum and maximum lipid percentage compositions for meibomian secretion from selected authors

Species	average %	min %	Max %
Hydrocarbons	10.3	1	38
Wax esters	42.8	18	51
Steryl esters	27.8	9.6	38
Triglycerols	12.9	3.7	43
Diesters	2.4	2	7.7
Free sterols	1.3	1.5	2
Free fatty acids	9.2	2.5	24
Polar lipids	6.1	0.5	13.3
Total%	112.7		

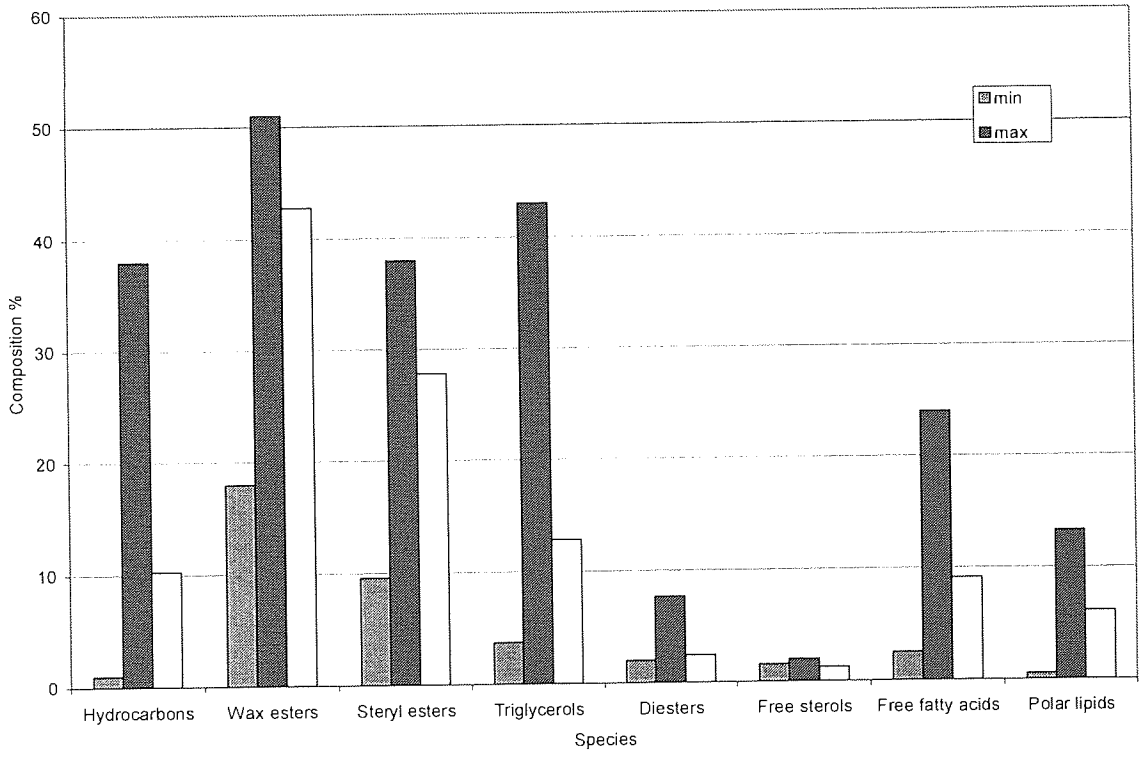

Figure 12. Minimum (blue), maximum (red) and average (yellow) lipid percentage compositions for meibomian secretion

Two significant features arise from comparison of the literature. Firstly the disparity in different authors' values as shown by the maximum and minimum values which in all cases but one (free sterols) differs by significant amounts. The second point is that although the authors agree that the bulk of the MGS is made up of non polar lipids such as wax esters, sterol esters and triglycerols species such as diesters, free sterols, free fatty acids and phospholipids are present in lower concentrations.

Problems associated with comparing the literature relate to the nature and specificity of the analytical techniques and also the use of descriptors for the polar lipid fraction, some authours unambiguously describe the phospholpids component whereas others use terms such as complex or polar lipids. It must be noted that when comparing the analysed data the question of subject to subject variation provides additional difficulty. A further part that is apparent from the literature is that both the method of collection and nature of the collection vessel can have effects on the analysis [32, 38].

1.3.7.1 Phospholipid composition in meibomian gland secretions

Whereas several authors have accepted to classify MGS by means of broad categories relatively little has done been on the detailed sub-classes of the polar lipids. One such study has been carried out by Mculley and Shine [39] wh descibe two types of normal human MGS, those with cholesterol esters and unsaturated ester fatty acids and alcohols (NCP), and those without cholesterol esters and unsaturated ester fatty acids and alcohols (NCA).

The phospholipids of NCA and NCP types and when analysed by Shine and McCulley who found the composition were found to be 38.3% phosphatidylcholine (PC), 7.4% sphingomyelin (SM), 16% phosphatidylethanolamine (PE) and 38.5% unknowns (U) for the NCP type whereas the NCA type had 31.6% PC, 33.4% PE, 18.6% PE and 16.5% U (Figure 13).

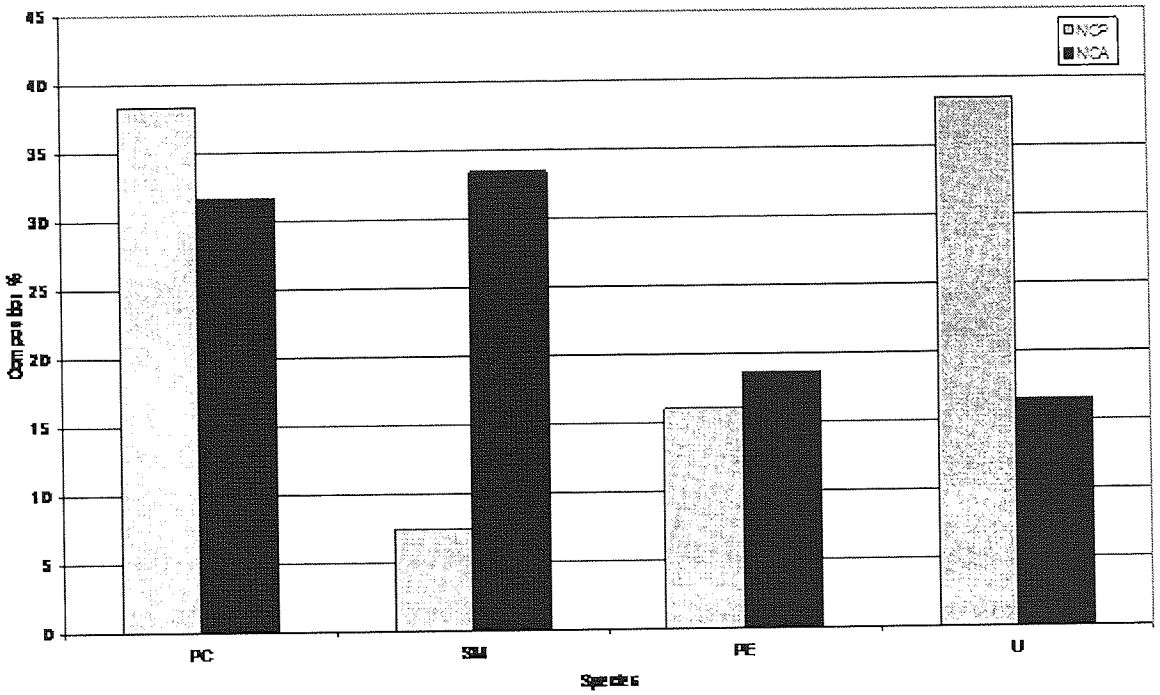

Figure 13. Chart showing the percentage of normal meibomian secretions with cholesterol esters and unsaturated ester fatty acids and alcohols (NCP), and without cholesterol esters and unsaturated ester fatty acids and alcohols (NCA). PC is phosphatidylcholine, SM is sphingomyelin PE is phosphatidylethanolamine and U in unknowns

Noye that these percentages are not of total meibomian lipid content but for the composition of phospholipids which have been described earlier as composing an average of 5.4% of the total lipid in the tear film.

It can be seen between the two groups that the ratios of PC to PE differ relatively little but the ratio of SM to U varies greatly which is an indication of effect of the inclusion of cholesterol esters and unsaturated ester fatty acids and alcohols into the MGS.

Meibomian gland phospholipids from rabbits have been studied by Greiner et al [40] using ^{31}P NMR and the major phospholipids components present were PC at 40%, PE at 18% and SM at 9%, which is similar to the concentrations reported by Shine and McCulley. Several new phospholipids were identified as components of the meibomian fluid including diphosphatidylglycerol (DPG) at 2.5%, dihydrosphingomyelin (DHSM) at 5.3%, phosphatidylsyrine (PS) at 6.9%, lysophosphatidylcholine (LPC) at 1.8%, phosphatidylinisitol (PI) at 4.7%, acylphosphatidylcholine (AAPC) at 4.1% and ethanolamine plasmalogen (EPLAS) at 8.6%, shown in Table 5.

Table 5. Phospholipids in rabbit meibomian gland secretions

%	Species	Abbr.
2.48	diphosphatidylglycerol	DPG
5.33	dihydrosphingomyelin	DHSM
17.79	phosphatidylethanolamine	PE
6.9	phosphatidylsyrine	PS
8.68	sphingomyelin	SM
1.79	lysophosphatidylcholine	LPC
4.73	phosphatidylinisitol	PI
4.08	acylphosphatidylcholine	AAPC
39.64	phosphatidylcholine	PC
8.58	ethanolamine plasmalogen	EPLAS

The fatty acids groups of phospholipids were found to be normal (straight) chains with a narrow range of lengths (C12-C18) and unsaturated in comparison to the non polar lipids which were found to have a greater variety of chain length and unsaturation [39]. The inclusion of LPC into the polar lipids indicates that cleavage of the lipids may be occurring.

1.3.8 Lipids in the tear film

Meibomian secretion is generally acquired directly from the meibomian gland for analysis and as a result the lipids taken directly from the tear film have not been studied in great detail. The composition of the tear film lipids is difficult to access; there are many reasons for this including: the low volume of the tear film, the problems of harvesting, the difficulty of analysing lipids and the dynamic nature of the tear film.

The whole the tear fluid has a volume of 7µl [19] and the lipids compose an average of 3.52µg/µl [31, 41, 42]. Capillary Liquid Chromatography Mass spectrometry (LCMS) can be utilized for overcoming this type of problem [43]. Capillary LC allows small volume analysis as capillary columns have internal diameter (ID) of less than 1mm (typically of 0.5 - 0.3mm) compared to standard chromatographic techniques (1-5mm ID).

The method of collection of lipid from the tear film and subsequent extraction of the lipid from this sample can be problematic. Lipids by their nature are difficult molecules to analyze, collection with glass capillary can cause adherence of lipids to the glass whereas

collection via a sponge method can interfere with detection, components can be extracted from the sponge and interfere with the detection technique [43].

The literature does not present many reports of human tear lipid compositions but Stuchell [35] described the collection of their samples as "lipid analysis of lacrimal secretions collected with capillary pipettes following nasal stimulation". Ham et al also used capillary collection to analyse phospholipids from the tear film, extraction of the lipids was by immobilized metal affinity chromatography (IMAC) prior to matrix assisted laser desorbtion ionization – time of flight (MALDI-TOF) MS with a novel matrix [44, 45]. Stuchell found the composition of phospholipids to be phosphatidic acid, lysophosphatidylcholine and sphingomyelin whereas Ham et al found dimyristoylphopatidylcholine (DMPC) and pyrophosphylated sphingomyelins (PSM).

While the non polar lipids of the tear film remain relatively similar to the composition of non polar lipids in the meibomian gland excretion there is evidence that oxidative degradation occurs [46]. It is the non saturated lipids such as the triglycerides that would be prone to this oxidation and not the saturated phospholipids. There is also evidence that the composition of the phospholipids of the tear film is not the same as that of the meibomian gland excretion [43]. The difference in lipid composition of meibomian gland secretion and tear film can be easily seen in the chromatograms from Gas Chromatography Mass Spectromerty (GCMS) analysis by Nagyova and Tiffany [47].

1.3.9 Interactions of Ocular Lipids

The lipid layer is known to have a retarding effect to the evaporation of the aqueous layer. Therefore any interaction of the lipid layer with anything that is placed in contact with it is of interest, contact lenses for example.

1.4 The Skin (the Dermal Environment)

The interaction of hydrogels with the skin is of interest in this work. These interactions primarily will involve adhesion of the hydrogels to the skin but may also include transcutaneous drug delivery; therefore greater attention will be paid to those parts of the

skin that will have effects upon these interactions. The epidermis is important in adhesion and for transcutaneous drug delivery. Sebum as a skin lipid may have a role in both of these interactions.

1.4.1 Anatomy of the skin

The skin is the largest organ of the body. It is a thin layer which ranges from 0.5mm on the eyelids to 4.0mm on the heels and covers the entire body. It has an area of about $2m^2$ and weighs approximately 4.5-4kg (16% of body weight). The skin consists of two layers the epidermis and dermis with subcutaneous tissue below (Figure 14 [48]).

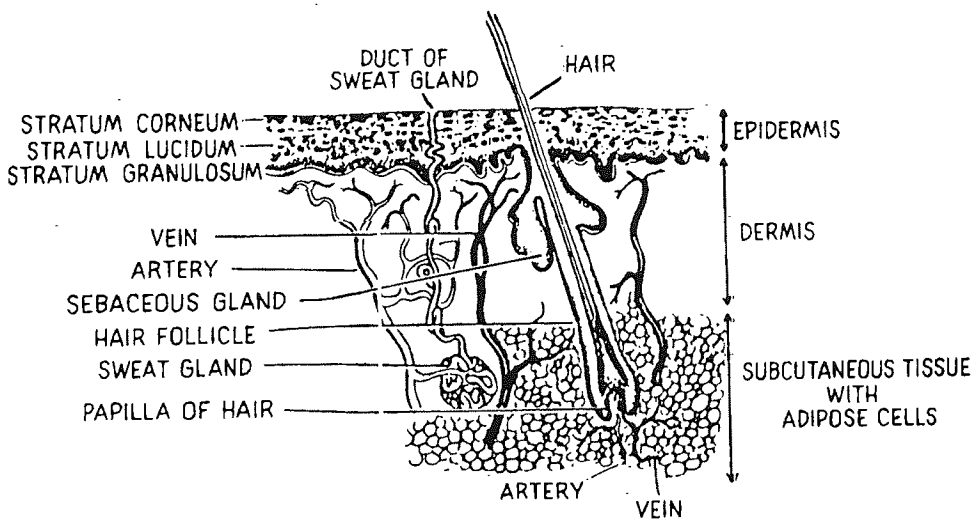

Figure 14. Cross-section of human skin [48]

It is the stratum corneum of the epidermis epidermis that provides the barrier function of the skin. Elias describes the stratum corneum as a "brick and mortar" conformation, where the brick are keratinised coreneocytes and the mortar is a lipid matrix. The composition of the skin has been designed by nature over millions of years to be a very effective barrier. This barrier function of the skin reduces the passage of water both ways and also stops many other biological species altogether.

1.4.2 Epidermal Lipids

The epidermal lipids are part of the skin's structure and found in the matrix of the stratum corneum. They are produced by a process known as differentiation. This leaves a continuous phase of a liquid crystalline nature that is hydrophobic and acts as the main barrier for the transport of water into and out of the body, it also acts as a barrier against the transportation of other species.

1.4.3 Composition of Epidermal Skin Lipids

The composition of epidermal lipids is unique amongst membranes as the percentage of phospholipids present is low. The composition of epidermal lipids differ as they undergo differentiation and progress through the strata of the epidermis as shown in Figure 15 [49] for a sample of abdominal skin.

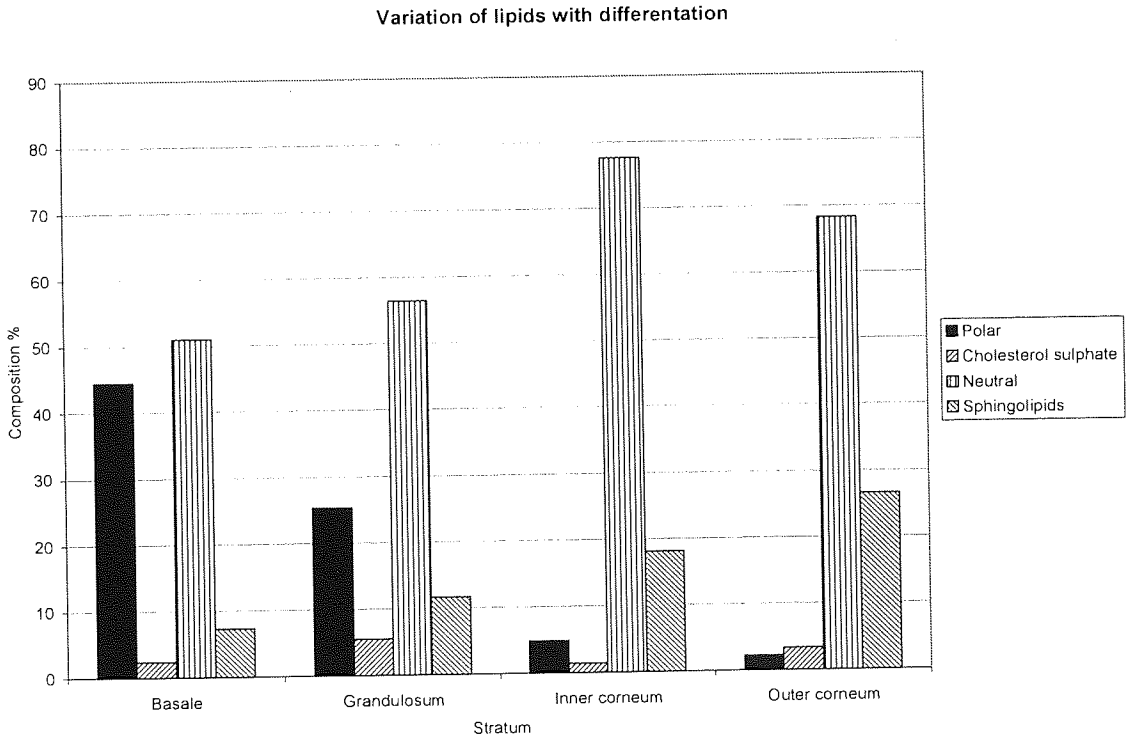

Figure 15. Variation of skin lipids with differentiation

Lampe et al [49] showed the polar lipids start as a high weight percentage (by weight) of the total present and this reduces as progression through the strata of the epidermis is

followed. While the non polar lipids start with a similar weight percentage of the total as the polar lipids, this percentage rises with progression through the strata, the sphingolipids weight percentage also rises with migration through the epidermis. This compositional change of lipids with migration through the epidermis is also reported by Elias and Menon and Yardley [50, 51].

More recently the composition of the lipids in the epidermis has been reported as 50% ceramides [52-54]; the ceramides unaccounted for were attached to the corneocyte envelope as the Bligh-Dyer [55] extraction technique did not remove them. Ceramides are shingolipids that are composed of fatty acids linked by an amide bond to a long-chain base; the long chain base is sphingosine to which the fatty acids are N-acylated.

1.4.4 Sebaceous Lipids (Sebum)

Sebum is another unique substance in compositional terms as it has a huge variety in its fatty acids chains [54, 56, 57]. Sebum is derived from sebaceous glands within the skin and is delivered directly to the skins surface. The fact that sebum constitutes a surface layer of lipids is the reason for the separate explanation.

1.4.5 Composition of Sebum

The composition of sebum changes during its progression through the sebaceous glands as lipases act upon it. The composition of sebum prior to the action of the lipases on the triacyl glycerols to produce free fatty acids has been reported by Downing and Strauss and Stewart et al [58, 59] as 12.8% squalene, 22.5% wax esters, 60.3% triacyl glycerol, 0.6% free fatty acids, 2.5% cholesterol esters, 1.3% cholesterol and 3% phospholipids (Figure 16 [58, 59]).

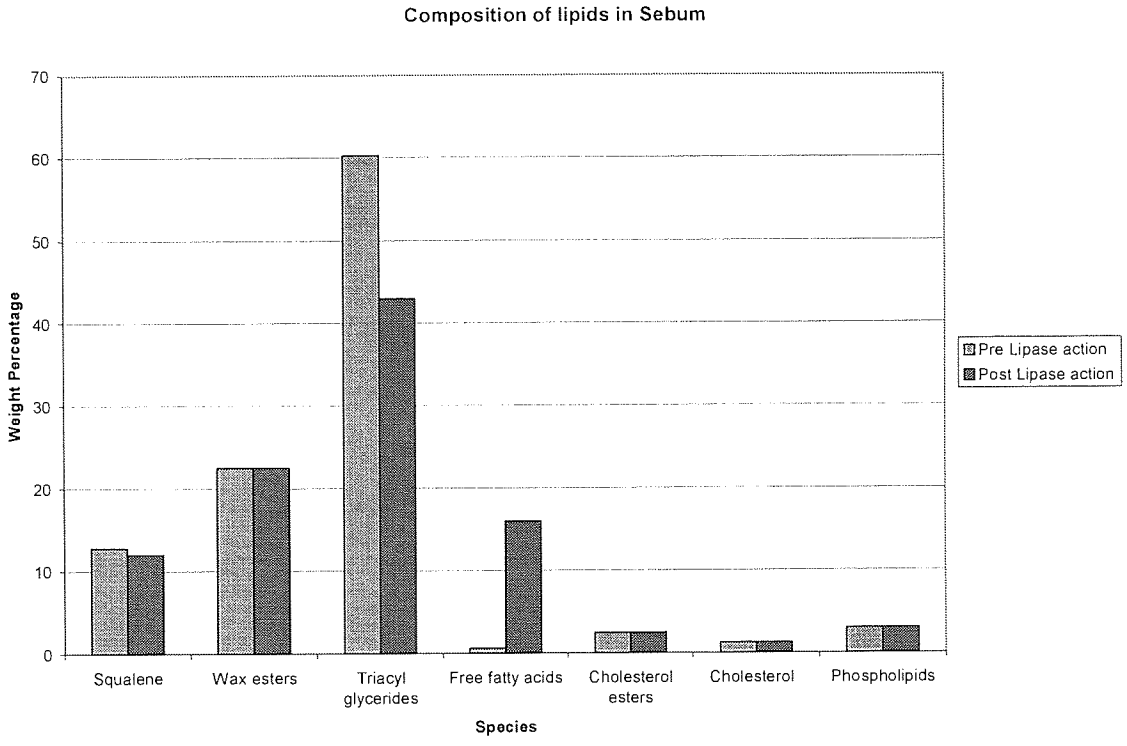

Figure 16. Composition of lipids in sebum prior to and after lipase action

After exposure to lipases the triacyl glycerols are hydrolysed to produce free fatty acids and the composition of sebum shifts to have 12% squalene, 22.5% wax esters, 43% triacyl glycerol, 16% free fatty acids, 2.5% cholesterol esters, 1.3% cholesterol and 3% phospholipids (Figure 16).

1.4.6 Oily skin and pressure sensitive adhesives (PSAs)

PSAs were discussed in section 1.1.5.3. There is some synthetic work in this thesis concerned with the designed of PSAs for use with oily skin and so a brief description of the problem of oily skin follows.

Oily skin is the term used when there is an excess of sebum on the skins surface and it is caused by the overproduction of sebum. Sebum is produced by the sebaceous glands which cover the majority of the skins surface. Sebum production is controlled by the activity of the androgen hormone on the sebaceous glands [60-62]. It is the concentration of dihydrotestosterone, a metabolite of testosterone that is thought to induce or inhibit sebum production [63].

The lipids on the skin interfere with the adhesion of the PSAs as they disrupt the bonding process. They do this in part by producing a thin film between the adhesive and the substrate. The surface free energy of the skins surface also plays a part as adhesives will only adhere to surfaces that have a higher surface energy level than the adherent.

Contact angle studies of the skin have reported the surface free energy to be between 38-56 mN/m [64, 65]. The removal of surface lipids (sebum) from the skin lowers the surface energy [65, 66], a value 32.9mN/m has been reported also using contact angle measurements. With the increased in sebum that oily skin brings the surface free energy would also increase. This is seen when comparing body sites in normal skin with the forehead having a higher surface free energy than the forearm where there are more sebaceous glands and higher expressions of lipids [56, 66].

1.4.7 Interactions of Skin Lipids

The composition of skin lipids is one of hydrophobic character which has a bearing on any adhesives that may be placed onto it, hydrogel skin adhesives for example. Therefore an understanding of its structure and interactions it has with adhesives will allow better design of materials.

Chapter 2 – Methods and Materials

"There are many methods for predicting the future. For example, you can read horoscopes, tea leaves, tarot cards, or crystal balls. Collectively, these methods are known as "nutty methods"

Scott Adams

Ethical declaration

The work contained in this thesis was conducted according to the Declaration of Helsinke and the research was approved by the human sciences research committee of Aston University. Where subjects were enrolled informed consent was given.

2.1 Reagents

The crosslinkers and initiators used are listed in Table 6. The monomers used in the synthesis of membranes are listed in Table 7. The monomers used in the synthesis of gels are listed in Table 8.

Table 6. Crosslinkers and initiators

Reagent	Abbreviation	M_r	Supplier
1-hydroxycyclohexyl phenyl ketone	Irgacure 184	204.3	Ciba
azo-iso-butyronitrile	AZBN	164.2	BDH
ethylene glycol dimethacrylate	EGDMA	242.3	Sigma
polyethylene glycol diacrylate	Ebacryl II		U.C.B.

Table 7. Monomers used in the synthesis of membranes

Reagent	Abbreviation	M_r	Supplier
2- hydroxyethyl methacrylate *	HEMA	130.1	Cognis Performance
2-(acrylamido-2-methyl propane sulphonate acid	AMPS	207.2	Lubrizol
2-(diethylamino) ethyl acrylate	-	171.2	Sigma
2-(diethylamino) ethyl methacrylate	-	185.3	Sigma
2-(dimethylamino) ethyl acrylate	-	143.2	Sigma
2-(dimethylamino) ethyl methacrylate	DMAEMA	157.2	Sigma
2-(dimethylamino) ethyl methacrylate dimethyl sulfate	-	283.4	Sigma
2-ethynyl-1--(3-sulfopropyl) inner salt	SPV	227.1	Raschig
2-methacryloyloxyethyl phosphorylcholine	MPC		
3-(dimethylamino) propyl acrylate	-	157.2	Sigma
3-(dimethylamino) propyl methacrylamide	DMAPMA	170.26	Sigma
3-(dimethylamino) propyl methacrylamide methyl chloride	-	206.7	Sigma
acryloylmorpholine	AMO	141.2	Sigma
N,N-dimethyl-N-(2-acryloylethyl)-N-(3-sulfopropyl) ammonium betaine	SPDA		Raschig
N,N-dimethyl-N-(2-methacrylamidopropyl)-N-(3-sulfopropyl) ammonium betaine	SPP	292.1	Raschig

Table 8. Monomers used in the synthesis of gels

Reagent	Abbreviation	M_r	Supplier
2-(acrylamido-2-methyl propane sulphonate sodium salt	NaAMPS	229.2	Lubrizol
acrylic acid-bis-(3-sulfopropyl)-ester, potassium salt	SPA	232.3	Raschig
N,N-dimethyl-N-(2-acryloylethyl)-N-(3-sulfopropyl) ammonium betaine	SPDA		Raschig
N-vinyl pyrrolidone	NVP	111.1	Vickers Laboratories

The structures of the crosslinkers and initiators used are shown in Figure 17. The structures of monomers used in the synthesis of membranes is shown in Figure 18. The structures of monomers used in the synthesis of gels is shown in Figure 19.

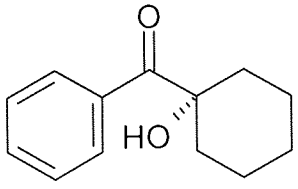

Irgacure 184 (1-hydroxycyclohexyl phenyl ketone)

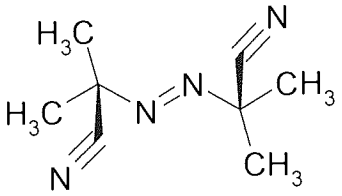

azo-iso-butyronitrile

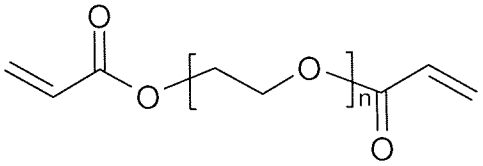

Ebacryl 11 (a poly(ethyllene glycol) diacrylate, where n = 2 to 4)

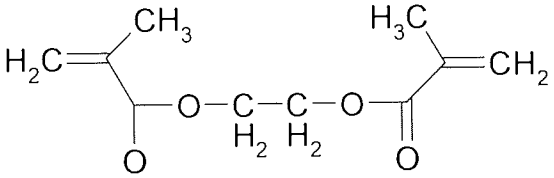

ethylene glycol dimethacrylate

Figure 17. The structures of crosslinkers, initiators and monomers

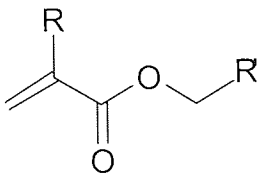

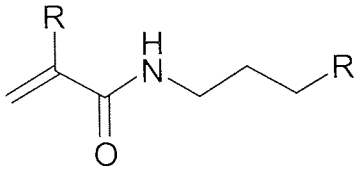

Where		
DMA EMA	$R = CH_3$	$R' = -CH_2N(CH_3)_2$
DMA EMA.DMSO	$R = CH_3$	$R' = -CH_2N^+(CH_3)_3$
DEA EMA	$R = CH_3$	$R' = -CH_2N(CH_2CH_3)_2$
DMA EA	$R = H$	$R' = -CH_2N(CH_3)_2$
DEA EA	$R = H$	$R' = -CH_2N(CH_2CH_3)_2$
DMA PA	$R = H$	$R' = -CH_2CH_2N(CH_3)_2$

Where	
NDMA PMAA	$R = -N(CH_3)_2$
NDMA PMAA.MeCl	$R = -N^+(CH_3)_3$

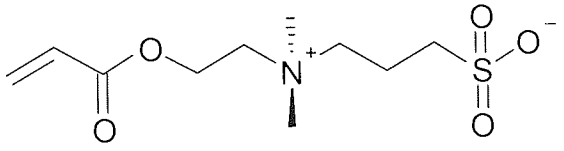

N,N-dimethyl-N-(2-acryloylethyl)-N-(3-sulfopropyl) ammonium betaine (SPDA)

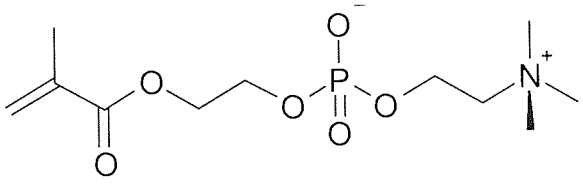

2-methacryloyloxyethyl phosphorylcholine (MPC)

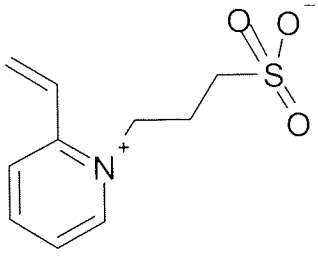

1-(3-Sulfopropyl)-2-vinylpyridinium-betaine (SPV)

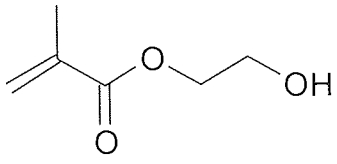

2-hydroxyethyl methacrylate

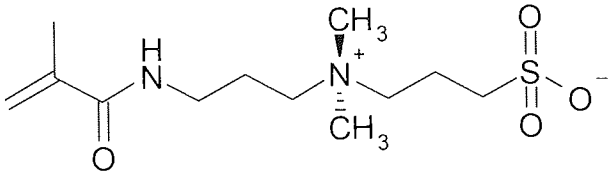

N,N-dimethyl-N-(2-methacrylamidopropyl)-N-(3-sulfopropyl) ammonium betaine (SPP)

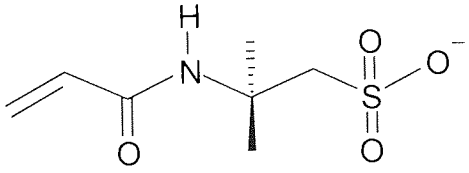

2-acrylamido-2-methyl propane sulfonic acid sodium salt (AMPS)

Figure 18. The structures of monomers used in membrane synthesis

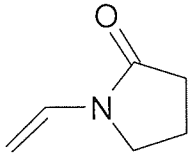

N-vinyl pyrrolidone

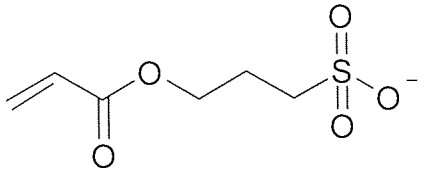

3-sulfopropyl ester acrylate (SPA)

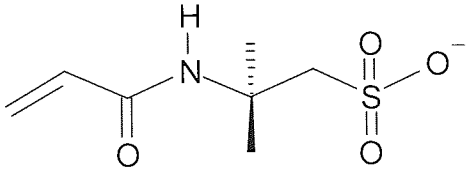

2-acrylamido-2-methyl propane sulfonic acid sodium salt (AMPS)

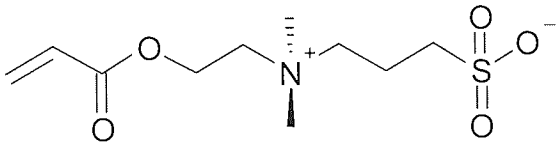

N,N-dimethyl-N-(2-acryloylethyl)-N-(3-sulfopropyl) ammonium betaine (SPDA)

Figure 19. The structures of monomers used in gel synthesis

All other reagents and materials are listed in Table 9.

Table 9. Other reagents and materials

Reagents	Abbreviation	M_r	Supplier
1,2,3-propanetriol	Glycerol	92.1	Sigma
acetonitrile	MeCN	41.1	Fisher
agarose	-	-	Sigma
ammonium formate	-	63.1	Sigma
Amplex® Red Phosphatidylcholine-Specific Phospholipase C Assay Kit	-	-	Molecular probes
antibody rabbit anti human phospholipase C	αPLC	-	abcam
boric acid	-	61.8	BDH
butylated hydroxyl toluene	BHT	220.4	Sigma
chloroform	$ChCL_3$	119.4	Fisher
cholesterol	Ch	386.7	Sigma
cholesterol myristate	ChMy	597.0	Sigma
cholesterol palmitate	ChPal	625.1	Sigma
Coomassie Brilliant Blue	-	826.0	BDH
diethyl ether	-	74.1	Fisher
diidomethane	-	267.8	Fisher
dilauroylphosphatidylcholine	DLPC	621.8	Sigma
dimyristoylphosphatidylcholine	DMPC	677.9	Sigma
dipalmitin	DAG	568.8	Sigma
dipalmitoylphosphatidylcholine	DPPC	734.0	Sigma
dipalmitoylphosphatidylethanolamine	DPPE	579.5	Sigma
ethylenediamine tetraacetic acid	EDTA	292.2	Sigma
glacial acetic acid	-	60.0	Fisher
hexane	-	86.2	Fisher
HPLC water	-	18	Fisher
immunoglobulin A	IgA	-	Sigma
iodine	I_2	253.8	Sigma
isopropanol	-	60.0	Fisher
lauric acid	-	200.3	Sigma
methanol	MeOH	32.0	Fisher
molybdenum	-	95.9	Sigma
molybdic anhydride	-	143.9	Sigma
nitrogen	N_2	28	
palmitic acid	-	256.4	Sigma
phosphate buffered saline	PBS	-	Sigma
sphingomyelin	SM	731.1	Sigma
stearic acid	-	284.5	Sigma
sulphuric acid	-	98.1	Fisher
tripalmitin	TAG	807.3	Sigma
Tris	Tris		Sigma

2.2 Collection of tear samples

Tear samples were collected using either glass capillaries or ophthalmic sponges. Non stimulated tear samples were taken whenever possible. The microcapillary (microcapillary pipettes, positive displacement, 1-5µl, P6679-1PAK, Sigma-Aldrich) was used to collect 5µl of tears taken from the meniscus of the inferior fornix (Figure 20).

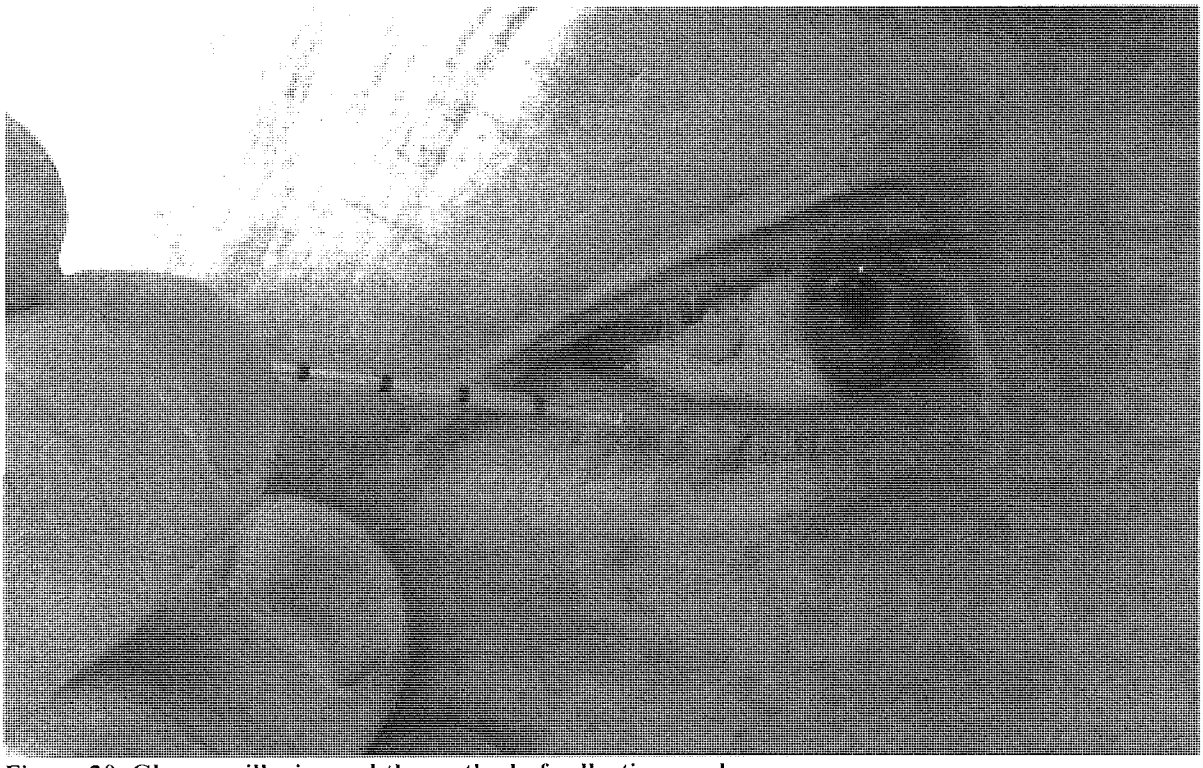

Figure 20. Glass capillaries and the method of collection used

The ophthalmic sponge was used in a similar way to the glass capillary but the whole of tear film would be collected onto the sponge. The ophthalmic sponges (BD Visitec, BD Visispear™ eye sponge, 7cm, 581089, BD Ophthalmic systems, FL, USA) (Figure 21).

Figure 21. Ophthalmic sponges (BD visitec, BD visispear™ eye sponge, 7cm, 581089, BD Ophthalmic systems, FL, USA)

After the samples were collected they were placed into 2ml vials and immediately frozen with liquid nitrogen. The vials containing the samples were then transferred to a -80°C freezer where they were stored until required for analysis.

2.3 Extraction of lipids from the tear film samples

The lipids of the tear film need to be separated from the other species present before they can be analysed. Different methods of extraction were tried as described below.

2.3.1 Methanol chloroform

Samples were removed from the -80°C storage and kept over ice. Stainless steel tweezers were used to remove the capillary tubes or sponges containing the samples from the 2ml vial. The samples were placed into 10ml glass vials with 5ml of methanol:chloroform (1:1). The sample was extracted for a given time with shaking, with or without having an atmosphere of nitrogen. The use of nitrogen at this point depended on the length of the extraction, for example if the extraction was overnight then nitrogen would not be used.

After the extraction step stainless steel tweezers were used to remove the glass capillary or sponge from the vial. The samples in the 5ml vial were then evaporated with nitrogen.

The samples were then re-suspended in 250µl of methanol:chloroform (1:1) and transferred to a 2ml vial, a further 250 µl of methanol:chloroform (1:1) was used to wash out the standard sample vial into the 2ml vial. The vial was capped ensuring there was an atmosphere of nitrogen. The samples were dried under a nitrogen atmosphere and resusped in solvents suitable for the analysis technique.The samples were now ready for analysis by Thin Layer Chromatography (TLC) or High Performance Liquid Chromatography (HPLC). If not analysed immediately the samples were stored at -80°C until ready to use.

2.3.2 Methanol

Samples were removed from the -80°C storage and kept over ice. Stainless steel tweezers were used to remove the capillary tubes or sponges containing the samples from the 2ml vial. The samples were placed into 20ml glass vials with 5ml of methanol. The sample was extracted for a given time with shaking, with or without having an atmosphere of nitrogen. The samples were left for extraction of times varying between 30 minutes to overnight. The capillary tubes or sponges were removed after extraction and the samples were dried under a nitrogen atmosphere and resuspended in solvents suitable for the analysis technique. The samples were now ready for analysis by TLC or HPLC. If not analysed immediately the samples were stored at -80°C until ready to use.

2.3.3 Modified Bligh and Dyer

This is a modified Bligh and Dyer method [67]. All glassware was chilled in a fridge and then kept over ice while being used. All Pyrex tubes were kept closed whenever possible. Samples were removed from the -80°C storage and kept over ice. Stainless steel tweezers were used to remove the capillary tubes or sponges containing the samples from the 2ml vial. The sample was placed into a Pyrex tube. 1ml of chilled phosphate buffered saline and 1ml of 0.15M acetic acid was added to the sample. 3.75ml of chloroform:methanol (1:2) was added to the sample. This mixture was inverted ad shaken for 1 minute. The mixture was then transferred to a second chilled Pryex tube. 3.75ml of chloroform:methanol (1:2) was added to the first Pyrex tube which was inverted and shaken for 1 minute and then transferred to the second Pyrex tube.

2.25ml of chloroform was added to the first Pyrex tube which was inverted and shaken for 1 minute and then transferred to the second Pyrex tube. 2.25ml of water was added to the first Pyrex tube which was inverted and shaken for 1 minute and then transferred to the second Pyrex tube. The mixture in the second Pyrex tube was inverted and shaken for 1 minute and the left to phase separate. The lower phase was pipetted off to a third Pyrex tube avoiding the carry over of the upper phase.

The chloroform in the third Pyrex tube was taken down to dryness on a drying block set to 80°C with nitrogen atmosphere. 0.5ml of chloroform was used to wash Pyrex tube 3 into an amber 2 ml vial. Pyrex tube 3 was washed with a further 0.5ml of chloroform twice into the amber vial.

The ~1.5ml of chloroform was then taken down to dryness on a drying block set to 80°C with an atmosphere of nitrogen. It was capped and placed on ice for 1 minute. 50 µl of chloroform was used to rinse the residue off the sides of the amber vial. The same 50 µl of chloroform was used to rimes the sides of the vial 3 times. The amber vial was capped ensuring there was an atmosphere of nitrogen. The samples were now ready for analysis by TLC or HPLC. If not analysed immediately the sample was stored at -80°C until ready to use.

2.4 *Chromatography*

The theory of chromatography is explained in the Appendix II - Chromatography.

2.4.1 High Performance Liquid Chromatography (HPLC)

The method used for HPLC is described in Chapter 3. This section describes the HPLC system employed for this work. The system used was an Agilent 1100 Series LC consisting of the following modules: G1376A Capillary Pump, G1389A Autosampler, G1330A Thermostatted Autosampler, G1315A Diode Array Dectector (DAD), G1321A Fluorescence Detector (FLD), G1379A Vacuum Degasser and G1316A Column Compartment (COLCOM) (Figure 22).

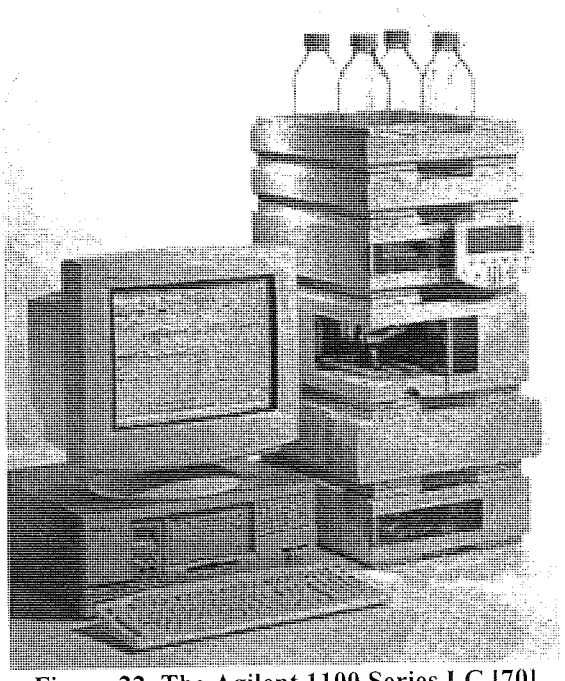

Figure 22. The Agilent 1100 Series LC [70]

The Agilent 1100 Series LC has a capillary capability which allows columns with internal diameter (ID) of less than 1mm typically of 0.5 - 0.3mm. This allows for lower volumes and concentration of sample to be introduced at lower flow rates when compared to standard chromatographic techniques, which typically have 1-5mm ID. The capillary columns allow increased system sensitivity due to decreased band broadening. An additional benefit is the low flow rates associated with capillary LC allowing for easier interfacing of LC to other detection systems such as mass spectrometry to produce Liquid Chromatography Mass Spectrometry (LCMS) techniques. Table 10 shows the ID of standard and capillary columns along with flow rates.

Table 10. Dynamic range of optimum flow rates for columns of different internal diameter

Column id [mm]	Capillary id [µm]	Flow rate [µl/min]
4.6		1000
2.1		200
1.0		50
-	800	20
-	500	8
-	180	2
-	75	0.2

2.4.2 Thin Layer Chromatograhy (TLC)

2.4.3 TLC method

The TLC plates were silica plates (Merck Silica gel 60, 20x20cm) were used for the TLC method. The mobile phase was made up fresh on the day it was to be used. Gloves were used to handle TLC plates to avoid contamination. The samples were removed from the fridge and kept over ice. The TLC plate was activated for ~15min at 80°C.

After activation of the plate a pencil was used to draw line of origin on the plate 2.5cm from bottom of the plate. The ruler was clean and only light pressure was used to avoid damaging the silica on the plate. The plate was marked for standards and samples at about 2cm apart on the origin line. The mobile phase being used (either polar or non polar, see section 2.4.4) was added to the trough.

7µl of standards and 25µl of sample were applied to plate. The samples were allowed to dry and then the plate was placed into the trough. The solvent front allowed was to run to near the top of the plate. The plate was removed and the solvent front was marked. The plate was dried and then stained for visualisation (see section 2.4.5).

2.4.4 Mobile phases used in TLC

Mobile phases used in this work were chloroform:methanol:acetic acid:water (170:30:20:7) for polar separations (note that solvents should be clear after they are made up) and hexane:diethyl ether:glacial acetic acid (70:30:1) for non polar separations [67].

2.4.5 Stains used in TLC

2.4.5.1 Iodine staining

20g of iodine was placed into a glass trough and allowed to sublime. Gloves were used to handle TLC plates to avoid contamination. The silica plate was then placed into the

trough and the iodine stains were allowed to develop [68]. The plate was removed and photographed. Air drying or oven drying will remove iodine staining.

2.4.5.2 Dittmer's staining solution

Dittmer's solution [69] is a sensitive spray reagent for phospholipids for use on TLC plates. Solution 1 was prepared by making up 8g of molybdic anhydride in 200ml of a 70% solution of sulphuric acid. This mixture was gentle boiled with stirring until a solution was obtained. Solution 2 was prepared by adding 0.4g of powdered molybdenum to 100ml of solution 1 and boiling for 1 hour before being cooled to room temperature. The solution is decanted from any residue that may be present.

Solution 3 was prepared by mixing solution 1 and 2 in equal volumes with two volumes of water. Finally for use with silica plates one volume of solution 3 is diluted with three equal volumes of glacial acetic acid.

Dittmer's solution is sprayed over the TLC plate and then left to dry. The phospholipids should stain a deep blue colour within minutes of the Dittmer's solution application.

2.5 Counter Immunoelectrophoresis (CIE)

2.5.1 Agarose/PEG8000 gels for the CIE analysis

The CIE method is explained in section 4.3.2. Agarose/PEG8000 gels were used for the CIE analysis which were synthesised from 1.2g agarose (Sigma A-0576) and 3g of polyethylene glycol 8000 (PEG8000, Sigma P-2139) diluted in 50mls of Tris-Borate-EDTA (TBE) buffer and 50ml of distilled water. TBE buffer is made up from 21.8g Tris, 11g Boric acid (BDH 10058), 1.86g EDTA (Sigma ED-2SS) made up to 1 litre with distilled water. This gel mixture was poured onto a melinex sheet measuring 7.6x7.6mm.

2.5.2 Coomassie Brilliant Blue stain

Coomassie Brilliant Blue stain is made up from 90mls methanol, 90mls distilled water, 10mls glacial acetic acid and 1.2g Coomassie Brilliant Blue (BDH 44329) and destain is made up from 30mls methanol, 80mls distilled water and 10mls glacial acetic acid.

2.6 Mass Spectrometry (MS)

2.6.1 Introduction to MS

The unit used for mass/charge (m/z) is equivalent the symbol Th, the Thompson. The MS used for this work was an Agilent 1100 Series LC/MSN (SL) Ion Trap equipped with electrospray ionization (ESI) interface. The Ion Trap MS and the ESI interface are explained in more detail elsewhere, briefly Ion Trap MS offers an alternative detection system that allows some chromatographic problems to be overcome and ESI allows HPLC system employed to deliver chromatographically resolved species into the MS. ESI acts as an interface between the HPLC and MS transforming the liquid phase which can not be detected by MS into a gas phase which may be detected by MS.

2.6.2 MS Sample Inlet

The Agilent 1100 Series LC/MSN (SL) Ion Trap has several choices for sample inlet and those available for this work were Liquid Chromatography (LC) or direct infusion.

2.6.2.1 LC Inlet

The LC sample inlet utilizes the Agilent 1100 Series LC at flow rates of 10–1000 µl/min, with a possible maximum of 5000 µl/min if LC is in non capillary mode. The LC sample inlet allows chromatographic separation of sample and inline detection with ultraviolet (DAD) and/or fluorescence (FLD) before it enters the MS. With this type of inlet we have a Liquid Chromatography Mass Spectrometry (LCMS) system.

2.6.2.2 Direct Infusion (DI)

The DI sample inlet employs a Kd Scientific Model 100 Series Syringe Pump shown in Figure 23 [70]. The syringe pump allows direct infusion of sample at flow rate of 1-10 µl/min, but flow rates can vary depending on the syringe size used. When employing DI there is no chromatographic separation of the species and MS detection is used. DI experiments used in this work had a flow rate of 0.3ml/hour (0.005ml/min).

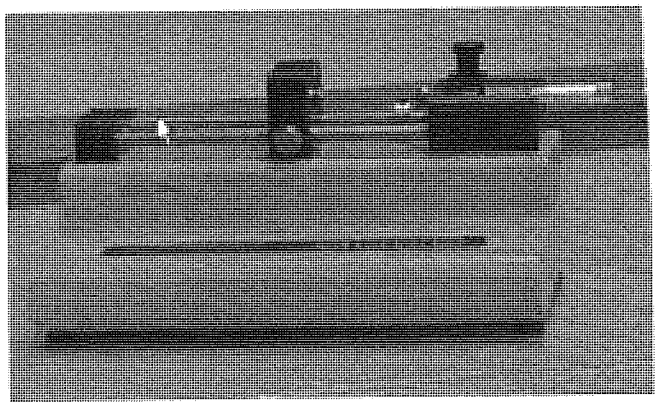

Figure 23. Kd Sceintific Model 100 Series Syringe Pump [70]

2.6.3 MS Parameters

The Agilent 1100 Series LC/MSN (SL) Ion Trap like any MS is a complicated instrument and has many parameters that can be controlled. This instrumental control is beyond the scope of this thesis but some of the more important parameters are Ion Charge Control (ICC), Smart Parameter Settings (SPS), capillary voltage, drying gas temperature and flow, nebulizer pressure and Smart Frag.

2.7 *Liquid Chromatography Mass Spectrometry (LCMS)*

2.7.1 LCMS System employed

The Agilent 1100 Series LC/MSD (SL) was used for this work. It is a complete LCMS system and is shown in Figure 24. This figure illustrates the different modules of the system. The Agilent 1100 Series HPLC (3), LC/MSD (SL) MS module (1) and the ESI interface (2) are described elsewhere.

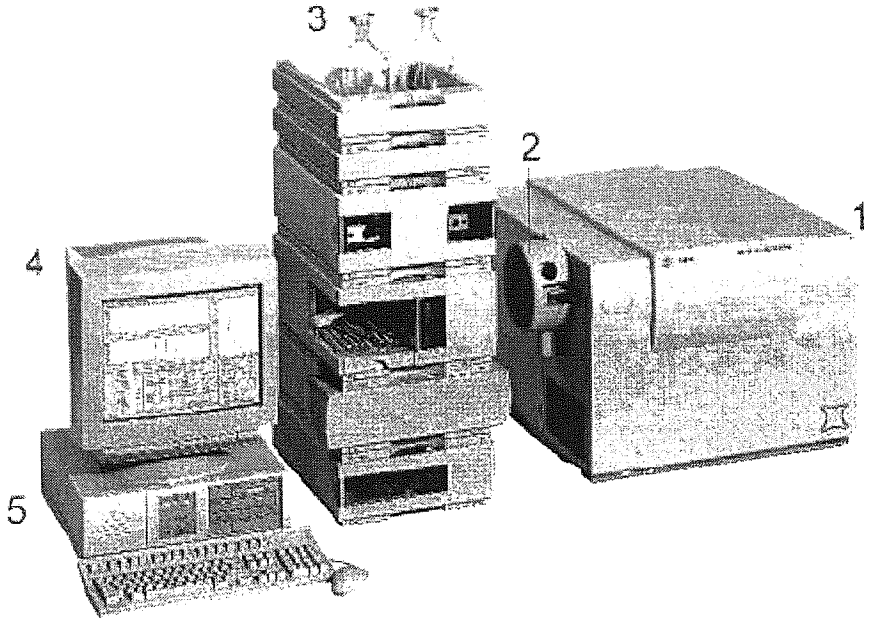

Figure 24. Agilent 1100 Series LC/MSD. The mass spectrometer (1) with its interface (2), the Agilent 1100 LC (3), monitor (4) and PC (5) [70]

2.7.2 Nature of data from MS - Total Ion Chromatogram (TIC), Extracted Ion Chromatogram (EIC) and Compound Mass Spectra (CMS)

2.7.2.1 Total Ion Chromatogram (TIC)

During a chromatographic separation the Mass Spectrometer is set to scan repetitively and continuously over a mass range. At the end of each scan a spectrum is stored and the

sum of the intensities of ions present is calculated and stored. This is the Total Ion Chromatogram (TIC) and it is the primary data from which all analysis is performed.

The TIC shows the variation with time of the total number of ions being detected by the MS. An example of a TIC of four phospholipids species separated by High Perfomance Liquid Chromatography is shown in Figure 25. At any point in time across the time the TIC we can extract a mass spectrum as shown in Figure 26 where at 4.9 minutes a mass spectrum was extracted from the total ion chromatogram. This shows the mass of 622.5 Th which is the mass of dilauroylphosphatidylcholine plus 1 amu.

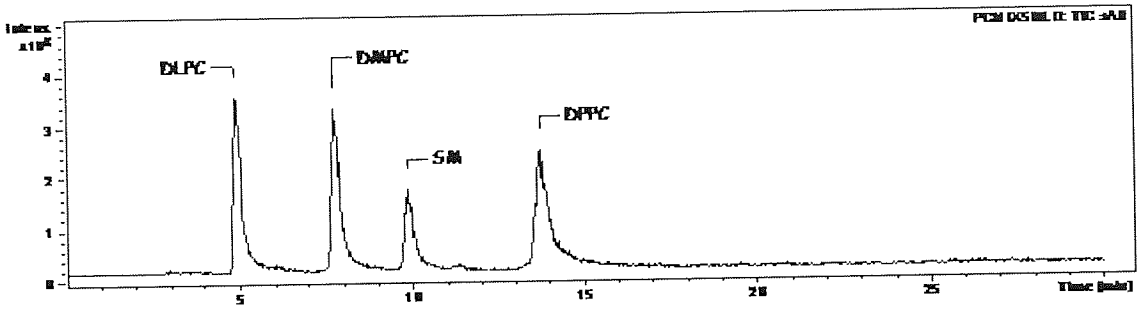

Figure 25. An example of a Total Ion Chromatogram (TIC) of sphingomyelin (SM), dilauroylphosphatidylcholine (DLPC), dimyristoylphosphatidylcholine (DMPC) and dipalmitoylphosphatidylcholine (DPPC).

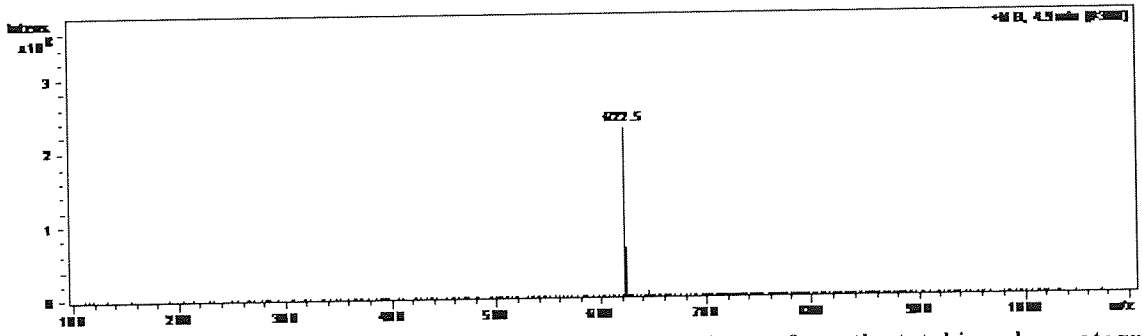

Figure 26. An example of a mass spectrum for the time 4.9minutes from the total ion chromatogram (TIC)

2.7.2.2 Extracted Ion Chromatogram (EIC)

An Extracted Ion Chromatogram (EIC) is data extracted from a TIC, an example is shown in Figure 27 where the positive ion of 622.5 Th has been extracted from the TIC in Figure 25. They show the variation with time of a single ion and are also known as Reconstructed Ion chromatograms (RIC). EIC can be based on mass or charge.

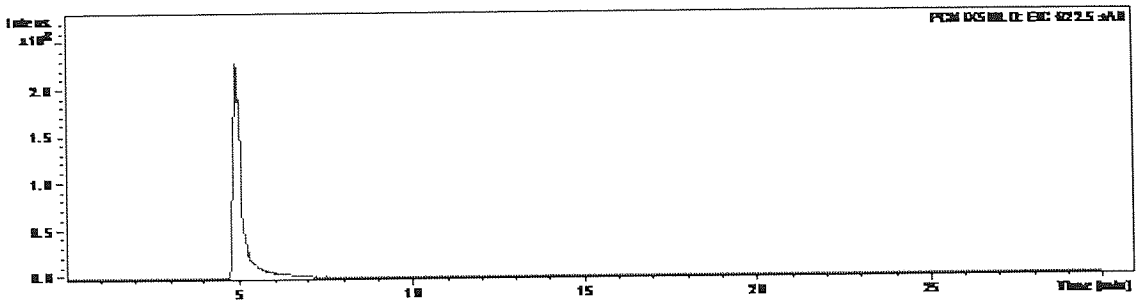

Figure 27. An example of a Extracted Ion Chromatogram (EIC) of ion 622.5 Th from the TIC

2.7.2.3 Compound Mass Spectra (CMS)

The Compound Mass Spectra (CMS) is used to display the mass spectra that are contained in the selected chromatogram analysis whose name is indicated. For example if we want the mass spectral data for a specified section of Figure 25 as indicated by the box at around 5 minutes in Figure 28. That data may be extracted and presented as shown in Figure 29; this is the CMS of 4.5-6.7 minutes of the TIC in Figure 25.

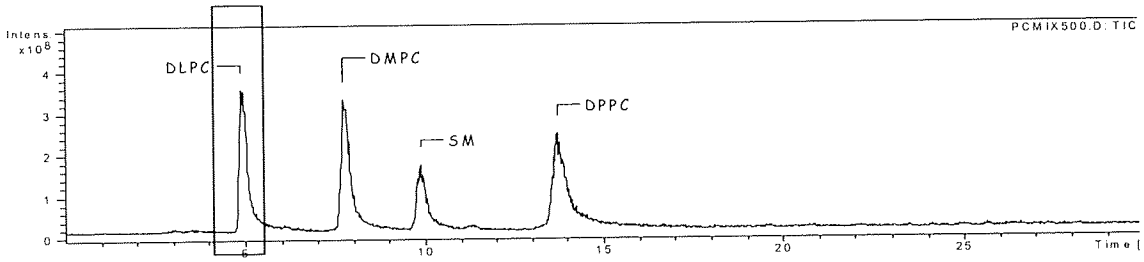

Figure 28. An example of a TIC with a section showing the data to be extracted from the TIC to produce a CMS

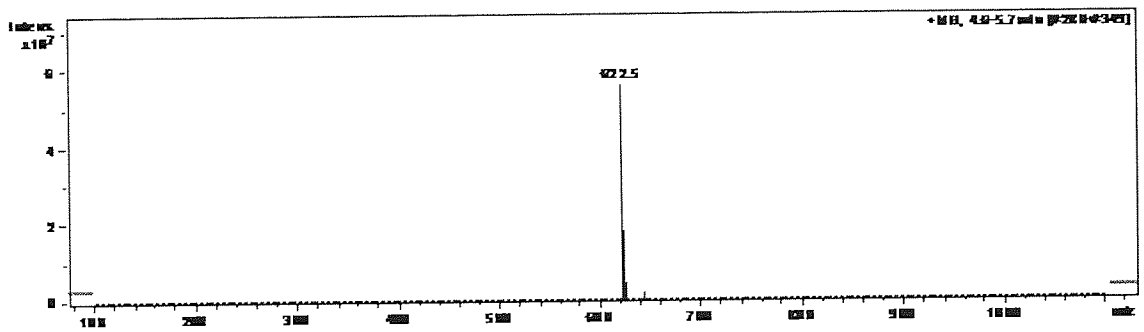

Figure 29. An example of the CMS of specified data. This shows a high intensity of peak 622.5 which is expected from the EIC

2.8 Partially hydrated hydrogels (gel) synthesis

Partially hydrated hydrogels are hydrogels that are below their equilibrium water content. They are known *"gels"* in this thesis to differentiate them from fully hydrated hydrogels (membranes) which are intended for different applications.

Partially hydrated hydrogels (gels) were synthesised by photopolymerisation of the monomer(s) in the presence of distilled water, glycerol, photoinitiator and a cross-linking monomer.

Monomer, glycerol and water were mixed together in a ratio of 4:3:3. They were typically made up to 100g in mass and mixed on a shaker to obtain a homogeneous solution (solution A). The mixture was degassed with a slow stream of nitrogen.

The cross-linker and initiator were made up in a ratio of 10:3 respectively. The cross-linker and initiator were mixed by a shaker to obtain a separate homogeneous solution (solution B) which was kept out of the light until needed. Solution B was added as a percentage of the mass, i.e. % w/w of solution A and was added just prior to the spreading step (see below). Solution A and B were mixed by a shaker to obtain a homogeneous solution (solution C).

Solution C was spread on a tray lined with release-paper and passed three times through a GEW ultraviolet lamp 310 at minimum belt speed. After cooling the adhesive gels were covered with a sheet of silicone release paper and stored in sealed plastic bags to prevent contamination and minimise water loss from the gel. Storage in this way has previously been shown to preserve the hydrogels for approximately six months.

2.9 Fully hydrated hydrogels (membrane) synthesis

Fully hydrated hydrogels or hydrogels at their equilibrium water content are known as membranes in this thesis to differentiate them from partially hydrated skin adhesive hydrogels (gels) as the two are intended for different applications.

Membrane were produced by thermal polymerisation of a monomer mixture in a glass mould [71] (Figure 30). Two glass plates, approximately 10cm by 15cm in size, were each covered by Melinex (polyethylene terephthalate) and separated by two polyethylene gaskets, each one 0.2mm thick. Spring clips hold the mould together.

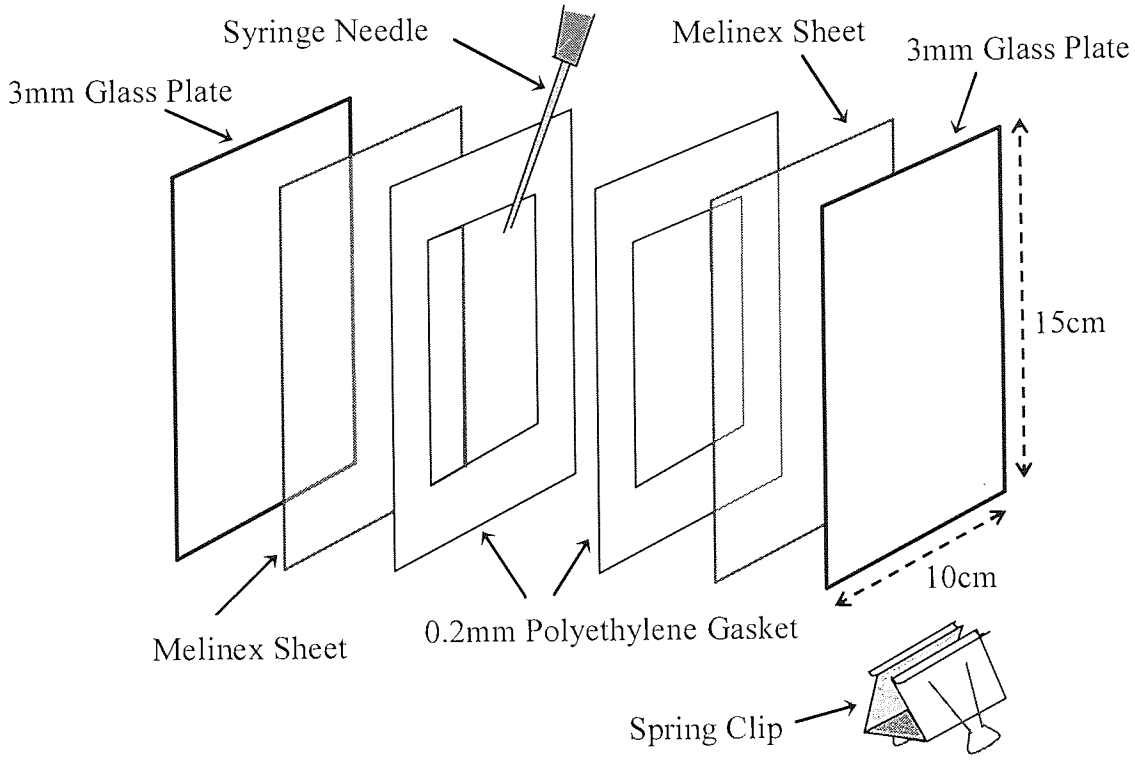

Figure 30. Diagram of a membrane mould (exploded view)

A homogeneous monomer mixture was injected into the mould cavity by insertion of a G22 syringe needle into the cavity space between the Melinex sheets.

The compositions were typically made up to 5g in mass and the desired cross-linker and initiator added as a percentage of that mass, i.e. % w/w. The composition was mixed by a shaker to obtain a homogeneous solution. The mixture was degassed with a slow stream of nitrogen prior to injection.

The injected mould would be placed in an oven at 60°C for three days followed by a three hour post-cure at 90°C. The membrane was then removed from the mould and separated from the Melinex sheets. It was allowed to hydrate in distilled water (approx.

pH 6.2) for at least seven days, changing the water daily. Previous experience had shown that this procedure allowed equilibrium hydration to be reached and the extraction of any water-soluble residual monomers.

2.10 Equilibrium water content (EWC)

The EWC of the membranes was recorded by a gravimetric method [6]. The EWC of samples was calculated by determining the weight difference between the hydrated and dehydrated material. Small samples of hydrogel were cut using a cork borer and blotted carefully with slightly damp filter paper to remove excess surface water.

After weighing, the samples were dehydrated to constant weight in a microwave and re-weighed. The EWC was calculated from a minimum of five samples from each membrane and the final value expressed as an average. The EWC is calculated using Equation 1.

$$\mathbf{EWC(\%)} = \frac{\mathbf{weight\ of\ water\ in\ hydrogel}}{\mathbf{Total\ weight\ of\ hydrated\ hydrogel}} \times \mathbf{100} \qquad \text{Equation 1}$$

2.11 Youngs modulus (ε)

The ε was recorded on a Houndsfield HTi tensometer interfaced with an IBM 55SX computer [72]. The tensometer was fitted with a 10N load cell (software allowed the load to be reduced to 1N) attached to the instrument crosshead which was able to move in a vertical plane only. A clamp was suspended from the load cell by a chain hung 8mm directly above a lower clamp that was permanently fixed to the tensometer.

The samples were cut into sections with widths of 3.3mm. The samples were measured for thickness with a micrometer immediately before being placed into the clamps in the vertical position. Specially designed mounting were used to avoid damaging the samples with the clamps.

The crosshead would then move at a constant rate of 10mm/min until the sample being assessed broke completely. The computer software then produces a graphical output and calculate the Young's modulus (ε), tensile strength at break (Ts) and the elongation to break (Eb) using the following equations:

$\varepsilon = stress / strain$ (MPa) Equation 2

Where

$stress = load / cross\text{-}sectional\ area$ Equation 3

$strain = extension\ of\ length / original\ length$ Equation 4

$Ts = load\ at\ break / cross\text{-}sectional\ area$ (MPa) Equation 5

$Eb = (extension\ of\ length / original\ length)\ x\ 100$ (%) Equation 6

To ensure the samples were kept in a fully hydrated state they were stored in solution after they were cut into sections and throughout the tensile testing (in the clamps) by the regular application of a fine mist of water from an atomiser. All samples were tested at room temperature and pressure. The aveage of five results was reported.

2.12 Oxygen permeability (Dk)

Oxygen permeability measurements were obtained using a Createch model 201T Permeometer. Polymer samples were cut to size using a size eight cork borer and the thickness was measured using a micrometer. Samples were placed over the electrode and a lens tissue, saturated in 0.1M potassium chloride was used as an electrode bridge situated in between the sample and the electrode.

A column was placed over the sample and a slow flow of gas, either nitrogen or oxygen, was passed through the sample. A constant stream of gas was passed through the sample until a steady current was obtained, which was noted. The steady current obtained when passing nitrogen gas through the sample was denoted as i_o. In all cases i_o was found to be

zero. The steady current reading obtained when oxygen was passed through the sample was denoted as i.

Oxygen permeability readings were calculated using equation 8 below and are given in the form of Dk, where D is the diffusivity of oxygen through a material and k is the solubility of oxygen in a given material

If $Dk/L = (i-i_o) / nFA\Delta P$ Equation 7

Where:
L – thickness (cm)
i_o – current obtained for nitrogen
i– current obtained for oxygen
F – Faraday constant = $96487x10^6$ μA s mol^{-1}
A – area of gold electrode = $0.1424cm^2$
ΔP – partial pressure = 155mm Hg (STP)
n – number of electrons generated at electrode = 4
V – standard gas constant = $22.415x10^3$ ml

If a constant (B) is calculated from $nFA\Delta P = 0.02629$ cm^3O_2 (STP)/cm^2 amperes s cmHg equation 7 becomes:

$Dk = i (\mu A) \times L (cm) \times (Bx10^{-9})$ Equation 8
(units 10^{-11} cm x ml O2 / sec x ml x mmHg)

In this method described by Fatt and colleagues [73, 74] the Dk from at least three thicknesses of the same material are measured. The thickness/Dk is plotted against the thickness of the sample and produces a linear relationship. The Dk is calculated from the slope of this line using linear regression. This method is independent of the "boundary effect" of the water layer between the lens and the sensor. The aveage of five results was reported.

2.13 Coefficient of friction (μ)

A Nano-Scratch Tester with Scratch Software V3.46 data management system was used to determine the coefficient of friction (μ). This instrument was identified and adapted for the study of contact lens biotribology [75]. This nanobiotribometer when used for studying membrane biotribology requires a set up that differs to the one used for contact lens studies. For membranes the hydrogel membrane is placed on the Melinex® sheet (polyethylene terephthalate) and these are both clipped onto the moving friction table (Figure 31). The whole instrument sits on an air table to isolate it from vibration; therefore it can measure low values of μ due to the reduced background "noise".

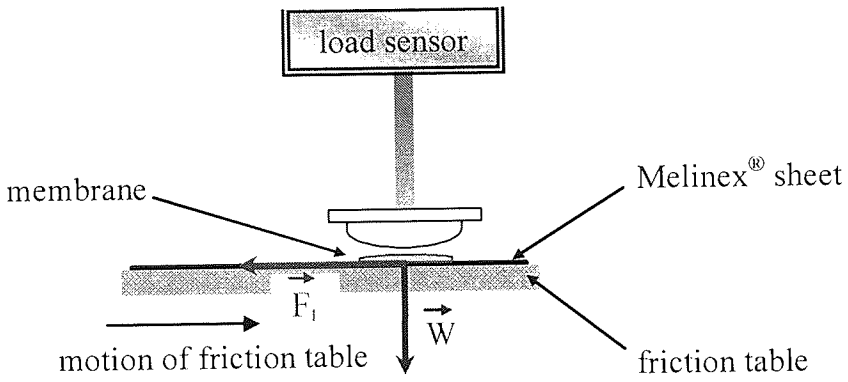

Figure 31. Schematic representation of a nanobiotribometer

The table is raised until the membrane comes into contact with the convex (polypropylene) mould at the bottom of the load sensor. The sample membrane was subjected to 10 cycles of sliding tests. A typical cycle was processed as a constant normal force was applied onto the membrane, then the friction table was moved in a straight line along 20 mm. The friction force experienced by the tested membrane was measured by the friction table monitoring system during the 20 mm slide. At the end of the 20 mm slide, the applied normal force was reset to zero and the friction table lowered in order to reposition itself at its initial starting point. μ is determined from equation 9.

$$\mu = \frac{F_t}{W} \qquad \text{Equation 9}$$

Where μ is the coefficient of friction, which is the ratio of the force causing movement (F_t) to the applied load (W).

Figure 32 illustrates a typical μ-distance measurement output indicating difference between μS ("start-up" or "static") and μD ("dynamic" or "sliding") friction.

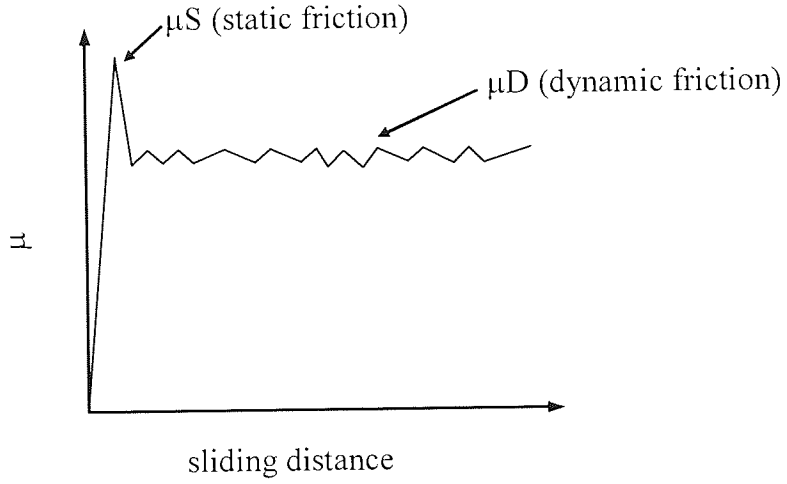

Figure 32. A schematic of a typical coefficient of friction vs distance trace

Experimental set-up values such as the applied load and the sliding speed as well as the properties of the material, lubricant and substrate will influence the value of the μ. Thus to enable the comparison of the μ for different materials and lubricants the applied constant load was set at 60 mN, the sliding speed at 30 mm/min, sliding distance 20mm.

The results from cycles three to ten were averaged and this gave the coefficient of friction for one run. Two runs were averaged to give a single result for one membrane.

2.14 The 90° perpendicular peel test

The 90° perpendicular peel test was recorded on a Houndsfield HTi tensometer interfaced with an IBM 55SX computer. The 90° perpendicular peel test consists of a base support platform and a plate that slides over this base. Strips of adhesive tape

measuring 1.27cm x 12.7cm (½"x 5") were pressed against the subject's forearm and left for 1 minute. The strips were subsequently peeled from the skin by a grip positioned directly above the end of the adhesive at a speed of 500mm/min using a 100N load cell. The subject's arm is placed on the sliding plate and this enables the arm to slide forward to ensure that the angle of peel to remain constant at 90°. This is shown in diagrammatically in Figure 33.

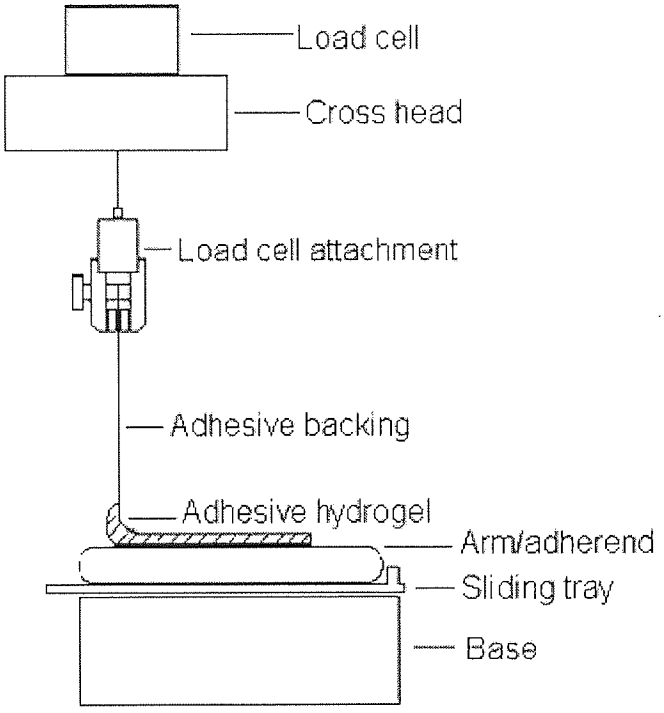

Figure 33. A diagrammatic representation of the 90 Degree Peel Test, adapted from a Hounsfield Hti tensometer

Results of the peel were automatically related to a computer that determined values for peel strength in N/mm of the samples. Five peel strength measurements were taken for each material tested, with a fresh gel sample used for each. Mean values of these measurements are quoted in the results.

2.15 Contact angle

The contact angle measurement is used to determine the polar and dispersive components of the hydrogel surface. The GBX Goniometer can be used to measure the contact angles

of liquid on a material instantly or over a period of time (kinetically, see below). In this case the test liquids were water and dididomethane. The GBX Goniometer is shown in diagrammatically in Figure 34.

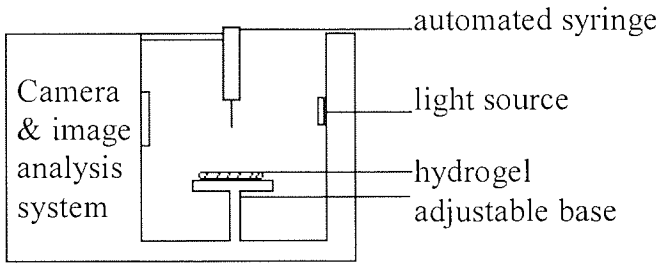

Figure 34. A diagrammatic representation of the GBX Goniometer.

2.15.1 Initial (instant) measurement

A ~3cm by 1cm sample is cut placed on the adjustable base of the GBX Goniometer. If the sample was a membrane (as described in section 2.9) then the residual water was removed from the surface before the contact angles were recorded. If the sample was a gel (as described in section 2.8) then the release paper was removed from the sample and the sample was allowed to "settle" for 1 minute before the contact angles were recorded.

The adjustable base is placed at the correct level to bring the sample into focus and a syringe containing HPLC water is loaded onto the instrument. Drops of water of a set volume, for example 2.5 µl are placed on the hydrogel and the angle of contact is measured from the image taken immediately after the drop has contacted the hydrogel.

The computer calculates the contact angle, thereby minimising human error. This is repeated three times to ensure the contact angle obtained is as accurate as possible and

typical for the material being analysed. This process is repeated for another sample of the same material using diiodomethane instead of water. The contact angle using diiodomethane and water provides information to determine the dispersive and polar components respectively and hence the total surface free energy, see Appendix VI - Contact angle.

2.15.2 Kinetic Measurements

Kinetic measurements are performed in the same way as initial contact angle measurements except the contact angle of the drop is recorded a preselected number of times over a specified period, for example 15 measurements made over 210 seconds. This gives information on the interaction of the drop with the hydrogel over time.

2.16 Rheology

Viscoelastic properties of partially hydrated hydrogels were measured on a Bohlin CVO Rheometer using the oscillatory rheometrical (frequency sweep) technique. Samples were subjected to a sweep of 20 sine wave completion frequencies from 0.5Hz to 25Hz. Low frequency oscillation relates to long stress time scales such as those occurring when a skin adhesive hydrogel is applied to the skin. Higher frequencies represent the shorter stress times of gel removal.

Samples of 20mm diameter were cut from hydrogel sheets using a size 13 cork borer and positioned in the centre of the base plate. The 20mm upper parallel plate was then lowered to the point of slight compression of the sample, ensuring good contact between the plates and the gel. This gap size varied with thickness of gel between 2.0 and 2.5mm. Correct loading of sample is important in order that measurements taken are from the area directly underneath the parallel plate only (Figure 35).

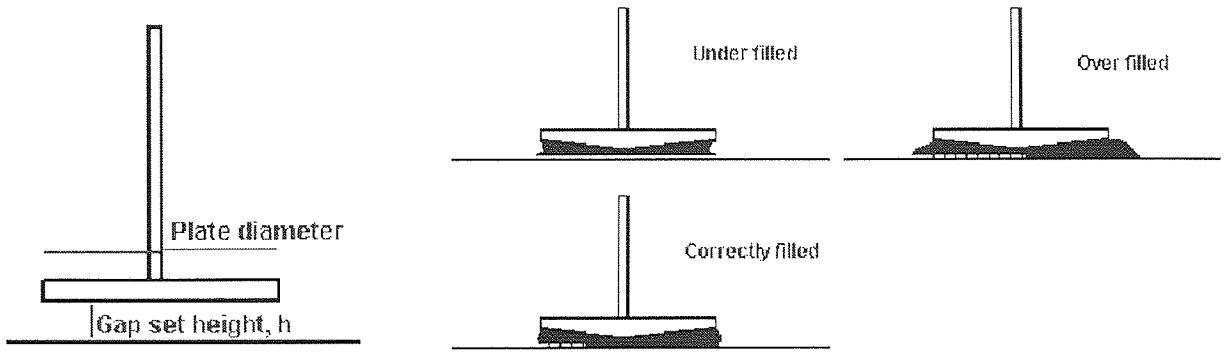

Figure 35. Correct loading of parallel plate measuring system (Bohlin Instruments)

To ensure uniform compression of the sample throughout the oscillation sweep a normal force control of 5% (100g) was specified. Tests were carried out at 37°C, normal body temperature, and repeated for each test material to verify reproducibility of data. Average values of at least three runs are quoted in the results.

2.17 Statistical analysis

A one-way analysis of variance (ANOVA) test was used to establish statistical significance between sets of data. ANOVA is a statistical method through which the differences between the means of two or more independent groups can be evaluated. A one-way ANOVA is carried out by partitioning the total model sum of squares and degrees of freedom into a between-groups (treatment) component and a within-groups (error) component. The significances of inter-group differences in the one-way ANOVA are then evaluated by comparing the ratio of the between and within-groups mean squares to a Fisher F-distribution. For each test, the level of confidence was taken at 0.05 at 95% confidence.

Chapter 3 - Lipid analysis of the tear film 1

"At first there were very few who believed in the existence of these bodies smaller than atoms. I was even told long afterwards by a distinguished physicist who had been present at my [1897] lecture at the Royal Institution that he thought I had been 'pulling their legs.'"

J.J. Thomson (1936). Recollections and Reflections

3.1 Introduction to lipid analysis of the tear film 1

Lipids are present in an anterior layer that covers the tear film which in turn covers the ocular surface [76]. These lipids have been shown to interact with and deposit onto materials that are placed in contact with them, i.e. contact lenses [77, 78]. Ever since the introduction of soft contact lens wearing modalities in 1971 lipid interactions have been problematic. Deposits of lipid and other tear film components onto lenses can lead to many problems including the lenses becoming uncomfortable to wear, infection and loss of visual acuity [79]. These deposits had to be removed if the lenes were to be worn on an extended basis.

The introduction of disposable lenses in 1987 removed some of the requirements for cleaning contact lenses and so the problem of lipid deposition was no longer in the limelight for contact lens research. Another significant change in wear modality came with the introduction of daily disposable lenses in 1993. The introduction of daily wear regimes essentially eliminated the need to understand lipid/lens deposition and interactions. The driving force for daily disposable lenses was multi factorial but lipid interactions/spoliation and corneal hypoxia being major reasons. Hypoxia was brought about the use of "conventional" hydrogel materials in long term and overnight wears modalities as the materials failed to provide the required corneal oxygen levels due to low oxygen transmissibility (Dk/t) [8].

The introduction of silicone hydrogel contact lens materials in about 2000 provided the high Dk/t needed to avoid hypoxia in continuous and long term wear modalities. However the use of these materials has reintroduced the lipid/lens interaction phenomena into the research arena. The use of silicone hydrogel materials is interesting in terms of lipid interactions as not only are the lenses being used for long term (30 days) and overnight wear but the materials themselves are hydrophobic.

Deposition of lipids in contact lens wear makes lipid/lens interactions important to understand and High Performance Liquid Chromatography (HPLC) has been utilised for the analysis of lipids that come into contact with lens materials in the past [80-83]. However the work in the literature has concentrated on the neutral lipids found in the

bulk of the lipid layer and little attention has been paid to the polar lipids (phospholipids). This is the case for both the literature concerning lipid/lens interactions and that related with the non contact lens wearing tear film.

It is these polar lipids that are believed to impart much of the tear film stability of the lipid-aqueous interface. An understanding of the concentration and behaviour of the polar lipids in the tear film is ideal before one can understand how these lipids interact with ocular biomaterials, e.g. contact lenses. The focus of this chapter is the nature and fate of the phospholipids of the tear film since a more qualitative understanding of these factors will illuminate the role played by phospholipids in tear film stability

Analysis of the phospholipids that are present in meibomian gland secretion and logically also thought to be present in the tear film required the development of an HPLC method. HPLC and Mass Spectrometry (MS) were used idividually and as a hyphenated technique (LCMS) to investigate the polar lipids of the tear film. The development of these methods is described in the following chapter.

3.2 High Performance Liquid Chromatography (HPLC) method development for tear film lipid analysis

3.2.1 Introduction to HPLC Method Development

Lipid separation is normally a multi stage operation with extraction of the lipids from samples required before they can be injected into HPLC systems. Lipids from organic sources such as the skin and the tear film are composed of highly complex mixtures that not only differ by classes of lipid but also differ within each class, see Chapter 1. As they are such mixtures of species with differing properties no single method is capable of separation of every species present [84].

As a first stage the lipids are normally separated from the source material and literature often quotes the method by Folsh et al [85] along with that of Bligh and Dyer [55] for this extraction. These extraction methods are based on chloroform, methanol and water mixtures.

Thin Layer Chromatography (TLC) can also be used for separation of the lipids from source material and into class before injection onto HPLC [86]. More recently Solid Phase Extraction (SPE) has been used for this type of separation [86, 87].

The mobile phases needed for chromatographic separations of all species of lipids are usually normal phase; some separation of species can be performed with reverse phase HPLC. The standard detector for a HPLC system is the Ultraviolet (UV) detector which normally detects in the 190-700nm range (UV to visible light). This can be problematic for lipid work as the lipids tend to absorb UV in the low nm region (~200nm) and require handling and extraction methods in solvents that also absorb in that range, chloroform for instance. Other detectors can be used such as Evaporating Light Scattering Detectors (ESLD) or Mass Spectrometry (MS) which reduces the problem of solvent interference [84].

Previous work from this laboratory has produced methods for lipoidal analysis using HPLC [83, 88]. The method from Franklin et al [83] used a Knauer HPLC equipped with a Rheodyne 7125 injector, a Lichrosorb 5μm (250mm x 4mm) SI60 column and Perkin-Elmer LC-75 UV and Perkin-Elmer Fluorescence detectors in series. The mobile phase was normal phase isocratic consisting of hexane: propan-2-ol: acetic acid (1000:5:0.5 v/v). The method reported by Tighe et al [88] was for fatty acid analysis and used a reverse phase system with a mobile phase acetonitrile: water (99:1) and a C18 column. Both of the methods HPLC systems employed columns of an internal diameter (ID) of 4mm which can be considered as standard ID for HPLC. Other workers have produced similar techniques for analysis of lipiodal species [89-91].

3.2.2 HPLC Method Development

The lipids of the tear film can be divided into non polar and polar classes. This defines the two separate areas of HPLC method development which could be explored, namely reverse and normal HPLC. The Agilent 1100 Series capillary pump came pre-installed with seals that were designed for reverse phase chromatography

alone and for this reason normal phase chromatography was not used. The HPLC system is described in Chapter 2.

3.2.3 Non polar lipid tear film Method Development

Both polar and non polar lipids are found in the tear film and although in this thesis primary interest lies in the polar (phospholipids) of the tear film, knowledge of the non polar lipids are useful. The retention times of other species that can be found in the system must be known otherwise they may be confused with the species of interest.

The Agilent 1100 Series HPLC instrument was equipped with an Agilent ECLIPSE XDB-C18 RR 3.5μm (0.5mm x 150m) column and detection by diode array detection (DAD) at 254nm and 210nm was used, but detecting 190-700nm with the diode array feature. The DAD was collecting at 254nm to detect if any protein was still in the system after lipid extraction and at 210nm to detect for the presence of lipids.

The reverse phase method reported by Tighe et al [88] was used as a starting point for non polar lipid detection. A buffered (5mM ammonium formate (pH3.8)) mobile phase was prepared with a composition of acetonitrile: water (99:1). Several variations of the Tighe et al method were tried including gradient mobile phases, temperature, flow rate, and injection volumes. No peaks were detected for the samples injected which were cholesterol (Ch), cholesterol palmitate (ChPal), lauric acid, stearic acid and palmitic acid shown in Table 11.

Table 11. Non polar samples injected

Species	mg/ml
Cholesterol (Ch)	0.105
Cholesterol palmitate (ChPal)	0.12
Lauric acid	0.102
Stearic acid	0.05
palmitic acid	0.049

It was thought that the detection of non polar lipids using modified Tighe et al methods did not allow the analytes of interest to elute off the column. As the Tighe et al method (isocratic acetonitrile: water (99:1)) did not produce any results for cholesterol, cholesterol palmitate or the free fatty acids injected a different mobile phase was tried consisting of acetonitrile: isopropanol (60:40) that had previously been shown to separate steryl esters and wax esters [92]. The mobile phase was buffered with 5mM ammonium formate (pH3.8).

A cholesterol sample (1.05mg/ml) was injected and a chromatographic peak was seen in UV at 210nm at 3.7min. A cholesterol myristate sample (1.01mg/ml) was injected and a chromatographic peak was seen in UV at 210nm at 3.7min. The chromatographic peaks appear at the same retention time. MS work related to this HPLC system is discussed in the LCMS section (3.4.3). Development of the non polar lipid HPLC system is required to gain separation of these species and this will be discussed in Chapter 7.

3.2.4 Polar lipid tear film Method Development

There are polar and non polar lipids in the tear film and it is the polar lipids, especially the phospholipids that are of particular interest as these species are believed to contribute significantly towards the stability of the tear film. Knowledge of how they phospholipids interact with foreign bodies placed in the ocular environment would not only help improve the basc science behind the tear film, as it is still (relatively) little understood but it may also allow for the development of improved materials.

A selection of the polar species included in the meibomian gland secretion (MGS) is dilauroylphosphatidylcholine (DLPC), dimyristoylphosphatidylcholine (DMPC) and sphingomyelin (SM). These were used as standards in this part of the phospholipids analysis. The concentrations of the standards used were 0.36mg/ml for DLPC, 0.6mg/ml for DMPC and 1.22 mg/ml for SM (Table 12).

Table 12. Polar samples injected

Species	mg/ml
Dilauroylphosphatidylcholine (DLPC)	0.36
Dimyristoylphosphatidylcholine (DMPC)	0.6
Sphingomyelin (SM)	1.22

The modified Tighe [88] method discussed earlier was used for phospholipid analysis. This method was used as it would allow separation of the phospholipids based on the fatty acids groups present on them. The Agilent 1100 Series HPLC instrument was equipped with an Agilent ECLIPSE XDB-C18 RR 3.5μm (0.5mm x 150m) column. The column temperature was 40°C. The DAD was set to scan at wavelengths of 254nm, 200nm, 205nm and 210nm, but also collecting 190-700nm with the diode array feature. The standards were injected at a volume 0.25μl into an acetonitrile: water (99:1), 5mM ammonium formate (pH3.8) mobile phase at a flow rate 10μl/min.

While no peaks were seen with UV detection the Mass Spectrometer (MS) could detect peaks for all three species. A 1:1 mixture of the DLPC and DMPC was prepared and injected into the HPLC system and MS detection showed separation of the species. Method development as discussed in the LCMS, Section 3.4.3, showed that this HLPC method could resolve these polar species.

3.2.5 Summary of tear film lipid HPLC analysis

The non polar lipid HPLC method needs further development to gain better separation using UV detection as will be discussed in further work. The presence of the non polar lipids in the extracted samples elute at earlier times than the polar and so should not interfere with the detection of the latter species. The polar lipids could not be detected with the UV method, however as the following sections show the HPLC separation method described above for polar lipids can be utilised with mass spectrometry as detection.

3.3 Mass Spectrometry (MS) detection in tear film lipids analysis: Direct infusion of non polar lipids

3.3.1 Introduction to MS

The MS system used in this work was an Agilent MSN (SL) Ion Trap equipped with electrospray ionization (ESI) interface. The Ion trap and ESI interface are described in Chapter 2 and in more detail in Appendix IV - Liquid Chromatography Mass Spectrometry.

MS is a useful tool in the analysis of lipids as when traditional detection LC techniques such as ultraviolet light (UV) are used certain extraction solvents used in the work up of lipid samples can interfere with the analysis as they absorb light in the area of interest, i.e approximately 200nm. The absorbance versus wavelength of some common solvents is shown in Figure 36. Because of this lipids are not generally analysed using UV detection.

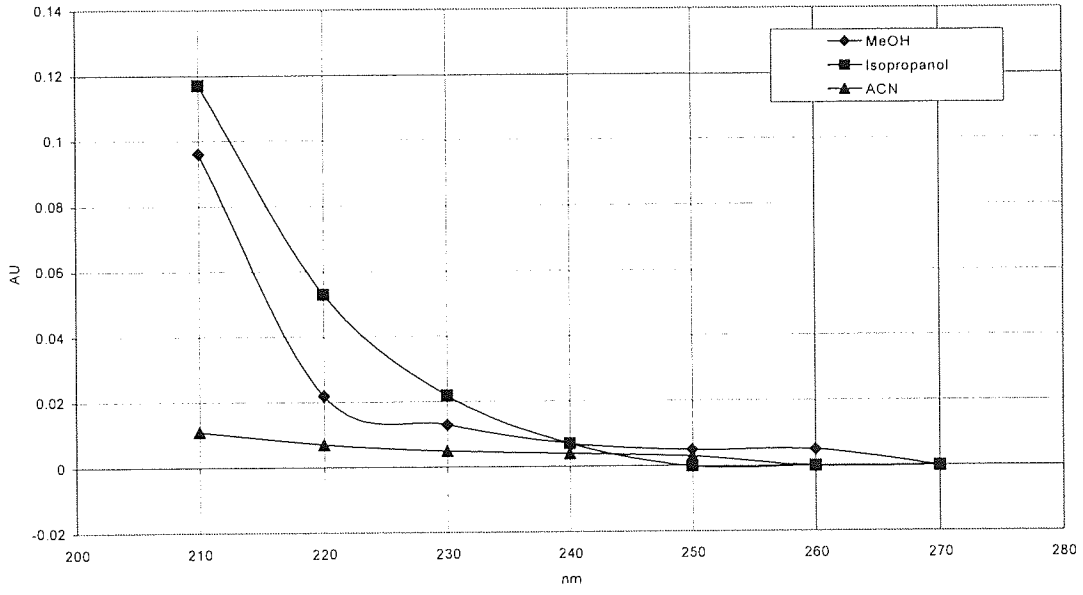

Figure 36. Absorbance versus wavelength for solvents

This section describes MS analysis only. As the combination of HPLC to MS is considered a method in its own right it will be described elsewhere in this thesis - any methodology using (HP)LC in conjunction with MS will be described in the Section 3.4, Liquid Chromatography Mass Spectrometry (LCMS).

3.3.2 Lipid MS: Direct Infusion of non polar lipids

Direct infusion experiments do not require the use of the HPLC system and are contained separately in this section. These experiments allow the species to be directly injected into the MS without the use of LC. The use of inducing fragmentation on the species can then be investigated without the complication that LC can sometimes add.

The cholesterol (Ch), cholesterol palmitate (ChPal) and cholesterol myristate (ChMy) samples shown in Table 13 were directly infused into the Agilent 1100 Series LC/MSN (SL) Ion Trap at 0.3ml/hour (0.005ml/min) with the polarity set to positive. This provided a Total Ion Chromatograms (TIC) from which a Compound Mass Spectrum (CMS) could be extracted. The terms TIC and CMS are explained in Chapter 2.

Table 13. Samples Directly Infused

Species	mg/ml
Cholesterol (Ch)	0.1
Cholesterol palmitate (ChPal)	0.101
Cholesterol myristate (ChMy)	0.1

The direct infusion of Ch provided a MS peak of 369.4 Th as shown CMS in Figure 37. Direct infusion of ChMy gave a MS peak of CMS shows peaks at 369.4 Th and 614.5 Th as shown in the CMS in Figure 38. Direct infusion of ChPal gave a MS peak of CMS shows peaks at 369.4 Th and 642.6 Th as shown in the CMS in Figure 39.

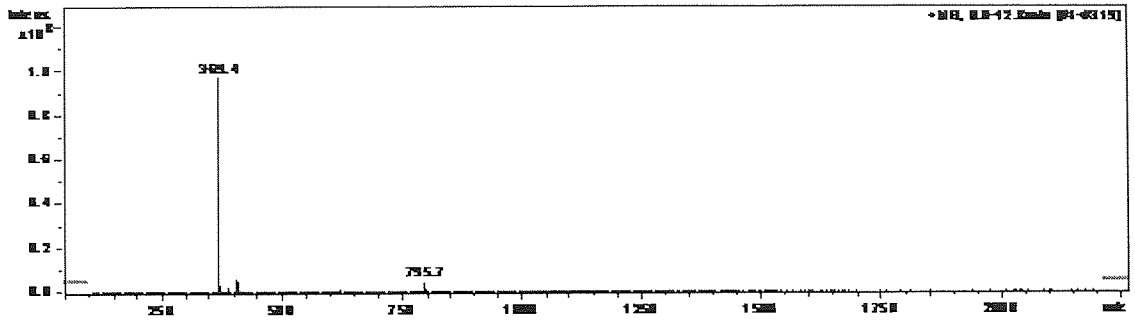

Figure 37. Compound Mass Spectrum (CMS) of the Direct Infusion of cholesterol, showing a MS peak of 369.4 Th

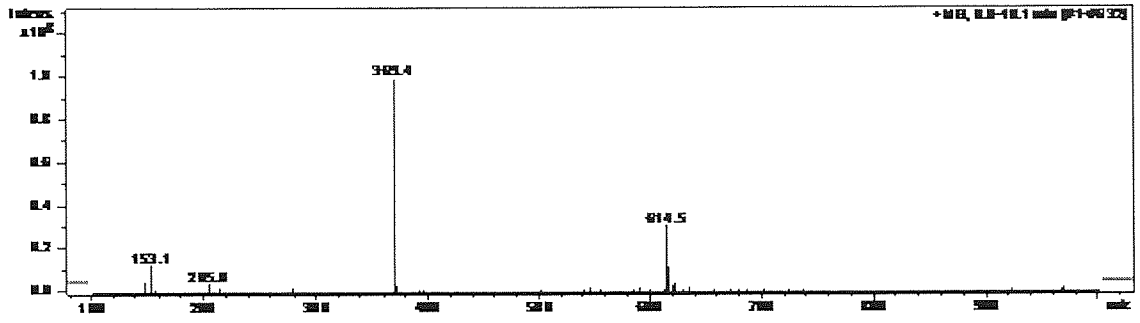

Figure 38. Compound Mass Spectrum (CMS) of the Direct Infusion of cholesterol myristate, showing peaks at 369.4 Th and 614.5 Th

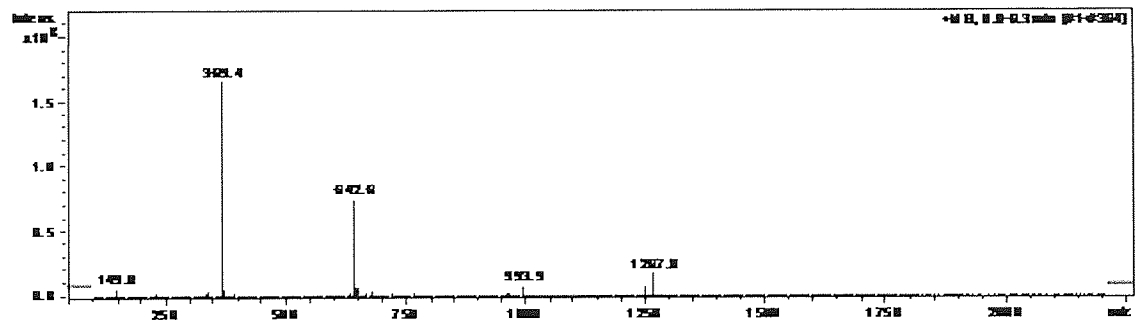

Figure 39. Compound Mass Spectrum (CMS) of the Direct Infusion of cholesterol palmitate, showing peaks at 369.4 Th and 642.6 Th

The MS peak for Ch is 17.25 mass units below the theoretical molecular mass (Mr) of 386.65g/mol, this could indicate the loss of a hydroxyl (OH) group. The cholesterol ester MS peaks were above the Mr of each ester by 17.49 mass units for ChMy and 17.53 mass units above for the ChPal and this could indicate the adduct of $NH4^{+}$, possibly gained from ammonium formate. The MS peaks and the Mr of each sample are summarized in Table 14.

Table 14. MS peaks and molecular weight (Mr) of samples

Species	MS peaks / Th	M_r / gmol-1
Cholesterol	369.4	386.65
Cholesterol palmitate	369.4 and 642.6	625.07
Cholesterol myristate	369.4 and 614.5	597.02

Where Th is the Thompson (m/z), Mr is the molecular weight; g/mol-1 is grams per mole

The cholesterol peak at 369.4Th appears in all three samples at a much higher intensity than the cholesterol ester peak indicating that the esters must undergo some fragmentation during analysis. To stop this fragmentation modification of the MS method is needed. The cone voltage can be altered to increase or decrease fragmentation and this needs to be explored as part of further work.

Kalo and Kuuranne [93] reported a peak for cholesterol of 369Th and cholesterol esters at $[M+NH4]^+$, for example 643Th for ChPal. The Kalo and Kuuranne experiments used direct infusion of sample into a Perkin-Elmer Sciex triple quadrupole LC–MS–MS instrument with ESI source. The results shown above indicate that MS can be used as a detection method for non polar species.

3.3.3 Lipid MS: fragmentation of phospholipids

The following section describes direct infusion (DI) of phospholipids into the MS. The use of DI allows a steady stream of the phospholipids to the MS. The advantage of this is that the fragmentation patterns of the different phospholipids could be established.

A standard solution of dilauroylphosphotadiylcholine (DLPC) at a concentration of 141µg/ml dissolved in the mobile phase described in Section 3.2.4. The standard was directly infused to the MS at 0.3ml/hour (5µl/min). Figure 40 shows the DLPC Compound Mass Spectra (CMS) extracted from the EIC's, which is an average of the data collected across the full time of accumulation.

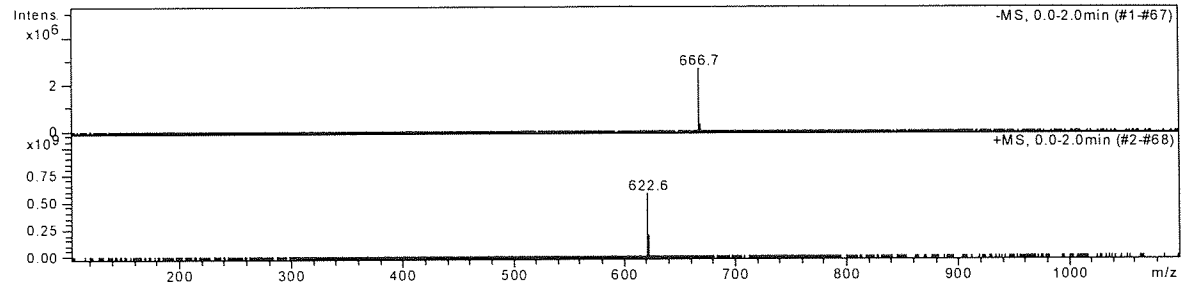

Figure 40. Compound mass spectra (CMS) of dilauroylphosphotadiylcholine (DLPC). This figure show the –ve and +ve mode polarity CMS

DLPC has a theoretical molecular weight of 621.83g/mol. The peak shown at 622.6m/z in the positive mode CMS corresponds to the $[M+H]^+$ ion. The peak shown at 666.7m/z in the negative mode CMS corresponds to an $[M+CHO_2]^-$ peak, the CHO_2^- ion (Mr of 44.85) could come from ammonium formate (CHO_2NH_4).

MS^2, MS^3 and MS^4 experiments were carried out in the positive mode polarity to study fragmentation allowing identification of DLPC. MS^n of 622.6m/z produced a peak of 184.1m/z and fragmentation of peak 184.1m/z produced a peak of 125.1m/z. This shows a fragmentation pattern of 622.6m/z → 184.1m/z → 125.1m/z. Further fragmentation of the 125.1m/z peak produced peaks not abundant enough for measurement.

The choline head group of PC, ($PO_4C_5H_{13}N$) has a molecular weight of 182.13g/mol and the PC end group $N(CH_3)_3$ has a molecular weight of 59.11g/mol. Therefore the fragmentation pattern is $[M+H]^+$ → [choline head group + 2H]$^+$ → [choline head group + 2H – $N(CH_3)_3$]$^+$. This fragmentation pattern for DPPC is shown in Table 15. This would allow for the identification of the PC containing phospholipids in the samples.

Table 15. MSn of dilauroylphosphotadiylcholine (DLPC). Peaks from DLPC and mass loss in positive polarity mode

	Number of peaks	Peaks produced	Mass Loss
MS	1	622.6	
MS^2 (662.6)	1	184.1	478.5
MS^3 (184.1)	1	125.1	59
MS^4 (125.1)	1	0	125.1

A similar direct infusion and MS^n experiment was carried out to identify the phospholipid headgroup ethanolamine using dilauroylphosphotadiylethanolamine (DLPE) as a standard. MS^n shows a fragmentation pattern of 580.5m/z → 439.5m/z → 183.2m/z, 165.2m/z and 123.2m/z. Also 183.2m/z → 165.2m/z, 123.2m/z and 109.2m/z.. Further fragmentation of the peaks 165.2m/z, 123.2m/z and 109.2m/z produced peaks which were not abundant enough for measurement. This fragmentation pattern of DLPE is shown in Table 16.

Table 16. MSn of dilauroylphosphotadiylethanolamine (DLPE). Peaks from DLPC and mass Loss in positive polarity mode

	Number of peaks	Peaks produced			Mass Loss		
MS	1	580.5					
MS^2 (580.5)	1	439.5			141		
MS^3 (439.5)	3	183.2	165.2	123.2	256.3	274.3	316.3
MS^4 (183.2)	3	165.2	123.2	109.2	18	60	74

DLPE has a theoretical molecular weight of 579.45g/mol therefore the peak at 580.5m/z can be assigned as the parent molecule with an "attached" proton or $[M+H]^+$. The loss of 141 to produce the 439.5m/z peak is the removal of the ethanolamine head group along with the H^+ (ethanolamine head group is 140.06g/mol).

Further fragmentation of 439.5m/z occurs with the loss 256.3 producing a peak at 183.3m/z this is equivalent to a $C_{12}H_{23}O^+$ ion which is the size of the fatty acid moiety of lauric acid present at the SN^1 ad SN^2 positions in the DLPE.

The 183.3m/z peak undergoes fragmentation with the loss of masses of 18, 60 and 74 to produce peaks at 165.2m/z, 123.2m/z and 109..2m/z respectively. The loss of 18 from the $C_{12}H_{23}O^+$ ion is removal of H_2O to produce a $C_{12}H_{21}^+$ ion, the loss of 60 from the $C_{12}H_{23}O^+$ ion is removal of C_3H_8O to produce a $C_9H_{15}^+$ ion and the loss of 74 from the $C_{12}H_{23}O^+$ ion is removal of $C_4H_{10}O$ to produce a $C_8H_{13}^+$ ion. This would allow for the identification of the PE containing phospholipids in the samples.

3.4 LCMS Method Development for tear film lipids analysis

3.4.1 Introduction to LCMS Method Development

As indicated in the Section 3.2 and 3.3 the tear film MS method development is explained here as it the combination of the LC and MS methods. The Agilent 1100 Series LC/MSD (SL) was used for this work.

The work carried out thus far is the analysis of extracted tear film lipids, the effect of varying the extraction technique and effect of the varying the collection technique. While dealing with the tear film lipids it became apparent that both the collection and extraction techniques affected the results. The HPLC method described in Section 3.2 was used to deliver chromatographically resolved species to the MS.

3.4.2 LCMS Method Development

The lipid layer of the tear film has been described in terms of polar and non polar components or phases and each phase needs a different approach to method development. This is due to the different behaviour of the different lipid phases when exposed to LC systems. The method development is separated into the non polar and polar sections.

3.4.3 Non polar Tear Film LCMS Method Development

The work described in this section is the follow up to HPLC and MS work on the non polar species described above in the HPLC and MS Sections. The work of the HPLC system provided chromatographic peaks that could be seen in the UV at 210nm. The direct infusion work of the MS section showed that the species can be detection by ESI MS and provided peaks to search for in the LCMS work.

The LCMS used the method described in the HPLC section (0.25µl injection volume, 10µl/min flow rate, acetonnitriile:isopropanol (60:40) mobile phase, 40°C column

temp, UV detection at 254nm, 200nm, 205nm and 210nm) allowed detection of the sample in the UV at 210nm prior to the sample passing into the MS. The samples injected were the same as for the direct infusion experiments and the resulting MS peaks are shown in Table 17.

Table 17. MS peaks and molecular weight (Mr) of samples

Species	MS peaks / Th	M_r / gmol-1
Cholesterol	369.4	386.65
Cholesterol palmitate	369.4 and 642.6	625.07
Cholesterol myristate	369.4 and 614.5	597.02

The chromatographic peaks were seen at approximately 3.7 minutes as expected. MS analysis provided the TIC from which the CMS could be extracted across the chromatographic peak at 3.7 minutes. The CMS peaks all showed the 'pseudo' cholesterol peak, i.e. 369.4 Th and none of the cholesterol ester peaks previously seen in the direct infusion experiments, i.e. 642.6 Th for cholesterol palmitate and 614.5 Th cholesterol myristate. This indicates that the cholesterol esters may not be stable under the LCMS conditions as only the 'pseudo' cholesterol peak is detected. Further development of the system is required to understand if fragmentation is occurring and this is discussed in the Chapter 7.

3.4.4 Polar Tear Film LCMS Method Development

Phospholipids species in the meibomian gland secretion (MGS) includes sphingomyelin (SM), dilauroylphosphatidylcholine (DLPC), dimyristoylphosphatidylcholine (DMPC) and dipalmitoylphosphatidylcholine (DPPC). The DLPC, DMPC and SM were shown to be resolvable by the modified Tighe [88] HPLC method so mixtures of these were made of these selected species along with the phospholipid DPPC.

PCMix1 is a mixture of DLPC, DMPC and DPPC at a concentration of 40μg/ml (0.04mg/ml). PCMix2, PCMix3 and PCMix4 are dilutions of PCMix1 to

concentrations of 20μg/ml (0.02mg/ml), 10μg/ml (0.01mg/ml) and 4μg/ml (0.004mg/ml) respectively. PCMix5 is a mixture of DLPC, DMPC, DPPC and SM (chicken egg yolk) at a concentration of 20μg/ml (0.02mg/ml). These solutions are shown in Table 18.

Table 18. PCMix Solutions, dilauroylphosphatidylcholine (DLPC), dimyristoylphosphatidylcholine (DMPC) and dipalmitoylphosphatidylcholine (DPPC) and sphingomyelin (SM)

Solution	Species	Concentration
PCMix1	DLPC, DMPC and DPPC	40μg/ml
PCMix2	DLPC, DMPC and DPPC	20μg/ml
PCMix3	DLPC, DMPC and DPPC	10μg/ml
PCMix4	DLPC, DMPC and DPPC	4μg/ml
PCMix5	DLPC, DMPC, DPPC and SM	20μg/ml

The solutions of PCMix 1, PCMix 4 and PCMix 5 were analysed by LCMS using the modified Tighe [88] method. The method chromatographically resolved the species as expected as shown in the TIC in Figure 41.

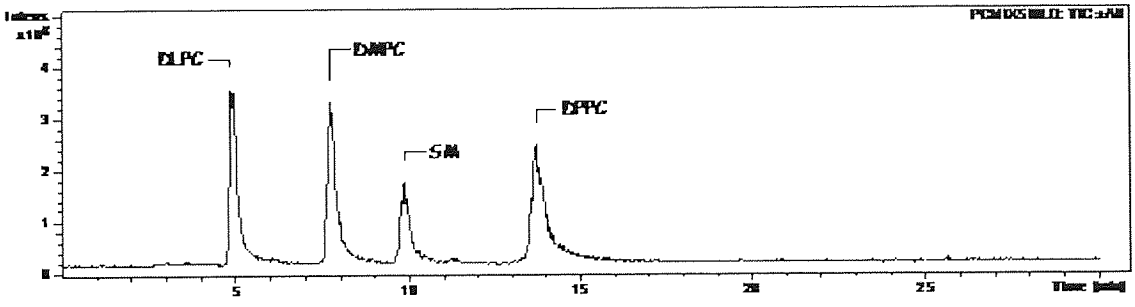

Figure 41. Total Ion chromatogram (TIC) of phospholipid species dilauroylphosphatidylcholine (DLPC), dimyristoylphosphatidylcholine (DMPC), dipalmitoylphosphatidylcholine (DPPC) and sphingomyelin,(SM).

DLPC, DMPC, DPPC and SM have $[M+H]^+$ molecular weights of 622.5 g/mol, 678.5 g/mol, 734.6 and 703.6 g/mol respectively. M is the molecular mass of the species and $[M+H]^+$ indicates the hydrogen adduct of the species that occurs in the electrospray ionization (ESI), see Appendix IV - Liquid Chromatography Mass Spectrometry.

The intensities of $[M+H]^+$ peaks versus sample were plotted versus concentration show a linear fit with an R2 of 0.9903, 0.9702 and 0.9458 for DLPC, DMPC and DPPC respectively are shown in Figure 42. After this calibration curve was created tear samples were taken as described in Chapter 2 and the method described above was used to analyse them.

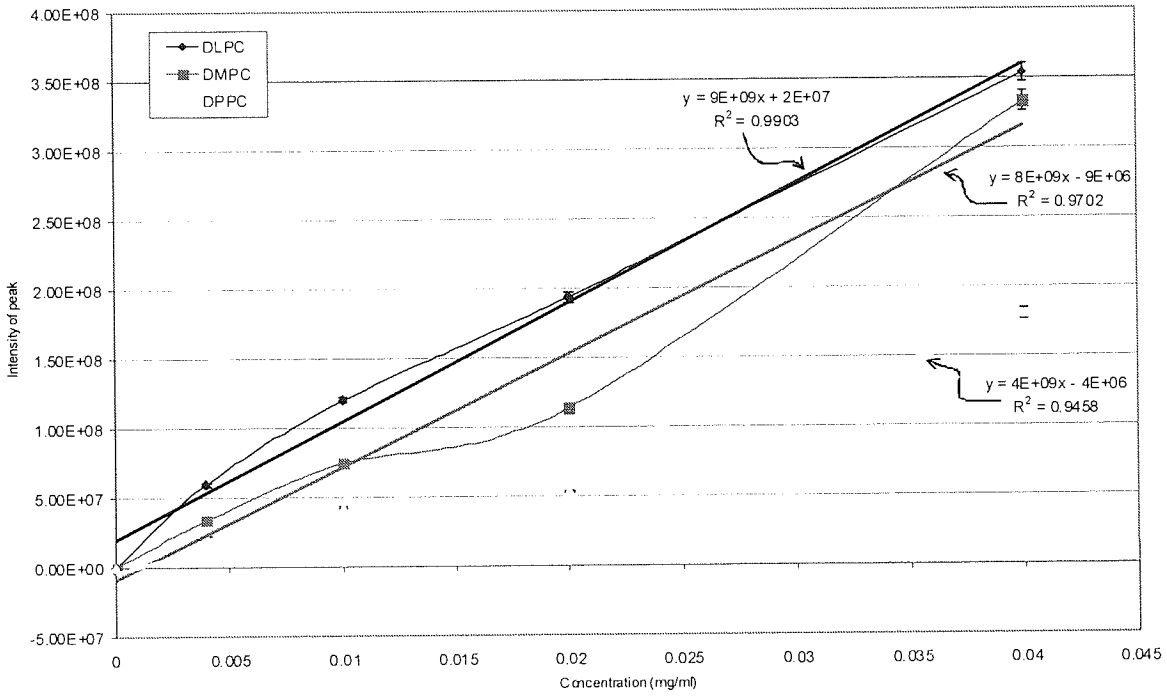

Figure 42. Intensity of Peak Vs Concentration of sample (mg/ml). N=3, ±SD

3.4.5 Tear film lipid samples analysed with LCMS

The Agilent 1100 series software uses a nomenclature for naming samples that has eight digits and so samples used in this thesis use this system also.

Tear samples were taken from various subjects with either glass capillary or ophthalmic sponges using the method described in Chapter 2. The extraction methods used were a modified Bligh and Dyer, methanol:chloroform and methanol as described in Chapter 2. A combination of collection and extraction methods were tried to extract phospholipids from the tear film. Examples of results obtained from

these combinations are samples TS000000, TS200000, TSDC0000, TSDC2000, TSAMCap0 and TSDCCap0.

TS000000 is an example of tear sample taken with an ophthalmic sponge and extracted using the methanol:chloroform method. TS200000 and TSDC0000 are examples of tear samples from different subjects taken with an ophthalmic sponge and extracted using the methanol method.

TSDC2000 is an example of a tear sample treated as TS200000 except the MeOH was made up as a 0.001% butylated hydroxyl toluene (BHT) solution. BHT was used to acertain if it would interefere with the analysis if used as an antoxidant to reduce possible oxidation f the lipids.

TSAMCap0 and TSDCCap0 are examples of a tear samples taken with a glass capillary and extracted using the methanol method.

Blank is a sample prepared from the extraction of an ophthalmic sponge alone and treated as TS200000. MeOH00001 is the solvent used as mobile phase in the system.

These extracted tear samples were subjected to the LCMS method described above. The resulting Total Ion Chromatograms (TIC's) are shown in Figure 43 for samples TS000000, TS200000, TSDC0000, TSDC2000, TSAMCap0 and TSDCCap0.

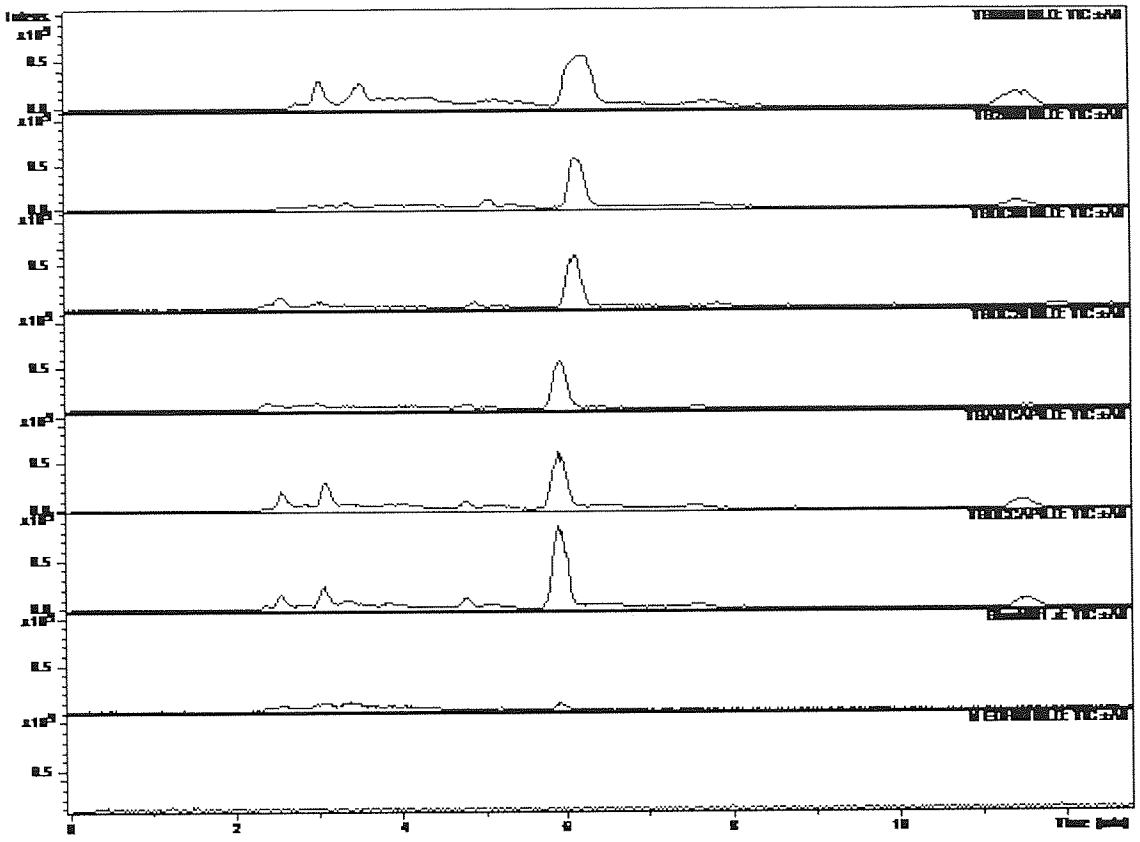

Figure 43. Total Ion Chromatograms (TIC) of samples. TS000000 is collected on an ophthalmic sponge and extracted in MeOH: ChCl3 (1:1), TS200000 and TSDC0000 were ophthalmic sponge and extracted in MeOH, TSDC2000 is collected on an ophthalmic sponge and extracted in MeOH (0.001% BHT), Blank is an ophthalmic sponge and extracted in MeOH, TSAMCap0 and TSDCCap0 were collected in a glass capillary and extracted in MeOH

It can be seen that all the TIC's are similar and the predominant chromatographic peak is that at 6 minutes. When the Compound Mass Spectra (CMS) of this chromatographic peak is inspected it showed strong MS peaks at 338.4Th and 675.7 Th. Another chromatographic peak appeared in the TIC at approximately 11.5 minutes and when the CMS was inspected this showed a strong peak at 429.4 Th.

These three MS (ion) peaks (338.4Th, 675.7Th and 429.4Th) were selected for further inspection. There are subject to subjects variations as the peak at 338.4Th is of a higher concentration in some subjects indicating that this may be a subject variable ion peak. The peak at 675.7Th is of lower concentration in the same subject.

The peak at 429.4 Th (which appears chromatographically in the TIC at ~11.5 minutes) was of a lower intensity when MeOH: CHCL3 (1:1) was used as the extraction medium and of lower intensity for ophthalmic sponge collection. The use

of the ophthalmic sponge as a collection method introduced contaminants to the samples which were presumed to be from the sponge.

It was not clear from these results if these were impurities or tear components as the peaks appear in the blank as well as the tear samples, although it is at an order of magnitude lower. The peaks of 338.4 Th, 675.7 Th and 429.4 Th do not correlate with the expected masses, i.e. those associated with phopholipid MGS components that would undergo ionisation to form $[M+H]^+$ ions easily.

Further inspection showed that the type of vial being used influenced the intensity of the 338.4 Th, 675.7 Th and 429.4 Th peaks and that changing the vials improved the situation by lowering the intensity of these peaks. The modified Bligh and Dyer method [67] used for lipids extraction further improved the impurities brought about by the vials as described above.

The extraction protocols were also changed with respect to the amount of time that the samples were left in the extraction medium. The times chosen ranged from 10 minutes to overnight.

Despite the variation of collection method, extraction method and extraction times the peaks of the phospholipids were not any of the predominate peaks seen in the samples. Therefore the concentration of phospholipid in the samples taken was presumed to be below those used for the standard curve shown in Table 18, i.e less than 4μg/ml of DLPC, DMPC and DPPC.

3.4.6 Extracted Ion Chromatograms (EIC) of tear film samples

The use of EIC is explained in Chapter 2. Briefly it allows the filtering of a single ion peak from all the other peaks present in the sample. EIC was used with the peaks of phospholipids expected in the ttear film and none of the species reported as being predominant in the meibomian gland secretions could be seen in the tear film samples.

3.4.7 Common Contaminants in ESI MS

Common contaminants in ESI are erucamide with a peak at 338 Th and diisooctyl phthalate (a plasticiser) with a peak at 429 Th which would help explain the presence of these ions in the samples but not the 675.7 Th peak.

3.4.8 Summary of tear film lipid LCMS analysis

The tear fluid has beea volume of 7μl and the lipids compose an average of 3.52μg/μl [31, 41, 42] with the phospholipids composing ~6.1% (0.215μg/μl) of this total [33-37]. A LCMS method was developed which was able access the concentration of phospholipid species to a sensitivity of 4μg/ml (0.04μg/μl) and it would appear that the phospholipids are present at lower concentration than this in the tear film. It was decided to utilise other methods to validate these results as discussed in Chapter 4.

3.5 Conclusions

While not being of primary interest in this work the knowledge that the non polar lipids elute with a different retention time to te species of interest indicates that they would not interfere with the analysis of the phospholipids in terms of chromatography. The HPLC analyis of the non polar lipids; cholesterol and cholesterol myristate as described in section 3.2.3 produced chromatographic peaks which appeared at ~3.7 minutes. The non polar lipidas have different tretntion times to the phospholipids.

The HPLC method, using UV as a detection method, produced no peaks for the standards used: dilauroylphosphatidylcholine, dimyristoylphosphatidylcholine and sphingomyelin. This is perhaps not surprising since these species have no conjugation and would not be expected to be detectable by UV. Any chromophoric behaviour that these species exhibit would probably not be seen if the extraction medium is considered, i.e. chloroform.

Direct infusion mass spectrometry (MS) was able to detect the presence of the non polar lipids and this shows that MS can be used as a detection method for non polar species. MS^2 can be used to induce fragmentation and identify the phospholipids if there is any ambiguity of exact species as a result of similar masses. The use of the Liquid Chromatograph Mass Spectrometry (LCMS) method for phospholipids showed that these species were stable under the conditions the MS method used The LCMS polar standards show the method works and separates based on fatty acid groups present on the phospholipids. MS/MS can be used to induce fragmentation and identify the phospholipids if there is any ambiguity of exact species as a result of similar masses.

The tear film contains concentrations of phospholipids as indicated by the LCMS analysis below those previous thought to exist. If we look at the literature on the lipids of the tear film we see that Ham et al [44] used ESI MS/MS to analyse non polar lipids in the tear film of rabbits. The rabbits had been operated on to instigate a dry eye model and a small number of normal human tear samples were also used whose results were similar to the normal samples from the rabbit.

The polar lipids were not studied but comments were made about the ionization efficiencies of the phospholipids being lowered in the presence of the glycerides [44]. ESI MS analysis of non polar lipids by Duffin et al [94] had shown that ionization efficiencies increase with polarity of the analyte, so as we see an increase in alcohol groups on glycerides we see an increase in the response of the detector (monoglycerides > diglycerides > triglycerides).

This statement on the acylglycerides seems peculiar as the phospholipids "lend" themselves to the ESI technique as they have polarity and should be expected to easily form the [M+H]+ species common to ESI. The n-acylglycerides on the other hand are less polar than the phospholipids and so their ionisation efficiencies should also be lower. Work in this laboratory showed that phospholipids had ionisation efficiencies that were not decreased in the presence of n-acylglyceries.

Polar lipids were studied by Ham et al [95] using MALDI-TOF MS where it was also suggested that the response to phospholipids were lower in the presence of glycerides

or other non polar lipids. They suggested the use of immobilized metal affinity chromatography (IMAC) ZipTip® Pipette Tips (Millipore Inc., Bedford, MA) allowed the removal of the non polar lipids and concentration of the phospholipids in the sample. The spectra from MALDI-TOF of the tear total chloroform extract acquired without and with the use of the IMAC ZipTip cleanup prior to spectral acquisition is shown in Figure (Figure 44) [95].

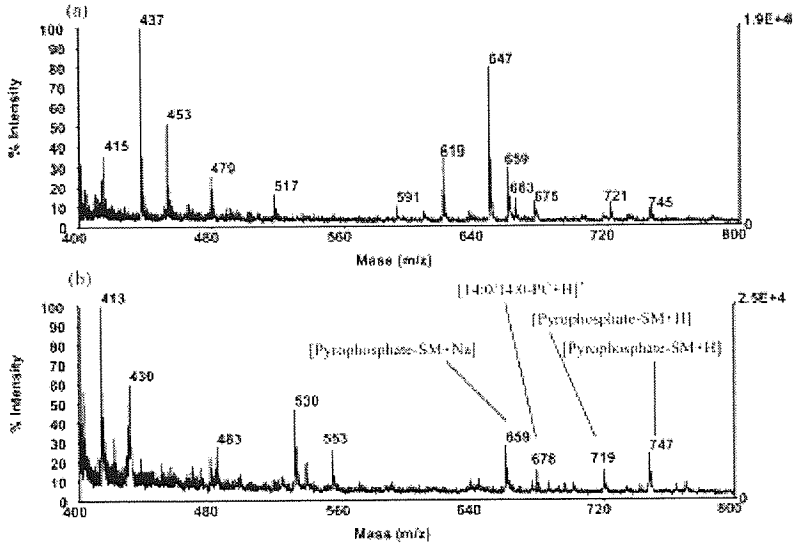

Figure 44. MALDI-TOF mass spectra of the tear total chloroform extractables acquired (Top) without the use of the IMAC ZipTip cleanup method and (Bottom) with the use of the IMAC ZipTip cleanup prior to spectral acquisition [97].

Dipalmitoylphosphatidoylcholine (DMPC) and pyrosphingomyelin (PSM) are the only phospholipids reported by Ham et al as being in the tear film using this extraction technique. PSM has not been previously reported in the tear film although sphingmyelin (SM) has been, it may be the extraction technique is converting SM to PSM. The literaturre [39, 40] shows that in meibomian gland secretions there is phosphatidylcholine (PC) appearing at 40% of phospholipids (or 1.71-2.07% of the total lipid composition). In addition to PC these reports show the other major classes of phospholipids as phosphatidylethanolamine (PE) and sphingomyelin (SM) appearing at 16 and 9% of phospholipids respectively (or 0.85-1% and 0.4-1.8% of the total lipid composition respectively). Greiner et al also report that other phospholipids are present in lower concentrations [40]. Ham et al reported PSM at higher peak intensities than the DMPC even though they are there in lower concentrations in meibomian gland secretions.

The lack of other phospholipids and higher peak intensity of the PSM could be explained by the fact that the phospholipids are being lysed by phospholipase A2 (PLA2) in the tear film while the SM is not. Comparing the structure of SM to PC (Figure 45 and Figure 46 respectively) we see there is no fatty acid at the sn2 position for SM which is where the PLA_2 acts to lyse a fatty acid group.

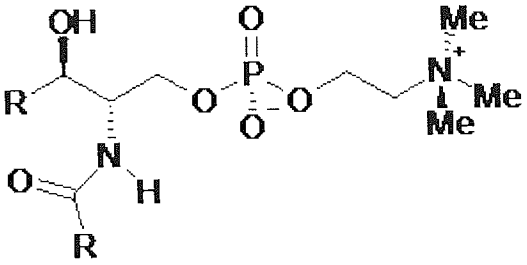

Figure 45. Structure of a sphingomyelin (SM)

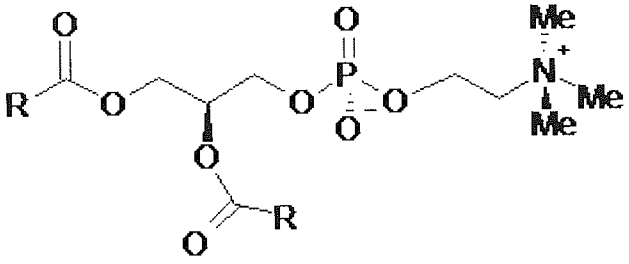

Figure 46. Structure of a phosphatidylcholine (PC)

The attack of the PLA_2 on the phospholipid species could explain why Ham et al analysis found SM in the tear film at higher concentrations than expected from literature values of meibomian gland excretions. The presence of the only other polar lipid present from Ham et al analysis was DMPC, could be explained by the fact that lipases preferentially attack those phospholipids having longer fatty chain deriveratives, such as palmitoyl or steroyl [96] and then move onto shorter fatty acid group such as myristoyl.

In summary the phospholipids in the tear film could be being processed into other species such as diacylglycerides by the action of lipases. The low concentration of phospholipids in the tear film as indicated by the analysis with LCMS in this work could be the normal state of tear film physiology.

Chapter 4 - Lipid analysis of the tear film 2

"For the tear is an intellectual thing"
William Blake, *I saw a Monk of Charlemaine*

4.1 Introduction to lipid analysis of the tear film 2

The literature describes the lipids of the tear film composing an average of 3.52μg/μl [31, 41, 42]. The phospholipids compose ~6.1% (0.22μg/μl) of this total [33-37]. Chapter 3 discussed the use of LCMS to analyse phospholipids of the tear film and showed that the ex vivo concentration of phospholipids was less than 4μg/ml. This is a lower concentration than previously thought. One possible explanation for the lower concentration reported in Chapter 3 is the fact that enzymes are lysing the phospholipids when they are presented to the tear film.

The literature shows that the lipids have mainly been analysed as meibomian gland secretions and not as components of the tear film. The lipids are secreted by the meibomian gland and are then spread across the ocular surface by the action of the eyelid [31]. If we consider the delivery of lipids to the skin by sebaceous glands, which are closely related to the meibomian glands, we see that the lipids are delivered to the skin by holocrine section and are acted on by lipases as they travel along the sebaceous gland and also as they reside on the skins surface. A similar situation can then be envisaged in the case of meibomian gland secretion where the lipids are also secreted by holocrine secretion and could be subjected to the action of lipases when present in the tear film. Examples of such lipases are that can act on phospholipids are phospholipase A_1, phospholipase A_2, phospholipase C and phospholipase D.

An isoform of phospholipase A_2 is found in the tear film, secretory phospholipase A_2 ($sPLA_2$). It is a lipolytic enzyme that catalyzes the hydrolysis of the acyl ester bond at the sn-2 of phospholipids producing a free fatty acid and lysophospholipid [97]. Group II $sPLA_2$ is the most abundant form of $sPLA_2$ in the tear film. It is present in the tear film at relatively high concentration. Concentration varies with individuals and the literature shows concentration values ranging from 1.45μg/ml to 80.6±47.8 μg/ml [98-101]. The concentration decreases with increase in age [102] and is diurnal with concentrations increasing towards midday and then a decreasing for the rest of the day [99]. As might be expected there is a decrease in concentration with tear reflexing [102].

Group II sPLA2 has been associated with the antimicrobial behaviour of the tear film [103, 104] and in disease states concentration and activity of group II $sPLA_2$ can alter, for example in atopic blepharoconjunctivitis there are decrease in concentration [105] and in chronic blepharitis increases in activity have been shown [106].

Contact lens wear intolerant subjects have been shown to have higher concentrations of group II $sPLA_2$ in the tear film [107]. The enzyme can be deposited into contact lenses [100, 101] but this does not alter its concentration or activity in the tear film and actually contributes to the prevention *Staphylococcus aureus* build up on lenses [101].

Phospholipase C (PLC) and phospholipase D (PLD) may also be present in the tear film and if so they would lyse phospholipids to produce headgroups and diacylglycerols. The presence and effect of PLC and PLD have not been studied in the tear film. This chapter is concerned with the low concentration of phospholipids and the elevated concentration of diacylglycerols in the tear film along with the relationship between the concentrations of these species and the activity of PLC.

4.2 Thin Layer Chromatography (TLC) for tear film lipid analysis

4.2.1 Introduction to TLC

It was decided that another method should be used to validate the LCMS experiments as to the concentration of the phospholipids present in the tear film. The method utilised was TLC.

TLC can be used for the separation of lipoidal species. Typically species are separated into classes on the TLC plate with identification using standards. Polar and non polar lipids are normally run on two different TLC plates as different mobile phases are required to elute and separate the species.

4.2.2 TLC of polar tear film lipids

TLC was used to verify the results of the LCMS experiments of Chapter 3, i.e. low concentrations of phospholipids in the tear film. Tear samples were taken as described in Chapter 2.

The samples were collected as described in Chapter 2 and were labelled DC, AM1, AM2 and ANO. Sample DC composed of 40µl of tear samples collected from subject DC, sample AM1 composed of 35µl of tear samples collected from subject AM1, sample AM2 composed of 25µl of tear samples collected from subject AM2 and sample ANO composed of 45µl of tear samples collected from various subjects. This is summarized in Table 19.

Table 19. Tear samples for Thin Layer Chromatography

Sample	# of samples	Volume used/µl
DC	8	40
AM1	7	35
AM2	5	25
ANO	9	45

A Pyrex tube was chilled with liquid nitrogen and place over ice. The samples were taken from the -80°C freezer and placed over ice. The lipids were then extracted from the tear sample using a modified Bligh and Dyer method [67] as described in Chapter 2. The samples were finally suspended in 50µl of chloroform and either used immediately or stored at-80°C until needed.

The lipids from 25µl of the samples were spotted onto a silica TLC plate which had been previously activated at 80°C for 15 minutes. The phospholipid standards phosphatidylserine (PS), phosphatidylinositol (PI), phosphatidylcholine (PC) and phosphatidylethanolamine (PE) were also applied to the plate for reference. The lipids were then separated using the polar mobile phase TLC method as descried in Chapter 2. The plate was allowed to dry before being visualised with iodine staining as described in Chapter 2. Figure 47 shows the iodine stained lipids on the plate.

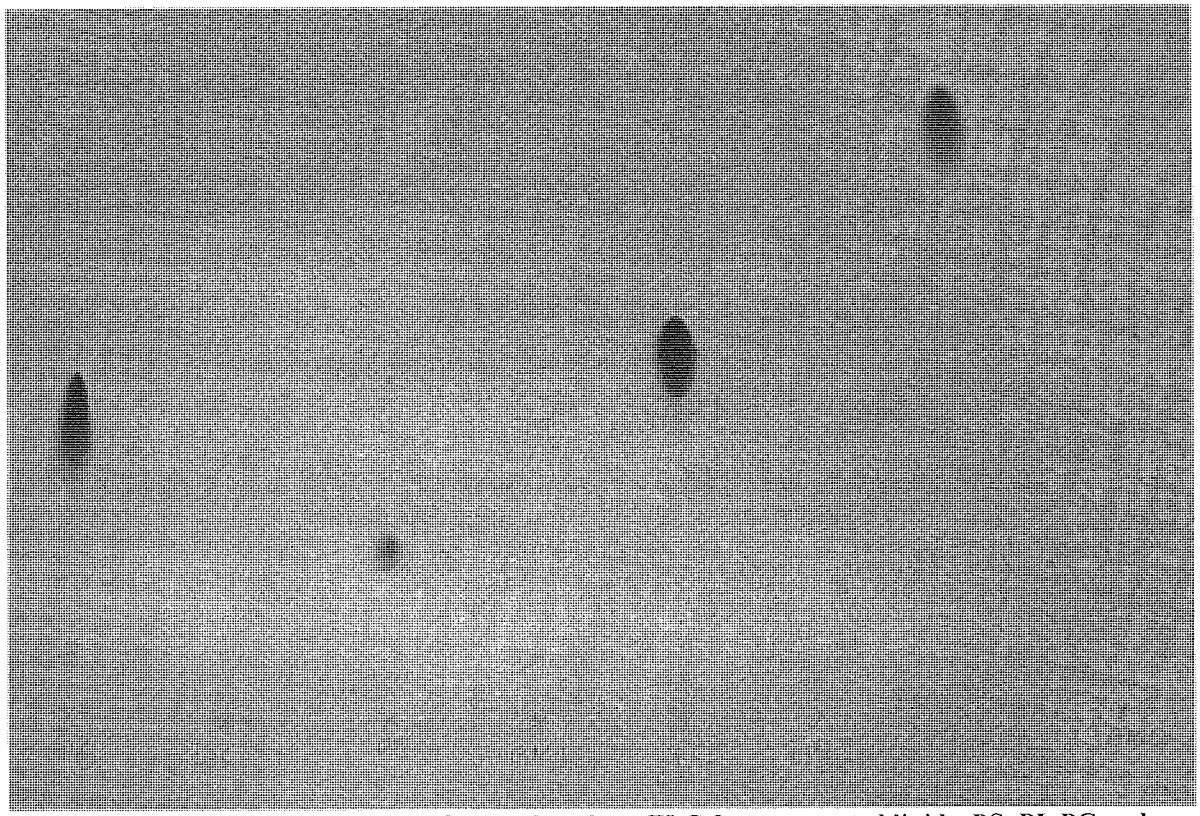

Figure 47. Iodine stained silica plate from polar phase TLC from extracted lipids. PS, PI, PC and PE are standard phospholipids (7µl). DC, AM1, AM2 and ANO are samples

The standards were visualized within minutes of the plate being exposed to the iodine. Table 20 shows the retention factor (Rf) values for the standards.

Table 20. Standards Rf values for polar TLC

Standard	Rf
PS	0.27
PI	0.15
PC	0.34
PE	0.56

Where PS is phosphatidylserine, PI is phosphatidylinositol, PC is phosphatidylcholine and PE is phosphatidylethanolamine

The sample lanes do not contain any spots where the standard phospholipids should appear indicating that phospholipids are not present in the samples. However a streak emerging off the origin did appear in the samples with an Rf value of 0.04.

Lysophospholipids (LPC) would appear as streaks off the origin and these spots on could be assigned to LPC.

Staining also appears at Rf values of 0.61-0.69 in the sample lanes. This staining faded quickly upon removal of the plate. Phosphatidic acid (PA) would run ahead of the lipids standards used and so these spots could be assigned to PA. The spots seen in the samples are summarized in Table 21.

Table 21. Sample Rf values for Thin Layer Chromatography of polar lipids. LPC is lysophospholipids and PA is phosphatidic acid

Sample	spot/assignment	Rf
DC	origin streak/LPC	0.04
"	PA?	0.61
AM1	origin streak/LPC	0.04
"	PA?	0.61
AM2	origin streak/LPC	0.04
"	PA?	0.64
ANO	origin streak/LPC	0.04
	PA?	0.69

Where LPC is lysophospholipids and PA is phosphatidic acid

4.2.3 Dittmer's solution for detection of polar lipids in TLC

As the iodine staining showed no phospholipids in the samples it was decided to use a more sensitive visualisation technique. Dittmer's solution is a known method of detection for phospholipid analysis in TLC. It is more sensitive to phospholipids than iodine staining. A molybdenum spray solution was prepared according to the method of Dittmer and Lester [69] as described in Chapter 2. The spray provides a vivid blue spot upon complex of the phosphate groups with molybdenum.

The iodine was removed from the plates by evaporating at room temperature overnight. There was still slight staining on the standards after evaporation of the iodine. The Dittmer's solution was sprayed over the TLC plate as described in Chapter 2. Figure 48 shows the plate after application of the Dittmer's solution.

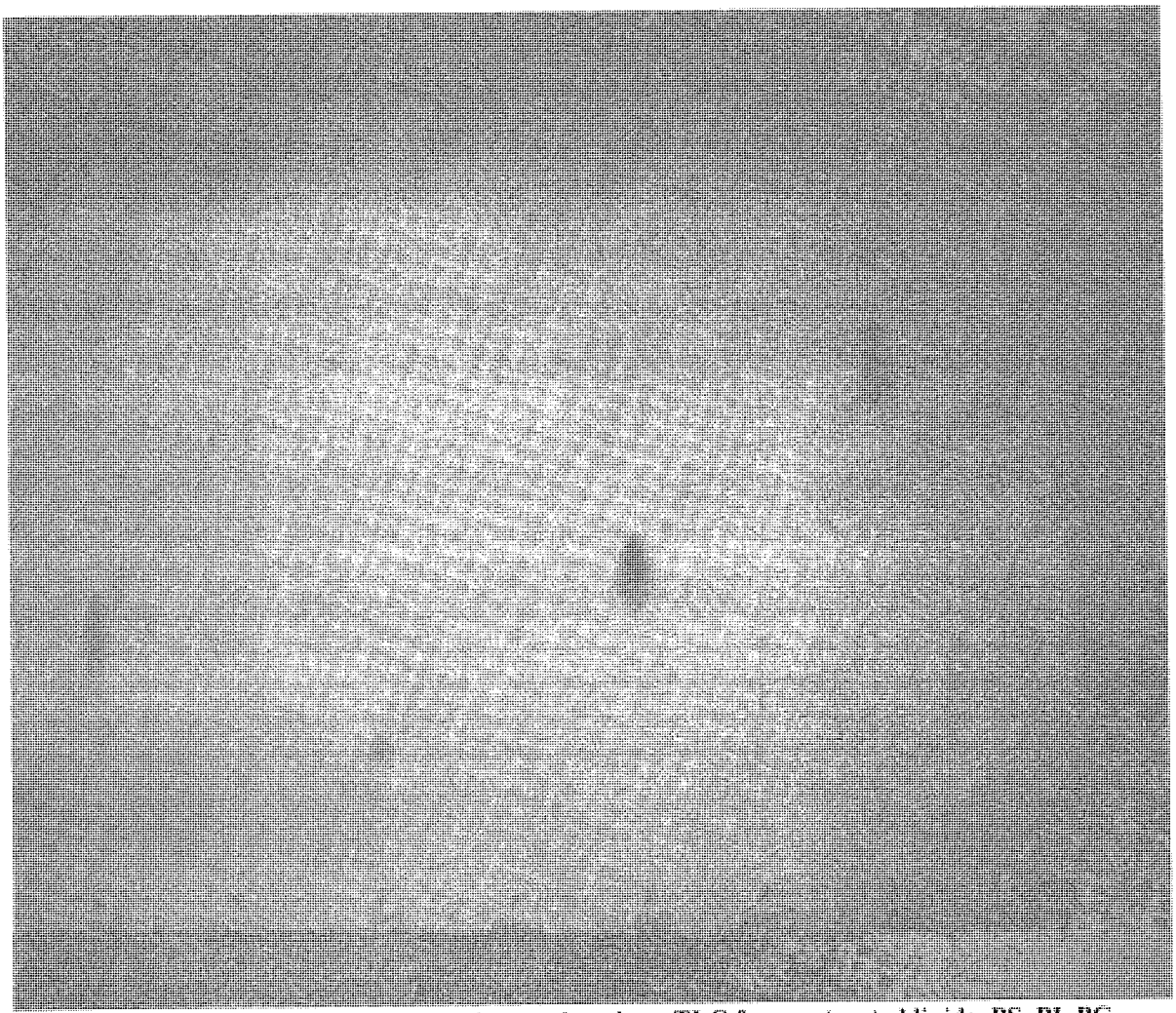

Figure 48. Dittmers sprayed silica plate from polar phase TLC from extracted lipids. PS, PI, PC and PE are standard phospholipids (7µl). DC, AM1, AM2 and ANO are samples. PC and PE were also respotted at the side of the plate

The standards PS, PI, PC and PE stained positively and there were no spots in the samples with Rf value of the standards indicating no phospholipids present in the tear film. The suspected LPC (Rf 0.04) and PA (0.61-0.69) in the samples did not appear when stained with Dittmers spray solution.

The amount of lipid in each sample can be calculated assuming the total lipid in the tear film to be averaged at 3.52µg/µl [31, 41, 42]. The samples were dissolved in 50µl and 25µl was used for spotting the plates so half of this amount is present on the plates. This gives us values of 70.4µg, 61.6µg, 44.0µg and 79.2µg for samples DC, AM1, AM2 and ANO respectively.

The polar lipids are present in the meibomian gland extract at an average of 6.1% from literature [33-36, 108] which gives the polar lipids at 4.29μg, 3.76μg, 2.68μg and 4.83μg for samples DC, AM1, AM2 and ANO respectively. The total lipids in sample, lipids on plate and polar lipid for each sample is shown in Table 22. The meibomian gland phospholipids have been studied by Greiner et al and Shine and McCulley [39, 40] and the major phospholipid components present were PC and PE at 40% and 18% of total polar lipids respectively allowing us to also calculate the μg of PC and PE as shown.

Table 22. Volume, lipid in samples, lipids on plate, polar lipid content, PC and PE in the samples at concentrations. * assuming 3.52μg/μl in tear film

Sample	volume/μl	lipid in sample/μg*	lipids on plate/μg*	polar lipid/μg*	PC/μg	PE/μg
DC	40	140.8	70.4	4.29	1.72	0.77
AM1	35	123.2	61.6	3.76	1.50	0.68
AM2	25	88	44	2.68	1.07	0.48
ANO	45	158.4	79.2	4.83	1.93	0.87

A modified Dittmers spray solution has a detection limit of 5μg LPC and 1μg for dipalmitoylphosphatidylethanolamine (DPPE) and dipalmitoylphosphatidylcholine (DPPC) species according to the method used by Ryu and MacCoss [109]. This is close to the expected concentration for polar lipids on the plate (from calculation). The limit of detection for phosphate containing lipids is 1μg for DPPC, LPC and SM. The calculated values for the phospholipids that should be on the plate are close to or above this limit of detection for PC in the samples. As there were no spots on the plate after the application of the Dittmer's solution this is another indication of low concentration of phospholipids in the samples.

4.2.4 TLC of non polar tear film lipids

The analysis of the non polar components of tear lipids was utilised to see if this could shed any light on the apparent lack of phospholipids in the tear film. Tear samples collected for non polar analyses were from subjects DC, AM1, AM2 and ANO. Each was composed of 25μl and the samples were collected and extracted in the same manner as the TLC of polar tear film samples.

After extraction the samples were each in 50µl chloroform and this was spotted onto a silica TLC plate which had been previously activated at 80°C for 15 minutes. The standards cholesterol myristate (SE), tripalmitin (TAG) and dipalmitin (DAG) were also applied to the plate for reference. The lipids were then separated using the non polar mobile phase TLC method as descried in Chapter 2

The plate was allowed to dry before being visaulised with iodine as described in Chapter 2. The stained plate is shown in Figure 49. The standards were photographed within minutes of the plate being exposed to the iodine vapour.

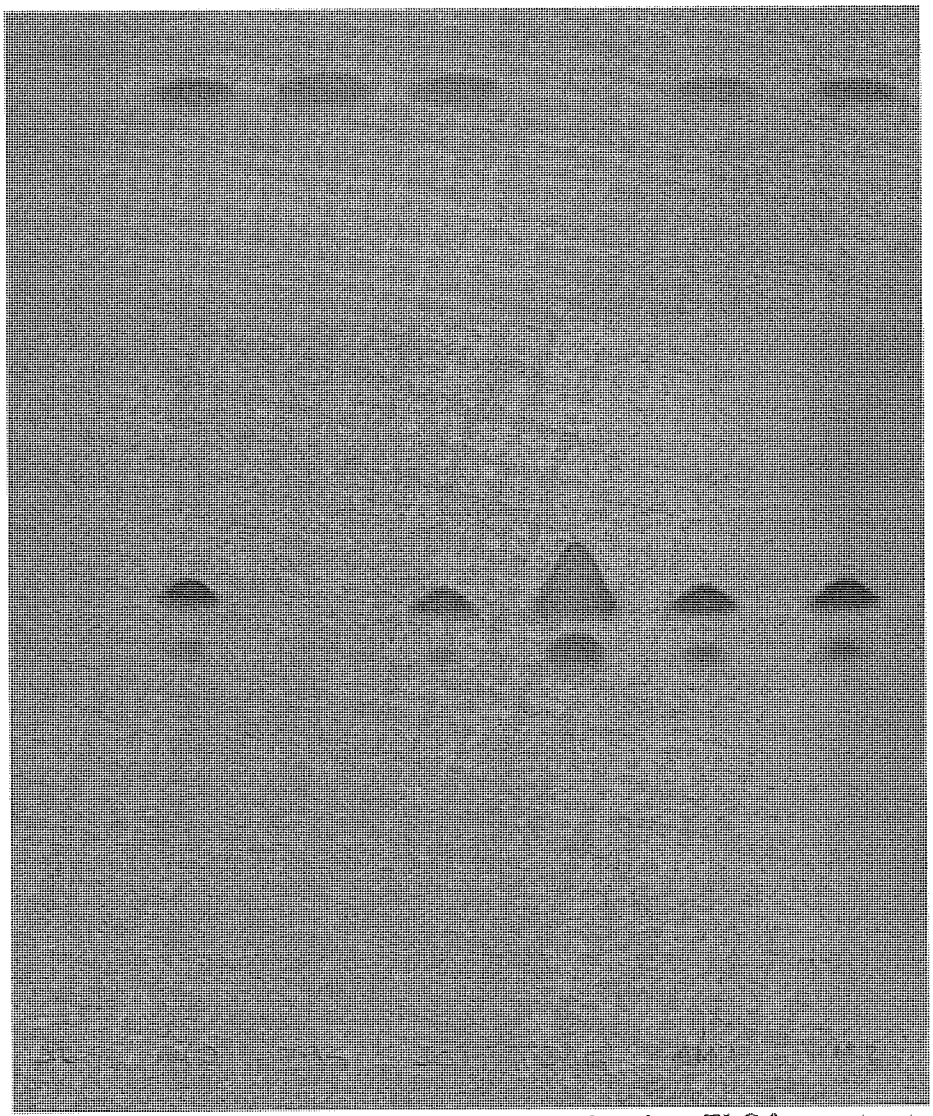

Figure 49. Iodine stained silica plate from non polar phase TLC from extracted lipids. SE, TAG and DAG are standard lipids (7µl). DC, AM1, AM2 and ANO are samples

The SE standard is seen at an Rf of 0.9 and the TAG standard is seen at an Rf of 8. The DAG standard is seen at an Rf of ~0.5, there are two spots representing the 1,2 DAG and the 1,3 DAG. The Rf's for the non polar lipids are shown in Table 23.

Table 23. Standard Rf values for non polar l TLC

Standard	RF
SE	0.9
TAG	0.8
DAG	0.5

Where SE is cholesterol myristate, TAG is triacylglycerols and DAG is diacylglycerol

The SE and TAG species are both seen in the samples as expected. The TLC plate also shows the presence of DAG in of the sample. This was unexpected as DAG was previously thought to be of low concentration in the meibomian gland secretion and therefore of low concentration in the tear film.

4.2.5 Summary of tear film lipids TLC analysis

Polar TLC revealed that phospholipids were not present in the tear film at concentrations previously thought. Non polar TLC reveals the presence of diacylglycerols (DAG) in the tear film. The concentration has not been established but the TLC plate's level of iodine staining indicates that the concentration is significant.

4.3 Detection of Phospholipase C (PLC) in the tear film

4.3.1 Detection of PLC in the tear film: Introduction

The presence of diacylglycerides (DAG) in the tear film has been demonstrated in section 4.2. A possible explanation for their presence is the action of phospholipase C (PLC) on phospholipids which would produce DAG by removing the head group from the phospholipids. The presence of PLC would also explain the low concentrations of phospholipids seen in the tear film as shown in section 4.2 and Chapter 3.

Two techniques were employed to detect the presence of PLC in the tear film. These were counter immunoelectrophoresis (CIE) and the Amplex® Red Phosphatidylcholine-Specific Phospholipase C Assay.

4.3.2 Detection of PLC in the tear film: Counter Immunoelectrophoresis (CIE) for tear film PLC analysis

CIE is an immunological technique using two wells of application along an electrical axis, the anodal well has positively charged antibody and the cathodal well has the negatively charge antigen; electrophoresis results in the antigen and antibody migrating cathodally and anodally, respectively, with time. A line of precipitation appears where the two meet and conjugate in concentrations of optimal proportions (Figure 50). This line of precipitation can be visualised by staining with reagents such as Coomassie brilliant blue or silver stain.

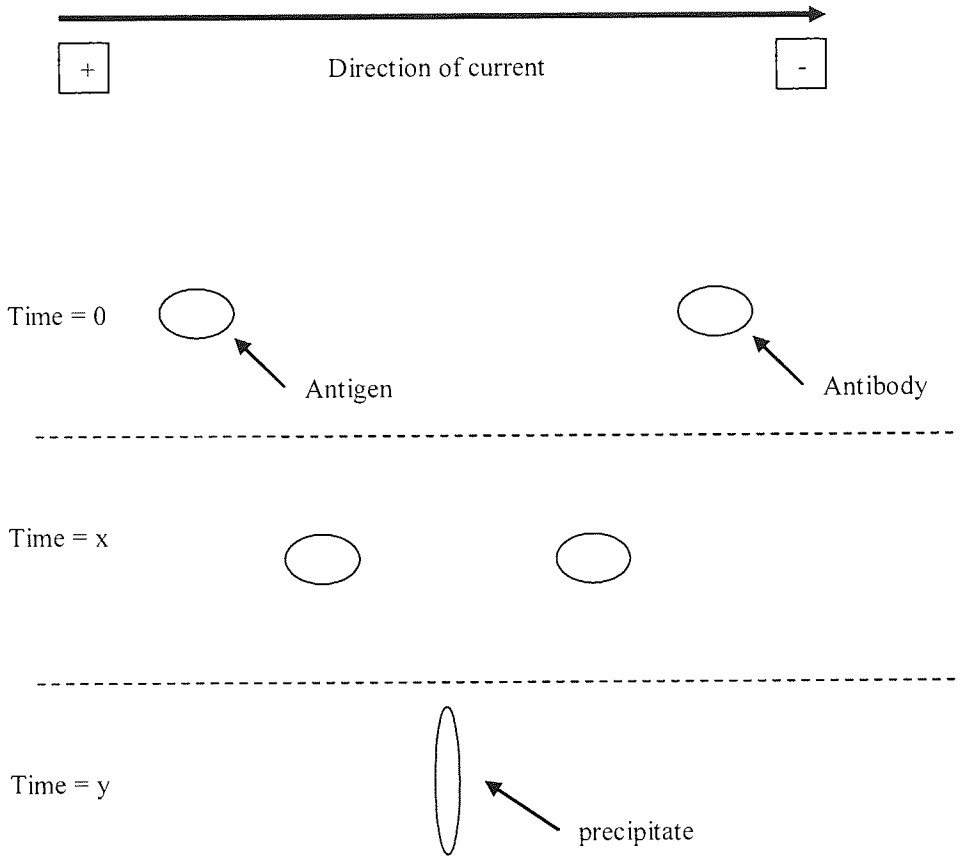

Figure 50. Principle of counter immunoelectrophoresis (CIE)

Agarose/PEG8000 gels as described in Chapter 2 were used in the CIE experiments. In the CIE technique the tear film was the antigen and an antibody rabbit anti human phospholipase C (αPLC, abcam ab32624) was selected. 5µl of tear film was collected with glass capillary as described in Chapter 2. The tear sample was this applied to the agarose/PEG8000 gel. The αPLC was applied to the gel opposite the tear samples at varying concentrations. A standard of 1mg/ml immunoglobulin A (IgA, Sigma I-1010) and (neat) rabbit anti human immunoglobulin A (αIgA, Sigma I-9889) was run along side the tear samples/αPLC lanes for verification of precipitation occurring.

The gel on the melinex was placed onto a Beckman Paragon Power Supply (Model 655803), bartbital buffer (B 5934) was used in the cells of the electrophoresis unit. Electrophoresis was induced by setting the voltage set at 50V for 60 minutes.

After electrophoresis the gel was immersed in 0.9% saline overnight to wash all unbound protein. The gels were then dried out by placing filter papers on top of the gel with a weight on top of the filter paper and placed by a window for approximately 24 hours. The filter paper and weights were removed and the gels were stained in Coomassie Brilliant Blue stain for 2 hours and transferred to destain until all background staining was removed. Coomassie Brilliant Blue stain and destain were made up as described in Chapter 2.

Figure 51 shows the results of a CIE experiment. This run included subject A tear film (TFA) versus αIgA, subject B tear film (TFB) versus αPLC at a concentration of 1:10 and TFA versus various concentrations of αPLC. The positive precipitation of TFA versus αIgA indicates that the electrophoresis had worked.

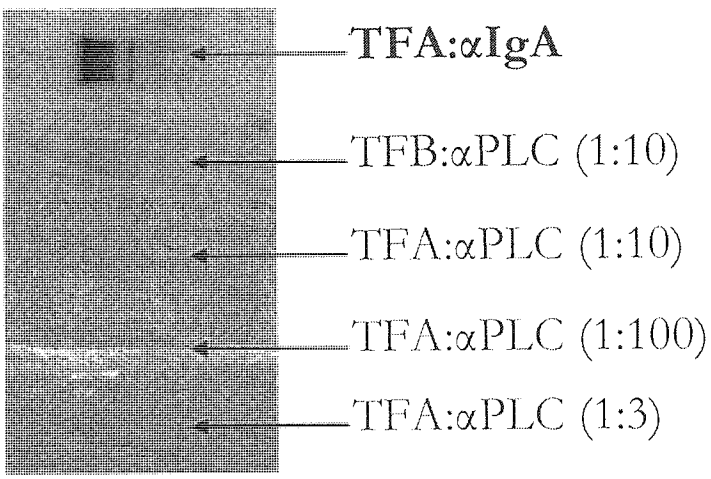

Figure 51. The results of counter immunoelectrophoresis (CIE) of TFA vs αIgA, TFA vs various concentrations of αPLC and TFB vs αPLC at a concentration of 1:10. Where TFA is tear film of subject A, TFB is tear film of subject B, αIgA is anti immunoglobulin A and αPLC is anti phopholipase C

The results of tear samples (TFA and TFB) versus the various concentrations of αPLC indicate that the presence of PLC in the tear film is below the level of detection for Coomassie brilliant blue staining which is 0.1μg/ml. Alternatively the chosen

antibody (rabbit anti human phospholipase C (αPLC, abcam ab32624)) was not specific for the isoform of PLC present in the tear film.

4.3.3 Detection of PLC in the tear film: Phosphatidylcholine-Specific Phospholipase C Assay for tear film PLC analysis

The Amplex® Red Phosphatidylcholine-Specific Phospholipase C Assay Kit (Molecular probes, A12218) provides a sensitive method for detecting the in vitro activity of phospholipase C (PLC) using a fluorescence microplate reader. This indirect method uses 10-acetyl-3,7-dihydrophenoxazine (Amplex Red reagent) (Figure 52) which acts as a fluorogenic probe for H_2O_2 [110].

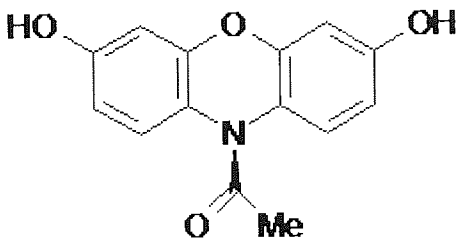

Figure 52. 10-acetyl-3,7-dihydrophenoxazine (Amplex red reagent)

The assay relies on the conversion of phosphatidylcholine to resorufin (7-Hydroxy-3-iso-phenoxazin-3-one); Initially PLC acts on the phosphatidylcholine substrate to produce phosphocholine (PC) and diacylglycerol (DAG). Alkaline phosphatise then hydrolyzes the PC to produce choline. The choline is oxidized by choline oxidase to form betaine and H_2O_2 [111]. The Amplex Red reagent reacts with H_2O_2, in the presence of horseradish peroxidise to form resorufin, with 1:1 stoichiometry [110-112]. The reaction scheme is shown in Figure 53.

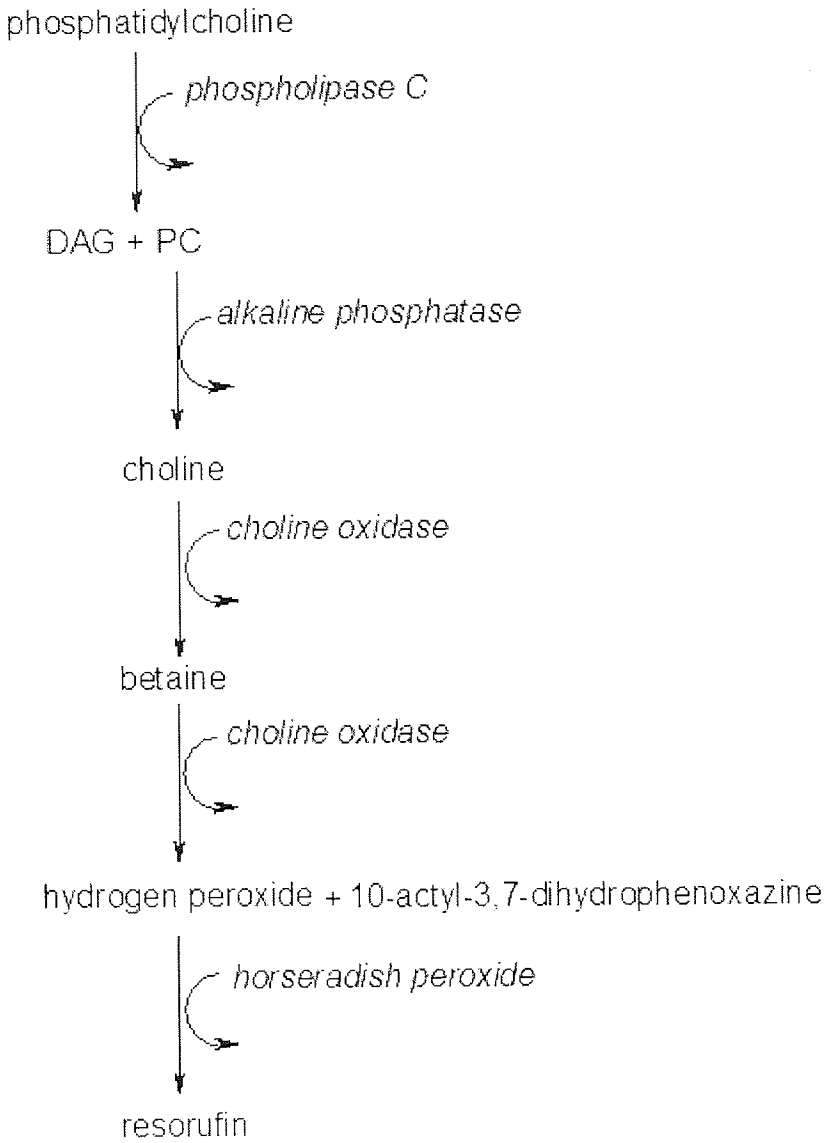

Figure 53. Reaction scheme for the conversion of phosphatidylcholine to resorufin

Resorufin has absorption and fluorescence emission maxima of approximately 571 nm and 585 nm, respectively and so there is little interference from autofluorescence in most biological samples.

The Amplex® Red Phosphatidylcholine-Specific Phospholipase C Assay Kit was used to determine the activity of PLC in tear samples. The assay allows the construction of a concentration curve from which the activity of tears can be calculated. A Spectra max M2 plate reader was used to perform the fluorescence spectroscopy. The Spectra max M2 plate reader was set to excite at 545nm and collect the emissions at 590nm.

Tear Samples of 5 and 10μL were taken from subjects AM and DC and were used immediately or stored at -80°C until required. The samples were collected by glass capillary as described in Chapter 2 and were applied to the 96 well plate immediately before the assay. The samples and standards were prepared as indicated in the kits methods.

The standards used for the calibration curve contained 100, 50, 25 and 10mU/ml of *B. cereus* phosphatidylcholine-specific phospholipase C (PC-PLC), these were produced from serial dilutions of a stock solution containing 100 mU/mL. The standards of 100, 50, 25 and 10mU/ml gave fluorescence emissions of 4987.62, 4571.90, 4461.26 and 4396.26 units respectively. This data and the calibration curve produced from the standards are shown in Figure (Figure 54). The slope calibration curve has an R^2 value of 0.98 but was found to be non linear in the region below 10mU/ml.

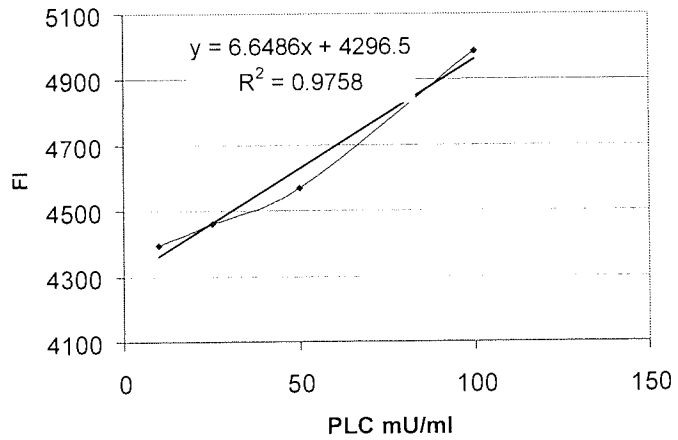

Figure 54. Standard curve for the detection of activity of phospholipase C. N=3, ±SD

The samples activity was then to be assayed by measuring the fluorescence emission and using the equation of the slope (y=mx+c) from the calibration curve to give an activity in mU/ml. The samples results were not on the linear part of the calibration curve so the results using y=mx+c gave negative mainly activities as shown in Table 24, where FI is the fluorescence intensity.

Table 24. PLC activity in the tear film

Sample	volume / µL	FI	mu/ml
AM1	10	3426.33	-131.33
DC2	10	3285.89	-152
AM12	20	3584386	-107.04
DC22	20	4465.38	25.4

It was decided to construct a calibration curve for the region below 10mU/ml PC-PLC using the data for 25 and 10mU/ml PC-PLC and a control with no PC-PLC. The control gave a fluorescence emission of 2.245units. The r^2 of this slope produced was 0.66 and so it is not a robust calibration curve. The activities of the samples were recalculated using this second calibration curve and the results are shown in Table 25.

Table 25. PLC activity in the tear film using second calibration curve

Sample	volume / µL	FI	mu/ml
AM1	10	3426.33	14.52
DC2	10	3285.89	16.69
AM12	20	3584386	15.51
DC22	20	4465.38	20.85

The tear film samples gave an activity of PC-PLC for 10µL of ~15mU/ml which is equivalent to the removal of head groups from PC at a rate of ~ 15µM/minute. The PC-PLC for 20µL of tear fluid is higher as would be expected but the relationship does not appear to be a linear one.

4.3.4 Detection of PLC in the tear film: Summary

The CIE showed the presence of PLC in the tear film is in concentrations below the level of detection for Coomassie brilliant blue staining (0.1µg/ml). Alternatively the chosen antibody (rabbit anti human phospholipase C (αPLC, abcam ab32624)) was

not specific for the isoform of PLC present in the tear film. The concentration of a lipase should be at low as species such as lipases and enzymes are generally not required at high concentrations to perform their function. The PC-PLC assay showed that PLC activity can be detected in the tear film at level that would lyse phospholipids.

4.4 Conclussions

The phospholipids were below the level of detection for the Dittmer's solution indicating they were present in the tear film at lower concentrations than previously thought. The TLC experiments supported the findings in Chapter 3.

The TLC also showed the presence of diacylglycerides (DAG) in the tear film which was unexpected. The concentration has not been established but the TLC plate's level of iodine staining indicates that the concentration is significant. The concentration of DAG in meibomian gland secretions is relatively low with the literature reporting diesters at 2.4% of the total lipid composition [33-36, 108]. When reading the literature most of these sources of DAG cite Nicoladides [34] and reviewing this paper shows that the DAG reported are split into three types. The type we are interested in for this work is the alpha, omega type II (consisting of alpha, omega-diols esterified to 2 moles of fatty acids). This type of DAG only represents a portion of the 2.4% as shown by Nicholaides. The low concentration of DAG in meibomian gland secretions has also been shown recently by TLC [113] and LCMS [114]. It would appear that DAG is not present in meibomian gland secretions or present at very low concentrations. Therefore the source of the DAG in the tear film is presumed not derived from MGS.

The lack of DAG in the tear meibomian gland secretions is also shown by Nagyová and Tiffany [47] who in the same publication show the appearance of a previously unidentified spot in TLC analysis of the tear film. This spot elutes where DAG should appear in the TLC experiment (Figure 55 [47]). The appearance of this previously unassigned spot now becomes more significant when the low concentrations of phospholipids and the activity of PLC in the tear film is highlighted.

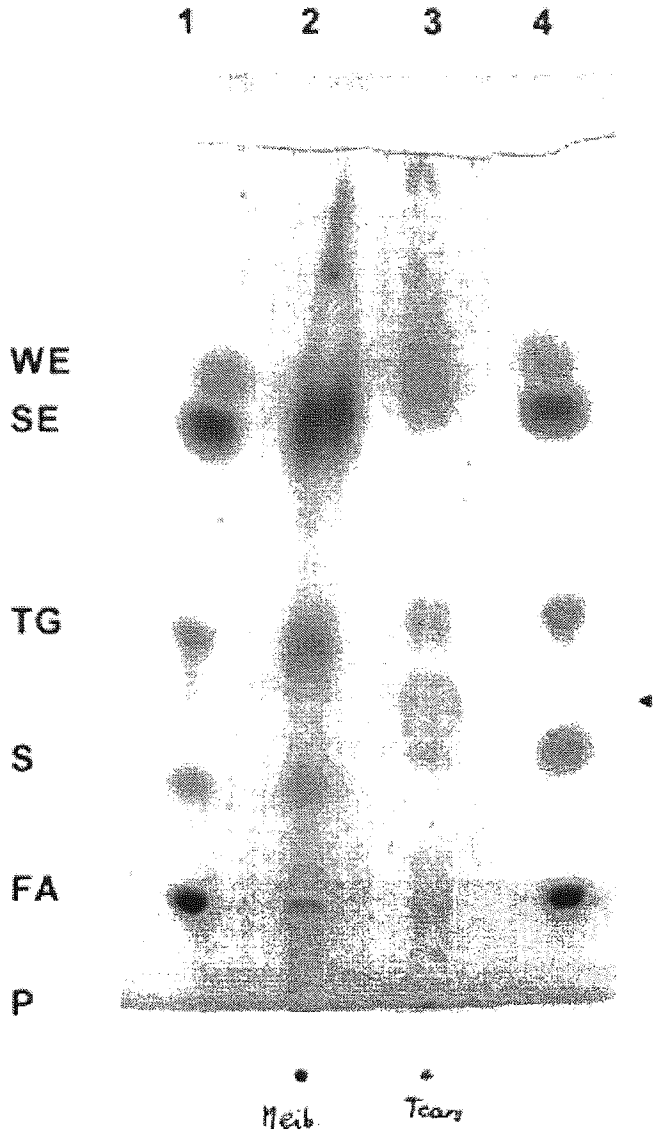

Figure 55. TLC plate of human tear lipids (lane 3) and meibomian gland lipids (lane 2). Lanes 1 and 4 are standards of lipid classes: WE, wax esters; SE, sterol esters; TG: triacylglycerides; S: free sterols; FA: free fatty acids; P: phospholipids. Unidentified additional spots indicated by the arrow head are present in the tears [47].

One potential route for the appearance of DAG in the tear film is the decomposition or degradation of species that are presented to it by the MGS. The presence of DAG in the tear film could occur via the action of a lipase such as PLC on the phospholipids to produce DAGs and the associated headgroup.

The possibly presence of LPC and PA in the tear film as indicated by the iodine staining of the plate show that the phospholipids could be degrading possibly via the action of lipases. The cleavage specificities of phospholipases are shown in Figure 56.

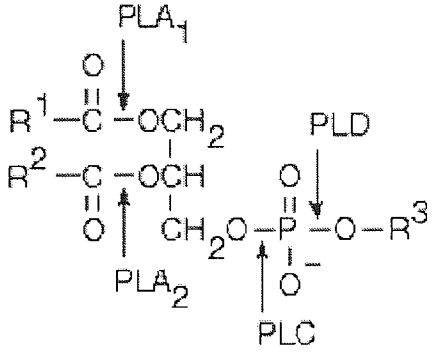

Figure 56. Cleavage specificities of phospholipases, PL indicates phosphlipase with the site specificity shown by the suffix A1, A2, C or D

The phopholipases are named by the site where they act on the phospholipid, for example phospholipase A_1 (PLA_1) is named because it acts on the SN_1 position in the phospholipids to cleave a fatty acid. The SN_1 position is where the fatty acid moiety is attached to the glycerol backbone of the phospholipids. The phospholipases then are phospholipase A_1 (PLA_1), phospholipase A_2 (PLA_2), phospholipase C (PLC) and phospholipase D (PLD).

The degradation of phospholipids via the PLA_1 or PLA_2 enzymes would produce LPC as seen at the origin on the iodine stained polar TLC plate as reported in section 4.2.4. The degradation of phospholipids via the PLD enzymes would produce PA as seen at R_f 0.61-0.69 on the iodine stained polar TLC plate also reporte in section 4.2.4. The degradation of phospholipids via the PLC enzymes would produce diacylglycerols (DAG). We see DAGS in the tear film at relatively high concentrations if we compare the intensity of staining of DAGs and TAGs on the non polar TLC plate. The appearance of high concentrations of DAGs in the tear film could be explained by the enzymatic action of PLC.

The PC-PLC assay showed there was an activity PLC in the tear film. This activity was ~15mU/ml for the 10μL samples which is equivalent to the removal of head groups from PC at a rate of ~15μM/minute and the PC-PLC activity for the 20μL samples is higher, as would be expected.

The lipids of the tear film are composed of an average of 3.52μg/μl [31, 41, 42] and the tear phospholipids are thought to be ~6.1% of this composition [33-36, 108]. If phosphatidylcholine (PC) composes of ~40% of the phospholipids [39, 40] then PC in the tear film should be represented of 0.08μg/μl of the lipids present.

If we take the average PC mass as 734g/mol (as the PC is made up from DMPC, DPPC and DPPC) we find that there should be ~117μM (micromoles) of PC present in the tear film. The measured activity of the PLC (~15mU/ml) could account for the removal of ~12.8% of the PC present in the tear film per minute. This would not account for the differences seen in the concentrations of PC in meibomian gland secretions from the literature and those described in section 4.2 and Chapter 3.

Although the activity of PLC is lower than required to explain the differences seen between the literature values of phospholipids and those seen in section 4.2 and Chapter 3 the activity is present. The PC-PLC activity assay was performed under different conditions than those found in the tear film and this may have altered the outcome of the assay. For example osmolarity and calcium ions concentration would all be expected to have an effect. The osmolarity of the assay kit is different from that of the tear film and this may have made a difference to the assay. Calcium levels are known to be of particular importance in the activity of phospholipases. The tear film contains other species that may act in synergy with or increase the activity of PLC to lyse the phospholipids at increased rates.

Further support for the low concentration of phospholipids is the monolayer requirement. Much less phospholipid is required to form a precorneal monolayer than is provided by the MGS. The current model of the tear film as proposed by McCulley and Shine [115] is one where the polar lipid layer acting as a bridge between the aqueous layer and a non polar lipid layer.

The area of this polar interface layer can be calculated. If we use DPPC as a model lipid of this layer which has a minimum area per molecule of DPPC is experimentally $85A^{o2}$ [116] and given that the area of the ocular aperture has been approximated to $1.5x10^{7}$ – $3.5x10^{7}$ A^{o2} [117], this would mean that the polar interface requires approximately $2.2x10^{-9}$ – $5.0x10^{-9}$ μg of material to form a monolayer film.

This calculation uses DPPC as a model lipid and considers a perfectly ordered lipid monolayer which would not be the case in the tear film. In the tear film there are other lipid species present and these would interact with the monolayer, for example the inclusion of cholesterol in the monolayer would create a much less expanded monolayer. However the monolayer requirement would still need a much lower concentration of phospholipid than the amount provided by the meibomian gland secretions (which is approximately 0.22μg - instantaneous average).

Chapter 5 – Zwitterionic and charge-balanced hydrogels

"Promising results have also been obtained in other experiments, for example, in manufacturing contact lenses"

Otto Wichterle

5.1 Introduction to zwitterionic and charge-balanced hydrogels

Zwitterionic compounds, or zwitterions, are electrically non polar compounds having an equal number of formal unit charges of opposite sign. They are a subclass of ampholytes which are molecules that contain both acidic and basic groups (and are therefore amphoteric) and exist as zwitterions at a certain pH. This pH is known as the molecule's isoelectric point. Zwitterions are sometimes referred to as betaines, dipolar ions (a misnomer), inner salts and ylides [118]. Zwitterions are polar molecules and usually have a high solubility in water and a poor solubility in most organic solvents.

Zwitterionic monomers are zwitterions with polymerisable functional groups and polyzwitterions are polymers prepared by polymerization of zwitterionic monomers. In common polyzwitterions the zwitterionic groups are usually located in pendent groups rather than the backbone of the macromolecule. They contain both the anion and cation in the same monomeric unit unlike a polyampholyte which can contain the anion and cation in different monomeric units.

Hydrogel materials produced from zwitterionic monomers have been proposed for use and are used in biomaterial applications such as tissue engineering scaffolds [119], coatings [120], bioactive membranes [121], drug delivery vehicles [122], bioassay media [123] and as contact lenses.

There is only one commercial zwitterionic material in the contact lens field. This material is known as omafilcon A and it used in the production of Proclear Compatible contact lenses marketed by Coopervision. Omafilcon A is a copolymer of 2-hydroxyethyl methacrylate (HEMA) and 2-methacryloyloxyethyl phosphoryl choline (MPC) crosslinked with ethyleneglycol dimethacrylate.

The MPC monomer used in the production of Proclear Compatibles is based on the patents of Hayward and Chapman [124] who produced a polyconjugated polymer from a diacytelenic phosphoryl choline containing monomer and Kadoma, Nakabayashi et al [125] who introduced the MPC monomer (Figure 57).

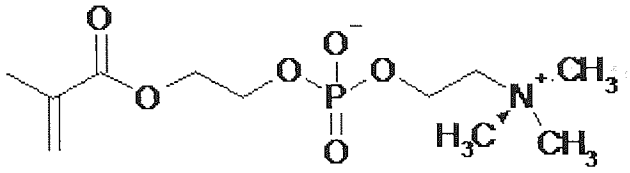

Figure 57. The structure of 2-methacryloyloxyethylphosphorylcholine (MPC)

The use of MPC in biomaterials is an example of the biomimetic approach to material design. The phosphoryl choline group of MPC are also found naturally in phospholipids which are prominent molecules at biomembranes. The MPC monomer used in a biomaterial is trying to replicate favourable interactions of the phosphoryl choline group with its environment.

Polymers containing zwitterionic groups or materials coated with zwitterionic groups have been shown to reduce bacterial adhesion [126-128], resist protein deposition [129, 130] and also have low water contact angles [131]. All of these features are valuable for biomaterials. Polymers containing sulfobetaines may have some advantage over phosphobetaines in these features, for example a lower proportion of sulfobetaine (compared to phosphobetaine) is required to provide the same degree of resistance to bacterial adherence [132] and reduced advancing contact angles when compared to similar polymers containing phosphobetaines [133].

Some synthetic routes used to producing polyzwitterions do not incorporate the monomer as it is used in the final material. A precursor monomer is used in the formulation and after polymerisation a subsequent reaction forms the zwitterion. This can be established for example on acrylates via sulfobetanisation using 1,3-propanesultone (Figure 58). This approach to zwitterionic material production can prove to be a problem as 1,3-propanesultone is toxic and so any residuals from the sulfobetanisation would need to be removed.

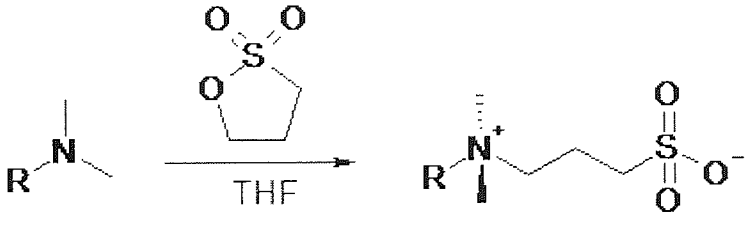

Figure 58. Sulfobetanisation reaction scheme

A sulfobetaine monomer was recently introduced by Raschig, GMBH. This monomer is N,N-dimethyl-N-(2-acryloylethyl)-N-(3-sulfopropyl) ammonium betaine (SPDA) (Figure 59). SPDA is the acrylate derivative of N,N-dimetyl-N-(2-methacryloylethyl)-N-(3-sulfopropyl) ammonium betaine (SPE). Both SPE and SPDA monomers can be structurally compared to MPC as both are acrylate-based monomers that contain quaternary nitrogen groups. The major difference is that MPC has a phosphorylcholine group while SPDA has a sulfonate group and these are positioned differently in the molecule. The use of SPDA in the copolymerisation step would remove the requirement for sulfobetanisation.

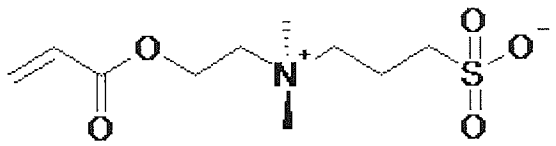

Figure 59. The structure of N,N-dimetyl-N-(2-acryloylethyl)-N-(3-sulfopropyl) ammonium betaine (SPDA)

As part of a programme investigating the potential of SPDA in ophthalmic biomaterials its co-polymerisation and compatibility with other contact lens forming monomers has been studied. This chapter describes some aspects of the polymerisation and properties of SPDA copolymers relevant to its potential use as a contact lens material and also compares the zwitterionic SPDA copolymer to synthesised charge-balanced (polyampholyte) copolymers.

5.2 *Synthesis of charge-balanced copolymer membranes*

5.2.1 Introduction to synthesis of charge-balanced copolymer membranes

This section describes the synthesis of charged-balanced (polyampholyte) copolymer membranes. Polyampholytes are macromolecules which contain anionic and cationic groups in different monomeric units. The cationic and anionic monomers were formulated to be present in equimolar ratios so the positive or negative charges associated with the monomers were balanced to give neutrality in the final polymer. The properties of the resulting charge-balanced copolymers could be used to compare to the "naturally" chage-balanced zwitterionic SPDA copolymers.

Cationic or potentially cationic monomers were chosen which contained amide or quaternary nitrogen functional groups. Throughout this thesis the term *cationic monomers* is used to represent both cationic and potentially cationic monomers. It is known that monomers containing amine functional groups can have a distinctive associated aroma. If such monomers are exposed to gamma (γ) ray irradiation the result can be the production of an additional aroma. The amine containing monomers are thought to undergo degradation as a result of exposure to γ ray. This property may stop the monomers use in products. It was decide that all of the selected monomers should be exposed to γ ray irradiation to establish which would undergo these degradative processes. This was used as a method of selection for monomers.

Two cationic monomers were selected after this process. It transpired that there was one acrylate and one acrylamide. These were 2-(diethylamino) ethyl methacrylate and 3-(dimethylamino) propyl methacrylamide. These differ in structure by the amide and ester functional groups but also by there being a propyl group in the acrylamide monomer but an ethyl group in the acrylate monomer. The selected cationic monomers were then copolymerised with the chosen anionic monomer, 2-acrylamido-2-methylpropane sulfonic acid (AMPS) in the presence of 2-hydroxyethyl methacrylate to produce the charged-balanced copolymer membranes.

5.2.2 Cationic monomers selected for charge-balanced copolymer membranes

This section outlines the cationic monomers initially chosen for synthesis. The cationic monomers were chosen as they contained quaternary nitrogen functional groups which were positively charged or tertiary nitrogen groups which had the potential to become charged under the appropriate conditions. The cationic monomers selected were:

- 2-(dimethylamino) ethyl methacrylate
- 2-(dimethylamino) ethyl methacrylate dimethyl sulfate
- 2-(dimethylamino) ethyl acrylate
- 2-(diethylamino) ethyl methacrylate
- 3-(dimethylamino) propyl acrylate
- 2-(diethylamino) ethyl acrylate
- 3-(dimethylamino) propyl methacrylamide methyl chloride
- 3-(dimethylamino) propyl methacrylamide

Figure 60 shows the structures of the chosen cationic monomers for 2-(dimethylamino) ethyl methacrylate, 2-(dimethylamino) ethyl methacrylate dimethyl sulphate, 2-(dimethylamino) ethyl acrylate, 2-(diethylamino) ethyl methacrylate, 3-(dimethylamino) propyl acrylate and 2-(diethylamino) ethyl acrylate.

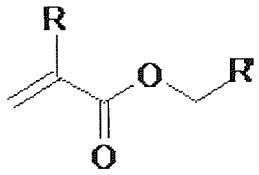

Figure 60. General structure of cationic monomers 1

Where

R = CH_3 and R' = $-CH_2N(CH_3)_2$	for 2-(dimethylamino) ethyl methacrylate
R = CH_3 and R' = $-CH_2N^+(CH_3)_3\ SO_4^-$	for 2-(dimethylamino) ethyl methacrylate dimethyl sulfate
R = CH_3 and R' = $-CH_2N(CH_2CH_3)_2$	for 2-(diethylamino) ethyl methacrylate
R = H and R' = $-CH_2N(CH_3)_2$	for 2-(dimethylamino) ethyl acrylate
R = H and R' = $-CH_2N(CH_2CH_3)_2$	for 2-(diethylamino) ethyl acrylate
R = CH_3 and R' = $-CH_2CH_2N(CH_2CH_3)_2$	for 3-(dimethylamino) propyl acrylate

Figure 61 shows the structures for 3-(dimethylamino) propyl methacrylamide and 3-(dimethylamino) propyl methacrylamide methyl chloride.

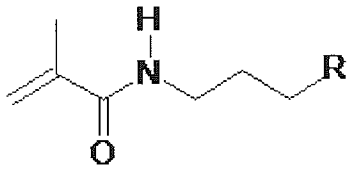

Figure 61. General structure of cationic monomers 2

Where

R = $-N(CH_3)_2$ for 3-(dimethylamino) propyl methacrylamide

R = $-N^+(CH_3)_3$ for 3-(dimethylamino) propyl methacrylamide methyl chloride

The structure of AMPS is shown inFigure 62.

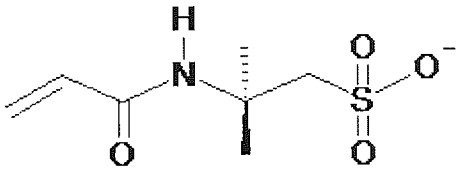

Figure 62. The structure of 2-acrylamido-2-methylpropane sulfonic acid (AMPS)

5.2.3 Sterilisation of monomers for charge-balanced membranes

This section describes the sterilisation of the selected cationic monomers. Sterilisation of biomaterials is important and common methods used are autoclave, ethylene oxide, electron beam, beta irradiation and gamma (γ) ray irradiation. The choice of method depends upon the material being sterilised and autoclaving is usually used in the manufacture of soft contact lens materials.

If a material, for example partially hydrated hydrogels can not undergo autoclaving because the material will swell under conditions of increased humidity γ ray irradiation can be used. As the synthesised materials may be utilised in applications

where γ ray irradiation is the chosen method of sterilisation it was thought that the effect of γ ray irradiation on the polymer and monomers should be known.

The monomers were sterilised by γ ray irradiation and this process induced an aroma from some of the selected monomers. Table 26 shows the aroma of cationic monomers before and after γ ray irradiation. It is known that some amine containing species have an associated aroma dependant on the volatility of the amine groups. The production of an aroma or an additional aroma during γ ray irradiation could be due to any amine groups in the monomers susceptibility to Hoffman degradation mechanisms. The Hoffman elimination reaction produces amines of higher substitution and therefore of lower boiling point.

Table 26. Aroma of cationic monomers before and after gamma (γ) ray irradiation

Monomer	aroma pre gamma	aroma post gamma
2-(dimethylamino) ethyl methacrylate	very smelly, fishy	no worse
2-(dimethylamino) ethyl acrylate	"	worse, fishy
2-(dimethylamino) ethyl methacrylate dimethyl sulfate	little smell	no worse
2-(diethylamino) ethyl methacrylate	"	worse, fishy
3-(dimethylamino) propyl acrylate	"	no worse
2-(diethylamino) ethyl acrylate	"	worse, fishy
3-(dimethylamino) propyl methacrylamide	medicinal smell	no worse
3-(dimethylamino) propyl methacrylamide methyl chloride	"	gained fishy smell

The monomers which produced no additional aromas after γ ray irradiation were 2-(dimethylamino) ethyl methacrylate, 2-(dimethylamino) ethyl methacrylate dimethyl sulphate, 3-(dimethylamino) propyl acrylate and 3-(dimethylamino) propyl methacrylamide.

The monomers which produced additional aromas after γ ray irradiation 2-(dimethylamino) ethyl acrylate, 2-(diethylamino) ethyl methacrylate, 2-(diethylamino) ethyl acrylate and 3-(dimethylamino) propyl methacrylamide methyl chloride.

The monomers were also sterilised by autoclave separately. The autoclave procedure was 121°C, under pressure for 30 minutes. The monomers sterilised by autoclave showed no increased aroma. There was a colour change of the 3-(dimethylamino)

propyl acrylate and the 3-(dimethylamino) propyl methacrylamide methyl chloride, from clear to cloudy.

2-(Diethylamino) ethyl methacrylate and 3-(dimethylamino) propyl methacrylamide which did not produce additional aromas were selected polymerisation studies. It was expected that they would produce polymers that were equally free from additional aromas after being exposed to γ ray irradiation.

5.2.4 Compositions for charge-balanced copolymer membranes

This section describes the monomer compositions that were used to synthesise the charged-balanced copolymer membranes. The cationic monomers chosen for their stability to γ ray irradiation as described in section 5.2.3 were 2-(dimethylamino) ethyl methacrylate (DMAEMA) and 3-(dimethylamino) propyl methacrylamide (DMAPMA).

A series of compositions was produced from the cationic and anionic monomers. The anionic monomer was 2-acrylamido-2-methylpropane sulfonic acid (AMPS). The cationic and anionic monomers were present in the compositions in stiochiometric ratios so that when polymerised they should produce membranes of overall charge neutrality. For example in a typical 5g monomer composition (DCNA31) there was 2.6%wt (0.13g) of DMAEMA and 2.9%wt (0.15g) of AMPS giving 2.15×10^{-4}mol of DMAEMA and 2.17×10^{-4}mol AMPS.

The compositions had ~5, 10 and 20%wt of the ionic monomers as shown in Table (Table 27). The other ~95, 90 or 80%wt was composed of 2-hydroxyethyl methacrylate (HEMA), the structure of which is shown in Figure 63. A control membrane was produced using HEMA as the monomer (DCNA30). The DMAEMA: AMPS series of compositions were labelled DCNA31-32 and the DMAPMA: AMPS series of compositions were labelled DCNA41-43 and are shown in Table 27.

Table 27. Composition of charge-balanced (polyampholyte) membranes

	DMA EMA / %	DMA PMA / %	AMPS / %	X / %	HEMA / %
DCNA30	0.0	0.0	0.0	0.0	100.0
DCNA31	2.6	0.0	3.0	5.6	94.4
DCNA32	4.4	0.0	5.0	9.4	90.6
DCNA33	10.0	0.0	11.3	21.3	78.7
DCNA41	0.0	2.6	2.9	5.4	94.6
DCNA42	0.0	4.4	5.0	9.5	90.5
DCNA43	0.0	9.1	10.0	19.1	80.9

Where DMA EMA is 2-(dimethylamino) ethyl methacrylate, DMA PMA is 3-(dimethylamino) propyl methacrylamide, AMPS is 2-acrylamido 2,2 methylpropane sulphonic acid, X is the total percentage of ionic monomers and HEMA is 2-hydroxyethyl methacrylate. % is by weight

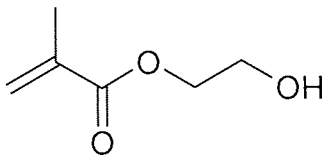

Figure 63. The structure of 2-hydroxyethyl methacrylate (HEMA)

5.2.5 Polymerisation of charge-balanced copolymer membranes

Monomer preparation and polymerisation were carried out as outlined in the Chapter 2. Polymerisation was thermally induced using 2,2-azobisisobutyronitrile (AIBN) as initiator at 0.5%wt. Ethylene glycol dimethacrylate (EGDMA) was used as a crosslinker at 1%wt.

The HEMA control (DCNA30), 2-(dimethylamino) ethyl methacrylate (DCNA31-32) and 3-(dimethylamino) propyl methacrylamide (DCNA41-43) composition solutions as described in section 5.2.4 all polymerised to produce clear and cohesive membranes. Once polymerised the membranes were then swollen to their equilibrium water content (EWC) by soaking in phosphate buffered saline for three days, changing to a fresh soaking medium daily.

5.2.6 Sterilisation of charge-balance copolymer membranes

Samples of the HEMA control membrane (DCNA30), 2-(dimethylamino) ethyl methacrylate copolymer membranes (DCNA31-32) and 3-(dimethylamino) propyl methacrylamide copolymer membranes (DCNA41-43) were autoclaved and sent for gamma (γ) ray irradiation separately. The use of γ ray irradiation was to ascertain if the polymers were stable to γ ray as some of the cationic monomers were shown to be unstable and degrade under these conditions.

The membranes did not change in appearance or produce an additional aroma after autoclaving or γ ray irradiation. This indicates that the cationic pendant groups were stable to sterilisation by γ ray irradiation after polymerisation.

5.3 Synthesis of N,N-dimethyl-N-(2-acryloylethyl)-N-(3-sulfopropyl) ammonium betaine (SPDA) copolymer membranes

5.3.1 Introduction to synthesis of SPDA copolymer membranes

The charged-balanced copolymers membranes described in section 5.2 are composed of cationic and anionic monomers. These monomers must be used in equimolar ratios if a neutrally charged copolymer was to be produced. Even when the cationic and anion monomers used in eqimolar ratios the charge-balanced copolymer membranes may have the charges distributed unevenly. This could produce a material with localised charges. The SPDA monomer is zwitterionic and as such has the positive and negative charged moieties on one monomeric unit. When SPDA or other zwitterionic monomers are polymerised they will always produce a charge-balanced polymer, as long as no other ionic species are present. Section 5.3 describes the synthesis of SPDA copolymer membranes.

5.3.2 Sterilisation of zwitterionic monomers

Gamma (γ) ray irradiation is used as a method of sterilisation when autoclaving is not possible (as explained earlier). Investigation of some of the cationic monomers showed that when they were subjected to γ ray irradiation they produced an additional aroma. This aroma possibly arose due to the degradation of amine groups present. The SPDA monomer also contains an amine group which could possibly degrade when subjected to γ ray irradiation. The SPDA monomer was γ ray irradiated to establish its stability when exposed to these conditions. A selection of other zwitterionic monomers was also subjected to γ irradiated for comparison. These monomers were:

- 2-methacryloyloxyethyl phosphorylcholine (MPC)
- 1-(3-Sulfopropyl)-2-vinylpyridinium-betaine (SPV)
- N,N-dimethyl-N-(2-methacrylamidopropyl)-N-(3-sulfopropyl) ammonium betaine (SPP)

The structures for the zwitterionic monomers SPDA, MPC, SPV and SPP are shown in Figure 64.

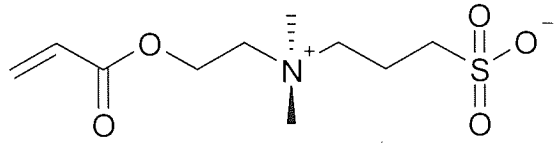

N,N-dimethyl-N-(2-acryloylethyl)-N-(3-sulfopropyl) ammonium betaine (SPDA)

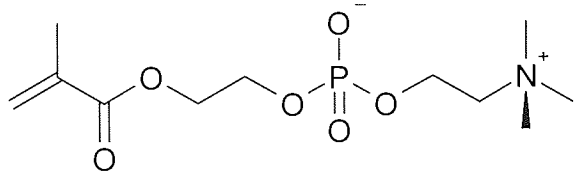

2-methacryloyloxyethyl phosphorylcholine (MPC)

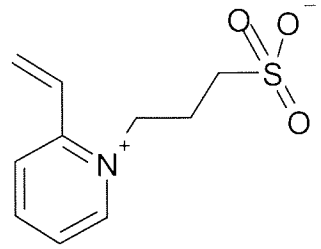

1-(3-Sulfopropyl)-2-vinylpyridinium-betaine (SPV)

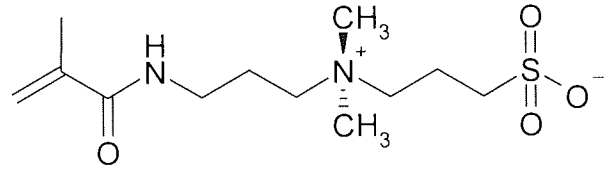

N,N-dimethyl-N-(2-methacrylamidopropyl)-N-(3-sulfopropyl) ammonium betaine (SPP)

Figure 64. Structures of zwitterionic monomers subjected to gamma (γ) ray irradiation

The SPDA, SPV and SPP monomers did not produce an additional aroma when γ ray irradiated. The MPC monomer produced an additional aroma after the γ ray irradiation. Comparison of the structures shows that the monomers that did not produce an additional aroma after γ irradiation were the sulfobetaines where the sulfonate placed as a terminal group of the inner salt. Whereas MPC where the quaternary nitrogen containing group placed terminally is a phosphobetaine.

5.3.3 Compositions for SPDA copolymer membranes

This section describes the compositions that were prepared for the SPDA copolymer membranes. 2-hydroxyethyl methacrylate (HEMA), N-vinyl pyrrolidone (NVP) and

acryloylmorpholine (AMO) are monomers that are used in many biomedical applications. To assess if SPDA would copolymerize with these monomers compositions of HEMA, NVP and AMO were prepared with SPDA in a ratio of 1:1 initially.

Monomer preparation and polymerisation were carried out as outlined in Chapter 2. Polymerisation of these compositions was thermally induced using 2,2-azobisisobutyronitrile (AIBN) as initiator (0.5%wt) and ethylene glycol dimethacrylate (EGDMA) as a crosslinker (1%wt). All three compositions polymerised to produce clear and cohesive membranes.

After the initial polymerisation of SPDA with HEMA, NVP and AMO produced suitable membranes it was decided to synthesise a series of copolymer membranes from HEMA and SPDA. HEMA was selected as conventional contact lens materials are commonly based on this monomer. The SPDA:HEMA compositions had the SPDA comonomer ranging from 0 to 100% (with the remaining composition percentage being HEMA) (Table 28). The SPDA:HEMA compositions were labelled DCNA1, 2, 5-10 and 12. A control membrane was also prepared from a composition of 100% HEMA (DCNA11).

Table 28. N,N-dimethyl-N-(2-acryloylethyl)-N-(3-sulfopropyl) ammonium betaine (SPDA) containing membranes

Gel	SPDA / %	HEMA / %
DCNA07	70	30
DCNA06	50	50
DCNA01	45	55
DCNA02	33	67
DCNA05	29	71
DCNA08	20	80
DCNA09	15	85
DCNA13	10	90
DCNA12	5	95
DCNA10	0	100
DCNA11	100	0

The two monomers in this series of membranes make up 70% of the total weight of the compositional solution with water composing the other 30%. For example a typical compositional solution for a SPDA membrane DCNA07 is composed of

~49%wt SPDA, ~21%wt HEMA and ~30%wt water, with SPDA constituting ~70%wt and HEMA ~30%wt of the monomer present.

5.3.4 Polymerisation of SPDA copolymer membranes

Monomer preparation and polymerisation were carried out as outlined in Chapter 2. The SPDA membranes were polymerised thermally using 2,2-azobisisobutyronitrile (AIBN) as initiator (0.5%wt) and ethylene glycol dimethacrylate (EGDMA) as a crosslinker (1%wt).

Once polymerised the membranes were swollen to their EWC by soaking in phosphate buffered saline for 3 days, changing the soaking medium daily. The series of compositions described in section 5.3.3 (DCNA1, 2, 5-10 and 12) polymerised to produce clear and cohesive membranes.

5.3.5 Sterilisation of SPDA copolymer membranes

Samples of the HEMA control (DCNA10) and the SPDA membranes (DCNA1, 2, 5-10 and 12) were autoclaved and also sent for gamma (γ) ray irradiation seperately. The use of γ ray irradiation was to ascertain if the polymers were stable to γ ray as some of the cationic monomers were shown to be unstable and degrade under these conditions as explained earlier.

The membranes did not change in appearance or produce an additional aroma after autoclaving. The zwitterionic membranes sent for γ ray irradiation were the 29 and 70% SPDA membranes (DCNA05 ad 07) and these produced a slightly ammonium aroma when γ ray irradiated. The SPDA monomer did not produced an additional aroma when exposed to γ ray so it was not expected for the SPDA membrane should be produce an aroma when γ ray irradiated.

5.3.6 NMR of SPDA monomer

As the γ ray irradiation of the SPDA membranes caused an aroma it was decided to analyse the SPDA monomers by proton NMR (^{1}H NMR) pre and post γ ray irradiation to see if additional information could be obtained even though the γ ray irradiation of SPDA monomer did not cause an additional aroma.

An explanation of NMR is beyond scope of this chapter. Briefly in ^{1}H NMR the protons that are different (chemically speaking) have different NMR frequencies because the chemical environment causes the local magnetic field for that nucleus to be unique. The "ppm" axis is used to report frequency differences that are scaled by the magnetic field strength. This allows the peak positions to be compared for spectra acquired at various magnetic field strengths, without having to do any conversions. Zero, on this PPM axis, is the frequency position (or chemical shift) of a compound called tetramethyl silane or TMS.

The NMR signals from the various chemically unique protons appear not as single peaks, but as multiplets of peaks. This is because the spins of the hydrogen nuclei bonded to neighbouring carbon atoms perturb the energy of the NMR signals.

The solvent used for the NMR analysis was deuterium oxide and the ^{1}H NMR spectra for the SPDA monomer prior to and after γ ray irradiation are shown Figure 65 and Figure 66 respectively.

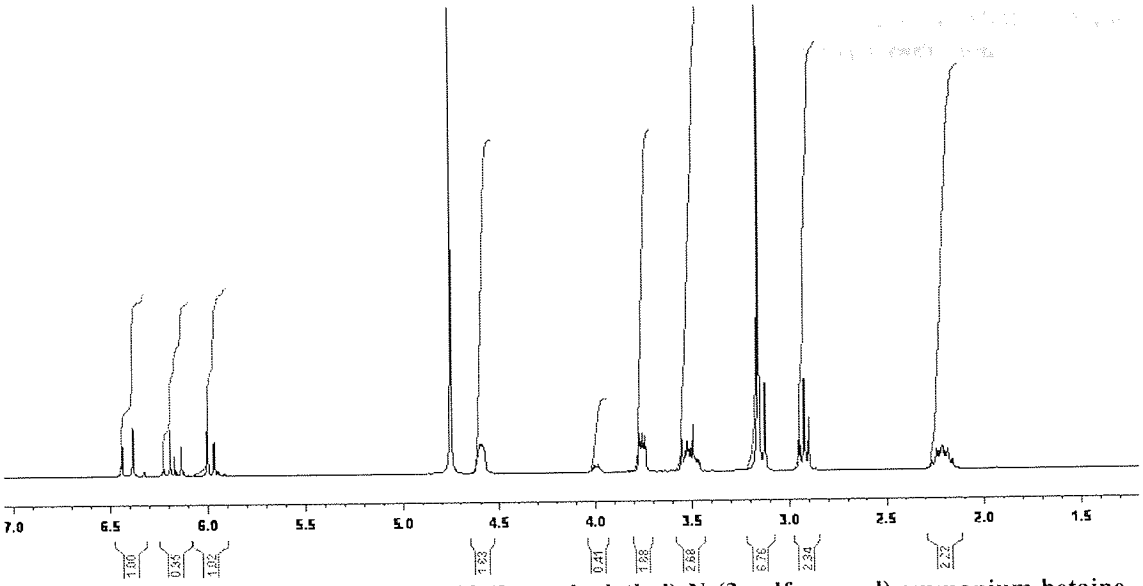

Figure 65. 1H NMR of N,N-dimethyl-N-(2-acryloylethyl)-N-(3-sulfopropyl) ammonium betaine (SPDA) before gamma ray irradiation

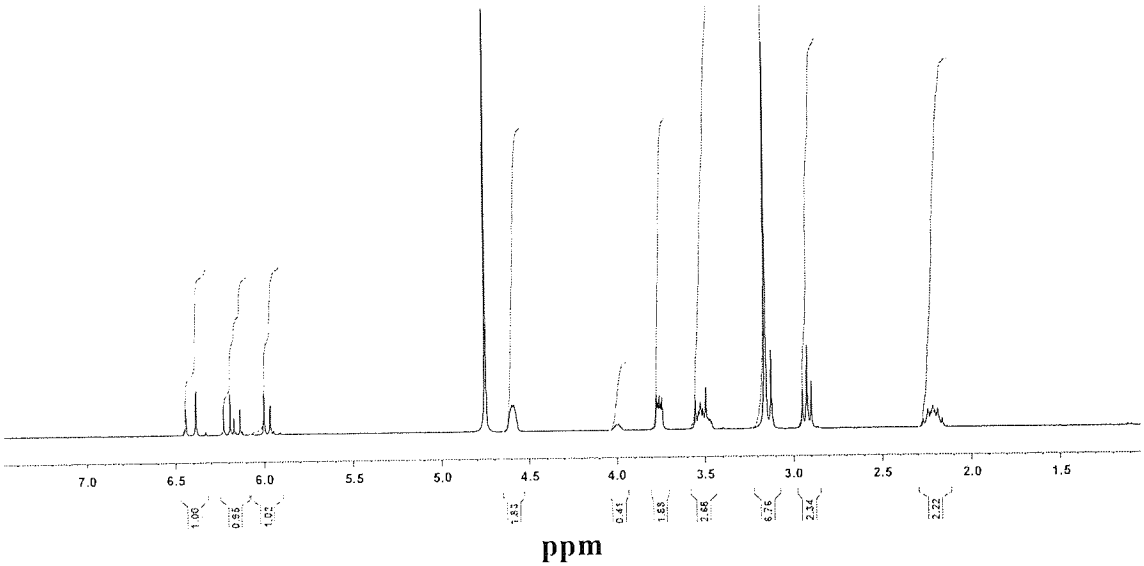

Figure 66. 1H NMR of N,N-dimethyl-N-(2-acryloylethyl)-N-(3-sulfopropyl) ammonium betaine (SPDA) after gamma ray irradiation

The peaks of interest in the SPDA monomer prior to γ ray irradiation are shown in Table 29. We see peaks at 2.3ppm, 2.9ppm, 3.5ppm and 4.6ppm with integrated values of ~2 which correspond to the four CH_2 groups present in the molecule. The peaks at 6ppm, 6.2ppm and 6.4ppm have an integrated value of ~1 and a splitting pattern which correspond to the allyl group. There is a peak at 3.2ppm with an integration value of 6.76 which correlates with the two methyl groups on the nitrogen.

Table 29. Peaks of interest in the 1H NMR specturm of N,N-dimethyl-N-(2-acryloylethyl)-N-(3-sulfopropyl) ammonium betaine (SPDA) proir to gamma ray irradiation

ppm	integration
2.3	2.42
2.9	2.37
3.2	6.62
3.5	2.68
3.8	1.88
4	0.41
4.6	1.83
6	1.02
6.2	0.95
6.4	1

ppm is parts per million

After γ ray irradiation there is the shifting and splitting of the peak at 3.2ppm to two peaks at 3.4ppm and 3.6ppm with integration values of 2.7 and 0.44 respectively. This along with the aroma reported from the membranes could indicate there is some instability of the polymer to γ ray irradiation. The possible degradation of the quaternary nitrogen could cause the production of amine species (Figure 67).

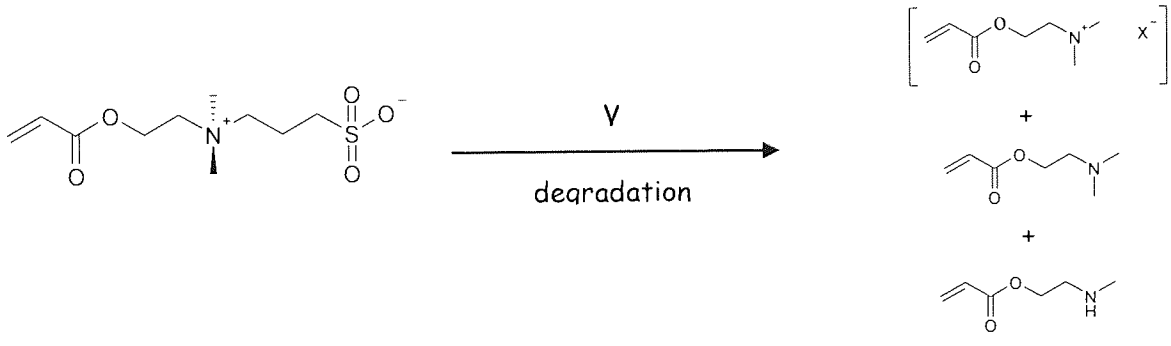

Figure 67. Possible degradation of N,N-dimethyl-N-(2-acryloylethyl)-N-(3-sulfopropyl) ammonium betaine (SPDA)

A similar peak splitting feature is seen in the ^{1}H NMR spectra of 3-(dimethylamino) propyl methacrylamide methyl chloride and 2-(dimethylamino) ethyl methacrylate dimethyl sulphate monomers. Both of these monomers have quaternary nitrogen within the molecule brought about by the presence of the methyl chloride or dimethyl sulphate additive. It may be the spectra seen for the SPDA monomer after γ ray

irradiation shows the presence of a group that is causing the quaternisation of the nitrogen in a similar way to these additives in the quaternised acrylates.

5.4 *Properties of charge-balanced copolymer and N,N-dimethyl-N-(2-acryloylethyl)-N-(3-sulfopropyl) ammonium betaine (SPDA) copolymer membranes*

Certain properties are important for the successful use of materials in contact lens applications. Among these properties are the equilibrium water content, mechanical properties, surface properties, oxygen permeability, optical transmittance and coefficient of friction. This section describes the analysis and results of these important properties for the charge-balanced copolymer and SPDA copolymer membranes.

5.4.1 Equilibrium water content (EWC) of copolymer membranes

EWC is described in Chapter 1. The EWC of the charge-balanced copolymer membranes and the SPDA copolymer membranes was determined by a gravimetric method [6]. The method is shown in Chapter 2.

5.4.1.1 Equilibrium water content (EWC) of charge-balanced copolymer membranes

The EWC of the control HEMA membrane (DCNA30) was 36.8±0.7% which is in good agreement with literature values. The EWC's of the HEMA control, 2-(dimethylamino) ethyl methacrylate (DCNA31-32) and 3-(dimethylamino) propyl methacrylamide (DCNA41-43) membranes are shown in Figure 68.

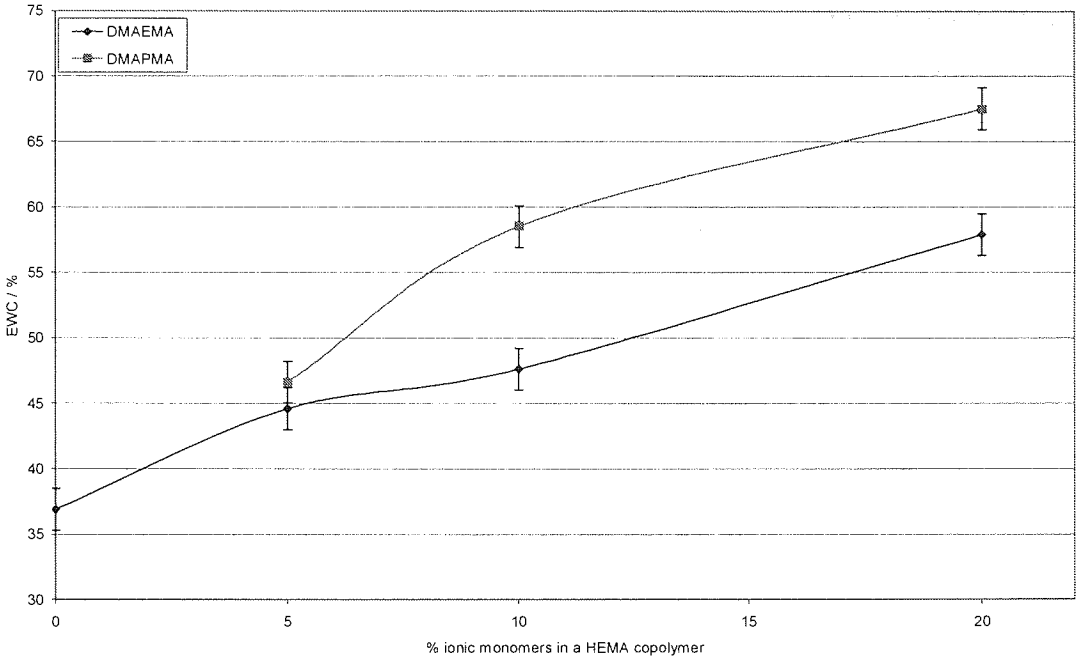

Figure 68. Equilibrium water content (EWC) of charge-balanced membranes. Where DMAEMA is 2-(dimethylamino) ethyl methacrylate, DMAPMA is 3-(dimethylamino) propyl methacrylamide and HEMA is 2-hydroxyethyl methacrylate. % ionic monomers is the weight percentage of the ionic pair in the HEMA copolymer, e.g. 5% ionic monomers in a HEMA copolymer for DMAEMA is 2.5% DMAEMA, 2.5% AMPS (2-acrylamido-2-methylpropane sulfonic acid) and 95% HEMA. N=5, ±SD

It can be seen that progressive increase of the ionic monomer pair 2-(dimethylamino) ethyl methacrylate:AMPS in the HEMA copolymer produces membranes with increased EWC. For example copolymerisation with ~5% of the 2-(dimethylamino) ethyl methacrylate:AMPS pair increases the EWC to 44.6±0.4%. Further increase to ~10% of the ionic pair in the copolymer produced a membrane with a EWC of 47.7±0.2%

Similarly the copolymerisation with ~5% of the 3-(dimethylamino) propyl methacrylamide:AMPS ionic pair increase the EWC to 46.7±0.7%. Further increase to ~10% of the ionic pair in the copolymer produced a membrane with a EWC of 58.5±0.4%.

While it is the sulfonate-containing AMPS monomer that would be expected to provide the majority of the increase in EWC, there is a difference between the

membranes containing the different ionic pairs. The 3-(dimethylamino) propyl methacrylamide:AMPS ionic pair copolymer membranes have higher EWC than the 2-(dimethylamino) ethyl methacrylate:AMPS ionic pair membranes copolymer. The difference between the two ionic pairs is not statistically significantly at ~5%. At higher percentages of ionic pair copolymerisation this difference becomes more apparent and statistically significant.

Comparing the structures of 2-(dimethylamino) ethyl methacrylate and 3-(dimethylamino) propyl methacrylamide (Figure 69) it can be seen that the acrylamide would be expected to be more hydrophilic than the acrylate. This expected increase is due to the presence of the amide group. The propyl group of the acylamide would be expected to produce a decrease in EWC but the amide group's contribution to the EWC overrides this negative effect. The increased hydrophilicity of the amide group provides explains the increased in EWC of the acrylamide containing membranes (DCNA41-43) compared to the acrylate containing membranes (DCNA31-32). This increase in hydrophilicity via the incorporation an amide group can be seen when comparing other acylates and acrylamides.

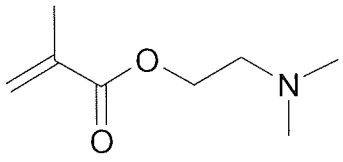

2-(dimethylamino) ethyl methacrylate (DMAEMA)

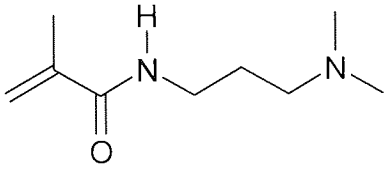

3-(dimethylamino) propyl methacrylamide (DMAPMA)

Figure 69. Comparison of 2-(dimethylamino) ethyl methacrylate (DMA EMA) and 3-(dimethylamino) propyl methacrylamide (DMA PMA)

5.4.1.2 Equilibrium water content (EWC) of SPDA copolymer membranes

The HEMA control membrane (DCNA10) had a EWC of 37.2±0.4%, this is in good agreement with the literature value for HEMA of ~39%. SPDA as a homopolymer had a EWC of 78±1.1%. The EWCs versus SPDA content for the series of SPDA:HEMA membranes is shown in Figure 70. We can see that progressive incorporation of SPDA into a HEMA membrane increases the EWC of the membranes, this is expected as both the quaternary nitrogen and sulfonate groups attract water.

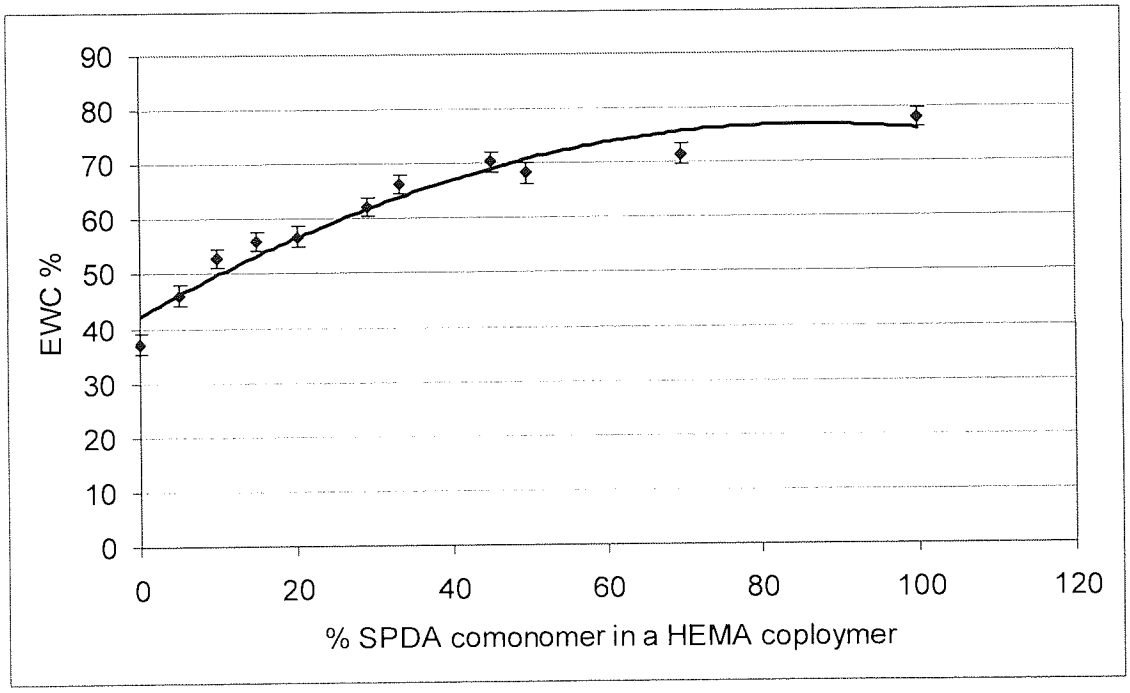

Figure 70. Equilibrium water content (EWC) of SPDA membranes. N=5, ±SD

5.4.1.3 Comparison of equilibrium water content (EWC) of charge-balanced copolymer and SPDA copolymer membranes

Conventional contact lens materials use hydrophilic monomers such as N-vinyl pyrrolidone to increase EWC. SPDA offers increased EWC compared to these monomers on a weight for weight basis. This can be shown if we compare the EWC's of the synthesised SPDA:HEMA copolymer membranes to NVP:HEMA copolymer

membranes (Figure 71). The same increase in EWC is seen for the charge-balanced:HEMA membranes in comparison to a NVP:HEMA membrane. If SPDA or the charge-balanced containing-copolymers were to be used in a contact lens application then the increase in EWC at reduced weights could be a useful property.

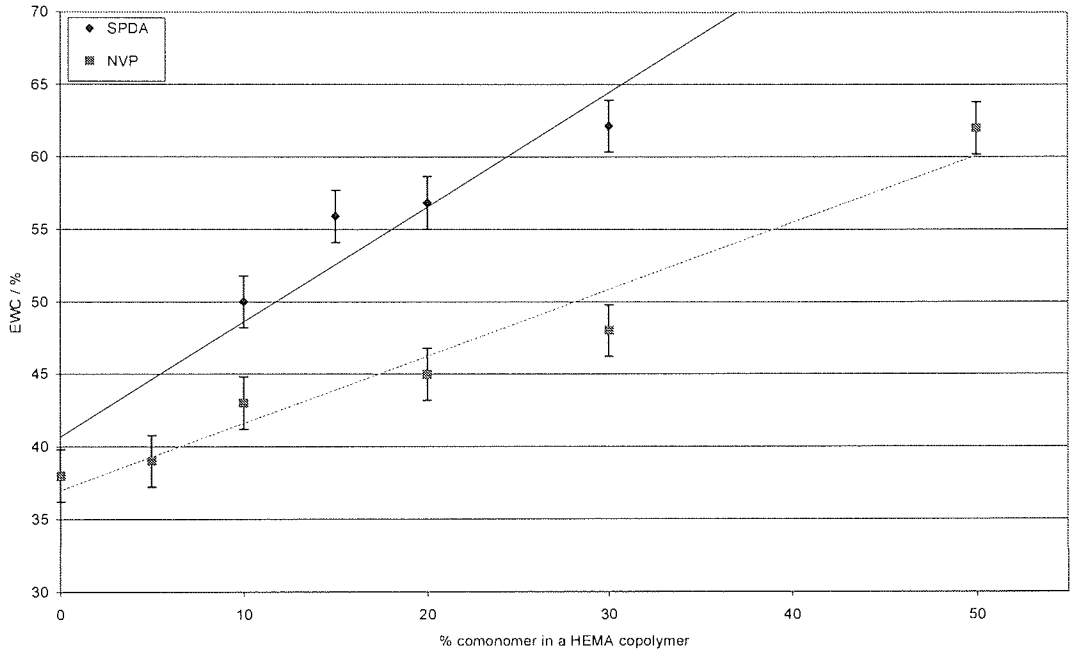

Figure 71. EWC vs % SPDA and % NVP comonomer in a HEMA copolymers. N=5, ±SD

The EWC of the SPDA copolymer membrane is closer to that of the 2-(dimethylamino) ethyl methacrylate :2-acrylamido-2-methylpropane sulfonic acid (DMAEMA:AMPS) ionic pair membranes (DCNA31-33) than that of the 3-(dimethylamino) propyl methacrylamide :2-acrylamido-2-methylpropane sulfonic acid (DMAPMA:AMPS) ionic pair membranes (DCNA41-43) (Figure 72). This is somewhat unexpected as the SPDA structure is more similar to the DMAPMA as both contain the quarternary nitrogen groups.

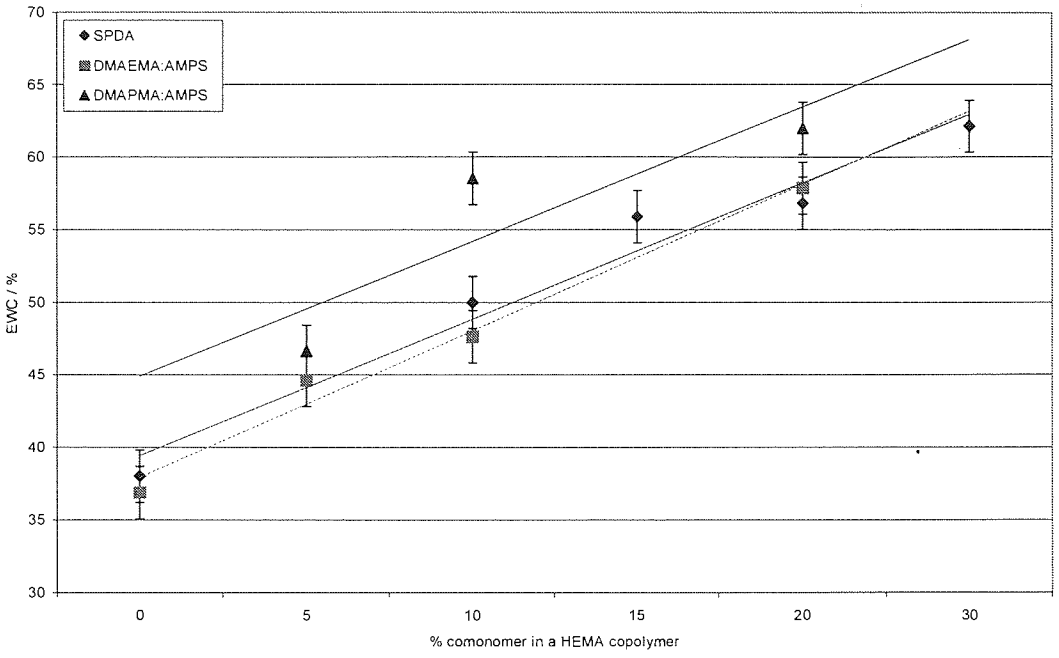

Figure 72. Comparison of the EWC of ionic comonomer and SPDA comonomer in HEMA copolymer. Where SPDA is N,N-dimethyl-N-(2-acryloylethyl)-N-(3-sulfopropyl) ammonium betaine, DMAEMA is 2-(dimethylamino) ethyl methacrylate, DMA PMA is 3-(dimethylamino) propyl methacrylamide, HEMA is 2-hydroxyethyl methacrylate and AMPS is 2-acrylamido-2-methylpropane sulfonic acid. % monomers is the weight percentage of the comonomer in the HEMA copolymer. N=5, ±SD

The inner salt of the SPDA and the charge attraction between the DMAEMA and AMPS in the acrylate membrane must allow less chain expansion of the polymer network that the of the acrylamide membrane (DMAPMA:AMPS).

The EWC's of the synthesised charged-balanced and the polyzwitterionic membranes are lower than that of membranes which have sodium 2-acrylamido-2-methylpropane sulfonic (NaAMPS) as the comonomer without the cationic comonomer to balance the charge [134]. The same is seen when other anionic sulfonate monomers such as 3-sulfopropyl ester acrylate (SPA) and bis-(3-sulfopropyl)-ester acrylate (SPI) are incorporated into membranes without a cationic group to balance the charge.

5.4.2 Mechanical properties of copolymer membranes

Initial (Young's) modulus, tensile strength and elongation to break were recorded on a Houndsfield HTi tensometer [72]. The method is shown in Chapter 2.

The Youngs modulus (ε) indicates the degree of stiffness of a material. Contact lenses with relatively low ε allow draping of the material over the cornea. Incorporation of hydrophilic monomers should reduce the ε as the EWC is increased. The reduction of ε is a result of the water plasticizing the material.

The tensile strength (Ts) indicates the materials resistance to deformation under tension and elongation to break (Eb) measures the materials ductility. In contact lens applications these are properties that are more related to the handling of the material rather than the on eye performance. The mechanical properties of hydrogels are normally but not always correlated to the EWC of materials [135].

5.4.2.1 Mechanical properties of charge-balanced copolymer membranes

The Youngs modulus (ε) for the HEMA control membrane (DCNA30) is 0.42±0.02 MPa which is in good agreement with the literature values. The progressive incorporation of the ionic comonomer pairs into the HEMA copolymer membranes reduces the ε as expected (Figure 73). The ε for both charged-balanced membranes seems to go through a rapid decrease at up to ~10% incorporation and then a gradual decrease at >10%.

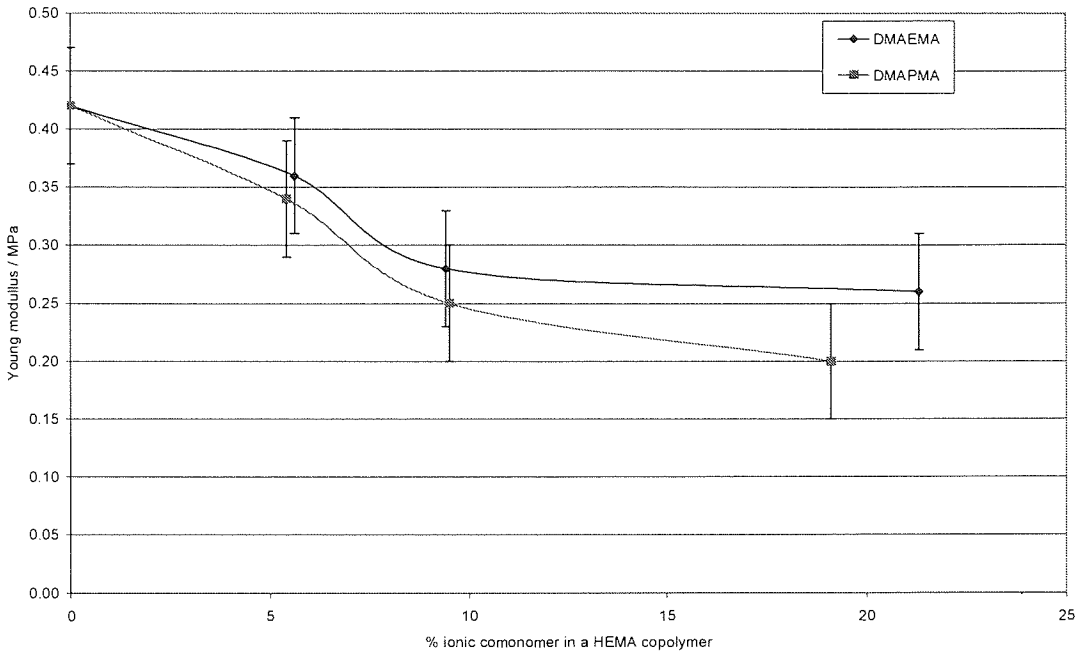

Figure 73. Youngs modulus (ε) of charge-balanced membranes. Where DMA EMA is 2-(dimethylamino) ethyl methacrylate, DMA PMA is 3-(dimethylamino) propyl methacrylamide and HEMA is 2-hydroxyethyl methacrylate. % ionic monomers is the weight percentage of the ionic pair in the HEMA copolymer, e.g. 5% ionic monomers in a HEMA copolymer for DMAEMA is 2.5% DMAEMA, 2.5% AMPS (2-acrylamido-2-methylpropane sulfonic acid) and 95% HEMA. N=5, ±SD

The ionic pair 2-(dimethylamino) ethyl methacrylate:2-acrylamido-2-methylpropane sulfonic acid (DMAEMA:AMPS) had a lower EWC than that of the ionic pair 3-(dimethylamino) propyl methacrylamide:2-acrylamido-2-methylpropane sulfonic acid (DMAPMA:AMPS). The different EWC's of the charged-balanced membranes would be expected to observable in the mechanical properties. There is a difference in the ε of the charged-balanced membranes (as shown in Figure 17) although the difference in is not statistically significant.

A similar situation is seen in the tensile strength (Ts) and elongation to break (Eb) of the both of the charge-balanced membranes. The increased EWC results in lowering of the Ts and Eb. The DMAEMA:AMPS copolymer membranes have higher Ts and Eb than the DMAPMA:AMPS copolymer membranes, but once again the differences are not statistically significantly (Figure 74). The DMAPMA:AMPS copolymer membranes having a higher EWC would be expected to have mechanical properties

that were of a lower value than the DMAEMA:AMPS copolymer membranes as the water plasticizes the membrane.

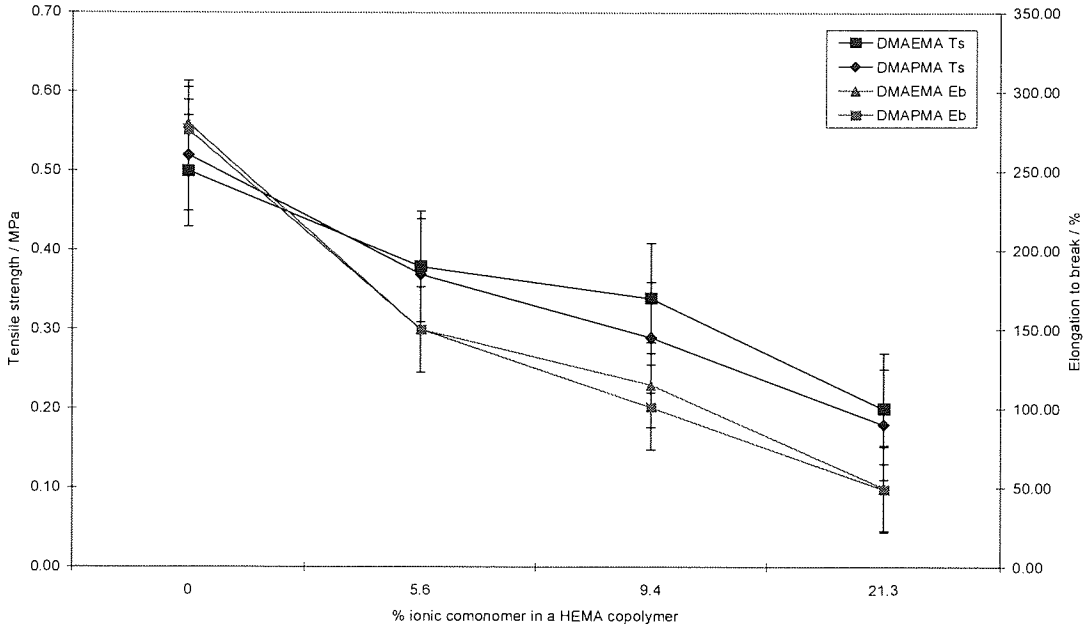

Figure 74. Tensile strength (Ts) and elongation to break (Eb) of charge-balanced membranes. Where DMA EMA is 2-(dimethylamino) ethyl methacrylate, DMA PMA is 3-(dimethylamino) propyl methacrylamide and HEMA is 2-hydroxyethyl methacrylate. % ionic monomers is the weight percentage of the ionic pair in the HEMA copolymer, e.g. 5% ionic monomers in a HEMA copolymer for DMAEMA is 2.5% DMAEMA, 2.5% AMPS (2-acrylamido-2-methylpropane sulfonic acid) and 95% HEMA. N=5, ±SD

The EWC is highly correlated to the mechanical properties for the charge-balanced membranes as shown in Figure 75 and Figure 76.

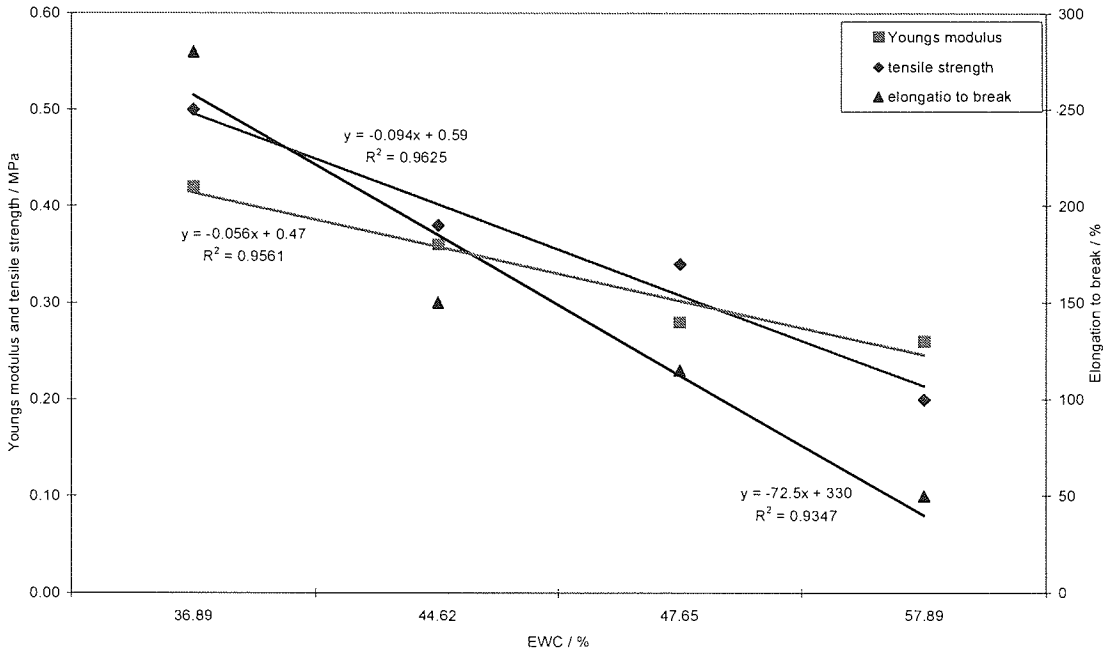

Figure 75. The correlation between EWC and mechanical properties of the DMAEMA:AMPS copolymer membrane

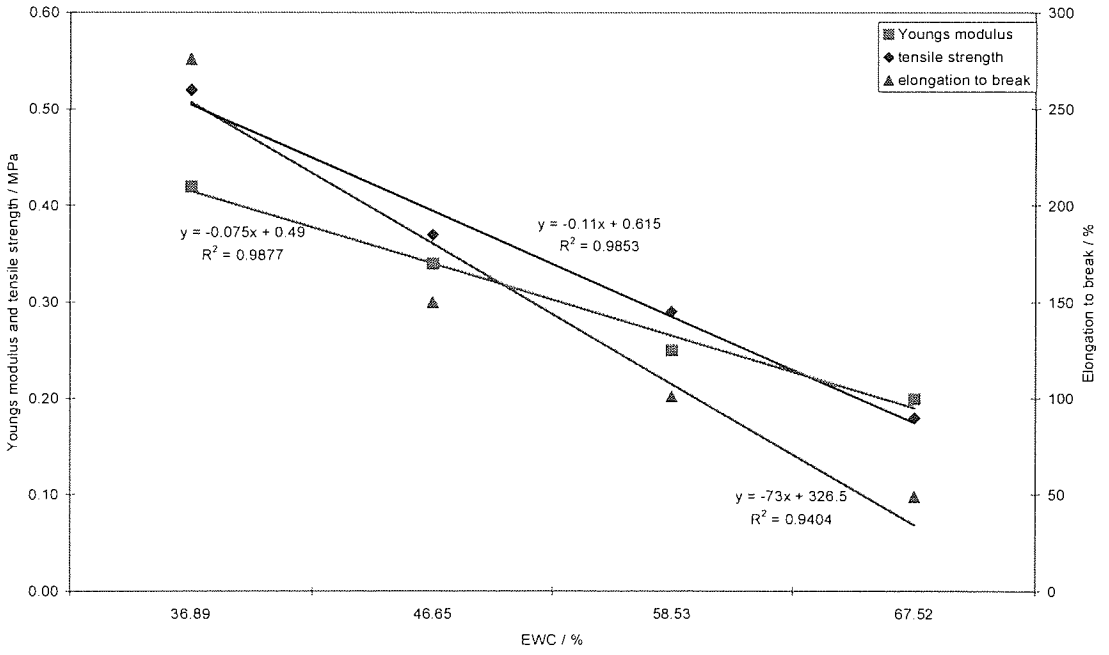

Figure 76. The correlation between EWC and mechanical properties of the DMAPMA:AMPS copolymer membrane

5.4.2.2 Mechanical properties of SPDA copolymer membranes

The Youngs modulus (ε) for the HEMA control membrane (DCNA10) is 0.42±0.02 MPa.. The progressive incorporation of SPDA into the HEMA copolymer membranes reduces the ε as expected (Figure 77).

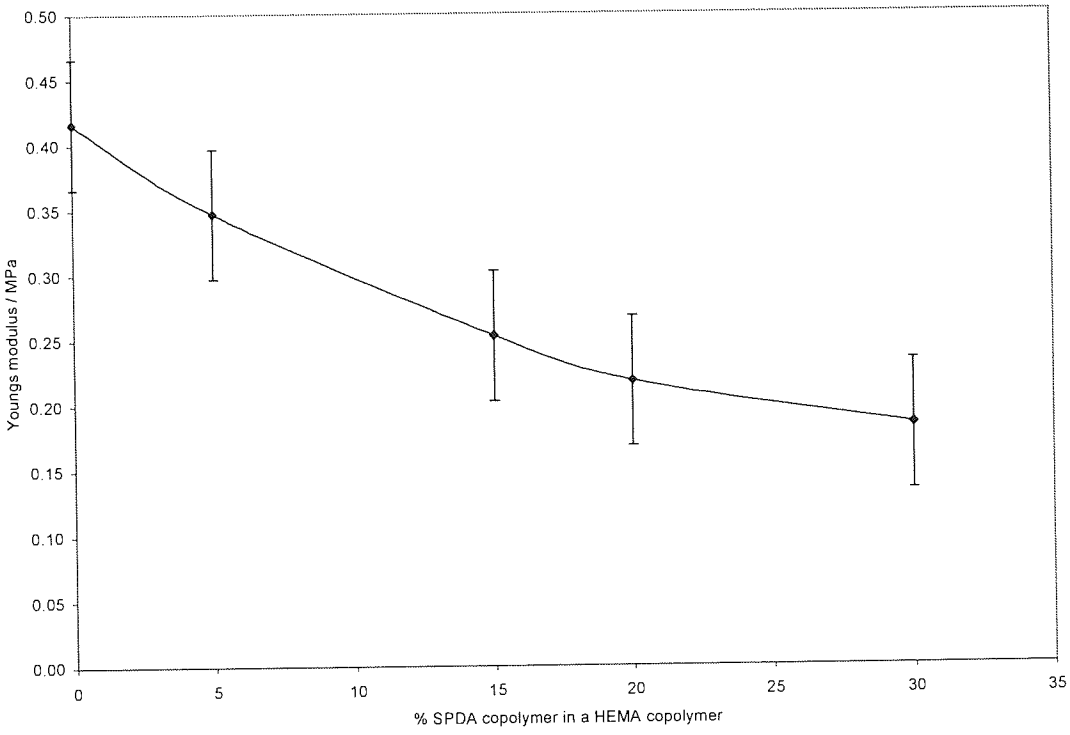

Figure 77. Youngs modulus (ε) of SPDA membranes. N=5, ±SD

The ε reduces as we increase the percentage of SPDA in the copolymer. It is a reflection the EWC of the membranes. The progressive incorporation of SPDA into the HEMA copolymer membranes reduces the tensile strength (Ts) and elongation to break (Eb) (Figure 78). As the percentage of SPDA is increased so the polymer network includes more of the sulfonate and amine hydrophilic pendant groups. These groups have an associated shell of water molecules which are plasticizing the membranes. This is having the effect of lowering the Ts and Eb.

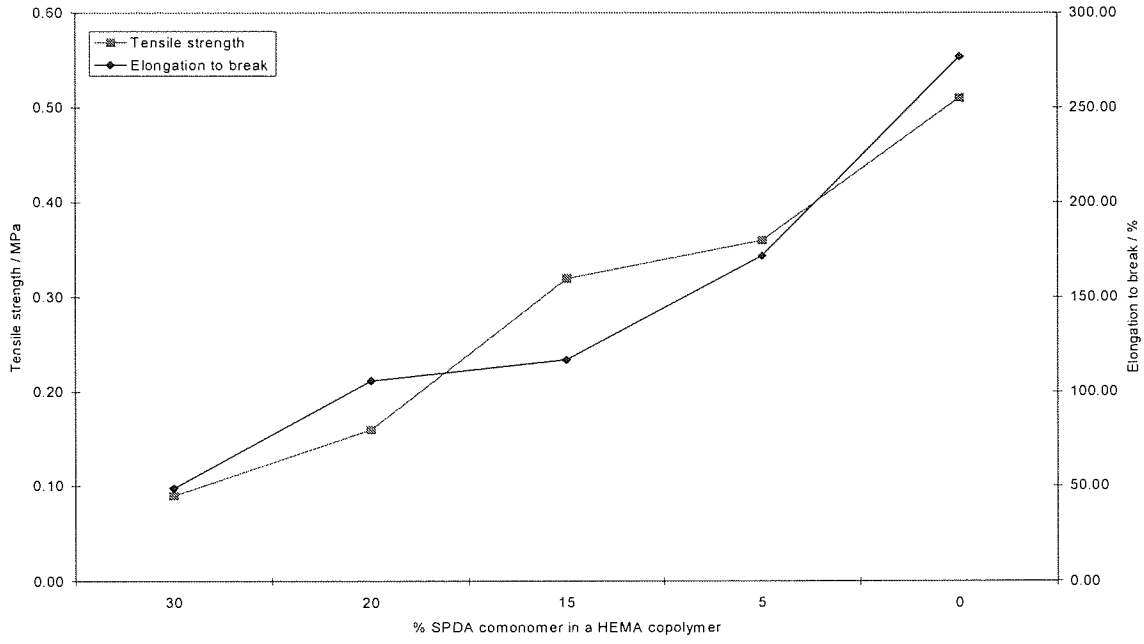

Figure 78. Tensile strength (Ts) and elongation to break (Eb) of SPDA membranes

There is a positive correlation between the EWC and these three mechanical properties. A plot of EWC vs ε, Ts and Eb as shown in Figure 79 gives slopes of r^2 of 0.96, 0.97 and 0.92 respectively, the slopes for Ts and Eb are close and one appears under the other in Figure 79.

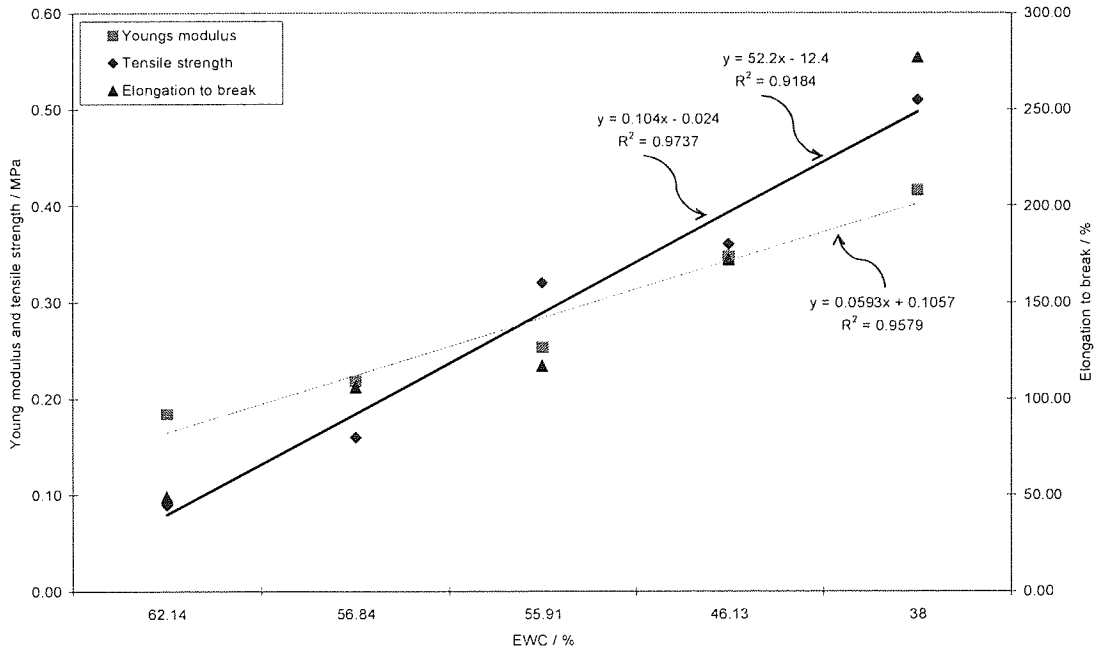

Figure 79. The correlation between EWC and mechanical properties of the SPDA copolymer membrane

The incorporation of >30% SPDA into the HEMA copolymer membranes (DCNA01-03, 06, 07 and 11) produced membranes with mechanical properties that were relatively low. The membranes were too fragile and broke while handling to place into the jaws of the tensometer and so were unsuitable for testing using this method.

5.4.2.3 Comparison of the mechanical properties of charge-balanced copolymer membranes and SPDA copolymer membranes

The ε of the SPDA membranes is higher (not statistically significantly) than that of the charged-balanced membranes. The Ts of the SPDA and charged-balanced membranes are similar and not significantly different although the actual values of the SPDA membrane is closer to those of the 2-(dimethylamino) ethyl methacrylate:2-acrylamido-2-methylpropane sulfonic acid copolymer membrane. The Eb of the SPDA membranes is higher than the charged-balanced membranes but once again there is no significant difference.

The ε of the charged-balanced and SPDA membranes are comparable to those of commercial conventional hydrogels soft lens materials of similar water contents, for example etafilcon A has an EWC of 58% and a ε of ~0.3MPa [136]. The mechanical properties of the membranes at the higher water contents are low and unfavourable for contact lens applications. It is the Ts and Eb that are taken into account in terms of handling contact lenses and these values for the zwitterionic and charged-balanced membranes are relatively low.

5.4.3 Surface free energy (γ) of copolymer membranes

Sessile drop contact angle measurement using well characterised liquids such as water and diidomethane provide a convenient method of determining the surface free energy (γ) of solid surfaces. The contact angle (θ) can be measured either as initial θ or kinetic θ using the sessile drop technique. A GBX Goniometer was used according to the method as described in Chapter 2.

The total free surface energy (γ_s^t) of a material can be found from the sum of the dispersive (γ_s^d) and polar components (γ_s^p) (see Appendix VI - Contact angle). Incorporation of a hydrophilic monomer into a polymer would be expected to increase the polar component of the surface free energy. The sessile drop technique is frequently used on surfaces when they are hydrated although it can be used on dehydrated samples to ascertain the γ of the sample [64, 137]. The samples were hydrated when analysed in these experiments.

5.4.3.1 Surface free energy (γ) of charge-balanced membranes

The total surface free energy (γ_s^t) for the HEMA control membrane (DCNA30) was calculated to be 51.9±2 mN/m. The contribution from the dispersive (γ_s^d) and polar components (γ_s^p) were 24±2 and 27.4±2mN/m respectively. As was expected the progressive incorporation of the ionic monomer pairs into a HEMA copolymer increased the γ_s^t of the membranes, shown Figure 80.

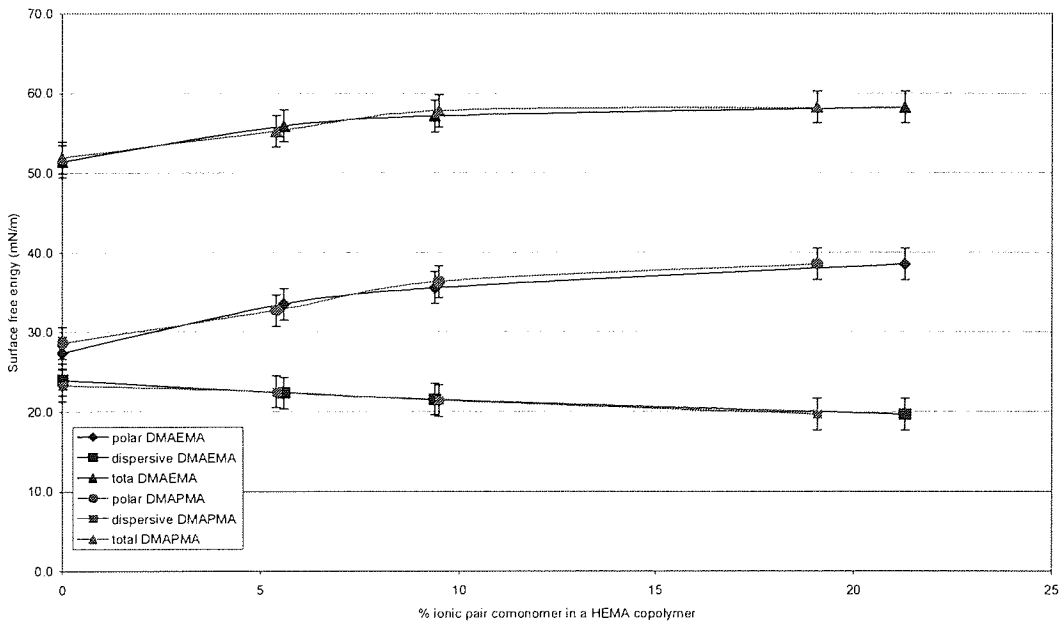

Figure 80. Surface free energy of charge-balanced membranes. Where DMAEMA is 2-(dimethylamino) ethyl methacrylate, DMA PMA is 3-(dimethylamino) propyl methacrylamide and HEMA is 2-hydroxyethyl methacrylate. % ionic monomers is the weight percentage of the ionic pair in the HEMA copolymer, e.g. 5% ionic monomers in a HEMA copolymer for DMAEMA is 2.5% DMAEMA, 2.5% AMPS (2-acrylamido-2-methylpropane sulfonic acid) and 95% HEMA. N=5, ±SD

As we the increase the ionic comonomers to ~5% in the charge-balanced copolymer membranes there is an increase in the γ_s^t to 56.9±2mN/m. This increase comes from a combination of a small reduction in the γ_s^d and a significant (p=0.001) increase in the γ_s^p. These polar increases come about from the ionic and hydrophilic nature of the membranes. As we increase the ionic comonomers further to ~10 and ~20% in the charge-balanced copolymer membranes this causes an increase of γ_s^t to 57.2 and to 58.3±2mN/m respectively (both statistically insignificant). This is a smaller increase than the one brought about by the initial introduction of ~5% ionic comonomers.

5.4.3.2 Surface free energy (γ) of SPDA membranes

The total surface free energy (γ_s^t) for the HEMA control membrane (DCNA10) was calculated to be 50.6±2 mN/m. The contribution from the dispersive (γ_s^d) and polar components (γ_s^p) were 23.6±2 and 27±2 mN/m respectively.

The progressive incorporation of SPDA into a HEMA copolymer was shown to increase the γ_s^t of the membranes as was expected (Figure 81). Incorporation of 5% SPDA into a HEMA copolymer (DCNA13) produced a membrane with a γ_s^t of 57.2±2 mN/m with the increase of the polar component and a decrease in the dispersive component. Further incorporation of 10 and 20% SPDA into the membrane (DCNA12 and 08) provided a small increase in the γ_s^t of the membranes.

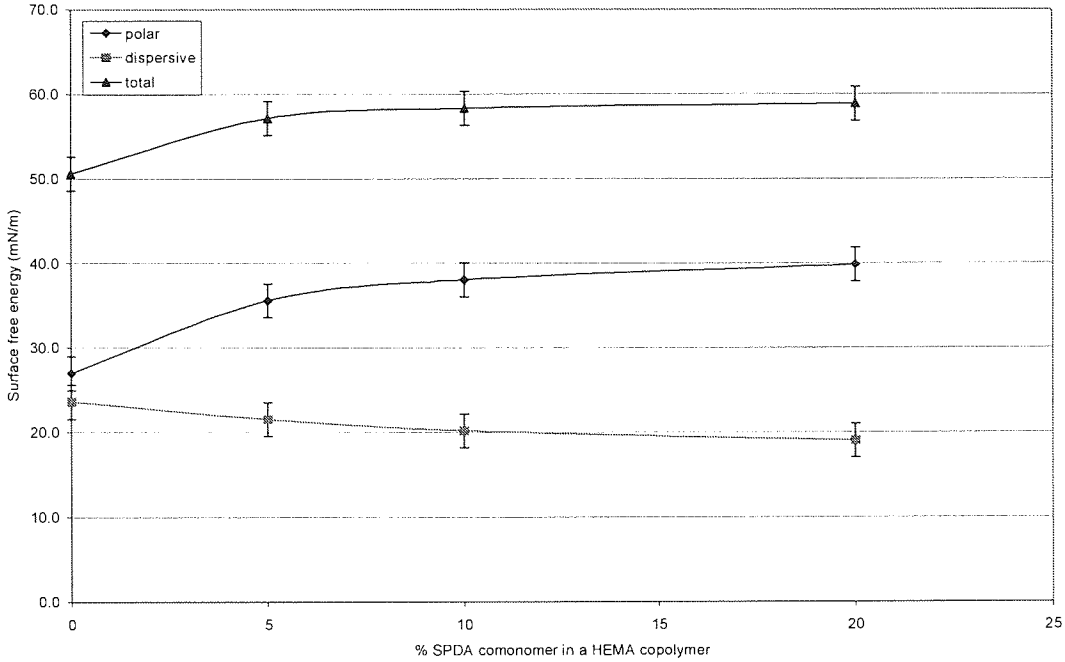

Figure 81. Surface free energy of SPDA membranes. N=5, ±SD

The increase in γ_s^t at ≤5% SPDA may be brought about by the hydrophilic sulfonate groups orientating themselves to the surface of the membrane when exposed to water. The increase of SPDA above 5% has a less pronounced effect on the contact angles of the probe solutions and thus the γ_s^t, with 10% SPDA wee see a ~1mN/m increase and 20% SPDA produced <1mN/m increase. This is unexpected as the increase from 0 to 5% gave a change of ~10mN/m and we would expect a more pronounced increase in γ_s^t when we double the amount of SPDA.

Betaines are known to have low water contact angles and so would give high surface free energies [131]. If the surface of the membrane was an even distribution of homogeneous SPDA the contact angle would be low. The HEMA component of the polymer must be distributed at the surface and playing a role in lowering the γ_s^t.

5.4.3.3 Comparison of the surface free energy of charge-balanced and SPDA membranes

The SPDA and charged-balanced membranes displayed similar values for γ_s^t. The contributions from the polar and dispersive components were also of similar values. This is perhaps not surprising if the structures are considered. The SPDA has the quaternary nitrogen and sulfonate moities on a single pendant group, the acrylamide charged-balanced also has quaternary nitrogen and sulfonate moieties but situated on separate pendants groups and the acrylate has a sulfonate and an ester moiety on separate pendant groups. The combined pendant groups of the charged-balanced ionic comonomers are similar to the single zwitterionic pendant group and so similar values should be expected.

The contact angle sessile drop technique is frequently performed on dehydrated surfaces although it can be used to determine the γ of hydrated surfaces [137]. Although the structures of the zwitterionic and charge-balanced copolymers are similar it may be that the hydrated nature of the membranes was interfering with the analysis and this is why both the zwitterionic and charged-balanced membranes had similar values for γ_s^t.

The relationship between the EWC and the γ_s^t for the charge-balanced membranes and SPDA copolymer membrane are correlated as shown in Figure (Figure 82). A plot of EWC vs γ_s^t for the 2-(dimethylamino) ethyl methacrylate:2-acrylamido-2-methylpropane sulfonic acid (DMAEMA:AMPS) has a slope with an r^2 of 0.84. The SPDA copolymer shows a similar slope with an r^2 of 0.86.

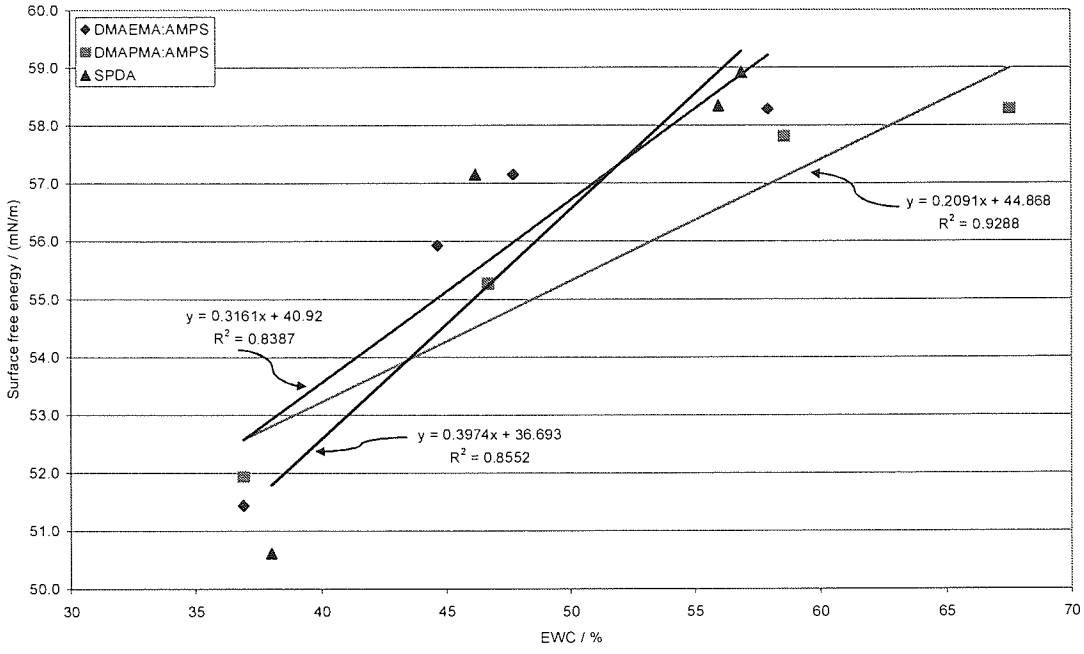

Figure 82. The correlation between EWC and surface free energies of the SPDA, DMAEMA:AMPS and DMAPMA copolymer membrane. Where DMAEMA is 2-(dimethylamino) ethyl methacrylate, DMAPMA is 3-(dimethylamino) propyl methacrylamide and HEMA is 2-hydroxyethyl methacrylate, AMPS (2-acrylamido-2-methylpropane sulfonic acid) and SPDA is N,N-dimethyl-N-(2-acryloylethyl)-N-(3-sulfopropyl) ammonium betaine

The 3-(dimethylamino) propyl methacrylamide:2-acrylamido 2,2 methylpropane sulfonic acid (DMAPMA:AMPS) copolymer membranes has a slope with a higher correlation with an r^2 of 0.93. The γ_s^t of the DMAPMA membrane is similar to that of the SPDA membrane as would be expected from the structural similaritie, this is I contrast to the difference in EWCs of these membranesas reported in section 5.4.1.3.

5.4.4 Oxygen permeability (Dk) of SPDA membranes

Dk was measured with the polarographic method [73, 74] using a Createch Model 201T permeometer. Dk has the units of 10^{-11} cm x ml O2 / sec x ml x mmHg which is equivalent to 1 Barrer or Fatt unit. The method is explained in Chapter 2.

The HEMA control membrane has a Dk of $6x10^{-11}$ Barrers measured at room temperature (24°C) is in good agreement with the literature value for HEMA lens

materials. The Dk of a SPDA:HEMA copolymer in a ratio of 33:77 membrane (DCNA02) is $16x10^{-11}$ Barrers.

In conventional hydrogel lens materials the rise in Dk is driven by water content. The relationship between EWC and permeability is not a linear one. The Dk of conventional hydrogels increases logarithmically with the EWC of the material [138]. The equation used to describe the relationship is

$$Dk = A^{e\,B\,EWC}$$

where

D = diffusivity of oxygen through a material

k = the solubility of oxygen in a given material

EWC = equilibrium water content

A and B = experimentally determined constants

Researchers have determined different values for A and B as shown in Table 30. Using these formulas we can calculate a value for the membrane based upon its EWC. The EWC of a membrane synthesised with SPDA:HEMA in a ratio of 33:77 (DCNA02) is 66% and the calculated values for its Dk are 23.1, 30.1 and 44.7 Barrers.

Table 30. Theoretical Dk from literature

Formula	Theoretical Dk / Barrers	Reference
Dk = 1.68 e 0.0397 EWC	23.1	Morgan [1]
Dk = 2 e 0.0411 EWC	30.1	Fatt [2]
Dk = 2.4 e 0.0443 EWC	44.7	Tighe [3]

1. Morgan, P.B., and Efron, N. (1998). The oxygen performance of contemporary hydrogel contact lenses. Contact Lens & Ant Eye *21*, 3-6.
2. Fatt, I., and Chaston, J. (1982). International Contact Lens Clinic *9*, 76.
3. Tighe, B.J. (1976). The design of polymers for contact lens applications. British Polymer Journal *8*, 71 - 77.

This experimental value in this work was determined at room temperature (24°C) and Dk is known to be temperature dependant. The Dk for hydrogel membranes has been shown to double on raising the temperature from 24°C to 34°C [139]. If we assume the EWC of the membrane is the same at 34°C as at 24°C then we can estimate the Dk of the membrane at 34°C could be as much as $32x10^{-11}$ Barrers which is a similar value to the calculated value using the Morgan and Efron [140] and Fatt and Chaston [73] formula.

A Dk of $32x10^{-11}$ Barrers would give an oxygen transmissibility (Dk/t) of $40x10^{-9}$ Barrers (assuming a thickness of 0.08mm). Holden and Mertz [8] showed a Dk/t of $24x10^{-9}$ Barrers was necessary for daily wear of contact lenses and $87x10^{-9}$ Barrers for extended wear to limit overnight corneal edema to 4%. Those values have been recently raised to $35x10^{-9}$ Barrers for daily wear and $125x10^{-9}$ Barrers for extended wear as suggested by Harvitt and Bonanno [9].

Most conventional contact lenses fall below the Harvitt and Bonanno criteria. Those materials with EWC's of 60% and over reach the Dk/t of $35x10^{-9}$ Barrers. The new generation of silicone hydrogel contact lenses easily meet the Dk/t values for daily wear and most of them meet the value for extended wear. The drive for higher Dk/t brought about the silicone hydrogels and they are slowly replacing the conventional materials. Manufacturing costs will eventually fall and allow their use on a daily wear basis.

The mechanical properties of the SPDA membranes are low as described in section 5.4.2 and a lens of 0.08mm thickness would be hard to handle. A thicker material would be needed to improve the "handleability" unfortunately this would reduce the Dk/t of the material. The SPDA membrane does not have suitable Dk for extended wear contact lens application.

5.4.5 Optical transmittance of SPDA membranes

Optical clarity is an obvious requirement of a contact lens. The transmission of light through a membrane can be measured by placing the membrane into a

spectrophometer and measuring the transmission across a range of wavelengths. A 5mm cork borer was used to cut sections of the (~0.5mm thick) membranes before placing them flat onto the side of a silica cuvette. The cuvette was then filled with HPLC water and the transmission of light measured from 440-800nm. A matched silica cuvette filled with HPLC water was used in the reference beam of the instrument. The clarity of series of SPDA membranes is shown by the transmission of light being >93.3% for any of the membranes as shown in Table 31. The value for the transmission of light indicates the zwitterionic membranes would mean they would be suitable in contact lens applications.

Table 31. Transmission of light across SPDA membranes

Membrane	SPDA / %	HEMA / %	Trans / %
DCNA07	70	30	96.6
DCNA06	50	50	94.9
DCNA01	45	55	94.7
DCNA02	33	67	94.4
DCNA05	29	71	93.4
DCNA08	20	80	96.7
DCNA09	15	85	95.9
DCNA10	0	100	92.7

Where SPDA / % is percentage of N,N-dimethyl-N-(2-acryloylethyl)-N-(3-sulfopropyl) ammonium betaine monomer in membrane, HEMA / % is percentage 2-hydroxyethyl methacrylate monomer in the membrane and Trans / % is transmission of light (UV from 440-800nm) through the membrane

5.4.6 Coefficient of friction (μ) of SPDA membranes

The coefficient of friction (μ) is a measurement that can be made during the relative motion of the surfaces of two materials against each other. When a blink occurs there is friction between the eye and the eyelid and the tear film acts as a lubricant to lower the μ. When a lens is inserted in the eye the situation changes and now during a blink and there is friction between the lens and the eyelid. The front surface properties of a contact lens are likely to affect the frictional forces between the eyelid and the lens.

Therefore experiments to determine the effect of the introduction of SPDA as a comonomer on the μ of the resulting membranes were carried out. The μ was determined for the HEMA control and SPDA copolymer membranes using a modified

Nano-Scratch Tester method [75] where the polypropylene probe was moving against the membrane which was resting on a Melinex® sheet. The method is explained in Chapter 2.

The μ is a relative figure that is method dependent. The μ for the HEMA control membrane (DCNA10) is 4.43 (after initial start up friction). The incorporation of 15% SPDA (DCNA08, 15:85, SPDA:HEMA) in the copolymer membranes significantly reduces the μ to 1.88 and a further increase of the SPDA content to 33% (DCNA02, 33:66, SPDA:HEMA) reduces the μ to 1.31, as shown in (Figure 83).

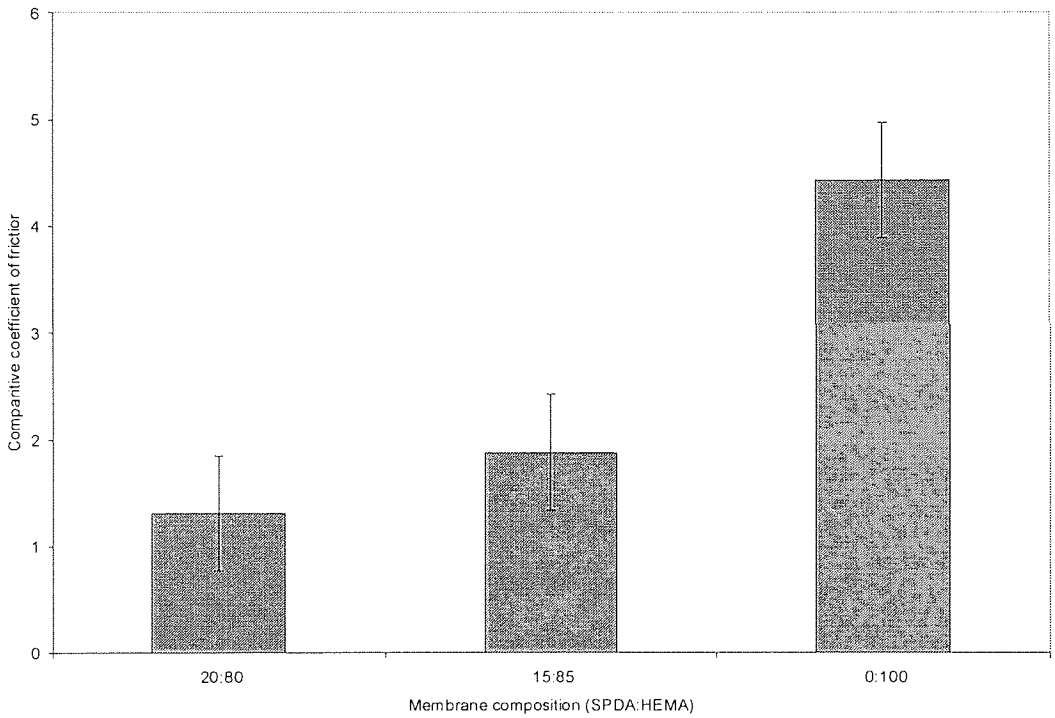

Figure 83. Coefficient of friction (μ) of SPDA membranes. Where membrane composition is the percentage ratio of N,N-dimethyl-N-(2-acryloylethyl)-N-(3-sulfopropyl) ammonium betaine (SPDA) to 2-hydroyethyl methacrylate (HEMA). N=5, ±SD

The presence of the SPDA in the membranes is causing a reduction in the μ. The lubricating ability of the SPDA present at the surface of the material lowered μ substantially. The increased EWC of the SPDA containing membranes may be having an effect upon the μ. The presence of the water may be acting as an internal lubricant but also as the polypropylene probe passes over the surface of the membrane it may be forcing water out of the polymer network and onto the surface out the membrane

where it may act as a lubricant. The presence of the SPDA at the surface may be acting to reduce μ as a result of reducing the boundary lubrication regime. If this effect is reproducible when the polymer is used as a coating could be an area for investigation.

5.5 Conclusions

A series of charged-balanced membranes were synthesised from cationic (or potentially) monomers 2-(dimethylamino) ethyl methacrylate (DMAEMA) and 3-(dimethylamino) propyl methacrylamide (DMAPMA) and the anionic monomer 2-acrylamido-2-methylpropane sulfonic acid (AMPS). The ionic monomers were present in equimolar ratios meaning any positive and negative charges were balanced overall in the final material. A series of zwitterionic membranes were synthesised from the N,N-dimethyl-N-(2-acryloylethyl)-N-(3-sulfopropyl) ammonium betaine (SPDA) monomer. 2-hydroxyethyl methacrylate (HEMA) was used as a copolymer in both the ampholyte and zwitterionic membranes.

The charged-balanced and zwitterionic membranes produced were clear and cohesive with the zwitterionic membrane having transmission of light being >93.3% showing its optical clarity. The charged-balanced membranes were stable to the effects of autoclave and gamma ray irradiation sterilisation. The zwitterionic membranes seem to be stable to the effects of autoclave but unstable to gamma ray irradiation. This could prove problematic if the zwitterionic material is used in applications in which autoclave sterilisation is not an option.

The α-methyl group is not present in the SPDA material and this leads to easier polymerisation and greater optical clarity when comparing to copolymers containing this group, such as the SPE (N,N-dimetyl-N-(2-methacryloylethyl)-N-(3-sulfopropyl) ammonium betaine) monomer [8].

The incorporation of ampholyte and zwitterionic character to the HEMA copolymer had the effect of increasing the EWC membranes in comparison to a control HEMA membrane. Unexpectedly the EWC of the zwitterionic component was closer to that of the acrylate copolymer than that of the acrylamide copolymer. The acrlyamide had a higher (not statistically significant) EWC than the acrylate and the zwitterionic membranes. The increased EWC provided by all the membranes could be advantageous for contact lens applications.

The mechanical properties of the charged-balanced and zwitterionic membranes were similar and comparable to conventional contact lens materials. The zwitterionic membrane has a higher (not statistically significant) Youngs modulus than the charge-balanced membranes. However with increased EWC the mechanical properties of charged-balanced and zwitterionic membranes became less favourable for contact lens application.

The zwitterionic membrane should have produced a material with higher surface free energy considering the structure of the SPDA monomer. The surface free energy of the charged-balanced and zwitterionic membranes were similar, with the zwitterionic being higher (not statistically significant) than the charged-balanced membranes. This implies that the bulk properties may not be being displayed as surface properties. The higher surface energy of these materials offers advantages in terms of wettability and biocompatibility. This is a feature of betaines that is well known and utilised in biomaterials.

The oxygen permeability (Dk) of the zwittterionic membrane is controlled by the EWC of the material. This is typical for conventional hydrogel materials and is a well known phenomenon. If EWC controls Dk then if we require the material to have higher Dk we need to need to increase the EWC of the material. The increase in EWC of the material would also introduce mechanical properties of lower values. Also a material that is dependant on EWC for Dk can never exceed $80x10^{-11}$ Barrers as this is the Dk of water. The material obviously can not be 100% water and this means the maximum oxygen transmissibility of a conventional hydrogel contact lens is probably more like $\leq 40x10^{-9}$ Barrers (assuming a thickness of 0.8mm). This is close to the value required for lower limit for safe daily wear ($35x10^{-9}$ Barrers). The dependence of Dk on EWC for the zwitterionic material is disadvantageous for contact lens applications

The incorporation of zwitterionic character into the membrane had the effect of lowering the coefficient of friction. This is an advantageous property for a contact lens as the material is constantly under the friction imposed by the action of the eyelid moving (~10 blinks per minute).

Although the zwitterionic and charged-balanced membranes appear to have similar properties an advantage of using the zwitterionic monomer over the ionic and cationic monomers is that of reactivity ratios. Although not studied here the use of one zwitterionic monomer as a comonomer would be easier to control than the use of a balanced ratio of cationic and anionic comonomers. The difficulty of controlling the incorporating of additional monomers into the growing chain is obvious.

The biomimetic nature of SPDA together with its compatibility with other monomers makes it a useful and complimentary addition to the building blocks of ophthalmic materials. However even though the SPDA has some suitable properties for application as contact lens material, as described above, it also has unsuitable properties making it inadequate for such applications. It does not offer advantages over the current silicon hydrogel materials, which are becoming the market driving force. The use of SPDA as component of a coating for contact lenses would be more likely as it surface properties are more useful than its bulk properties.

Chapter 6 – Hydrogel skin adhesives and lipid interaction

"Two polish'd marbles,... by immediate contact stick together"

Isaac Newton, Opticks

6.1 *Introduction to hydrogel skin adhesives and lipid interaction*

Hydrogel pressure sensitive adhesives (PSAs) as described in Chapter 1 can be used for applications involving the skin. Excess lipid associated with oily skin can cause a lack of adhesion for the PSA. This chapter is concerned with the synthesis of PSAs which might be less susceptibly to loss of adhesion under these conditions.

Two approaches were used based on two hypotheses. One was related to the known affinity for lipids for N-vinyl pyrrolidone (NVP) and the second related to the possibility that N,N-dimethyl-N-(2-acryloylethyl)-N-(3-sulfopropyl) ammonium betaine (SPDA) might intercalate by charge interactions with the phosphatidylcholine headgroup of phospholipids.

To investigate the first hypothesis the copolymerisation of NVP, acrylic acid bis-(3-sulfopropyl)-ester potassium salt (SPA) and 2-acrylamido 2,2-methyl propane sulfonic acid sodium salt (AMPS) was carried out to provide partially hydrated gels that may increase the adhesion to oily skin through PSA and lipid interaction. The lipid could interact with the hydrophobic regions of the NVP and be absorbed by the PSA. The effect of the possible absorption and reduction of the excess lipid at the adhesive-substrate interface could result in increased adhesion.

The second hypothesis was investigated by the copolymerisation of SPDA, SPA and AMPS to provide partially hydrated gels that may also increase the adhesion to oily skin through PSA and lipid interaction. The lipids, particularly the phospholipids could intercalate with the SPDA copolymer which may also lead to absorption. The absorption of the lipids from the might also result in an increased adhesion. This work on SPDA was undertaken as an extension the lipid based studies in Chapter 3 and 4. It was in part an extension of the previous work undertaken in this laboratory on zwitterionic hydrogels.

6.2 *N-vinyl pyrrolidone (NVP) copolymer pressure skin adhesives (PSA)*

6.2.1 Introduction to NVP copolymer PSA

The patent literature shows NVP (Figure 84) has been used in PSAs for various reasons, for example as a complexing agent for iodine [141] and for its ability to acts as a hydrogen bonding acceptor [142]. Poly(N-vinyl pyrrolidone) has been used to enhance adhesion of PSA [143, 144] but neither the polymer or the copolymerised monomer has been suggested for use for enhancement of adhesion in oily skin applications.

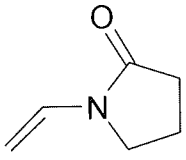

Figure 84. N-vinyl pyrrolidone (NVP)

While the NVP monomer is considered to be hydrophilic in character the structure contains a ring composed of a nitrogen atom, a carbonyl and three CH_2 groups. While the amide functional group imparts hydrophilic characteristic the three carbon ring structure would have give a certain amount of hydrophobic character. This hydrophobic character could allow interaction with the other hydrophobic species, such as lipids.

Furthermore when NVP is polymerised the ring structures contained within the polymer may rotate to associate with each other (or other hydrophobic moieties present if copolymerised) through van der Waals interactions to create domains of hydrophobicity, this is illustrated in Figure 85. There would also be a certain amount of hydrophobic shielding of the amide hydrophilicity from the carbon back bone of the polymer and the ring structure.

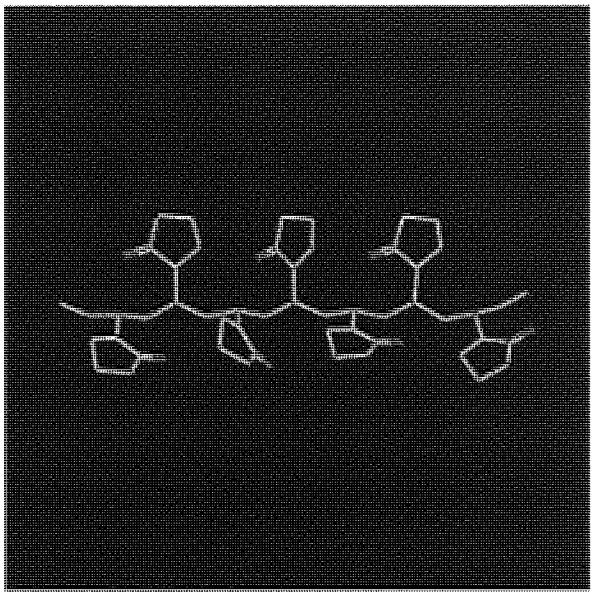

Figure 85. The structure of poly(N-vinyl pyrrolidone) using Weblab Viewerlite

NVP-containing contact lenses have been shown to be particularly susceptible to lipid uptake, resulting in high levels of ocular spoilation [77, 145], i.e. they have increased in vivo and in vitro lipid uptake when compared to other contact lenses. This phenomenon has been attributed to the fact that the lipids are attracted to the NVP or poly(N-vinyl pyrrolidone) contained within the lens.

If a small amount of NVP is included in the composition of PSAs then it may enhance their adhesion to oily skin through the "intentional spoliation" of the material. The NVP is added to take up the lipid and remove it from the adhesive-skin interface.

6.2.2 Composition of NVP copolymer gels

Chapter 1 described work by Fleming [11] and Cartwright [12] on the synthesis of PSAs for use as skin adhesives. Fleming suggested that the preferred ratio of components for this application would be 40:30:30 ionic monomer:glycerol:water (by wt%). Cartwright recommended that the most favourable ionic monomers to use within this composition would be acrylic acid bis-(3-sulfopropyl)-ester potassium salt (SPA) and 2-acrylamido-2-methyl propane sulfonic acid sodium salt (AMPS) in the

ratio of 6:4. The combination of these suggestions is a composition of SPA:AMPS:glycerol:water, 24:16:30:30 (by wt%).

In this thesis the SPA:AMPS:glycerol:water 24:16:30:30 (by wt%) composition described above was used as the basis for a composition upon which changes were to be made. The compositional changes were made only to the monomer component, the glycerol and water remained at the same ratio. Therefore all formulations in this work had the composition monomer:glycerol:water 40:30:30 (by wt%).

Each of the monomer compositions described below was 40g in mass and was mixed with 30g of glycerol and 30g of water to make a 100g final composition. Any compositions described after this point are related to the 40g monomer contribution to the final composition. Glycerol and water each contribute 30g to the final composition but are not described.

A series of compositions was prepared from SPA, AMPS and NVP monomers to investigate the effects of copolymerising NVP with the ionic monomers. The series started with the ionic:NVP monomers in a of ratio 39:1. The series continued with the progressive incorporation of NVP to provide compositions with ionic:NVP monomers in ratios of 19:1, 5.6:1, 3:1 and 1.5:1. The ionic monomers (SPA:AMPS) were present in a ratio of 6:4 for these compositions. These compositions were labelled series A.

A second series of compositions was prepared from SPA and NVP monomers to investigate the effects of copolymerising SPA with NVP. The series started with the SPA:NVP monomers in a of ratio 7:1. The series continued with the progressive incorporation of the NVP to provide compositions with SPA:NVP monomers in ratios of 3:1, 1.8:1 and 1:1. These compositions were labelled series B.

Two compositions were prepared from AMPS and NVP monomers to investigate the effects of copolymerising AMPS with NVP. These compositions had the AMPS:NVP monomers in ratios of 1:0.4 and 1:1 and were labelled series C.

A control composition was prepared from SPA and AMPS in the ratio of 6:4. A second control was prepared from SPA and AMPS monomer in the ratio of 4:6. The monomer compositions of the controls and series A-C are shown in Figure 86.

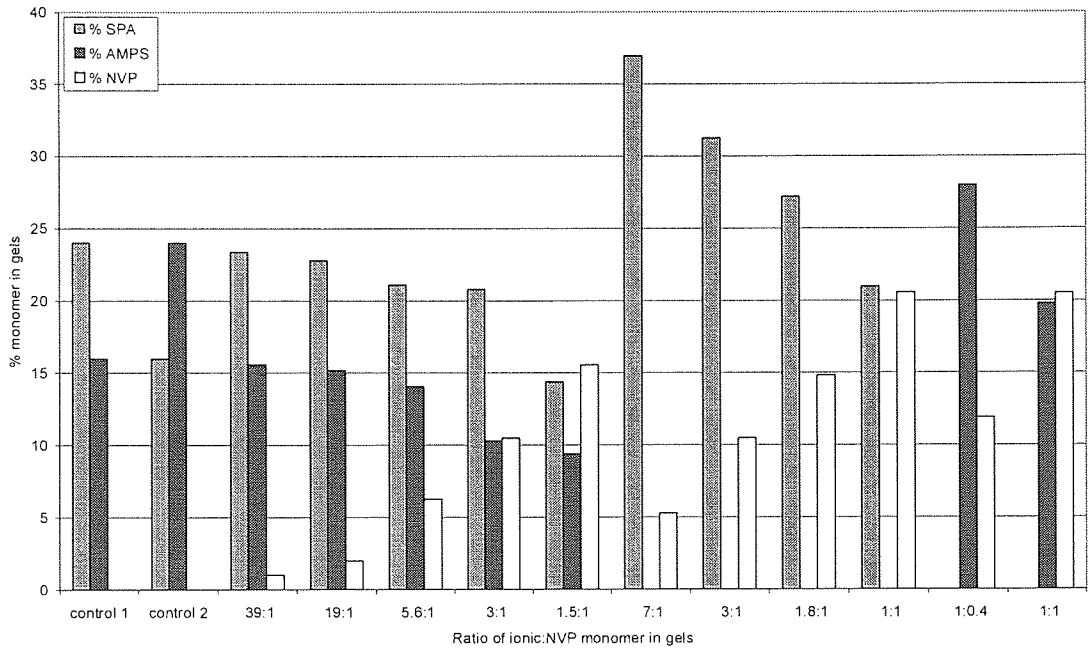

Figure 86. Monomer composition for SPA, AMP and NVP gels. Where SPA is acrylic acid bis-(3-sulfopropyl)-ester potassium salt, AMPS is 2-acrylamido-2-methyl propane sulfonic acid sodium salt and NVP is N-vinyl pyrrolidone

The structures of SPA, AMPS and NVP are shown in Figure 87.

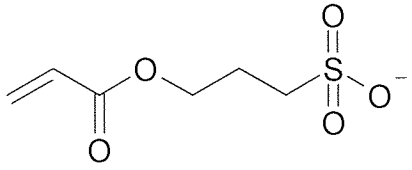

acrylic acid bis-(3-sulphopropyl)-ester potassium salt (SPA)

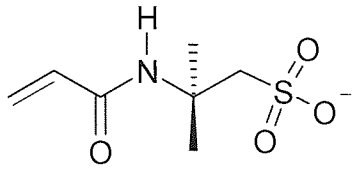

2-acrylamido 2,2-methyl propane sulfonic acid sodium salt (AMPS)

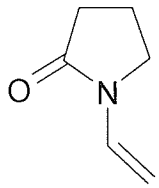

N-vinyl pyrrolidone (NVP)

Figure 87. The structure of acrylic acid bis-(3-sulfopropyl)-ester potassium salt (SPA), 2-acrylamido-2-methyl propane sulfonic acid sodium salt (AMPS) and N-vinyl pyrrolidone (NVP)

6.2.3 Polymerisation of NVP copolymer gels

The monomer, crosslinker and initiator were prepared and polymerised as described for partially hydrated gels in Chapter 2. The crosslinker and initiator were Ebacryl 11 and Irgacure184 respectively. The crosslinker:inititor (10:3) solution was used at ~0.33% (by wt) of the total composition. The structures of Ebacryl 11 and Irgacure184 are shown in Figure 88.

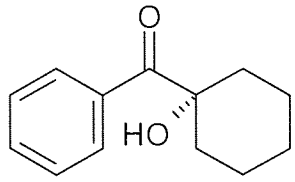

Irgacure 184 (1-hydroxycyclohexyl phenyl ketone)

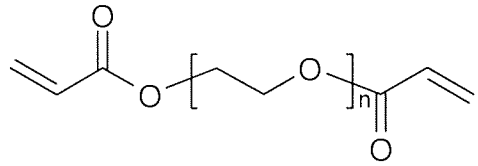

Ebacryl 11(polyethylene glycol diacrylate, where n = 2 to 4)

Figure 88. The structure of Irgacure 184 and Ebacryl 11

The controls and the series A (SPA:AMPS:NVP copolymers) formed cohesive, transparent and adhesive gels. Series C (AMPS:NVP copolymers) also formed cohesive, transparent and adhesive gels. After polymerisation there was an aroma of the NVP monomer along with a surface film which was thought to be residual NVP for all of these gels except the 39:1 and 19:1 ratio ionic:NVP gels of series A. It is known that the reactivity ratio of NVP towards acrylates is low and the presence of the NVP aroma could indicate the presence of residual NVP. Series B (SPA:NVP copolymers) formed cohesive and adhesive gels but were less "tacky" than the other gels.

6.2.4 Peel strengths of NVP copolymer gels

The 90° perpendicular peel test is a measure of the force required to remove the gel from the surface of the skin. It is a measure of the adhesive bond between the gel and the skin and can give a useful comparative measure for gels of different compositions. The 90° perpendicular peel test as described in Chapter 2 was used to determine the peel strength of the NVP copolymer gels. The peel strengths of the controls, series A and series C gels are shown in Figure 89.

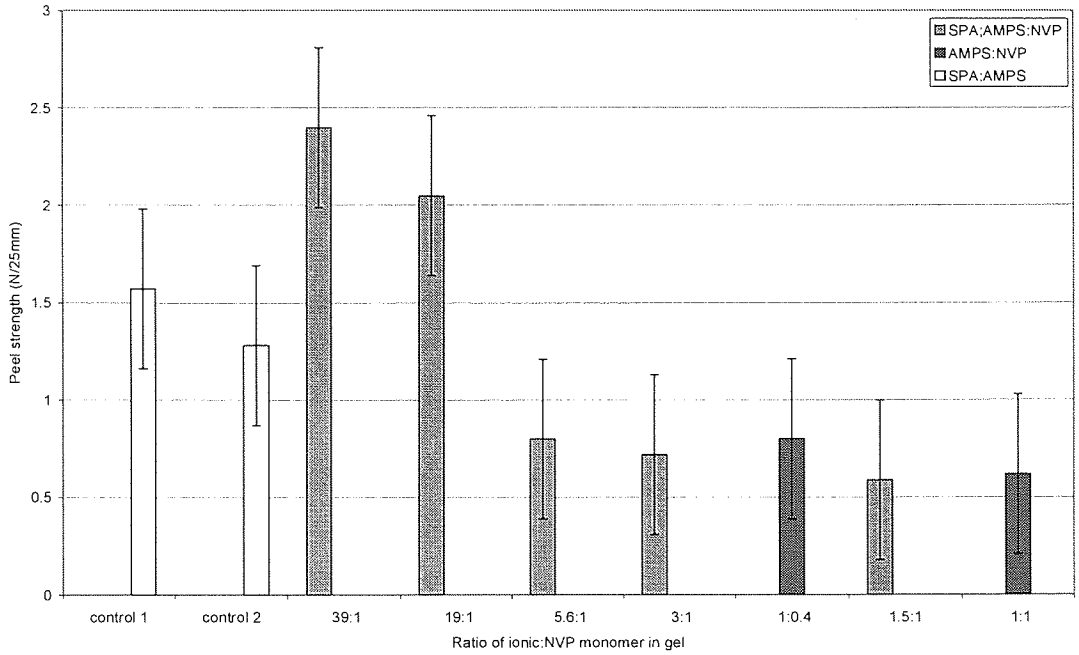

Figure 89. Peel strengths of SPA, AMPS and NVP copolymer gels. Where SPA is acrylic acid bis-(3-sulfopropyl)-ester potassium salt, AMPS is 2-acrylamido-2-methyl propane sulfonic acid sodium salt and NVP is N-vinyl pyrrolidone. N=5, ±SD

6.2.4.1 Peel strengths of controls 1 and 2 gels

Control 1 composed of the monomers SPA:AMPS in the ratio of 6:4. Control 2 composed of the monomers SPA: AMPS in the ratio of 4:6.

The peel strengths of the controls 1 and 2 were 1.57±0.45 and 1.28±0.43 N/25mm respectively (not statistically significant different, p=0.328). There is a trend for the lowering of peel strength when the composition is changed from SPA:AMPS 6:4 to SPA:AMPS 4:6. The effect of increasing the AMPS monomer while reducing the SPA monomer implies that a higher ratio of SPA is needed for gels to achive higher peel strengths with the surface of the skin.

6.2.4.2 Peel strengths of series A (SPA:AMPS:NVP) gels

This series consisted of gels with ionic monomers:NVP at ratios 39:1,19:1, 5.6:1, 3:1 and 1.5:1. The ionic monomers were SPA:AMPS and present in a ratio of 6:4.

The gel composed of ionic:NVP at a ratio of 39:1 had a peel strength of 2.39±0.45N/25mm. The gel composed of ionic:NVP at a ratio of 19:1 had a peel strength of and 2.05±0.7N/25mm respectively. These peel strengths are statistically significantly higher ($\leq p$=0.019) than the 6:4 SPA:AMPS copolymer control 1.

The gels composed of NVP at higher ratios gave the following peel strengths:

ionic:NVP 5.6:1	0.8±0.39N/25mm
ionic:NVP 3:1 0.	0.72±0.31N/25mm
ionic:NVP 1.5:1	0.59±0.38N/25mm

These peel strengths were all respectively reduced compared to control 1. The values are statistically significantly ($\leq p$=0.02) lower than control 1.

These results indicate that if the SPA:AMPS monomer content is at a ratio of 6:4 and the NVP component is of a low enough concentration then the addition of NVP increases the peel strength.

NVP has a tendency for alternation when polymerised with AMPS [146] and this alternating copolymer should have the effect of providing defined sequence distributions of the AMPS and NVP comonomers. However the copolymer also includes SPA and so the reactivity ratios would not be the same as the NVP:AMPS copolymer. Differing reactivity ratios when the SPA was involved would lead to different comonomer sequence distributions than a NVP:AMPS copolymer. If the NVP:SPA:AMPS copolymer does have a tendency to alternate then this may be enhancing the effect of mechanical interlocking between the copolymer and the skin, which will uncrease the adhesion of the PSA.

The aroma of NVP noted when these gels were polymerised indicated that residual NVP may be present. If the residual NVP is at low concentrations then this may have the effect of increasing peel strength as it could interact with the lipids present. It may increase the tack of the copolymer and lubricise the lipids.

6.2.4.3 Peel strengths of series C (AMPS:NVP) gels

This series consisted of gels with AMPS:NVP at ratios of 1:0.4 and 1:1. The AMPS:NVP copolymer gel in the ratio of 1:0.4 had a peel strength of 0.81±0.24N/25mm which is significant (p=0.01) lower than that of control 1. Additional increase of the NVP comonomer to a ratio of 1:1 lowers peel strength insignificantly further to 0.62±0.29N/25mm. The introduction of NVP at the expense of SPA in the copolymer had the effect of reducing the peel strength.

Hydrogen bonding may occur between the amide in the AMPS pendant group and the sulfonate in the SPA pendant group (Figure 90). The sulfonate could act ass a hydrogen bond acceptor. The hydrogen bonding could hold the sulfonate groups of both the SPA and AMPS to face in similar orientations. This hydrogen bonding may also slow down chain rotation.

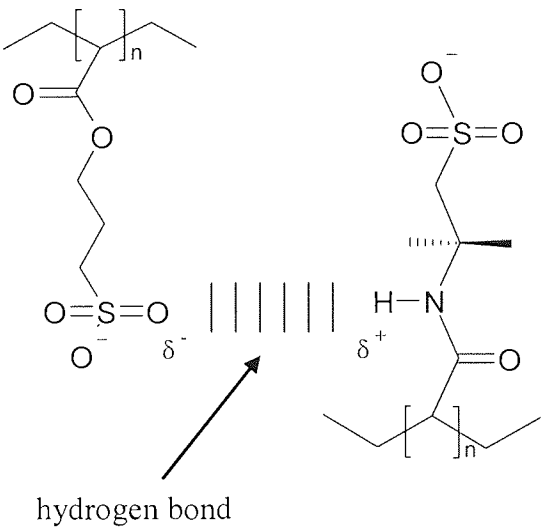

Figure 90. Proposed hydrogen bonding between AMPS and SPA

The use of NVP as a comonomer in place of the SPA comonomer could still allow hydrogen bonding to occur between the carbonyl on the NVP and the amide of the

AMPS Figure (Figure 91) where NVP acts as a hydrogen bond acceptor. In this case the hydrophobic CH_2 ring of the NVP would be presented in the same orientation as the sulfonate pendant group of the AMPS. This could introduce a degree of heterogeneous character at the surface of the gels which may account for the low peel strengths of these gels.

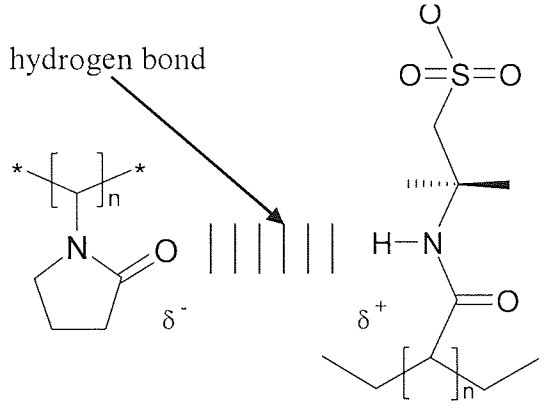

Figure 91. Proposed hydrogen bonding between AMPS and NVP

6.2.4.4 Peel strengths of series B (SPA:NVP) gels

This series consisted of gels with SPA:NVP at ratios of 7:1 3:1, 1.8:1 and 1:1.The SPA:NVP gels peel strengths could not be tested as the gels did not form adequately strong bonds with the skin. This was unexpected as the SPA should have provided higher peel strength if we consider the differences between the control gels.

The removal of the AMPS removed the bonding capability of the gel. The SPA would not hydrogen bond with the NVP as SPA does not contain an easily accessible δ^+ moment. This would allow the pendant groups of SPA and NVP to rotate more freely, the free rotation would lead to hydrophobic and hydrophilic domains from the NVP ring and the SPA sulfonate respectively. The domains could be presented at the surface when the gel is exposed to different environments, i.e. hydrophilic or hydrophobic.

6.2.4.5 The effect of skin moisturiser on peel strengths of NVP copolymer gels

In an effort to replicate a "greasy" skin a moisturiser was applied to the skin of the subject. A small amount of moisturiser was applied to the skin and rubbed in. The peel tests were repeated after five minutes of the application of a skin moisturiser. The results for all the gels were that the peel strengths were not recordable. The adhesive was removed from the skin without the Houndsfield tensiometer being able to make a recording. In retrospect it was apparent that the application of the moisturiser was too liberal as it affected all of the gels ability to adhere to the skins surface.

6.2.4.6 Comments on peel strengths of NVP copolymer gels

The gels with NVP at higher concentrations had an associated aroma of NVP. If the aroma of NVP was residual monomer this may have reduced the peel strengths the peel strength. Cartwright [12] had previously showed that residual monomers can reduce peel strength of adhesive gels. The gels with NVP at lower concentrations did not have an aroma of NVP but there still may have been residual NVP. At these lower residual concentrations the NVP residuals may have made a contribution to increasing the peel strength of the gel.

None of the NVP-containing gels produced peel strengths of $\leq$2.4 N/25mm and a peel strength of 3 N/25m has been suggested as a target figure for a PSA A peel strength of ~3N/25mm should provide good adhesion of over an extended period of time and also minimum discomfort upon removal [12]. Allthough the gels had a lower peel strength than ths suggested target figure they remained adhered to the skin of the subject until removed.

The skin of the subject used during the peel tests in this thesis may have been of the "greasy" type. A second subject was used in peel tests and this increased the peel strengths of the gels by ~0.25 N/25mm which was an insignificant increase.

6.2.5 Surface free energy (γ) of NVP copolymer gels

The contact angles of test liquids such as water and diidomethane allows the calculation of the γ of a material. The total free surface energy (γ_s^t) of a material can be found from the sum of the dispersive (γ_s^d) and polar components (γ_s^p), see Appendix VI - Contact angle. Using the sessile drop technique the contact angle can be measured either as an initial contact angle or a kinetic contact angle. The initial contact angle is the angle measured the instant that the drop comes into contact with the substrate.

The recording of the kinetic contact angle involves recording the initial contact angle and then the continued recording of the contact angle from the same drop over time, e.g. every 30 seconds until the experiment is ended, in this case 210 seconds. The angle measured at 210 seconds gives the final contact angle. A GBX Goniometer was used to record the contact angles as described in the Chapter 2.

The sessile drop technique is frequently used on surfaces when they are hydrated although it can be used to ascertain the γ of the sample on dehydrated samples [64, 137]. The samples were hydrated when analysed in these experiments.

Copolymerisation of a hydrophilic monomer would be expected to increase the polar component of γ of the resulting polymer. While NVP is hydrophilic it has hydrophobic character as described earlier and it is less hydrophilic than sulfonate containing monomers such as SPA and AMPS therefore it should be expected to produce a reduction in the γ if copolymerised with SPA or AMPS. However when the gels are hydrated it is the water that will make the greatest contribution to the γ.

The results of the γ have been spilt into two types of gel composition for analysis. The first set of data deals with series A (SPA:AMPS:NVP gels) and the second set of data deals with series C (AMPS:NVP gels). As the peel strengths of series B were too low to be measured the contact angles of water and diidomethane were not determined.

6.2.5.1 Surface free energy (γ) of series A gels (SPA:AMPS:NVP)

This series consisted of gels with ionic monomers:NVP at ratios 39:1,19:1, 5.6:1, 3:1 and 1.5:1. The ionic monomers were SPA:AMPS and present in a ratio of 6:4.

The initial contact angles are different from the final contact angles for series A. Because the contact angle is used to calculate γ, the initial and final of γ of the gels are also different. The values of initial and final γ for these gels are shown in Figure 92 and Figure 93 respectively.

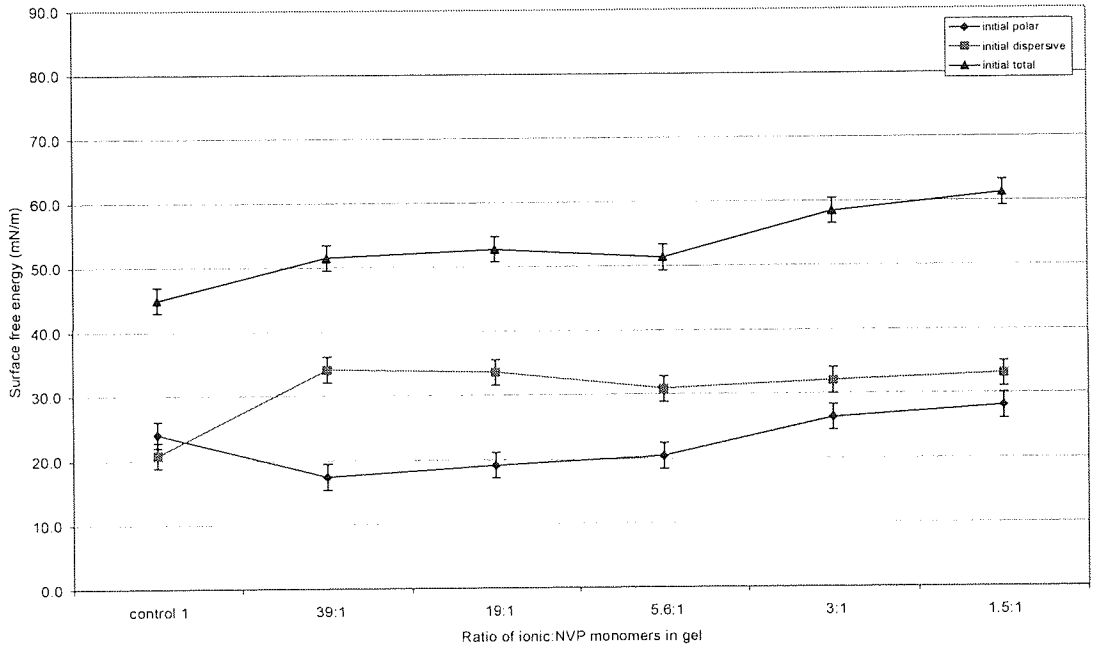

Figure 92. Initial surface free energy of SPA:AMPS:NVP gels. Where the ionic monomer is SPA:AMPS in the ratio of 6:4. AMPS is 2-acrylamido-2-methyl propane sulfonic acid sodium salt, SPA is acrylic acid bis-(3-sulfopropyl)-ester potassium salt and NVP is N-vinyl pyrrolidone. N=5, ±SD

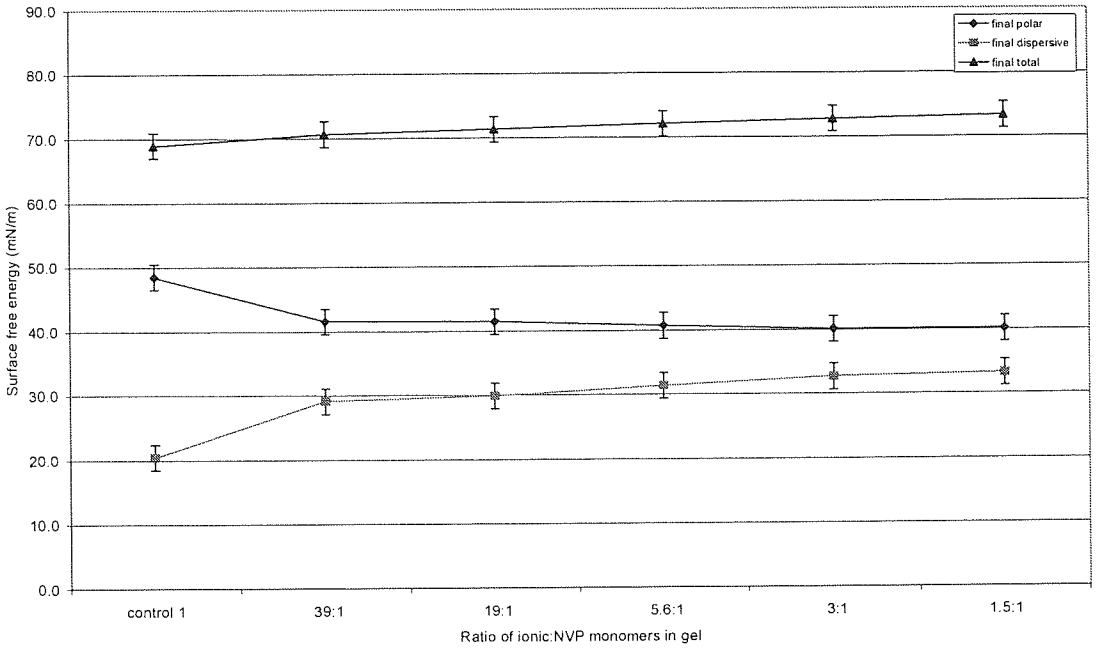

Figure 93. Final surface free energy of SPA:AMPS:NVP gels. Where the ionic monomer is SPA:AMPS in the ratio of 6:4. AMPS is 2-acrylamido-2-methyl propane sulfonic acid sodium salt, SPA is acrylic acid bis-(3-sulfopropyl)-ester potassium salt and NVP is N-vinyl pyrrolidone. N=5, ±SD

Two points are immediately apparent on comparison of the values for initial and final γ of the gels:

- the γ_s^t is higher for the final values
- the contributions from the γ_s^d component are higher than the γ_s^p with the initial values but the γ_s^p become dominate in the final values

This difference between the initial and final values of γ for the gels can be attributed to a combination of the gels being stored on a silicon paper and the absorption of water into the gel. The silicon paper would bring about the chain rotation of the hydrophobic groups of the polymer to the surface during storage. This is reflected in the initial values of γ as we see the γ_s^d being the dominating contribution to γ_s^t. As the contact angle experiment continues (in time) we see the γ_s^p becoming the dominating component to γ_s^t. This would indicate that the hydrophilic groups are reorientating themselves to the surface when the backing paper is removed.

The gels are below their EWC and designed to have the capacity to imbibe more water. The absorption of the medium that is being used as a probe would reduce the contact angle values obtained. The contact angles of the water and diidomethane changed from the initial values to the final values within 60 seconds of the kinetic experiment (data not shown).

Closer inspection of the values for initial γ shows the γ_s^d of control 1 gel is 20.9±2 mN/m and this increases significantly (p= 0.001) to 34.1±2 mN/m with the copolymerisation of NVP at a ratio of 39:1 ionic:NVP. The progressive increase of the NVP comonomer does not significantly change the γ_s^d from the value of the 39:1 ratio gel. The values change by ±1.3mN/m. It appears the copolymerisation of NVP at 2.5% (the percentage value for the 39:1 ratio) maximises the γ_s^d contribution to γ_s^t.

The copolymerisation of NVP at higher ratios produces a different trend in γ_s^p. The control 1 gel has an initial γ_s^p of 24.1±2 mN/m. With the copolymerisation of NVP at a ratio of 39:1 ionic:NVP gel we see a significant reduction (p=0.015) in the γ_s^p to 17.4±2 mN/m. With further increase in the NVP comonomer we see a gradual increase in γ_s^p with the 1.5:1 ionic:NVP ratio gel having a γ_s^p of 28.1±2 mN/m, significantly (p=0.03) higher value than the 39:1 ratio gel. The γ_s^t rise with the increase of NVP comonomer at higher ratios is a reflection of the γ_s^p contribution. It appears that NVP comonomer is affecting the surface in a polar manner with the initial contact angles.

The values for final γ shows the control 1 gel has γ_s^d of 20.4±2 mN/m and this increases significantly (p= 0.006) to 29.2±2 mN/m with the copolymerisation of NVP at a ratio of 39:1 ionic:NVP. There is a slight insignificant increase in γ_s^d with the increase of the NVP comonomer to a value of 33.2±2 mN/m at a ratio of 1.5:1 ionic monomer:NVP.

The opposite trend is seen for the final values in γ_s^p with the increase of NVP comonomer. The control has a γ_s^p of 48.5±2 mN/m which is reduced significantly (p=0.01) to 41.5±2 mN/m for the 39:1 ionic:NVP gel. This is followed by slight insignificant decrease in γ_s^p with increase of the NVP comonomer to a value of

40.1±2 mN/m for the 1.5:1 ionic:NVP gel. The γ_s^t increases with the higher ratios of the NVP comonomer. This is a reflection of the γ_s^p contribution but at a lower rate of increase that that seen with the initial values of γ. The hydrophobic character of the NVP is acting to reduce the γ_s^p while increasing the γ_s^d.

6.2.5.2 Surface free energy (γ) of series C gels (AMPS:NVP)

This series consisted of gels with AMPS:NVP at ratios of 1:0.4 and 1:1. The initial and final γ of the series C gels showed a similar trend to those of the series A gels described above. Again there was a difference between the initial and final γ of the series C gels as shown in Figure 94 and Figure 95 respectively.

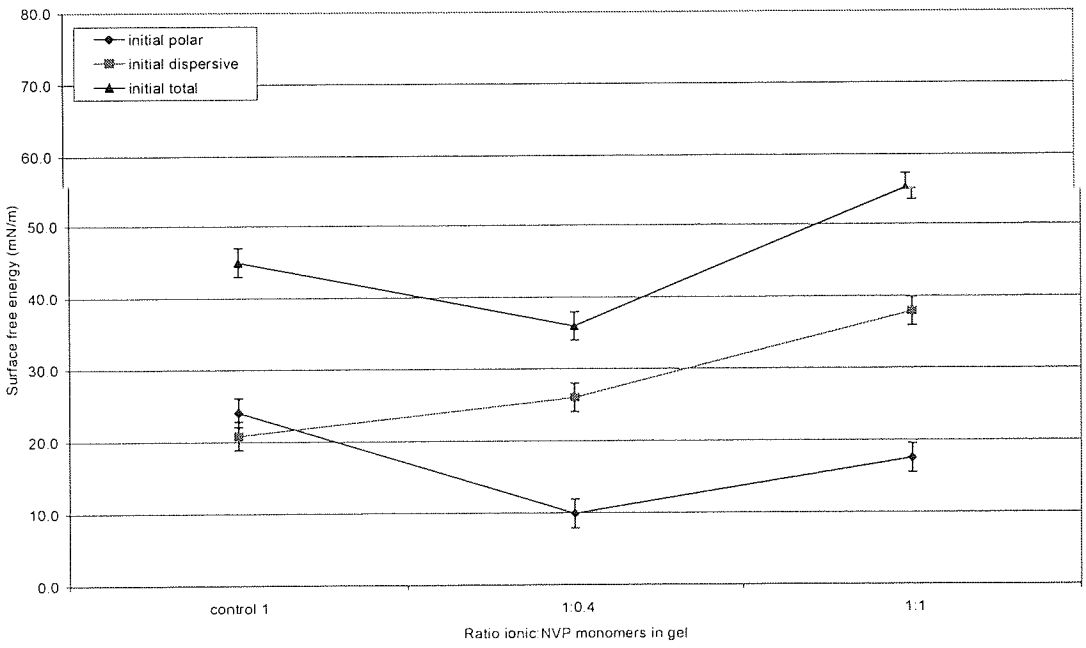

Figure 94. Initial surface free energy of AMPS:NVP gels. Where the ionic monomer is AMPS (2-acrylamido-2-methyl propane sulfonic acid sodium salt) and NVP is N-vinyl pyrrolidone. N=5, ±SD

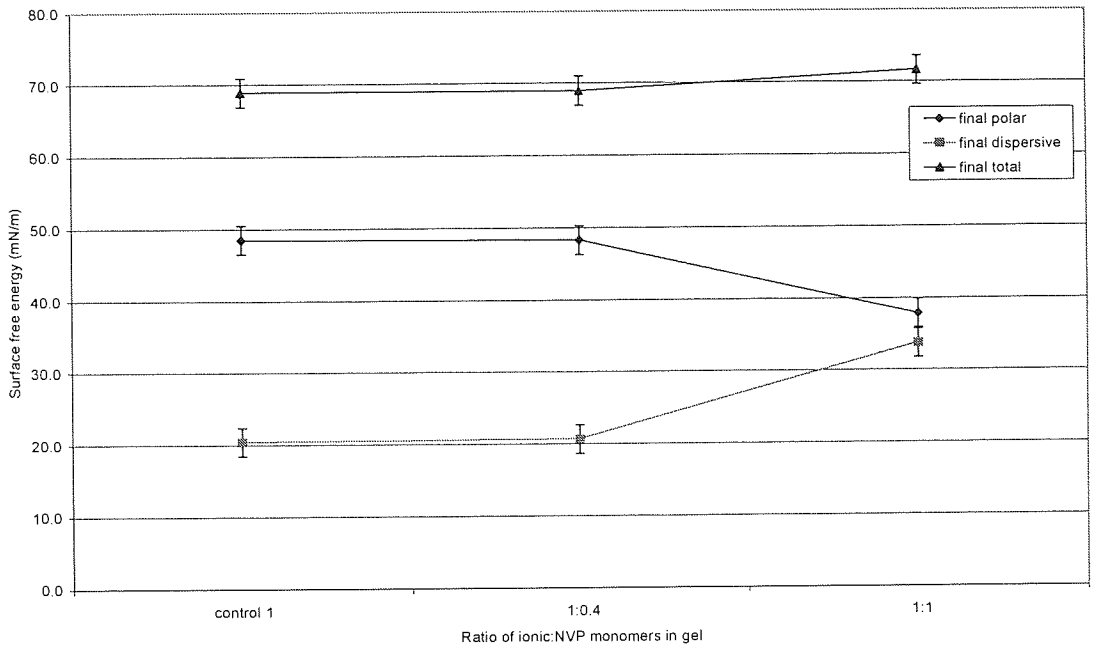

Figure 95. Final surface free energy of AMPS:NVP gels. Where the ionic monomer is AMPS (2-acrylamido-2-methyl propane sulfonic acid sodium salt) and NVP is N-vinyl pyrrolidone. N=5, ±SD

Comparing the initial and final γ for the series C (AMPS:NVP) gels in we see:

- the γ_s^t is higher for the final values
- the contributions from the γ_s^d component are higher than the γ_s^p in the initial values but the γ_s^p become dominate in the final values

The difference between the initial and final values of γ for the series C (AMPS:NVP) can again be attributed to a combination of the gels being stored on a silicon paper and the absorption of water into the gel. The contact angles of the water and diidomethane changed from the initial values to the final values within 60 seconds of the kinetic experiment (data not shown).

The trends in γ were similar to the previous described series A gels. The initial γ values of the control 1 gel were 24.1±2 mN/m and 20.9±2 mN/m for γ_s^p and γ_s^d components respectively. Incorporation of NVP as a comonomer in the ratio of 1:0.4 AMPS:NVP significant decreased the γ_s^p to 9.9±2 mN/m. Further increase of the NVP comonomer produced a gradual increase in γ_s^p to 17.6±2 mN/m at a ratio of 1:1

AMPS:NVP. While the γ_s^d increase significantly to 37.9±2 mN/m as the ratio of NVP comonomer increased. The initial γ_s^t is a reflection of the polar values. Once again the NVP comonomer is affecting the surface in a polar manner with the initial contact angles.

In the final γ values for the series C gels the control has a γ_s^p of 48.5±2 mN/m and γ_s^d of 20.4±2 mN/m. The copolymerisation of NVP at a ratio of 1:0.4 AMPS:NVP produced a small change in γ_s^d and γ_s^p. Increasing the ratio of the NVP comonomer to 1:1 AMPS:NVP insignificantly reduced the to 37.9±2 mN/m. These values of γ_s^d are the opposite of the γ_s^d. The γ_s^t remains the same as the control. The NVP comonomer is displaying its hydrophobic character and reduce the γ_s^p while increasing the γ_s^d.

6.2.5.3 Comments on the Surface free energy (γ) of series A and C gels

The thermodynamic requirement for adhesion is that γ adhesive < γ substrate. The γ for skin has been reported to be between 38-56 mN/m [64, 65]. The initial values of γ_s^t for both series A and C gels are close to or below this value and this indicates adherence should occur. At the final values of γ_s^t for both series A and C gels above the γ of the skin and so they should not adhere. When the patches were worn they did adhere to the skin and remained adhered to the skin until removed.

6.2.6 Rheology of NVP copolymer gels

Viscoelasticity can be studied using rheology. Dynamic mechanical analysis, in particular the oscillatory frequency sweep experiment allows the adhesive properties of the gel to be determined. The dynamic-mechanical properties (the elastic modulus (G'), viscous modulus (G") and tan δ (G''/G') have been correlated to tack and peel [147-154], see Appendix II – Rheology and viscoelastic materials.

As the gels from series A containing ionic monomer:NVP in ratios of 39:1 and 19:1 showed the most favourable peel strength and free surface energies these were analysed by rheology.

Figure 96 is a sample graph of an oscillatory frequency sweep of a gel showing G', G'' and tan δ against frequency, all of the series A gels studied had a plot similar to the example shown this figure. We can see that tan δ increases over time and this is a requirement for PSAs in terms of the bonding (application) and de-bonding (removal) processes.

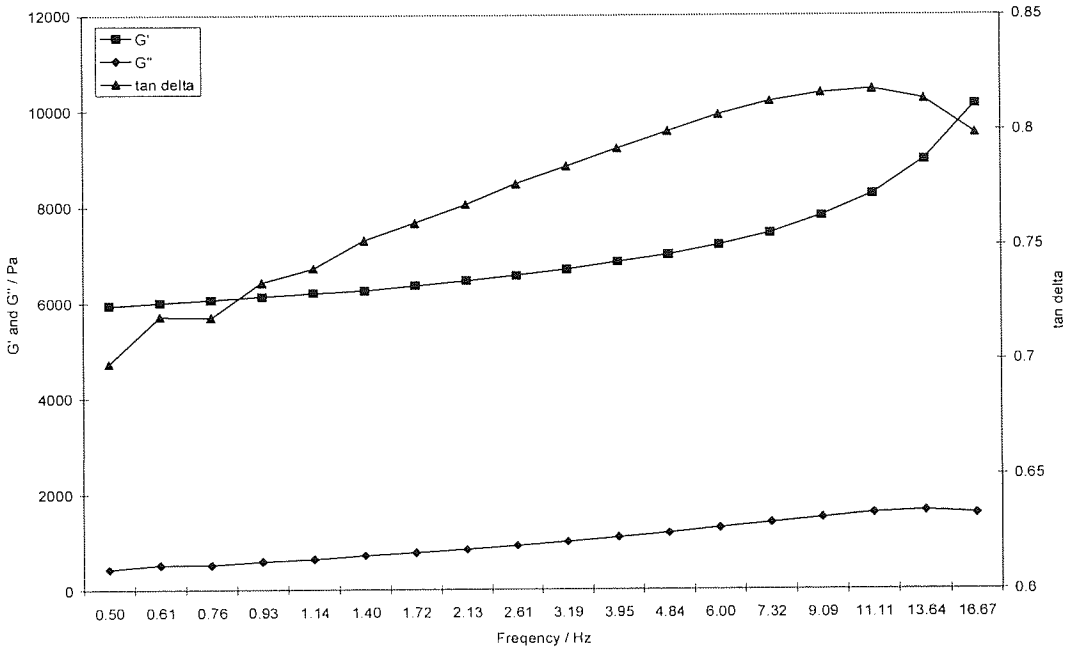

Figure 96. Sample graph of an oscillatory frequency sweep of a gel showing the storage modulus (G') loss modulus (G')' and tan delta against frequency

Viscoelastic behaviour at low frequency (~1Hz) is representative of the shear forces involved during the application of a gel or adhesive. Whereas higher frequency (~10Hz) is representative of the shearing forces involved in the removal of a gel or adhesive removal. The skin adhesive requires a dominant elastic component during application to allow the flow of the material over the skin; a reduced viscous component is also favourable at this time. During removal a reduced elastic and increased viscous component will be favourable. The tan δ plotted against ω are also be expected to have a positive gradient for good adhesive properties of gels [152-154].

As the G', G'' and tan δ at 1Hz and at 10Hz are important figures in terms of application and removal of skin adhesives. These data points for the control 1 and the gels with ionic monomer:NVP in ratios of 39:1 and 19:1 and are shown in Figure 97 and Figure 98 respectively.

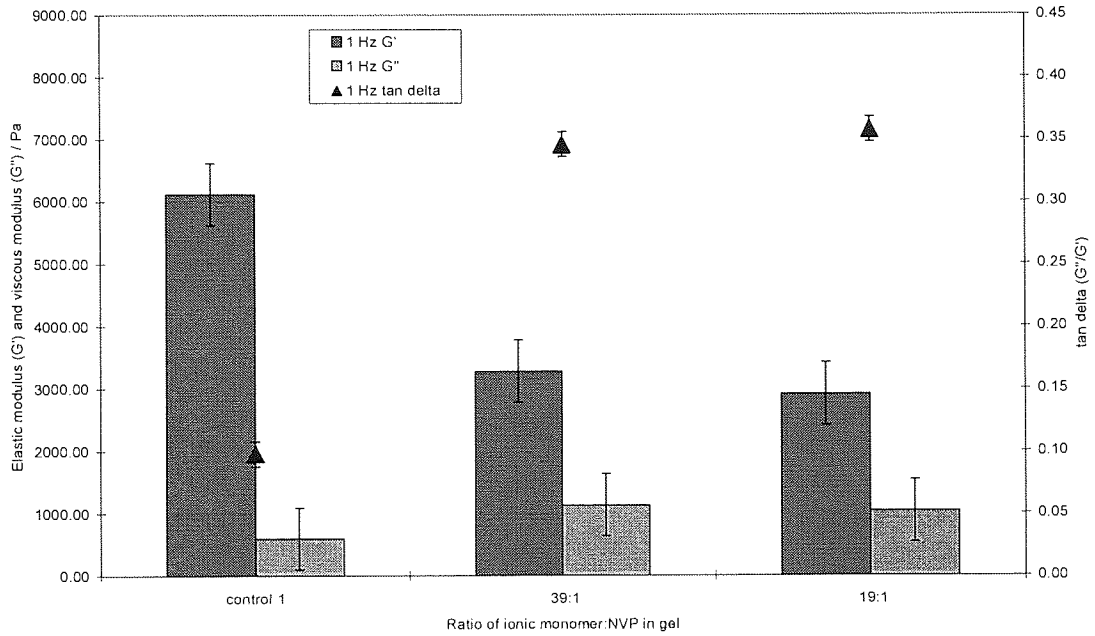

Figure 97. Elastic modulus (G'), viscous modulus (G'') and tan delta (G''/G') at 1Hz for control and SPA:AMPS:NVP gels. Where the ionic monomers are SPA (acrylic acid bis-(3-sulfopropyl)-ester potassium salt) and AMPS (2-acrylamido-2-methyl propane sulfonic acid sodium salt) and NVP is N-vinyl pyrrolidone. N=5, ±SD

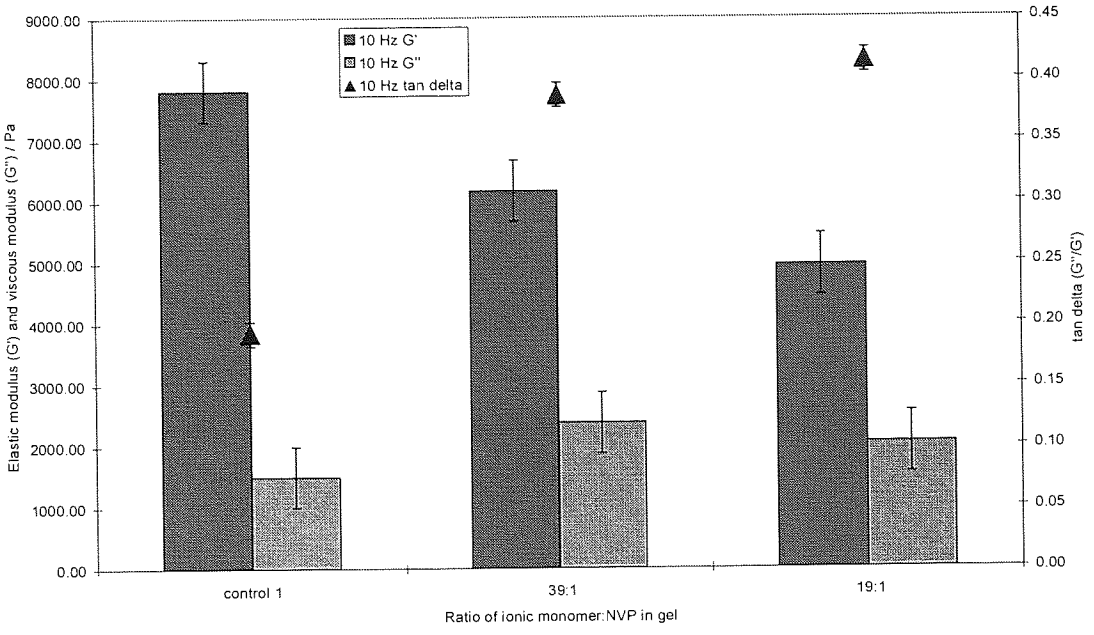

Figure 98. Elastic modulus (G'), viscous modulus (G'') and tan delta (G''/G') at 10Hz for control and SPA:AMPS:NVP gels. Where the ionic monomers are SPA (acrylic acid bis-(3-sulfopropyl)-ester potassium salt) and AMPS (2-acrylamido-2-methyl propane sulfonic acid sodium salt) and NVP is N-vinyl pyrrolidone. N=5, ±SD

At ~1Hz the control 1 gel has a G' 6125±500 Pa, a G'' 600±180 Pa and a tan δ 0.1. These values are within the criteria for good pressure sensitive adhesives as described by Chu and other workers [149, 150, 155]. The Chu criteria are:

$$\text{(i) } G' \ (\omega = 0.1 \text{ rad/s}) \sim 2 \text{ to } 4\times10^5 \text{ dynes/cm } (0.2 - 4\times10^4 \text{ Pa})$$

and

$$\text{(ii) } 5 < [G' \ (\omega = 100)/G'' \ (\omega = 0.1)] < 300$$

Good cohesive properties can be expected from gels with a G' (1 rad/s) of between 1000 – 10000 Pa and a G" (1 rad/s) of between 300 – 5000 Pa [147].

With the incorporation of NVP in a ratio of 39:1 (ionic monomer:NVP) significantly (p=0.002) reduces the G' to 3280±500 Pa while significantly (p=0.022) increasing the G'' to 1134±180 Pa. This has the effect of increasing the tan δ to 0.35. A similar trend is seen at ~10Hz.

An NVPcoAMPS polymer may allow hydrogen bonding to occur between the carbonyl of the NVP and the amide of the AMPS as shown in section 6.2.4.3. There may also be van der Waals interactions between the NVP carbon ring and the methyl's on the AMPS. Both of these would the affect the viscoelastic nature of the copolymer as reflected in the reduction of G' and increase in G''.

Increasing the NVP comonomer to a ratio of 19:1 sees the insignificant reduction of G' to 2915±500 Pa and the insignificant reduction of G'' to 1043±180 Pa. The values of G' and G'' for these gels fall within the criteria required for a good PSA [12, 147, 156]. A similar trend is seen at ~10Hz.

6.3 *N,N-dimethyl-N-(2-acryloylethyl)-N-(3-sulfopropyl) ammonium betaine (SPDA) copolymer pressure skin adhesives (PSA)*

6.3.1 Introduction to SPDA copolymer PSA

Zwitterionic monomers have been used to produce hydrogel materials for biomaterial applications but in the PSA area there are few examples. There have been PSA applications using cationic and anionic monomers in combination to provide overall neutrality [157] but the use of zwitterionic monomers for this application can only be been seen in patents by the Minnesota Mining and Manufacturing Company [158, 159] and the Chesebrough-Pond's USA Co. [160].

The section describes copolymerisation of SPDA, acrylic acid bis-(3-sulfopropyl)-ester potassium salt (SPA) and 2-acrylamido-2-methyl propane sulfonic acid sodium salt (AMPS) to provide partially hydrated gels that could increase the adhesion to oily skin through PSA and lipid interaction. The lipids, particularly the phospholipids may intercalate with the SPDA and possible be absorbed by the PSA thus reducing the excess lipid at the interface. The structurally related 2-methacryloyloxyethyl phosphoryl choline (MPC) has an affinity for lipids through the interaction of its phosphatidylcholine headgroup [161]. The charged headgroup of the

phosphatidylcholine and phosphatidylethanolamine could interact with the charged groups of the SPDA through dipole-dipole interactions as shown in Figure 99.

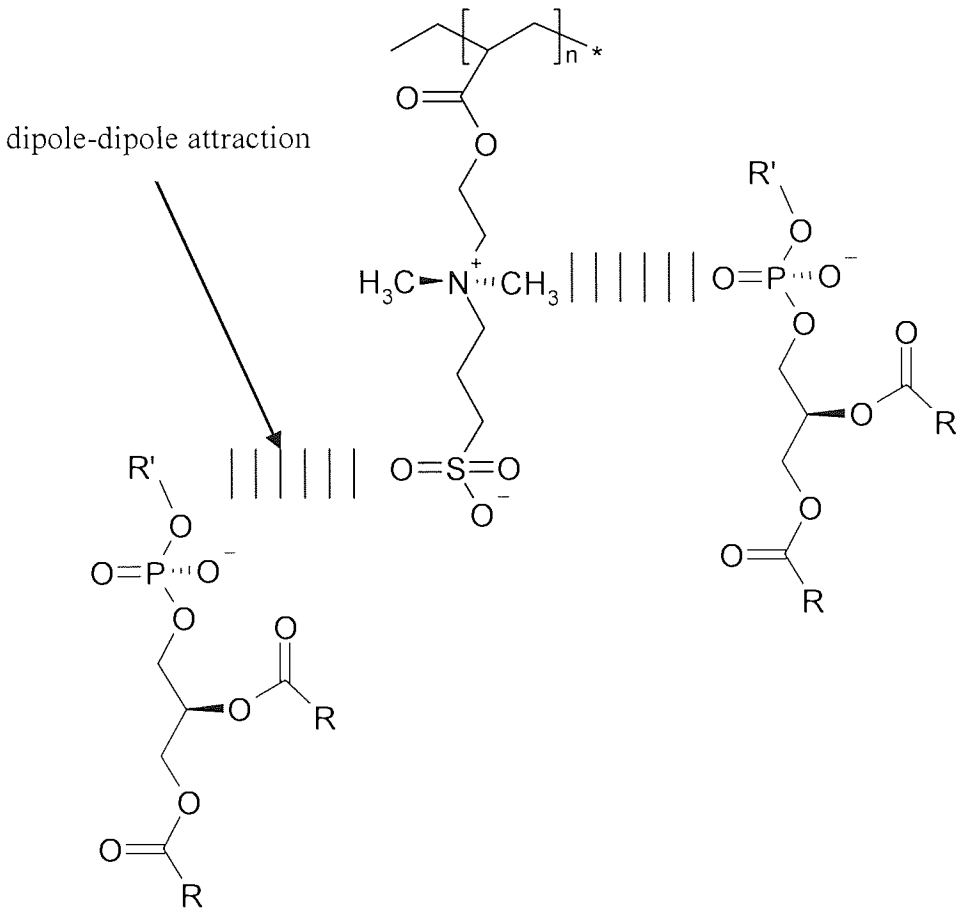

Figure 99. Intercalation of phosphatidylcholine and phosphatidylethanolamine with N,N-dimethyl-N-(2-acryloylethyl)-N-(3-sulfopropyl) ammonium betaine (SPDA)

The absorption of the lipids from the skin-adherant interface might also result in an increased adhesion. This work on SPDA was undertaken as an extension the lipid based studies in Chapter 3 and 4. It was in part an extension of the previous work undertaken in this laboratory on zwitterionic hydrogels [11].

6.3.2 Composition of SPDA copolymer gels

The compositions of SPDA gels were based on the 6:4 SPA:AMPS gels as described for the NVP copolymer gels in section 6.2.2. All gel described after this point only

show the monomer contribution of 40% to the total composition of the gels. Glycerol and water each contribute 30% to the total composition of the gel but are not described.

A series of compositions were prepared from of SPDA, AMPS and SPA monomers to investigate the effect of copolymerising SPDA with SPA and AMPS. The series started with a ratio of 7.7:1 ionic monomers:SPDA. The series continued with the progressive incorporation of SPDA to provide compositions with ratios of 3:1 and 1:1 ionic:SPDA. The ionic monomers (SPA:AMPS) were present in a ratio of 6:4 for these compositions. This series was labelled series D.

Two more series of compositions were prepared, one from SPDA and SPA monomers and another from SPDA and AMPS monomers. These were labelled series E and series F respectively.

Series E composed of SDPA and SPA monomers in ratios of 1:1 and 1:3. Series F composed of SPDA and AMPS monomers in ratios of 1:1 and 1:3. The SPDA containing compositions are shown in Figure (Figure 100). The control is the same as that described earlier in section 6.2.2.

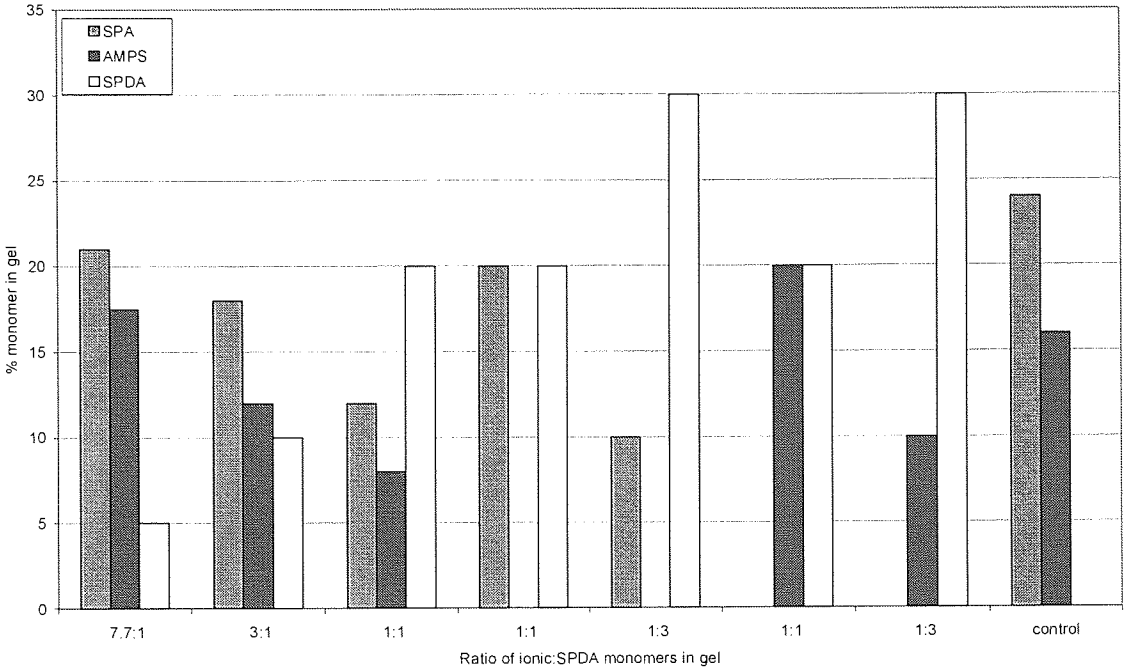

Figure 100. Monomers composition in SPDA, AMPS and SPA gels. Where SPA is acrylic acid bis-(3-sulfopropyl)-ester potassium salt, AMPS is 2-acrylamido-2-methyl propane sulfonic acid sodium salt and SPDA is N,N-dimethyl-N-(2-acryloylethyl)-N-(3-sulfopropyl) ammonium betaine

6.3.3 Polymerisation of SPDA gels

Monomer preparation and polymerisation were carried out as outlined in Chapter 2 for partially hydrated gels. The cross linker used was Ebacryl II and the initiator was Irgacure184. This crosslinker:initiator (10:3) solution was used at ~0.33% of the total composition weight. The composition all polymerised to form cohesive, transparent and adhesive gels.

6.3.4 Peel strength of SPDA copolymer gels

The 90° perpendicular peel test as described in Chapter 2 was used to determine the peel strength of the SPDA copolymer membranes. The peel strengths of series D (SPDA:AMPS:SPA), series E (SPDA:SPA) and series F (SPDA:AMPS) gels are shown in Figure 101.

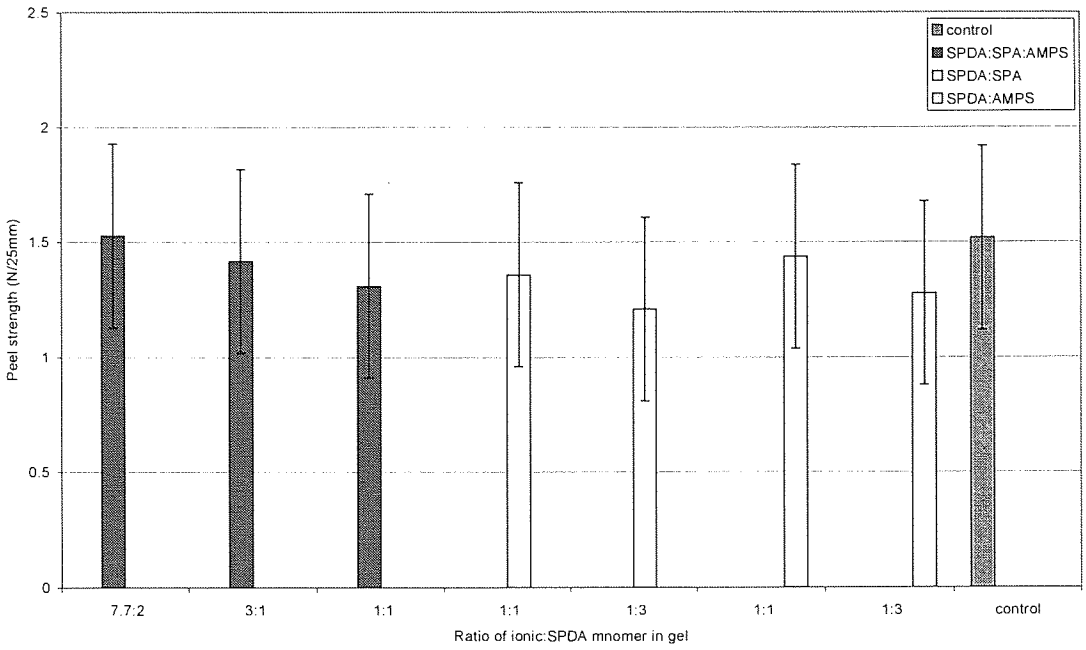

Figure 101. Peel strengths of SPDA, AMPS and SPA gels. Where SPA is acrylic acid bis-(3-sulfopropyl)-ester potassium salt, AMPS is 2-acrylamido-2-methyl propane sulfonic acid sodium salt and SPDA is N,N-dimethyl-N-(2-acryloylethyl)-N-(3-sulfopropyl) ammonium betaine . The control is a copolymer of SPA:AMPS at a of 6:4 ratio. N=5, ±SD

The peel strengths of all the SPDA gels are between 1.28 and 1.53 N/25mm and are not significantly different. There is a trend for the decrease in peel strength with the increase of SPDA comonomer in the gels. The structure of SPDA is similar to the structure of AMPS and SPA and the group that would be present at the surface of the gels are the sulfonate groups in the case of all of these comonomers. It seems that the hypothesised intercalation between the SPDA and the lipids does not occur.

6.3.4.1 The effect of skin moisturiser on the peel strengths of SPDA copolymer gels

In an effort to replicate a "greasy" skin a moisturiser was applied to the skin of the subject. A small amount of moisturiser was applied to the skin and rubbed in. The peel tests were repeated after five minutes of the application of a skin moisturiser. The results for all the gels were that the peel strengths were not recordable. The adhesive was removed from the skin without the Houndsfield tensiometer being able to make a

recording. In retrospect it was apparent that the application of the moisturiser was too liberal as it affected all of the gels ability to adhere to the skins surface.

6.3.5 Surface free energy (γ) of SPDA copolymer gels

The contact angles of test liquids such as water and diidomethane allows the calculation of the γ of a material. The total free surface energy (γ_s^t) of a material can be found from the sum of the dispersive (γ_s^d) and polar components (γ_s^p), see Appendix VI - Contact angle. The contact angle can be measured either as initial contact angle or kinetic contact angle using the sessile drop technique as described in Chapter 2.

A GBX Goniometer was used to record the kinetic contact angles of water and diidomethane on the surface of the series D, E and F gels as described in the Chapter 2. The samples were hydrated when analysed in these experiments.

The initial contact angles are different to the final contact angles for series D, E and F gels. This is once again due to the storage of the gels on a silicone release paper which allows the hydrophobic groups to reorientation themselves to the surface of the gel. Although the initial and final values γ are different they do not follow the trend as the NVP containing gels as described in section 6.2.5.

6.3.5.1 Surface free energy (γ) of series D (SPDA:AMPS:SPA)gels

Series D consisted of gels with the AMPS:SPA:SPDA monomers in the ratios of 7.7:1, 3:1 and 1:1 ionic:SPDA. With the ionic monomers present in the ratio of 6:4 SPA:AMPS.

The difference between the initial and final γ for the series D gels are that the γ_s^t and γ_s^p are higher in the final values. The initial γ_s^d of control 1 gel is 20.9±2 mN/m and an initial γ_s^p of 24.1±2 mN/m. These values do not change significantly with the incorporation of SPDA as a comonomer at any of the ratios tested.

The SPDA structure has features of both the SPA and AMPS structures. These structural features may explain why the replacement of AMPS and SPA with SPDA is having little effect on the γ of the resulting gels. SPDA has the sulfonate as the terminal group the same as SPA and AMPS. It also has the amide group similar to AMPS. The amine of the SPDA has two methyl groups placed between the quaternary nitrogen and the sulfoante groups and there are two methyl groups placed similarly in the AMPS structure. The same structural features are able to rotate to present them selves to the environment they are exposed to.

The initial γ and final γ in are shown in Figure 102 and Figure 103 respectively.

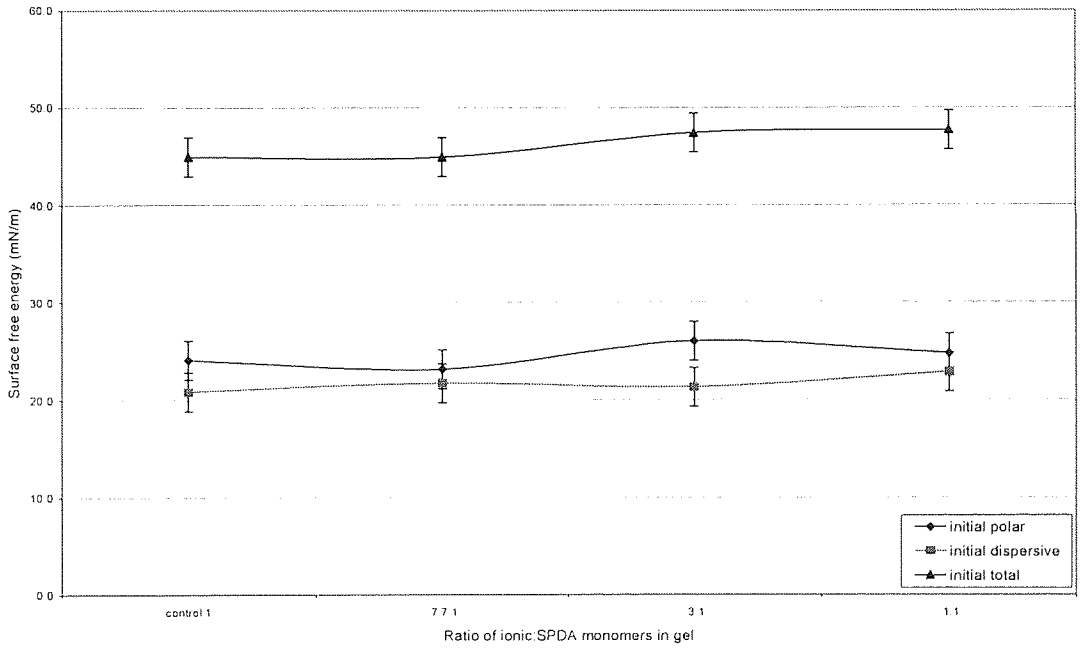

Figure 102. Initial surface free energy of SPDA:AMPS:SPA gels. Where the ionic monomers are SPA (acrylic acid bis-(3-sulfopropyl)-ester potassium salt) and AMPS (2-acrylamido-2-methyl propane sulfonic acid sodium salt) and SPDA is N,N-dimethyl-N-(2-acryloylethyl)-N-(3-sulfopropyl) ammonium betaine. N=5, ±SD

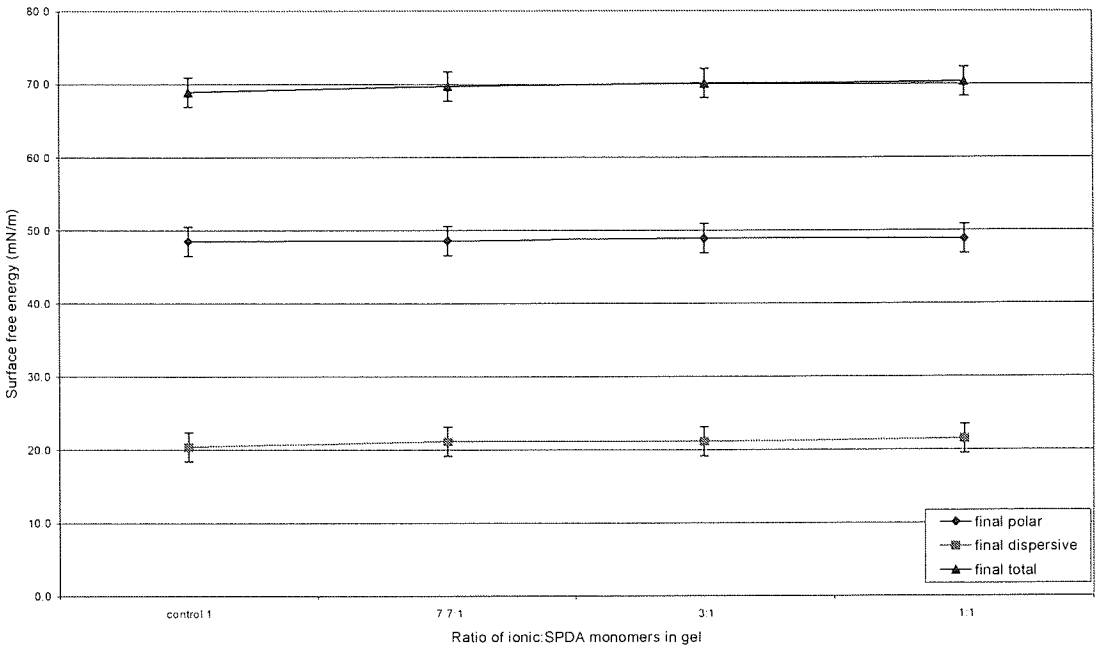

Figure 103. Final surface free energy of SPDA:AMPS:SPA gels. Where the ionic monomers are SPA (acrylic acid bis-(3-sulfopropyl)-ester potassium salt) and AMPS (2-acrylamido-2-methyl propane sulfonic acid sodium salt) and SPDA is N,N-dimethyl-N-(2-acryloylethyl)-N-(3-sulfopropyl) ammonium betaine. N=5, ±SD

6.3.5.2 Surface free energy (γ) of series E (SPDA: SPA) and F (SPDA:AMPS) gels

Series E consisted of gels with the monomers SPDA:SPA in the ratios of 1:1 and 1:3 ionic:SPDA. Series F consisted of gels with the monomers SPDA:AMPS in the ratios of 1:1 and 1:3 ionic:SPDA.

The initial and final γ for series E are shown in Figure 104 and Figure 105 respectively. The initial and final γ for series F are shown in Figure 106 and Figure 107 respectively. These figures show that all the gels have values of γ that do not differ significantly from the control. The use of SPDA as a copolymer does not significantly alter the γ of these gels when hydrated. The reasons for this are the structural similarities between SPDA and AMPS as indicated earlier for the series D (SPDA:SPA;AMPS) gels in section 6.3.5.1.

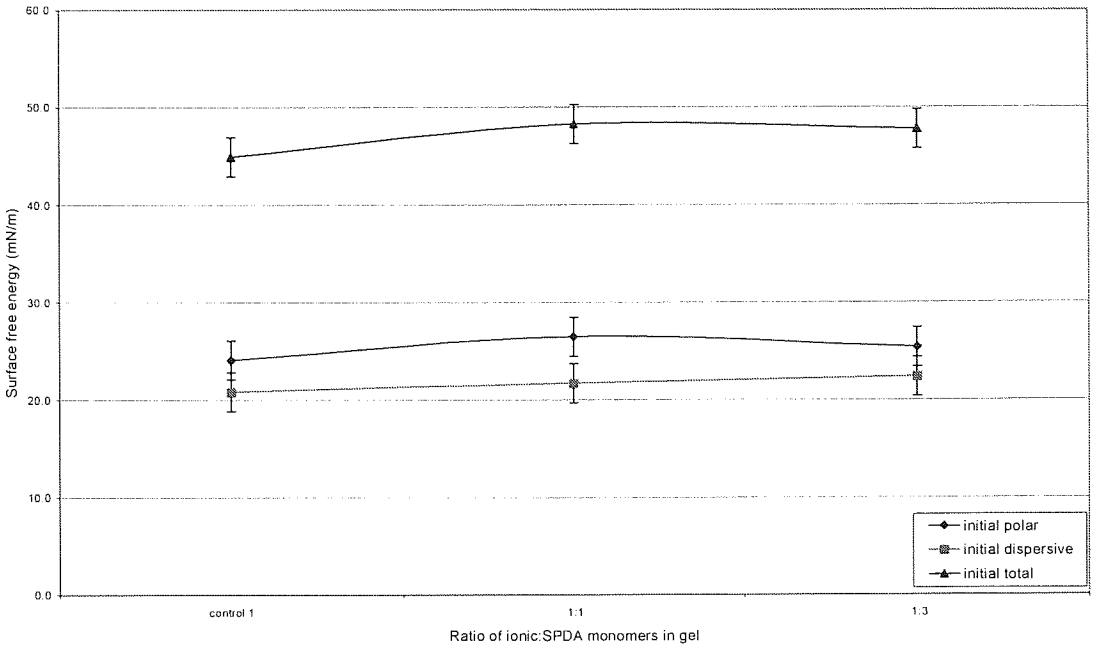

Figure 104. Initial surface free energy of SPDA:SPA gels. Where the ionic monomer is SPA acrylic acid bis-(3-sulfopropyl)-ester potassium salt and SPDA is N,N-dimethyl-N-(2-acryloylethyl)-N-(3-sulfopropyl) ammonium betaine. N=5, ±SD

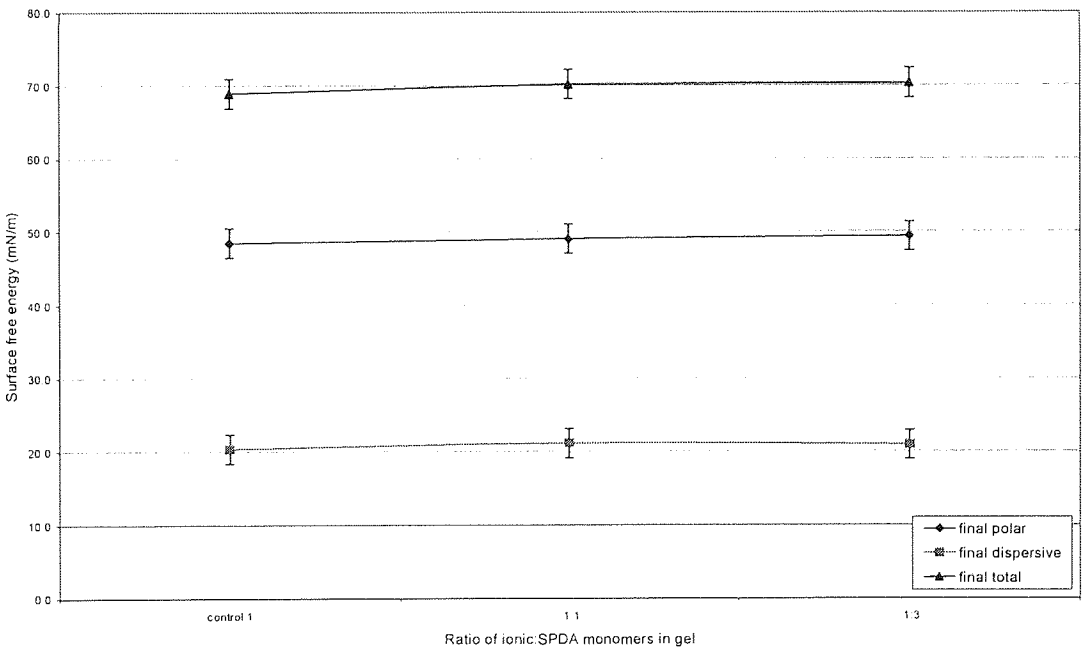

Figure 105. Final surface free energy of SPDA:SPA gels. Where the ionic monomer is SPA acrylic acid bis-(3-sulfopropyl)-ester potassium salt and SPDA is N,N-dimethyl-N-(2-acryloylethyl)-N-(3-sulfopropyl) ammonium betaine. N=5, ±SD

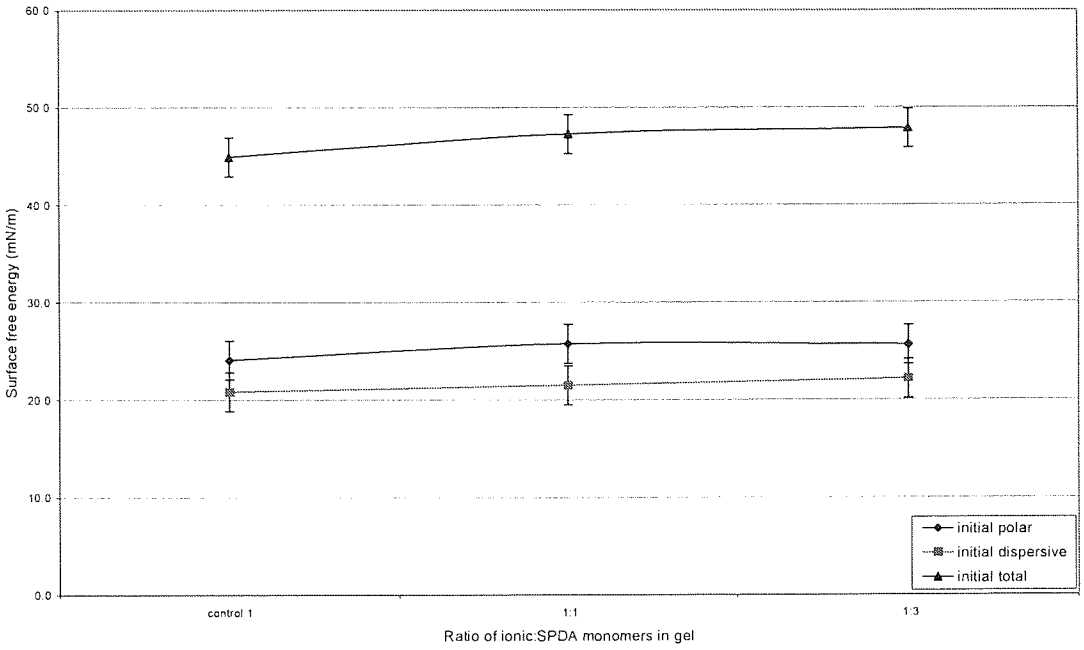

Figure 106. Initial surface free energy of SPDA:AMPS gels. Where the ionic monomer is AMPS (2-acrylamido-2-methyl propane sulfonic acid sodium salt) and SPDA is N,N-dimethyl-N-(2-acryloylethyl)-N-(3-sulfopropyl) ammonium betaine. N=5, ±SD

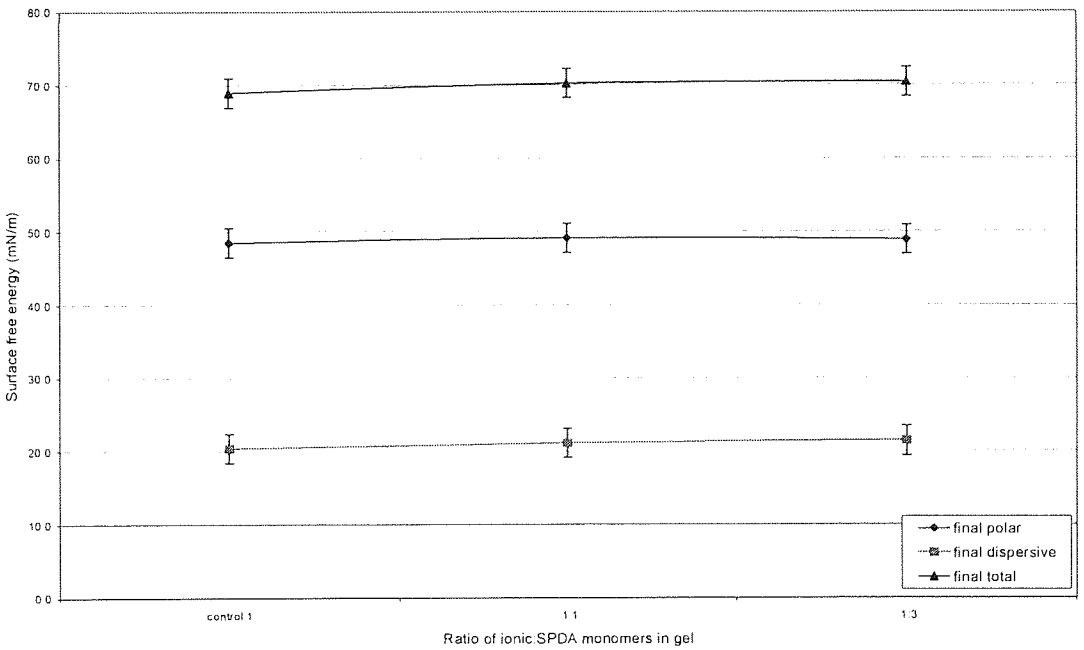

Figure 107. Final surface free energy of SPDA:AMPS gels. Where the ionic monomer is AMPS (2-acrylamido-2-methyl propane sulfonic acid sodium salt) and SPDA is N,N-dimethyl-N-(2-acryloylethyl)-N-(3-sulfopropyl) ammonium betaine. N=5, ±SD

6.3.6 Rheology of SPDA copolymer gels

Only Series D (SPDA:SPA:AMPS) gels rheological properties were determined as the series E and F showed similar properties in other respects. An example of a plot of G', G'' and tan δ vs frequency for an SPDA gel is shown in Figure 108. This figure shows that the tan δ has a positive gradient which is a suggested requirement for PSAs. The value of G' and G'' for the series D gels are within suggested criteria values as outlined in section 6.2.6.

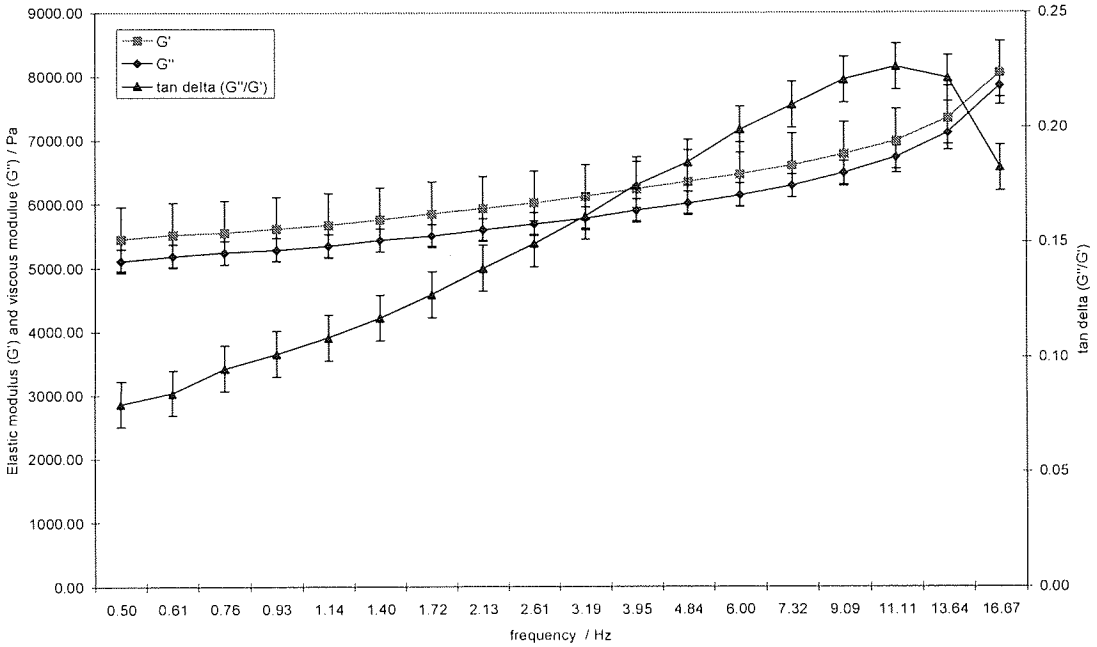

Figure 108. Example graph of an oscillatory frequency sweep of an SPDA containing gel showing the storage modulus (G') loss modulus (G')' and tan delta against frequency. N=5, ±SD

The G'' has a positive gradient but does not reach a maximum at higher frequencies as seen with the NVP containing gels (section 6.2.6). The reduction of G'' at higher frequencies (~10Hz) is normally seen with PSAs. The inner salt of the SPDA must be having an effect on the G''. The dipolar bonds between SPDA on different chains must be causing a retractive force causing the gel to be more viscous at higher frequencies. The G', G'' and tan δ for the SPDA:AMPS:SPA gels at 1 Hz and 10 Hz are shown in Figure 109 and Figure 110 respectively.

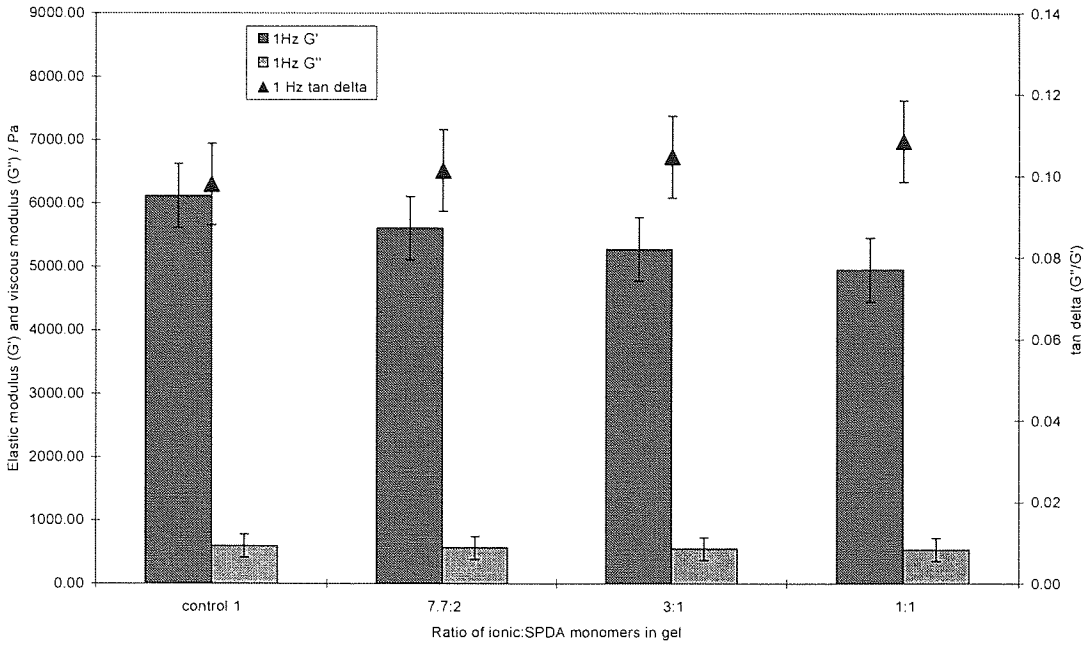

Figure 109. Elastic modulus (G'), viscous modulus (G") and tan delta (G"/G') at 1Hz for control and SPDA:AMPS:SPA gels. Where the ionic monomers are SPA (acrylic acid bis-(3-sulfopropyl)-ester potassium salt) and AMPS (2-acrylamido-2-methyl propane sulfonic acid sodium salt) and SPDA is N,N-dimethyl-N-(2-acryloylethyl)-N-(3-sulfopropyl) ammonium betaine. N=5, ±SD

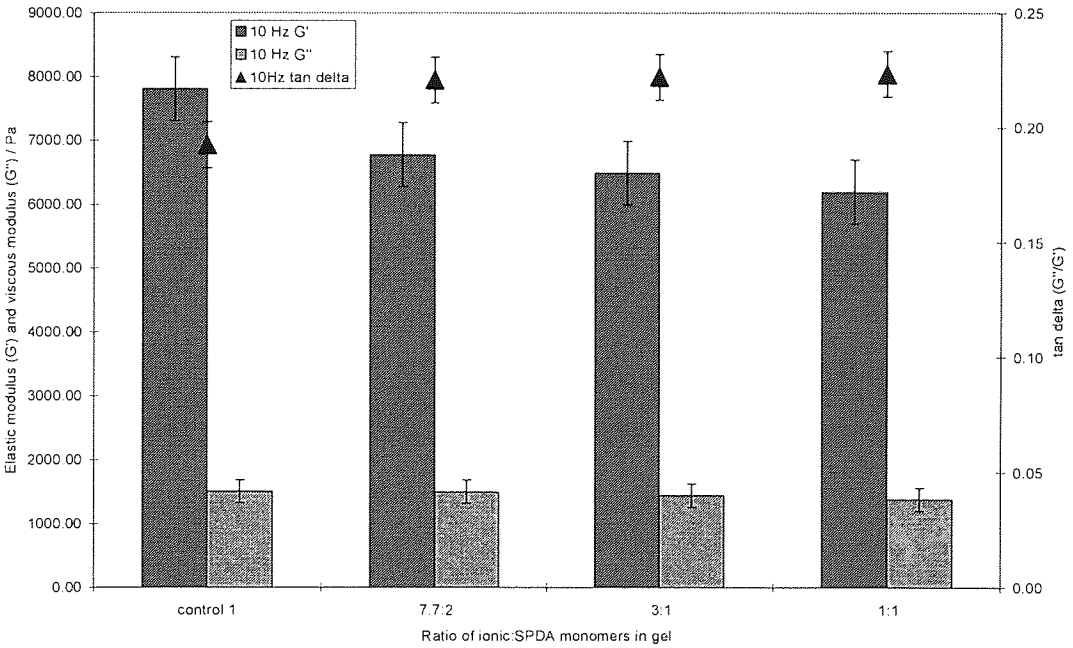

Figure 110. Elastic modulus (G'), viscous modulus (G") and tan delta (G"/G') at 10Hz for control and SPDA:AMPS:SPA gels. Where the ionic monomers are SPA (acrylic acid bis-(3-sulfopropyl)-ester potassium salt) and AMPS (2-acrylamido-2-methyl propane sulfonic acid sodium salt) and SPDA is N,N-dimethyl-N-(2-acryloylethyl)-N-(3-sulfopropyl) ammonium betaine. N=5, ±SD

At 1 Hz there is an insignificant decrease in the G' and no change in the G'' as we increase the percentage of SPDA in the gel. At 10 Hz the increase of SPDA copolymer had the effect of significantly reducing the G'. There is no change in the G''. This reduction in G' may be the effect of the charged groups of the inner salt creating dipolar bonds with inner salt groups on other chains. This would cause the network to have less free chain rotation and resulting in a lower elasticity. The values of G' and G'' for these gels falls within the suggested criteria required for a good PSA, as outlined in section 6.2.6.

6.4 Conclusions

A series of partially hydrated hydrogels was synthesised from N-vinyl pyrrolidone (NVP), acrylic acid bis-(3-sulfopropyl)-ester potassium salt (SPA) and 2-acrylamido-2-methyl propane sulfonic acid sodium salt (AMPS) monomers. All the gels were clear, cohesive and tacky. There was an aroma of NVP after polymerisation which may have indicated residual NVP.

Among the important properties for pressure sensitive adhesive (PSA) are namely peel strength, surface free energy (γ) and dynamic mechanical properties; these were investigated for the synthesised gels. The peel strengths of the SPA:AMPS:NVP copolymers gels was higher (~2.4 N/25mm) than a control gel (1.52 N/25mm) when the ratio of ionic:NVP monomers was kept low (39:1 or 19:1). The SPA:AMPS:NVP and AMPS:NVP copolymers gels had peel strengths that were low ($\leq$2.4 N/25mm) compared to the preferred peel strengths for skin adhesive applications ($\geq$3 N/25mm). The SPA:NVP copolymers gels had peel strengths to low to recorded using the 90° perpendicular peel test. It was thought that the subject used to record the peel strengths may have had greasy skin and so lowered the peel strength but a different subject did not produce significantly different results. Intersubject variation therefore was not considered to be a relevant parameter in the low peel strength of these gels.

The contact angles of the test liquids SPA:AMPS:NVP and AMPS:NVP copolymers gels revealed that the γ were within the requirements for the adhesives application, i.e. below the adherents when they were initially recorded.

However over time (~60 seconds) the contact angles changed and the γ became above those of the adherent indicating that the gels should not adhere to the skins surface. The contact angles of the test liquids and the SPA:NVP copolymers were not determined.

When applied to the subject's skin the gels did adhere to the skin for several hours until they were removed, at the point at which the gels were removed they were still adhered to the skin. This would not be predicted to be the case from the peel strength and value of the γ reported. The dynamic mechanical properties of the SPA:AMPS:NVP copolymer were detemined as these gels produced the most suitable peel strengths and γ for use as PSA for the skin. The elastic modulus (G'), viscous modulus (G'') and tan δ of the SPA:AMPS:NVP gels were all within the suggested criteria for PSAs.

Another series of partially hydrated hydrogels was synthesised from N,N-dimethyl-N-(2-acryloylethyl)-N-(3-sulfopropyl) ammonium betaine (SPDA), SPA and AMPS monomers. All the gels were clear, cohesive and tacky. The peel strength, surface free energy (γ) and dynamic mechanical properties of these gels were also determined. The peel strengths and γ of these gels did not differ significantly from a control gel. The G', G'' and tan δ of the SPDA:SPA:AMPS copolymer gels were all within the suggested criteria for PSAs. The use of SPDA as a comonomer in these gels causes a lowering of viscosity at higher (~10Hz) which is unusual for PSAs.

The high level of the γ of NVP and SPDA gels is in agreement with the low peel strengths. These results indicate that the NVP and SPDA copolymer gels are unsuitable for use as skin adhesives. However the initial values of γ and the values of G', G'' and tan δ of these gels does not agree with the other results and indicates that the gels are suitable for use as skin adhesives. Overall the gels synthesised in this thesis would not be suggested as suitable for use in greasy skin applications. The SPDA copolymers gels do have antipolyelectroltye properties that may give them advantages in certain applications such as wound dressing.

Chapter 7 – Discussion and Further work

"Make everything as simple as possible, but not simpler"
Albert Einstein

7.1 Introduction

The aims of the thesis can be broadly divided into two areas; the first was to collect and analyse the lipids of the tear film and of the skin. The second was to synthesise novel phospholipid analogous materials for ocular and dermal applications using the information gained from the analytical studies of the lipids. This chapter starts with a summary and discussion of the analytical work carried out in Chapters 3 and 4 along suggestions of further work for the area. This is followed by a summary and discussion of the synthetic work carried out in Chapter 5 and 6 along with suggestions of further work for that area.

7.2 Summary of the analytical studies

The analytical work of the thesis is concerned with the lipids of the tear film and those on the surface of the skin. These are body sites where biomaterials are used and exposed to the surrounding lipids. Hydrogel biomaterials applied in such body sites are known to become spoiled with biological species while in situ.

These eye and skin body sites are also easily accessible allowing the introduction and removal of a biomaterial with minimum invasiveness making them ideal sites, in this respect, for the study of material-host interactions. Lipids are among the biological species that have been shown to interact with and deposit onto materials that are placed in contact with them, e.g. contact lenses [77, 78]. In additional to this spoilation the presence of contact lenses in the tear film presents other problems, such as the reduction in the stability of the tear film [162]. It is the phospholipids which are believed to impart much of the tear film stability, at least at the lipid-aqueous interface of the tear film [44, 76, 115, 163].

Generally in the ocular environment the studies presented in the literature concentrate on the non polar lipids and little attention has been paid to the polar lipids. This is the case both for the literature concerning lipid/material interactions and also that of the natural tear film. A better understanding of the concentration and behaviour of the polar lipids in the tear film in the natural state is needed to help improve understanding of how these lipids will interact with a material when it is placed into

that environment. This knowledge of the tear film polar lipids in the absence of materials should provide additional information into why problems occur in the presence of materials and potentially lead to the development of materials to overcome such problems.

Chapters 3 and 4 describe the analysis of the phospholipid presence and activity in the tear film. Tear samples were collected using glass capillaries or opthalmic sponges with the method as described in Chapter 2. The lipids need to be extracted from the whole of the tear sample before analysis; te extraction methods used were a modified Bligh and Dyer, methanol:chloroform and methanol as described in Chapter 2. The High Performance Liquid Chromatography (HPLC) method developed as described in section 3.2 allowed separation of the target phospholipid molecules from the non polar lipids. The non polar lipids eluted with a retention time different from that of the phospholipid indicating that they should not interfere with chromatography. There is further scope for the development of the non polar HPLC method and as will be explained later there is now more of an interest in the non polar lipids; in particular the diacylgylcerides.

The HPLC method allowed separation of the individual phospholipids classes based on their fatty acid groups. Predictably, the ultraviolet detector used in the HPLC development could not detect phospholipid; consequently mass spectrometry (MS) was utilised as the detection technique. Direct infusion of polar and non polar lipids into the MS was used to establish fragmentation patterns of the species as described in section 3.3. This process allows the identification of individual species of phospholipids by MS detection.

The LCMS method involves hyphenation of LC and MS methods and is described in section 3.4. It combines the separation provided by the HPLC with the detection capability of the MS. The LCMS method developed was calibrated to a sensitivity of 4μg/ml. The LCMS of the non polar lipids indicated that some lipids, the cholesterol esters, may not be stable to the conditions nedded for the MS. The development of non poar LCMS is an area for further work. Allthough the LCMS methos allows the separation and identification of phospholipids there is still developmental work required for the LCMS phospholipid method because the fragmentation patterns of

other phospholipids need to be established; specifically phosphatidylinositol and phosphatidylglycerol.

The extracted lipids were analysed with the LCMS method as described in section 3.4. The LCMS analysis of extracted tear film lipids showed that the meibomian gland secretion (MGS) and tear film do not have the same concentrations of phospholipid as previously reported. The tear fluid has been reported as having a volume of 7μl and the lipids reported as composing an average of 3.52μg/μl [31, 41, 42]. Within this the phospholipids compose ~6.1% (0.215μg/μl) [33-37]. Previous workers in this area concentrated on analysing only meibomian gland secretion and wrongly assumed the same lipids were present in similar concentrations in the tear film. The LCMS analysis showed that the phospholipid in the tear film was in fact present at concentrations lower than previously reported. The concentration of phospholipids in the tear film was below 0.004μg/μl, the limit of detection for this method.

The cited literature shows limited reports which focus on the lipids of the tear film however one recent study [164] indicated that only two phospholipids were present in the tear film, namely dipalmitoylphosphatidoylcholine (DMPC) and pyrosphingomyelin (PSM). This conflicts with the presence of phospholipid in the meibomian gland secretion (MGS) as indicated in the literature [39, 165]; where PSM had not been reported and DMPC was found only at low concentrations. The finding of low concentration of phospholipid in the tear film as reported in Chapter 3 is also consistent with the fact that the monolayer model [115] phospholipid concentration requirement is lower than the concentration of the phospholipid provided by the MGS (as described in Chapter 4). The information gathered by the analysis of the tear film lipids using the LCMS method and comparison with the literature indicates that phospholipid is present in lower concentrations in the tear film than in the MGS. The thin layer chromatography (TLC) as reported in section 4.2 also demonstrated that the phospholipid was not present at concentrations previously thought by incorrectly assuming the tear film and MGS had the same composition of phospholipid.

The TLC studies in section 4.2 indicated that diacylgylceride (DAG) was present in the tear film at relatively high concentrations. If MGS has the same composition as

tear fluid then this finding also conflicts with the previous reports on MGS lipids where DAG was not present at high concentrations [33-37]. It appeared that phospholipid was at a lower concentration and DAG was at a higher concentration than those levels found in MGS. The findings of Chapter 3 and those presented in the literature took the work in a new direction – namely to try to find the reason for the concentration difference of phospholipid and DAG in the MGS and tear film.

A potential explanation behind these findings is that lipases are present in the tear film and process the phospholipids into DAG and free fatty acids (FFA). One phospholipase, phospholipase A_2 (PLA_2) is known to exist in the tear film at a relatively high concentration. PLA_2 would produce a reduction in levels of phospholipid in the tear film but it cleaves phospholipids in a different manner to that which would produce DAG and FFA as is explained in section 4.4, it would not produce DAGs and FFA. The presence of another lipase, phospholipase C (PLC) in the tear film could account for this reported reduction of phospholipids and the increase in DAG. PLC has different cleavage specificity on phospholipids than that of PLA_2, also described in section 4.4. This theory was investigated as described in Chapter 4 using two techniques: counter immunoelectrophoresis (CIE) and a PLC activity assay.

The CIE analysis reported in section 4.3 found the levels of PLC to be below 0.1mg/ml, which is the lower level of detection using Coomassie blue as the stain. The PLC is likely to be below this concentration as it is an enzyme and these are know to be required in only low concentration to fulfil their function. Alternatively there may a lack of detection due to specificity problems with the antibody. Antibodies to other isoforms of PLC should be investigated using the CIE technique. The activity assay as reported in section 4.3 indicated that PLC was active in the tear film at 15mU/ml which could account for the removal of ~12.8% of the PC present in the tear film per minute. Although the activity assay proved positive with tear samples, the levels detected were inadequate to account for the difference between concentrations of phospholipids in the MGS and those in the tear film. However PLC activity was detected and this activity could account the transferral of some of the phospholipids into DAG and FFA. The activity of PLC in the tear film has not been reported previously.

Although the PLC activity in the tear film was established there is the possibility that the activity of the PLC in the tear film in vivo may be different to that in the assay due to the differences between the environment of the assay and those of the tear film. The activity of PLC in the tear film may be higher than the activity as established by the assay. Further studies on the activity of PLC in tear film should be performed to investigate the effect of differing the osmolarity of the assay and also conducting the assay in the presence of certain ions, in particular calcium ions. The investigation of phospholipases of the tear film were only preliminary in this work and should be investigated further by exploiting techniques such as western blotting, silver staining detection or analysis on the Agilent 2100 bioanalyser. The presence and activity of the similarly important phospholipase D would also be of interest and could be determined using similar techniques.

The experimental findings of Chapter 3 and 4 indicate that the phospholipid of the tear film are at lower concentrations than those found in MGS and that PLC plays a part in the lowering of this concentration. As the DAG appears to be at higher concentrations than previous workers described there is also now (for the author) more of an interest in the non polar lipids of the tear film. The LCMS method for the non polar lipids as described in Chapter 3 was only performed to verify there was no interference with the analysis of the phospholipids. The concentrations of the DAG in the tear film using LCMS or HPLC would now be of interest to verify the findings of the TLC experiments reported in Chapter 4.

The analysis of the phospholipid of the skin or sebaceous lipids was originally a part of the analytical work; this part of the analytical work was not completed due to the interesting findings relating to the low PL levels in tears leading to a reassessment of project objectives and a concentration upon this interesting observation. The sebaceous lipids still require investigation by HPLC and LCMS and although they contain similar lipid species to the tear film the method would need to be developed and verified.

7.3 Summary of the synthetic work

The second aim of this thesis was the synthesis of novel materials. The synthetic area of this work was itself divided into two sections: firstly that of zwitterionic and charge-balanced membranes for potential contact lens application and secondly that of hydrogel skin adhesives.

7.3.1 Zwitterionic and charge-balanced hydrogel membranes

The hypothesis for the synthesis of hydrogel membranes for potential contact lens materials was based on the incorporation of a sulfobetaine monomer into materials. As described in Chapter 5, polymers containing zwitterionic groups or materials coated with zwitterionic groups have been shown to have some advantages for application as biomaterials [126-131] and sulfobetaine containing biomaterials may have some advantage over those containing phosphobetaines [132, 133]. The potential of a newly introduced sulfobetaine monomer, N,N-dimethyl-N-(2-acryloylethyl)-N-(3-sulfopropyl) ammonium betaine (SPDA) was investigating for incorporation into ophthalmic biomaterials. The zwitterionic SPDA copolymer was also compared to synthesised charge-balanced (polyampholyte) copolymers.

Chapter 5 describes the synthesis and characterisation of the potential contact lens materials: a series of zwitterionic membranes and two series of charge-balanced membranes. The zwitterionic membrane series were synthesised from the monomers SPDA and 2-hydroxyethyl methacrylate (HEMA), as described in section 5.3

The two charge-balanced membranes series are described in section 5.2. The two charge-balanced membranes series were synthesised from 2-(dimethylamino) ethyl methacrylate (DMAEMA) or 3-(dimethylamino) propyl methacrylamide (DMAPMA) in conjugation with the anionic monomer 2-acrylamido-2-methylpropane sulfonic acid (AMPS). The DMAEMA and DMAPMA monomers were chosen based upon their apparent stability for sterilisation by gamma ray irradiation. DMAEMA or DMAPMA was used used in equimolar ratios with the AMPS monomer with the aim of the resulting copolymer being balanced with respect to charge.

The monomers used in these charge-balanced and zwitterionic membranes were copolymerised with HEMA in various compositions to provide the two series. The two series of charge-balanced membranes were then copolymers composed of three monomers: HEMA and AMPS conjugated with DMAEMA or HEMA and AMPS conjugated with DMAPMA.

The membranes produced from both the charge-balanced and zwitterionic monomers were clear and cohesive, which is a favourable property for a hydrogel to possess and is a requirement in some applications, e.g. contact lenses. The concentrations of residual monomers were not investigated and this is an obvious area for further work. The different crosslinkers and/or initiators for this system are also potential route of investigation. The reactivity ratios of the system could be studied as they may provide the optimal monomer feeds to be used to lead to the synthesis of copolymers containing precise equimolar quantities of the monomers used. As biomaterials the gels should be non-toxic and this initially could be determined via a cytotox assay.

It was observed that the charge-balanced membranes were stable to the effects of autoclave and gamma ray irradiation sterilisation (section 5.2.6) whereas the zwitterionic membranes were only stable by autoclave but unstable to gamma ray irradiation (section 5.3.5). This could prove problematic if the zwitterionic material was to be used in applications in which autoclave sterilisation is not an option. The effect of other sterilisation methods on the membranes would need to be established if the autoclaving method could not be used.

The equilibrium water content (EWC) of the zwitterionic and charge-balanced membranes series were similar to each other as reported in section 5.4. This was expected as the charge-balanced membranes were formulated as analogues of zwitterionic membranes. Increasing of the hydrophilic comonomers in the membranes had the effect of increasing the EWC as was expected. The charge-balanced DMAPMA-containing acrylamide copolymer series had a slightly higher EWC than that of the charge-balanced acrylate copolymer series and the zwitterionic copolymer series. This was also expected as the acrylamide membrane has the hydrophilic amide group whereas the acrylate has the ester group.

Somewhat unexpectedly the EWC of the SPDA copolymer membrane series is closer to that of the DMAEMA:AMPS membrane series than it is to that of the DMAPMA:AMPS membrane series. As the SPDA and acrylamide copolymers contain a quaternary nitrogen group it would be expected that these were of similar EWC. The charge attraction between the positive and negative containing functional groups present in the zwitterionic membrane and the complex formed between DMAEMA and AMPS in the acrylate membrane may be allowing less chain expansion compared to that of the charge attractions present in the acrylamide membrane.

Membranes synthesised from AMPS without a comonomer containing a functional group to allow the charge to be balanced have higher EWCs than those membranes presented in Chapter 5. The water is attracted to the sulfonate group and expands the polymer network, the presence of the balancing charge restricts the chain expansion.

The increase in EWC provided by the presence of the zwitterionic and/or charge-balanced monomers in all of the membranes, as reported in Chapter 5, could be advantageous for contact lens applications. One advantage is that the increased EWC of these membranes is achieved without the addition of a charged functional group to the material which is often utilised to increase EWC of hydrogels, for example acrlylic acid and its derivatives. The advantage of using a system with a charge balance is that there is no attraction by the membrane of species of opposite charge (to that of the membrane). Another advantage is that less charge-balanced material by weight can be used to affect a similar increase in EWC, for example as compared to N-vinyl pyrrolidone as described in section 5.4.1.2.

The values of the freezing and non-freezing water of the membranes are unknown and can be determined by dynamic scanning calorimetry. It would be expected that the freezing water would be relatively high compared to conventional contact lens materials and this could be beneficial in terms of the membranes retaining water under dehydrating conditions.

The mechanical properties of the charge-balanced and zwitterionic membranes, which were described in section 5.4, were found to be similar to each other and comparable

to conventional contact lens materials with similar EWCs, for example etafilcon A has an EWC of 58% and a Youngs modulus (ε) of ~0.3MPa [136]. The increase of the ionic monomers from 0 to 10% in the charge-balanced membrane series brought about a rapid decrease in the value of ε and a further increase of the ionic monomers to 20% brought about a gradual reduction in the value of ε, as shown in section 5.4.2.1. The tensile strength (Ts) and elongation to break (Eb) had an almost linear reduction correlated to the increase in ionic monomer. The increase of SPDA as a comonomer in the membranes causes a linear reduction in the mechanical properties of these membranes as shown in section 5.4.2.2. The zwitterionic membranes had a higher ε than the charge-balanced membranes between 5 and 10%, the reasons for this are unknown.

The ε of the SPDA membranes was higher (not statistically significantly) than that of the charge-balanced membranes. The tensile strength of the SPDA and charge-balanced membranes were similar and not significantly different, although the actual values of the SPDA membrane was closer to those of the 2-(dimethylamino) ethyl methacrylate:2-acrylamido 2,2 methylpropane sulfonic acid copolymer membrane. The elongation to break of the SPDA membranes was higher than the charge-balanced membranes but once again there was no significant difference.

The similarities between the mechanical properties of the charge-balanced and zwitterionic membranes were to be expected as the charge-balanced membranes were formulated to be analogues of the zwitterionic membranes. The mechanical properties are a reflection of the EWCs of the materials which have already been described as being similar. It is the Ts and Eb that are taken into account in terms of the manual handling of contact lenses and these values were relatively low for the membranes of the series with higher EWCs; therefore these higher EWC membranes would be unsuitable for contact lens applications.

The surface free energies (γ_s) of the charge-balanced and zwitterionic membranes as reported in section 5.4.3 were shown to be similar to each other but higher than that of conventional contact lens materials. This is perhaps not surprising when the structures are considered. The SPDA has the quaternary nitrogen and sulfonate moities on a

single pendant group, the acrylamide charge-balanced has amide and sulfonate moieties but situated on separate pendants groups and the acrylate has a sulfonate and an ester moiety on separate pendant groups. The combined pendant groups of the charge-balanced ionic comonomers were similar to the single zwitterionic pendant group and so similar values should be expected.

The relatively high γ_s values shown by these materials offers advantages in terms of wettability towards water and perhaps also to the tear film. The γ_s values might also offer biocompatibility in terms of reduced spoilation from proteinacious species. The spoilation profiles of the membranes were not determined but the surface free energies indicate that the spoilation profiles for proteins for the materials should be low and this could be established during any further work.

The contact angles were determined on hydrated surfaces but more information may be obtained if the contact angles were determined using the sessile drop technique when the copolymers were in a dehydrated state. The subtle contributions from polar and dispersive components of the copolymer to the surface free energies of the membranes could also be explored using the captive bubble method. Dynamic contact angle and hysteresis could also be determined as it would be expected that the presence of the pendant sulfonate groups should provide a low contact angle hysteresis as has been demonstrated by Nasso [166].

The EWC and the γ_s for the charge-balanced membranes and SPDA copolymer membrane are highly correlated as is shown in sections 5.4.2.1 and 5.4.2.2 where EWC is plotted versus γ_s. A slope with an r^2 0.84 is seen for the 2-(dimethylamino) ethyl methacrylate:2-acrylamido-2-methylpropane sulfonic acid membranes when EWC is plotted vs γ_s. A similar correlation was found between EWC and γ_s for the SPDA copolymer membranes where the slope had an r^2 of 0.86. The 3-(dimethylamino) propyl methacrylamide:2-acrylamido-2-methylpropane sulfonic acid copolymer membranes has a higher correlation with a slope of r^2 of 0.93 when EWC is plotted vs γ_s. The mechanical properties are correlated to the EWCs of the membranes and as the EWCs of the charge-balanced and zwitterionic membranes are similar so the mechanical properties would be expected to be similar.

The oxygen permeability (Dk) of a SPDA:HEMA copolymer in a ratio of 33:77 was $16x10^{-11}$ Barrers as described in section 5.4.4. The zwittterionic membranes have a Dk similar to that of conventional hydrogels which are controlled by the EWC of the material. While a high EWC can offer some advantages in contact lens applications it can be disadvantageous to have a material Dk dependent on EWC, as the Dk of water limits the Dk of the material. The Dk was determined at room temperature (24°C) and while the Dk can be extrapolated to the temperature of the ocular surface (34°C) the experiment could be repeated at ocular temperature to establish the Dk at that temperature.

The zwitterionic membrane had a relatively low coefficient of friction (μ) and this is an advantageous property for a contact lens material. As shown in section 5.4.6 a HEMA membrane had a μ of 4.43 and increasing the SPDA comonomer concentration in the membrane to 15% reduced the μ significantly to 1.88. The presence of the SPDA in the membranes is clearly causing a reduction in the μ. The lubricating ability of the SPDA present at the surface of the material lowered μ substantially. The presence of the SPDA at the surface may be acting to reduce μ as a result of reducing the boundary lubrication regime. The increased EWC of the SPDA containing membranes may have an influence upon the μ. The presence of the water may be acting as an internal lubricant but also as the polypropylene probe passes over the surface of the membrane it may be forcing water out of the polymer network and onto the surface out of the membrane where it may act as a lubricant. If this effect is reproducible when the polymer is used as a coating it could be an exciting area for further investigation.

The biocompatibility in terms of cell toxicity is also an important but thus far remains an unknown area for these systems. Sulfobetaines are known to be relatively non-toxic materials and it is expected that for the zwitterionic membranes offer low toxicity to cells. A cytotox assay of the copolymers could establish this and should be completed as further work.

Although the zwitterionic and charge-balanced membranes appear to have similar properties there are advantages of using the zwitterionic copolymer over the charge-balanced copolymers. The biomimetic nature of SPDA together with its compatibility with other monomers makes it a useful and complimentary addition to the building blocks of ophthalmic materials and its potential as a coating material in ocular applications should be explored.

7.3.2 Hydrogel skin adhesives

The second area of synthetic work investigated was that of hydrogel pressure sensitive adhesives (PSAs). As described in Chapter 1 PSAs can be used for applications involving the skin and excess lipid associated with oily skin can cause a lack of adhesion of the PSA. This section of the synthetic work was attempting to address that situation by synthesising PSAs which might be less susceptible to loss of adhesion under these unfavourable "oily" conditions.

Two approaches were used based on two hypotheses. One was related to the known affinity for lipids for N-vinyl pyrrolidone (NVP) as described in section 6.2.1. An NVP containing PSA may increase the adhesion to oily skin through NVP and lipid interaction. The lipid could interact with the hydrophobic regions of the NVP and be absorbed by the PSA. The effect of the possible absorption and reduction of the excess lipid at the adhesive-substrate interface could result in increased adhesion.

The second hypothesis related to the possibility that N,N-dimethyl-N-(2-acryloylethyl)-N-(3-sulfopropyl) ammonium betaine (SPDA) might intercalate by charge interactions with the phosphatidylcholine headgroup of phospholipids as described in section 6.3.1. PSAs containing SPDA may then increase the adhesion to oily skin through PSA and lipid interaction. The lipids, particularly the phospholipids could intercalate with the SPDA copolymer which may also lead to absorption. The absorption of the lipids from the skin-adhesive interface might also result in increased adhesion.

Chapter 6 describes the synthesis and characterisation of these NVP and SPDA containing PSAs. Several series of gels were synthesised using these monomers in copolymers. The gels in this thesis were based PSAs gels from previous work performed in this laboratory by Flemming [11] (see section 1.1.5.3). Flemming described the three key components of hydrogel PSAs as an unsaturated water soluble monomer, water and a humectant/plasticiser. Glycerol is a typical humectant/plasticizer used in PSA formulations. Flemming also defined the upper and lower limits of these three key components of hydrogel PSAs for the production of cohesive, adhesive hydrogels gels. Flemming's work used 2-acrylamido-2-methyl propane sulfonic acid sodium salt (AMPS) as the monomer and glycerol as the humectant to produce a series of hydrogel membranes with differing ratios AMPS, water and glycerol.

Cartwright [12] continued Flemming's work using AMPS and used the ionic comonomer; acrylic acid bis-(3-sulfopropyl)-ester potassium salt (SPA) and found that a ratio of 6:4 AMPS:SPA provided PSAs with better adhesion while still remaining cohesive and clear. From the work of Flemming and Cartwright the chosen starting point for composition of gels in this thesis were 40% monomer(s), 30% water and 30% glycerol with 6:4 ratio of AMPS:SPA. All formulations for PSA gels in this work had the composition monomer:glycerol:water 40:30:30 (by wt%). Any monomer added to gels in this thesis are part of the 40% monomer overall in the gels and the ratio of AMPS:SPA kept at 6:4 in these gels.. The compositional changes were made only to the monomer component, the glycerol and water remained at the same ratio.

In the NVP work (section 6.2) a series of partially hydrated hydrogels were synthesised from NVP, SPA and AMPS monomers, this was labelled series A. A second series was synthesised from NVP and SPA and labelled series B. A third series was synthesised from NVP and AMPS and labelled series C. Two control gels were synthesised from SPA and AMPS.

The series A, series C and the controls formed cohesive, transparent and adhesive ("tacky") gels. After polymerisation there was an aroma of the NVP monomer along with a surface film which was thought to be residual NVP for all of these gels except

those gels with a low ratio of NVP gels of series A (see section 6.2.3). The NVP aroma along with the known low reactivity ratio of NVP towards acrylates indicates the presence of residual NVP. Series B (SPA:NVP copolymers) formed cohesive and adhesive gels but these were less "tacky" than the other gels.

In the N,N-dimethyl-N-(2-acryloylethyl)-N-(3-sulfopropyl) ammonium betaine (SPDA) work (section 6.3) a series of partially hydrated hydrogels were synthesised from SPDA, SPA and AMPS monomers which were labelled series D. SPDA and SPA were synthesised in another series and labelled series E. A final series was synthesised from SPDA and AMPS and labelled series F. Series D, E and F were synthesised to form cohesive, transparent and adhesive gels. The residual monomer content of all the gels should be investigated in future work. This possible further work on residual monomer also leads to another area of further work; that of establishing the effects of the numerous sterilisation methods on all of the gels synthesised. This should be investigated as the properties of the gels may be different after sterilisation and any residual monomers should, but may not, be removed during sterilisation processes.

Similar to the zwitterionic and charge-balanced membranes synthesised in Chapter 5 the use of different crosslinkers and/or initiators for the NVP and SPDA containing gels are a potential route of investigation for further analysis. If the reactivity ratios of these systems were studied they should provide information for the optimal monomer feeds to be used in the synthesis.

The principal properties of the NVP and SPDA containing PSA gels were investigated: namely peel strength, surface free energy (γ) and dynamic mechanical properties.

The peel strengths of series A (SPA:AMPS:NVP) gels were higher than that of a control gels provided that the ratio of ionic:NVP monomers was kept low, i.e. 39:1 or 19:1, ionic:NVP (as described in section 6.2.4.2). All other compositions of the NVP copolymer gels had peel strengths lower than that of the control gels. NVP has a tendency for alternation when polymerised with AMPS [146] and if the same

alternating tendency occurs with the SPA:AMPS:NVP copolymers then this may have the effect providing defined sequence distributions. This in turn may enhance the mechanical interlocking between the copolymer and the skin. If the NVP is left as residual monomer it may increase the tack of the copolymer and lubricise the lipids. If there is excess NVP at the surface, as indicated by the aroma, with the higher content NVP gels then this may be lowering the peel strengths.

The peel strengths of the series C (AMPS:NVP) gels were all lower than that of the control gel. The introduction of NVP at the expense of SPA in the copolymer had the effect of reducing the peel strength. As described in section 6.2.4.3 hydrogen bonding may occur between the amide in the AMPS pendant group and the sulfonate in the SPA pendant group. When NVP replaces SPA in this series hydrogen bonding could still occur between the carbonyl of the NVP and the amide of the AMPS. This could result in the NVP and AMPS having a similar orientation along the backbone of the polymer introducing a heterogeneous character at the surface of the gel and possibly resulting in reduced peel strength.

The series B (SPA:NVP) gels did not form adequately strong bonds with the skin and as a result the test for the gels peel strengths could not be conducted. The removal of the AMPS removed the bonding capability of the gel with the skin. SPA does not contain an easily accessible δ^+ moment and thus would not hydrogen bond with the NVP. The pendant groups of SPA and NVP could rotate more freely, the free rotation could lead to hydrophobic and hydrophilic domains from the NVP ring and the sulfonate of the SPA respectively. These domains within the gels could then be presented at the surface when the gel is exposed to different environments, i.e. hydrophilic or hydrophobic.

The peel strengths of series D (SPDA:AMPS:SPA), series E (SPDA:SPA) and series F (SPDA:AMPS) gels did not differ significantly from the control gel. This was somewhat expected as the structure of SPDA is similar to the structure of AMPS and SPA. In the case of all of these comonomers the group that would be present at the surface of the gels are the sulfonate groups. It seems that the hypothesised intercalation between the SPDA and the lipids may not occur.

Although the peel strengths of the SPDA and NVP copolymer gels was lower than the preferred peel strengths for skin adhesive applications (≥3 N/25mm) they remained on the skin for several hours before removed from the skin, at which point they were still adhered to the skin.

Contact angles of diidomethane and water with the gels of series A were recorded and used to calculate the surface free energies (γ) of the gels. The total surface free energy (γ_s^t) is a combination of the dispersive surface free energy (γ_s^d) and the polar surface free energy (γ_s^p) components. The contact angles were taken at the point of initial contact of the probe solution but were also recorded over a time of 210 seconds.

The γ of series A (SPA:AMPS:NVP) copolymer gels are described in section 6.2.5.1. The γ_s^t for series A gels is higher for the final values (after 210 seconds) and the contributions from the γ_s^d component are higher than the γ_s^p with the initial values but the γ_s^p become dominate in the final values. This difference between the initial and final values of γ for the gels can be attributed to a combination of the gels being stored on a silicon paper and the absorption of water into the gel. The initial values of γ_s^d shows that the copolymerisation of NVP at 2.5% maximises the γ_s^d contribution to γ_s^t as at this percentage a further increase in the NVP percentage does not change the value of γ_s^d. The initial values of γ_s^p are reduced with the NVP at 5% but then rise with the increase of NVP comonomer at higher ratios. The final values of γ_s^t show a different trend to the initial values. At 5% NVP the γ_s^d reaches a maximum and remains the same as the percentage of NVP is increased, whereas the γ_s^p is reduced at 5% NVP and remains the same as the percentage of NVP is increased. The NVP comonomer is affecting the surface in a polar manner with the initial contact angles. The NVP is less hydrpophillic in comparison to the ionic monomers and this is being displayed in the γ_s^p component becoming lower over time as expected. The γ_s^d component increases with the increase of NVP as a comonomer in the copolymer.

The γ of series C (AMPS:NVP) copolymer gels are described in section 6.2.5.1. These gels showed a similar trend to those of the series A gels described above. The γ_s^t is higher for the final values and the contributions from the γ_s^d component are higher

than the γ_s^p in the initial values but the γ_s^p become dominant in the final values. This can also be attributed to a combination of the gels being stored on a silicon paper and the absorption of water into the gel.

The thermodynamic requirement for adhesion is that γ adhesive < γ substrate. The γ for skin has been reported to be between 38-56 mN/m [64, 65]. The initial values of γ_s^t for both series A and C gels are close to, or below, this value and so adherence should occur. At the final values of γ_s^t for both series A and C gels are above the γ of the skin and so they should not adhere. This should indicate that the gels should not adhere to the surface of the skin, however when applied to the subject's skin the gels did adhere for several hours until they were removed. This would not be predicted to be the case from the peel strength and surface free energies results. Further information on the surface free energies should be determined by investigating the materials when dehydrated employing either the sessile drop method or the captive drop method. The contact angles of the test liquids and the series B (SPA:NVP) copolymers gels were not determined as these did not provide higher peel strengths than the control gel.

The γ of the series D (AMPS:SPA:SPDA) are described in section 6.3.5.1. The difference between the initial and final γ for the series D gels are that the γ_s^t and γ_s^p are higher in the final values. The γ of these SPDA gels did not differ significantly from a control gel. The SPDA structure exhibits features of both the SPA and AMPS structures and these structural features may explain why the replacement of AMPS and SPA with SPDA had little effect on the γ of the resulting gels. SPDA has the sulfonate as the terminal group the same as SPA and AMPS. SPDA also has the quaternary nitrogen group similar to AMPS. The amine of the SPDA has two methyl groups placed between the quaternary nitrogen and the sulfonate groups and there are two methyl groups placed similarly in the AMPS structure. The same structural features are able to rotate to present themselves to the environment to which they are exposed to.

The γ of the series E (SPA:SPDA) and F (AMPS:SPDA) copolymer gels are described in section 6.3.4.2. The initial and final γ for series E and series F gels did

not differ significantly from the control. The use of SPDA as a copolymer did not significantly alter the γ of these gels when hydrated. The reasons for this are the structural similarities between SPDA and AMPS as indicated earlier for the series D (SPDA:SPA;AMPS)

Viscoelasticity can be studied using rheology. Dynamic mechanical analysis, in particular the oscillatory frequency sweep experiment allows the adhesive properties of a gel to be determined. The dynamic-mechanical properties (the elastic modulus (G'), viscous modulus (G") and tan δ (G''/G') have been correlated to tack and peel [147-154]. Viscoelastic behaviour at low frequency (~1Hz) is representative of the shear forces involved during the application of a gel or adhesive. Whereas higher frequency (~10Hz) is representative of the shearing forces involved in the removal of a gel or adhesive removal. A skin adhesive requires a dominant elastic component during application to allow the flow of the material over the skin; a reduced viscous component is also favourable at this time. During removal of an adhesive from a skin a reduced elastic and increased viscous component will be favourable. The tan δ plotted against frequency (ω) is also expected to have a positive gradient for good adhesive properties of gels [152-154].

The dynamic mechanical properties of the series A (SPA:AMPS:NVP copolymer) gels with low ratios of NVP were determined as these gels produced the most suitable peel strengths and γ for use as PSA for the skin (see section 6.2.6). The G', G'' and tan δ when plotted against ω for this series of gels gave slopes typically associated with skin adhesive hydrogels with favourable adhesive properties. The G' and G" of the series A gels were within the suggested upper and lower limits for PSAs as suggested by Chu and other workers [149, 150, 155]. A plot of tan δ against ω for these gels had a positive gradient indicating favourable adhesive properties.

The control 1 gel has a G' 6125±500 Pa, a G'' 600±180 Pa and a tan δ 0.1 at ~1Hz. Copolymerisation of NVP with AMPS and SPA introduced a reduction in G' and an increase in G''. A ratio of 39:1 ionic:NVP monomer significantly reducing the G' (3280±500 Pa) and significantly increasing the G'' (1134±180 Pa). This increased the tan δ to 0.35. As the ratio of NVP in the gel was increased to 19:1 ionic:NVP

monomer there was a reduction (not statistically significant) in both G' and G". This indicates that the gels were becoming less suitable as adhesives as was also suggested by the lowering of peel strengths when the NVP ratio was increased. A similar trend was seen at ~10Hz.

The presence of NVP and AMPS in the copolymer should allow hydrogen bonding to occur between the carbonyl of the NVP and the amide of the AMPS. There may also be van der Waals interactions between the NVP carbon ring and the methyls on the AMPS. Both of these would the affect the viscoelastic nature of the copolymer as reflected in the reduction of G' and increase in G''.

Only the rheological properties for the series D (SPDA:SPA:AMPS) gels were determined (see section 6.3.6) as the series E and F showed similar properties in other respects. The G', G'' and tan δ of these gels were all within the limits for PSAs as suggested Chu and other workers [149, 150, 155]. The G' and tan δ when plotted vs ω gave slopes characteristic of skin adhesive hydrogels but the G'' vs ω did not. The G'' vs ω plot has a positive gradient but does not reach a maximum at higher frequencies as seen with the NVP containing gels (section 6.2.6). The reduction of G'' at higher frequencies (~10Hz) is normally seen with PSAs. The inner salt of the SPDA may influence the G'' of these gels. This could occur as the dipolar bonds between SPDA on different polymer chains may cause a retractive force resulting in the gel being more viscous at higher frequencies. The plot of tan δ vs frequency for the series D gel shows tan δ has a positive gradient.

At ~1 Hz there was an insignificant decrease in the G' and no change in the G'' as we increase the percentage of SPDA in the gel. At ~10 Hz the increase of SPDA copolymer had the effect of significantly reducing the G'. There was no change in the G''. This reduction in G' may be directly influenced by the effect of the charged groups within the inner salt creating dipolar bonds with inner salt groups on other chains. This may cause the network to have less free chain rotation and resulting in a lower elasticity and a higher G''.

The high level of the γ of NVP and SPDA gels was in agreement with the low peel strengths. These results indicate that the NVP and SPDA copolymer gels are unsuitable for use as skin adhesives. However the G', G'' and tan δ of these gels did not agree with the other results and indicates that the gels are suitable for use as skin adhesives. Also the gels were able to remain on the skin for several hours before being removed indicating that they have capability for long term use. Overall the gels synthesised in this thesis are suitable for general skin PSA applications but not ideal for use in greasy skin applications. The SPDA copolymers gels do have antipolyelectroltye properties that may give them advantages in certain applications such as in wound dressings. The charge balanced copolymers would also be expected to have a certain degree of antipolyelectrolyte properties when compared to charged materials or those that that have the potential to be charged. This behaviour could give them beneficial properties for applications in wound healing because the swelling of the gel can be controlled.

References

1. Peppas N.A, Ed. (1987). Hydrogels in Medicine and Pharmacy, Volume 3 (Florida: CRC Press).
2. Hoffman A.S (2002). Hydrogels for Biomedical Applications. Advanced Drug Delivery Reviews *43*, 3-12.
3. Wichterle O and Lim D (1960). Hydrophilic Gels for Biomedical Use. Nature *185*, 117-118.
4. Mark H.F, Ed. (2007). Encyclopedia of polymer science and technology, 3rd Edition (New York, Chichester: Wiley-Interscience).
5. Li J (2004). Polymeric hydrogels. In Engineering materials for biomedical applications, T.S. Hin, ed. (Singapore: World Scientific Publishing Company).
6. Corkhill P.H, Hamilton C.J and Tighe B.J (1990). The design of Hydrogels for Biomedical Applications. Critical Reviews in Biocompatibility *5*, 363-436.
7. Alsarra I.A, Neau S.H and Howard M.A (2004). Effects of preparative parameters on the properties of chitosan hydrogel beads containing Candida rugosa lipase. Biomaterials *25*, 2645-2655.
8. Holden B and Mertz G (1984). Critical oxygen levels to avoid corneal edema for daily and extended wear contact lenses. IOVS *25*, 1161-1167.
9. Harvitt D and Bonanno J (1999). Re-evaluation of the oxygen diffusion model for predicting minimum contact lens Dk/t values needed to avoid corneal anoxia. Optom Vis Sci *76*, 712-719.
10. Tan H.S and Pfister W.R (1999). Pressure Sensitive Adhesives for Transdermal Drug Delivery Systems. Pharmaceutical Science and Technology Today *2*, 60-69.
11. Flemming M.C (1999). Skin Adhesive Hydrogels for biomedical applications, Aston University, Birmingham.
12. Cartwright H.R (2003). Hydrogels for dermal applications, Aston University, Birmingham.
13. Christie W.W (1982). Lipid Analysis. Isolation, separation, identification amd structural analysis of lipids, 2nd Edition (Pergamon Press).
14. Whikehart D.R (2003). Biochemistry of the Eye, 2nd Edition (Butterworth-Heinemann Medical).
15. McMurrey J (1999). Organic Chemistry, 5th Edition (Brooks/Cole Publishing Company).
16. Larke J.R, Ed. (1997). The Eye in Contact Lens Wear, 2nd Edition Edition (Buterworth Heinmann).
17. Bron, A.J., Tiffany, J.M., Gouveia, S.M., Yokoi, N., and Voon, L.W. (2004). Functional aspects of the tear film lipid layer. Experimental Eye Research *78*, 347-360.
18. McCulley J.P and Shine W.E (2004). The lipid layer of tears: dependant on meibomian gland function. Experimental Eye Research *78*, 361-365.
19. Mishima S, Gasset A, Klyse S.D and Bowd J.L (1966). Determination of tear volume and tear flow. IOVS *5*, 264-276.
20. Wang J, Fonn D, Simpson T.L and Jones L (2003). Precorneal and pre- and postlens tear film thickness measured indirectly with optical coherence tomography. Invest Ophthalmol Vis Sci *44*, 2524-2528.

21. Prydal J.I, Artal P, Woon H and Campbell F.W (1992). Study of human precorneal tear film thickness and structure using laser interferometry. Invest Ophthalmol Vis Sci *33*, 2006-2011.
22. Stern J et.al. (1998). A unified theory of the role of the ocular surface in dry eye. In Adv Exp Med Biol, Volume 438, D.A. Sullivan, ed.,pp. 643-651.
23. Rolando M and Zierhut M (2001). The ocular surface and tear film and their dysfunction in dry eye disease. Survey of Opthalmology *45*, S203-S210.
24. Bonavida B, Sapse A.T and Sercarz E.E (1969). Specific tear lipocalin: a unique lachrymal protein absent from serum and other secretions. Nature *221*, 375-379.
25. Jonssen P.T and van Bijsterveld, O.P. (1983). Origin and biosynthesis of human tear fluid proteins. Invest Ophthalmol Vis Sci *24*, 623–630.
26. Josephson A.S and Lockwood D.W (1964). Immunoelectrophoretic studies of the protein components of normal tears. J Immunol *93*, 532–539.
27. McClennan B.H, Whitney C.R, Newman L.P and Allansmith M.R (1973). Immunoglobulins in tears. Am J Ophthalmol *76*, 89–101.
28. Gachon A.M, Verrelle P, Betail G and Dastague B (1979). Immunological and electrophoretic studies of human tear proteins. Exp Eye Res *29*, 539–553.
29. Zhou L, Beuerman R.W, Foo Y, Liu S, Ang L.P.K and Tan D.T.H (2006). Characterisation of human tear proteins using high-resolution mass spectrometry. Annals Academy of Medicine Singapore *35*, 400-407.
30. de Souza G.A, Godoy L.M.F and Mann M (2006). Identification of 491 proteins in the tear fluid proteome reveals a large number of proteases and protease inhibitors. Genome Biology *7*, -.
31. Bron A.J and Tiffany J.M (1998). The Meibomian Glands and the Tear Film Structure Function and Control, Volume 438.
32. Tiffany J.M (1995). Physical functions of the meibomian glands. Progress in Retinal and Eye Research *14*, 47-74.
33. Baron C and Blough H.A (1976). Compostion of the neutral lipids of bovine meibomian secretions. Journal of Lipid Research *17*, 373-376.
34. Nicolaides N (1981). Meibomian gland studies: comparison of steer and human lipids. IOVS *20*, 522-536.
35. Stuchell R.N, Slomiany B.L, Jozwiak Z, Murty V.L.N, Slomiany A and Farris R.L (1984). Lipid Composition of Human Tears. IOVS *25*, 320.
36. McCulley J.P and Shine W.E (2003). Eyelid Disorders The Meibomian Gland, Blepharitis, and Contact Lenses. Eye & Contact Lens *29*, S93-S95.
37. Tiffany J.M (1987). The lipid secretion of the meibomian glands, Volume 22 (Academic Press Inc).
38. Stuchell R.N, Feldman J.J, Farris R.L and Mandel I.D (1984). The effect of collection technique on tear composition. IOVS *25*, 374-377.
39. Shine W.E and McCulley J.P (2003). Polar lipids in human meibomian gland secretions. Current Eye Research *26*, 89-94.
40. Greiner J.K, Glonek T, Korb D.R and Leahy C.D (1996). Meibomian gland phospholipids. Current Eye Research *15*, 371-375.
41. Ham B.M, Jacob J.T, Keese M.M and Cole R.B (2004). Identification, quantification and comparison of major non-polar lipids in normal and dry eye tear lipidomes by electrospray tandem mass spectrometry. Journal of Mass Spectrometry *39*, 1321-1336.

42. Bright A.M and Tighe B.J (1993). The composition and interfacial properties of tears, tear substitites and tear models. Journal of the British Contact Lens Association.
43. Mann A.M, Campbell D and Tighe B.J (2004). The Application of Capillary Liquid Chromatography Mass Spectrometry Techniques to the Study of patient to patient variations in Tear Chemistry. Ophthalmic Research Journal for Research in Experimental and Clinical Ophthalmology *36*, 34.
44. Ham B.M, Jacob J.T, Keese M.M and Cole R.B (2004). Identification quantification and comparison of major non polar lipids in normal and dry eye tear lipodomes by electrospray tandem mass spectrometry. Journal of Mass Spectrometry *39*, 1321-1336.
45. Ham B.M, Jacob J.T, Keese M.M and Cole R.B (2005). Identification and comparison of proteins in normal versus dry eye rabbit tears by MALDI-TOF MS. Investigative Ophthalmology & Visual Science *46*, -.
46. Campbell D, Mann A, Griffiths G and Tighe B.J (2005). The Nature and Fate of Lipids in Contact Lens Wear. Ophthalmic Research Journal for Research in Experimental and Clinical Ophthalmology *37*, 26.
47. Nagyová B and Tiffany J.M (1999). Components responsible for the surface tension of human tears. Current eye research *19*, 4-11.
48. Encyclopaedia of Polymer Science and Technology.
49. Lampe A.L et. al. (1983). Human stratum corneum lipids: characterisation and regional variations. Journal of Lipid Research *24*, 120-130.
50. Elias P.M and Menon G.K (1991). Structural and lipid biochemical correlates of the epidermal permiability barrier. In Advances in Lipid Research, Volume 24, P.M. Elias, ed. (San Diego).
51. Yardley H.J (1987). Epidermal lipids. International Journal of Cosmetic Science *9*, 13-19.
52. Downing D.T (1992). Lipid and protein structures in the permiability barrier of mammalian epidermis. Journal of Lipid Research *33*, 301-313.
53. Wertz P.W and van den Bergh B (1988). The physical, chemical and functional properties of lipids in the skin and other biological barriers. Chemistry and Physics of Lipids *91*, 85-96.
54. Menon G.K (2002). New insights into skin structure: scratching the surface. Advanced Drug Delivery Reviews *54*, S3-S17.
55. Bligh E.G and Dyer W.J (1959). A rapid method of total lpid extraction and purification. Canadian Journal of Biochemical and Physiology *37*, 912-917.
56. Clarys P and Barel A (1985). Quantitative evaluation of skin surface lipids. Clinics in Dermatology.
57. Nicolaides N (1974). Skin lipids: their biochemical uniqueness. Science *186*, 19-26.
58. Downing D.T and Strauss J.S (1974). Journal of Investigative Dermatology *62*, 228-244.
59. Stewart M.E et.al. (1978). The fatty acids of human sebaceous gland phosphatidylcholine. Biochim Biophys Acta *529*, 380-386.
60. Pochi P.E and Strauss J.S (1974). Endocrinological control of the development and activity of the human sebaceous gland. J Invest Dermatol. *62*, 191-201.
61. Strauss J.S and Pochi P.E (1963). The hormonal control of human sebaceous glands. In Biology of Skin, the Sebaceous Glands, Volume IV, Montaana W, Ellis R.A and Silver A.F, Eds. (Oxford: Pergamon Press), p. 220:254.

62. Jacobsen E, Billings J.K, Frantz R, Kinney C.K, Stewart M.E and Downing D.T (1985). Age-related changes in sebaceous wax ester secretion rates in men and women. J. Invest. Dermatol. *85*, 483-485.
63. Takayasu S and Adachi K (1970). Hormonal control of metabolism in hamster costovertebral elands. J Invest Dermatol *55*, 13-19.
64. Kenney K.F (1992). Medical grade acrylic adhesives for skin contact. J Appl Polm Sci *45*, 355.
65. Thomsen F, Measuring the surface free energy of human skin.
66. Mavon A et al (1997). Sebum and stratum corneum lipids increase human skin surface free energy as determined from contact angle measurements: A study on two anatomical sites. Colloids and Surfaces B: Biointerface *8*, 147-155.
67. Griffiths G, Jones H.E, Eaton C.E and Stobart K (1997). Effect of n-6 polyunsaturated fatty acids on growth and lipid composition of neoplastic and non-neoplastic prostate epithelial cell cultures. The Prostate *31*, 29-36.
68. Jork H.H, Funk W, Fischer W and Wimmer H (1990). Thin-Layer Chromatography Reagents and Detection Methods, Vol. 1a: Physical and Chemical Detection Methods: Fundamentals, Reagents I (New York: Wiley).
69. Dittmer J.C and Lester R.L (1964). A simple, specific spray for the detection of phospholipids on thin-layer chromatograms. Journal of Lipid Research *5*, 126-127.
70. Agilent Technologies, Basics of LCMS: a primer.
71. Corkhill P.J, Jolly A.M, Ng C.O and Tighe B.J (1987). Synthetic hydrogels: 1. Hydroxyalkyl acrylate and methacrylate copolymers – water binding studies. Polymer *28*, 1758-1766.
72. Tighe B and Trevett A (1990). The characteristics of mechanical properties of soft contact lenses. Trans. Br. Contact Lens Assoc. Ann. Clin. Conf *13*, 57–61.
73. Fatt I and Chaston J (1982). International Contact Lens Clinic *9*, 76.
74. Fatt I and B.A Weissmann (1989). Optom Vis Sci *66*, 235-238.
75. Mahomed A, Nasso M and Tighe B.J (2005). Frictional and lubricity changes in contact lenses during wear. Ophthalmol. Res. *37*, 27 & 161.
76. Bron A.J, Tiffany J.M Gouveia S.M, Yokoi N and Voon L.W (2004). Functional aspects of the tear film lipid layer. Experimental Eye Research *78*, 347-360.
77. Maissa C, Franklin V, Guillon M and Tighe B.J (1998). Influence of contact lens material surface characteristics and replacement frequency on protein and lipid deposition. Optom Vis Sci *75*, 697-705.
78. Bowers R.W.J and Tighe B.J (1987). Studies of the ocular compatibility of hydrogels. A review of the clinical manifestations of spoliation. Biomaterials *8*, 83-88.
79. Gellatly K.W, Brennan N.A and Efron N (1988). Visual decrement with deposit accumulation of HEMA contact lenses. Am J Optom Physiol Opt. *65*, 937-941.
80. Jones L, Evans K, Sariri R, Franklin V and Tighe B (1997). Lipid and protein deposition of N-vinyl pyrrolidone-containing group II and group IV frequent replacement contact lenses. CLAO J *23*, 122-126.
81. Bontempo A.R and Rapp J (1994). Lipid deposits on hydrophilic and rigid gas permeable contact lenses. Clao J *20*, 242-245.
82. Wollensak G, Mur E, Mayr A, Baier G, Gottinger W and Stoffler G (1990). Effective Methods for the Investigation of Human Tear Film Proteins and

Lipids. Graefes Archive for Clinical and Experimental Ophthalmology *228*, 78-82.
83. Franklin V.J (1990). Lipoidal species in ocular spoilation processes, Aston University.
84. Myher J.J and Kuksis A (1995). General strategies in chromatographic analysis of lipids. Journal of Chromatography B: Biochemical Applications *671*, 3-33.
85. Folsh J, Lees, M and Stanley G.H.S (1956). A simple method for the isolation and purificaion of total lipides from animal tissue. Journal of Biol. Chem. *226*, 497.
86. Touchstone J.C (1995). Thin layer chromatographic procedures for lipids separation.Journal of Chromatography B: Biomedical Applications *671*, 169-195.
87. Christie W.W (1992). Solid phase extraction columns in the analysis of lipids.
88. Tighe B.J and Franklin V.J (1997). Lens deposition and spoilation. In The Eye in Contact Lens Wear, 2nd Edition Edition, J.R. Larke, ed. (Buterworth Heinmann).
89. Lorentz H and Jones L (2007). Lipid deposition on hydrogel contact lenses: how history can help us today. Optometry & Vision Science *84*, 286-295.
90. Maziarz E.P, Stachowski M.J, Liu X.M, Mosack L, Davis A, Musante C and Heckathorn D (2006). Lipid Deposition on Silicone Hydrogel Lenses, Part I: Quantification of Oleic Acid, Oleic Acid Methyl Ester, and Cholesterol. Eye & Contact Lens *32*, 300–307.
91. Guillon M, Maissa C, Girard-Claudon K and Cooper P (2002). Influence of the tear film composition on tear film structure and symptomatology of soft contact lens wearers. Advances in Experimental Medicine & Biology *506*, 895-899.
92. Billheimer J.T, et. al. (1983). Seperation of steryl esters by reverse phase liquid chromatography. Journal of Lipid Research *24*, 1646-1651.
93. Kalo P and Kuuranne T (2001). Analysis of free and esterified sterols in fats and oils by flash chromatography, gas chromatography and electrospray tandem mass spectrometry. Journal of Chromatography A *935*, 237-248.
94. Duffin K, Obukowicz M, Raz A and Shieh J.J (2000). ESI tandem MS for quantitative analysis of lipid remodelling of essentail fatty acid deficient mice. Analytical Biochemistry *279*, 179–188.
95. Ham B.M, Jacob J.T and Cole R.B (2005). MALDI-TOF MS of Phosphorylated Lipids in Biological Fluids Using Immobilized Metal Affinity Chromatography and a Solid Ionic Crystal Matrix. Analytical chemistry *77*, 4439-4447.
96. Bomalaski J.S and Clark M.A (1987). The effect of sn-2 fatty acid substitution on phospholipase C enzyme activities. Biochem. Journal *244*, 497-502.
97. Dennis E (1997). The growing phospholipase A2 superfamily of signal transduction enzymes. Trends Biochem Sci. *22*, 1–2.
98. Nevalainen T.J, Aho H.J and Peuravuori H (1994). Secretion of Group 2 Phospholipase-a2 by Lacrimal Glands. Investigative Ophthalmology & Visual Science *35*, 417-421.
99. Aho V.V, Paavilainen V, Nevalainen T.J, Peuravuori H and Saari K.M (2003). Diurnal variation in group IIa phospholipase A(2) content in tears of contact lens wearers and normal controls. Graefes Archive for Clinical and Experimental Ophthalmology *241*, 85-88.

100. Yamada M, Mochizuki H, Kawashima M and Hata S (2006). Phospholipids and their degrading enzyme in the tears of soft contact lens wearers. Cornea *25*, S68-S72.
101. Hume E.B.H, Cole N, Parmar A, Tan M.E, Aliwarga Y, Schubert T, Holden B.A and Willcox M.D.P (2004). Secretory phospholipase A(2) deposition on contact lenses and its effect on bacterial adhesion. Investigative Ophthalmology & Visual Science *45*, 3161-3164.
102. Saari K.M, Aho V.V, Paavilainen V and Nevalainen T.J (2001). Group IIPLA(2) content of tears in normal subjects. Investigative Ophthalmology & Visual Science *42*, 318-320.
103. Moreau J.M, Girgis D.O, Hume E.B.H, Dajcs J.J, Austin M.S and O'Callaghan R.J (2001). Phospholipase A2 in Rabbit Tears: A Host Defense against Staphylococcus aureus. Invest. Ophthalmol. Vis. Sci. *42*, 2347-2354.
104. Girgis D.O, Dajcs J.J and O'Callaghan R.J (2003). Phospholipase A2 activity in normal and Staphylococcus aureus-infected rabbit eyes. Invest Ophthalmol Vis Sci *44*, 197-202.
105. Peuravuori H, Kari O, Peltonen S, Aho V.V, Saari J.M, Collan Y, Maatta M and Saari K.M (2004). Group IIA phospholipase A2 content of tears in patients with atopic blepharoconjunctivitis. Graefes Archive for Clinical and Experimental Ophthalmology *242*, 986-989.
106. Song C.H, Choi J.S, Kim D.K and Kim J.C (1999). Enhanced secretory group IIPLA(2) activity in the tears of chronic blepharitis patients. Investigative Ophthalmology & Visual Science *40*, 2744-2748.
107. Glasson M.J, Stapleton F and Willcox M.D.P (2002). Lipid, lipase and lipocalin differences between tolerant and intolerant contact lens wearers. Current Eye Research *25*, 227-235.
108. Tiffany J.M (1987). The lipid secretion of the meibomian glands, Volume 22 (Academic Press Inc).
109. Ryu E.K and MacCoss M (1979). Modification of the Dittmer-Lester reagent for the detection of phospholipid deriveratives on thin layer chromatograms. Journal of Lipid Research *20*, 561-563.
110. Zhou M, Diwu Z, Panchuk-Voloshina N and Haugland R.P (1997). A Stable Nonfluorescent Derivative of Resorufin for the Fluorometric Determination of Trace Hydrogen Peroxide: Applications in Detecting the Activity of Phagocyte NADPH Oxidase and Other Oxidases. Anal Biochem *253*.
111. Zhou M, Zhang C and Haugland R.P (2000). Choline Oxidase: A Useful Tool for High-Throughput Assays of Acetylcholinesterase, Phospholipase D, Phosphatidylcholine-Specific Phospholipase C and Sphingomyelinase. Proc SPIE-Int Soc Opt Eng *3926*, 166.
112. Mohanty J.G, Jaffe J.S, Schulman E.S and Raible D.G (1997). A highly sensitive fluorescent micro-assay of H_20_2 release from activated human leukocytes using a dihydroxyphenoxazine derivative. J. Immunol Methods *202*, 133.
113. Kutsuna M, Kodama T, Sumida M, Nagai A, Higashine M, Zhang W, Hayashi Y, Shiraishi A and Ohashi Y (2007). Presence of adipose differentiation-related protein in rat meibomian gland cells. Exp Eye Res *84*, 687-693.
114. Butovich I.A, Uchiyama E, Pascuale M.A and McCulley J.P (2007). Liquid Chromatography-Mass Spectrometric Analysis of Lipids Present in Human Meibomian Gland Secretions. Lipids.

115. McCulley J.P and Shine W (1997). A compositional based model for the tear film lipid layer. Trans Am Ophthalmol Soc *95*, 79-88; discussion 88-93.
116. Martinez-Landeira P et. al. (2002). Surface Tensions, Critical Micelle Concentrations, and Standard Free Energies of Micellization of C8-Lecithin at Different pHs and Electrolyte Concentrations. J.Chem.Eng.Data *47*, 1017-1021.
117. Zaman M. L, Doughty M. J and Button N. F (1998). The Exposed Ocular Surface and its Relationship to Spontaneous Eyeblink Rate in Elderly Caucasians. Exp. Eye Res. *67*, 681-686.
118. IUPAC Compendium of Chemical Terminology (1997), 2nd Edition Edition.
119. Zhang Z, Lingyun L, Chao T, Chen S and Jiang S (2006). Nonfouling and Responsive Zwitterionic Hydrogels with Improved Mechanical Properties. In *The 2006 Annual Meeting San Francisco*: San Francisco, USA.
120. Lewis A.L, Tolhurst L.A and Stratford P.W (2002). Analysis of a phosphorylcholine-based polymer coating on a coronary stent pre- and post-implantation. Biomaterials *23*, 1697–1706.
121. Ishihara K, Fukomoto K, Iwasaki Y and Nakabayashi N (1999). Modification of polysulfone with phospholipid polymer for improvement of the blood compatibility. Part 1. Surface characterization. Biomaterials *20*, 1545-1551.
122. Nederberg F, Bowden T and Hilborn J (2004). Synthesis, Characterization, and Properties of Phosphoryl Choline Functionalized Poly epsilon-caprolactone and Charged Phospholipid Analogues. Macromolecules *37*, 954-965.
123. Huang W, Ngola S and Voivodov K (2006). Zwitterionic polymers, Ciphergen Biosystems Inc.
124. Hayward J and Chapman D (1984). Biomembrane Surfaces as Models for Polymer Design: The Potential for Haemocompatibility. Biomaterials *5*, 135-142.
125. Kadoma Y, Nakabayashi N, Masuhara E and Yamauchi J (1978). Synthesis and Hemolysis Test of the Polymer Containing Phosphorylcholine Groups. Kobunshi Ronbunshu *35*, 423-427.
126. Chenga G, Zhanga Z, Chena S, Bryersb J.D and Jiang S (2007). Inhibition of bacterial adhesion and biofilm formation on zwitterionic surfaces. Biomaterials *28*, 4192–4199.
127. Lewis A.L (2000). Phosphorylcholine-based polymers and their use in the prevention of biofouling. Colloids and Surfaces B: Biointerfaces *18*, 261–275.
128. Baumgartner J.N, Yang C.Z and Cooper S.L (1997). Physical property analysis and bacterial adhesion on a series of phosphonated polyurethanes. Biomaterials *18*, 831-837.
129. Holmlin R.E, Chen X, Chapman R.G, Takayama S and Whitesides G.M (2001). Zwitterionic SAMs that resist nonspecific adsorption of protein from aqueous buffer. Langmuir *17*, 2841-2850.
130. Kitano H, Kawasaki A, Kawasaki H and Morokoshi S (2005). Resistance of zwitterionic telomers accumulated on metal surfaces against nonspecific adsorption of proteins. Journal of Colloid and Interface Science *282*, 340–348.
131. Cho W.K, Kong B and Choi I.S (2007). Highly efficient non-biofouling coating of zwitterionic polymers: Poly((3-(methacryloylamino)propyl)-dimethyl(3-sulfopropyl)ammonium hydroxide). Langmuir *23*, 5678-5682.
132. Lowe A.B, Vamvakaki M, Wassall M.A, Wong L, Billingham N.C, Armes S.P and Lloyd A.W (2000). Well-defined sulfobetaine-based statistical

copolymers as potential antibioadherent coatings. Journal of Biomedical Materials Research *52*, 88-94.
133. West S.L, Salvage J.P, Lobb E.J, Armes S.P, Billingham N.C, Lewis A.L, Hanlon G.W and Lloyd A.W (2004). The biocompatibility of crosslinkable copolymer coatings containing sulfobetaines and phosphobetaines. Biomaterials *25*, 1195-1204.
134. Benning B.K (2000). Novel high water content hydrogels, Aston University, Birmingham.
135. Tranoudis I and Efron N (2004). Tensile properties of soft contact lens materials. Contact Lens and Anterior Eye *27*, 177-191.
136. French K (2005). Contact lens material properties Part 2 - mechanical behaviour and modulus. Optician *230*, 29-34.
137. Zhao L, Xu L, Mitomo H and Yoshii F (2006). Synthesis of pH-sensitive PVP/CM-chitosan hydrogels with improved surface property by irradiation. Carbohydrate Polymers *64*, 473–480.
138. Ng C and Tighe B.J (1976). Polymers in contact lens applications VI. The 'dissolved' oxygen permeability of hydrogel and the design of materials for use in continuous wear lenses. Brit Polymer J *8*, 118-123.
139. Tighe B.J (1976). The design of polymers for contact lens applications. British Polymer Journal *8*, 71 - 77.
140. Morgan P.B and Efron N (1998). The oxygen performance of contemporary hydrogel contact lenses. Contact Lens & Ant Eye *21*, 3-6.
141. Rosso P.D and Moss M.Y (1982). Pressure-sensitive adhesive containing iodine, Minnesota Mining & Manufacturing Company.
142. Engel M.R (1989). Electrically-conductive, pressure-sensitive adhesive and biomedical electrodes, Minnesota Mining and Manufacturing Company.
143. Jenve A.H, Vegoe B.R, Holmblad C.M and Cahalan P.T (1984). Hydrophilic pressure sensitive biomedical adhesive composition, Medtronic Inc.
144. Feldstein M.M (2004). Adhesive hydrogels: Structure, properties, and application. Vysokomolekulârnye soedineniâ Seriâ A *46*, 1905-1936.
145. Jones L, Mann A, Evans K, Franklin V and Tighe B.J (2000). An in Vivo Comparison of the Kinetics of Protein and Lipid Deposition on Group II and Group IV Frequent-Replacement Contact Lenses. Optometry and Vision Science *77*, 503–510.
146. Schultz D.N, Kitano K, Danik J.A and Kaladas J.J (1988). Copolymers of N-vinylpyrrolidone and sulphonate monomers: Synthesis and solution properties. In Polymers in aqueous media.pp. 165-174.
147. Cinelli F, Colaianni A, Tordone A.A, Munro H.S and Tighe B.J (2002). Disposable absorbent articles with improved adhesive for attachment to the skin to facilitate adhesion in oily conditions, The Proctor and Gamble Company.
148. Venkatramen S and Gale R (1998). Skin Adhesives and Skin Adhesion 1. Transdermal Drug Delivery Systems. Biomaterials *19*, 1119-1136.
149. Chu S-G (1991). Adhesive bonding (New York: Plenum Press).
150. Dahlquist C.A (1999). Creep. In Handbook of Pressure Sensitive Adhesive Technology, 3rd Edition, D. Satas, ed. (Warwick: Satas & Associates), p. 121–138.
151. Mazzeo F.A Characterization of Pressure Sensitive Adhesives by Rheology, TA Instruments: New Castle.

152. Huskey R.A, Chang E.P, Caldwell C.A, Avalon G.A, Huang Y.H, Soerens D.A and Lachapell R.A (1997). Refastenable adhesive taping system, Avery Dennison Corporation.
153. Malek W (1999). Self-adhesive protective film, Beiersdorf AG: Germany.
154. Batrabet C.S, Huang Y.H, Lachapell R.A and Yu L-C (1997). Adhesive composition comprising a polysiloxane, Kimberly-Clark Coporation.
155. Skiest I (1971). Adhesive compositions. In Encyclopaedia of polymer science and technology, Volume Vol I, N. Bilkales, ed.,p.482.
156. Venkatraman S and Gale R (1998). Skin adhesives and skin adhesion 1. Transdermal drug delivery systems. Biomaterials *19*, 1119-1136.
157. Lucast D.H and Zhu D-W (2002). Pressure sensitive adhesives having quaternary ammonium functionality, articles, and methods, 3M Innovative Properties Company.
158. Knoepfel B and Spencer F (1973). Pressure sensitive adhesive copolymer formed from vinyl monomer and zwitterioinc monomer and tapes made therewith, Minnesota Mining and Manufacturing Company.
159. Nielsen K.E, Li K, Kantner S.S, Koski N.L and Everaerts A.I (1998). Ionically conductive adhesives prepared from zwitterionic materials and medical devices using such adhesives, Minnesota Mining and Manufacturing Company.
160. Crotty B.A, Miner P.E, Johnson A, Znaiden A.P, Corey J.M, Vargas A, Meyers A.J and Lange B.A (1998). Delivery of skin benefit agents via adhesive strips, Chesebrough-Pond's USA Co.
161. Ho S.P, Nakabayashi N, Iwasaki Y, Boland T and LaBerge M (2003). Frictional properties of poly(MPC-co-BMA) phospholipid polymer for catheter applications. Biomaterials *24*, 5121–5129.
162. Bruce A.S, Mainstone J.C and Golding T.R (2001). Analysis of tear film breakup on etafilcon A hydrogel lenses. Biomaterials *22*, 3249-3256.
163. Peters K and Millar T (2002). The role of different phospholipids on tear break-up time using a model eye. Curr Eye Res *25*, 55-60.
164. Ham B.M, Jacob J.T and Cole R.B (2005). MALDI-TOF MS of Phosphorylated Lipids in Biological Fluids Using Immobilized Metal Affinity Chromatography and a Solid Ionic Crystal Matrix. Analytical chemistry *77*, 4439-4447.
165. Greiner J.V, Glonek T, Korb D.R and Leahy C.D (1996). Meibomian gland phospholipids. Current Eye Research *15*, 371-375.
166. Nasso M (2007). Improving comfort in contact lens wear.
167. Adams R.D, Ed. (2005). Adhesive Bonding (Woodhead Publishing, Limited).
168. Houwink R and Salomon G, Eds. (1967). Adhesion and adhesives, Volume I, 2nd Edition (Amsterdam, London: Elsevier).
169. Comyn J (1997). I Edition (Cambridge: Royal Society of Chemistry).
170. Vakula VL and Pritykin L.M, Eds. (1991). Polymer adhesion, physico-chemical principles (New York, London: Ellis Horwood).
171. Han C.D (1976). Rheology in polymer processing (New York: Academic Press).
172. Vinogradov G.V and Malkin A.Y (1980). Rheology of polymers, viscoelasticity and flow of polymers (Moscow, Mir, New York: Springer-Verlag).
173. Rosen S.L (1993). Fundamental principles of polymeric materials, 2nd Edition (New York, Chichester: Wiley).

174. Cowie J.M.G (1991). Polymers: Chemistry and Physics of Modern Materials, 2nd Edition (Glasgow and London: Blackie).
175. Williams D.J (1971). Polymer Science and Engineering (London: Prentice-Hall).
176. Ardrey R.E (2003). Liquid Chromatography-Mass Spectrometry: an introduction (John Wiley and Sons Inc).
177. Lemière P (2001). Interfaces for LCMS. In *Guide to LCMS*. pp. 2-8.
178. Dole M, Mack L.L, Hines R.L, Mobley R.C, Ferguson L.D and Alice M.B (1968). Molecular Beams of Macroions. The Journal of Chemical Physics *49*, 2240-2249.
179. March R.E (1997). An Introduction to Quadropole Ion Trap Mass Spectometry. Journal of Mass Spectrometry *32*, 351-369.
180. Jonscher K.R and Yates J.R, The Whys and Wherefores of Quadrupole Ion Trap Mass Spectrometry.
181. de Hoffman E and Stroobant V (2003). Mass Spectrometry Principles and Applications (John Wiley and Sons LTD).
182. Young T (1805). An essay on the cohesion of fluids. Phil. Trans. Roy. Soc., 65-87.
183. Dupre A (1869). Theorie mechanique de la chaleur. *Guthier Villars*, 369.
184. Owens D.K and Wendt R.C (1969). Estimation of the surface free energy of polymers. J. Appl. Polym. Sci. *13*, 1741-1747.
185. Fowkes F.M (1962). Determination of interfacial tensions, contact angles and dispersion forces in surfaces by assuming additivity of intermolecular interactions in surfaces. J. Phys. Chem *66*, 382.

Appendices

8.1 Appendix I - Adhesion

Adhesion and theories of adhesion

Adhesion is the molecular attraction exerted between bodies in contact and is the sum of a number of mechanical, physical, and chemical forces that overlap and influence one another.

It is not possible to separate these forces from one another and several theories have been proposed in an attempt to provide an explanation for adhesion phenomena, no single theory explains adhesion fully. The most common theories of adhesion are named after and based on the following mechanisms: mechanical, adsorption, electrostatics and diffusion. They are explained briefly but for a fuller discussion of these theories see the literature [167-169].

The mechanical (or mechanical interlocking) thoery is based upon the adhesive penetrating into pores, holes and other irregularities of the adherent surface. The adhesive is mechanically locked into the substrate. To do this the adhesive must be able to wet the substrate and have suitable rheological properties.

The adsorption theory is dependant on if the adhesive can wet the surface of the adherent. The adhesive must spread spontaneously. The adhesive must have a lower surface free energy than the adherent surface.

Electrostatic theory is based on the materials having different electronegativities. The adhesive force can be attributed to the electron transfer between the materials and the resulting positive and negative charges attract each other.

Diffusion theory applies only to bonding polymers. The carbon chains that make the backbone of the polymers interpenetrate at the interface where the materials interface. There is a molecular interlocking mechanism.

Requirements for adhesion

In order to adhere to a surface an adherent must have certain thermodynamic and kinetic requirements. The thermodynamic requirement for adhesion is that the measured surface free energy (γ) of the adherent must be lower than the γ of the substrates in order for adhesion to occur. For good wetting and resulting strong adhesion forces: γ adhesive << γ substrate. For poor wetting and low adhesion forces: γ adhesive >> γ substrate. For an explanation of the thermodynamic requirements of adhesion see the literature [167, 169, 170].

We can use the adsorption theory and in particular contact angles to determine the thermodynamic requirements of a pressure sensitive adhesive based on the theory of adsorption. Contact angle measurements can be made using diiodomethane and water as probes on the adhesive to provide the necessary information to determine the dispersive (γs^d) and polar components (γs^p) of surface free energy and hence the total surface free energy (γs^t). $\gamma s^t = \gamma s^d + \gamma s^p$. See Appendix VI - Contact Angle.

The kinetic requirements of adhesion are that the adherent must flow adequately to allow intimate molecular contact between adhesive and adherent [148]. These kinetic requirements are harder to quantify and techniques such as tack, peel adhesion and shear strength are used. Each technique tests a different parameter of adhesion.

- Tack is a measurement of how easily and quickly an adhesive can be applied to a surface. It can be thought of as bond formation. A typical experiment for tack would be measuring the distance a rolling ball travelled before stopping while passing over the adhesive.
- Peel Adhesion is a measurement of how difficult it is to remove an adhesive from a surface after it has been firmly attached and so is bond breaking. The Houndsfield tensiometer can be used to perform 90° or 180° peel tests to measure peel adhesion.
- Shear strength is a measurement of cohesive strength. A measure of if the adhesive will withstand the pulling force of being removed. The Houndsfield tensiometer can be used to test cohesive strength.

Tack and peel strength have been empirically correlated to dynamic-mechanical properties. Tack can be thought of as a bonding process that occurs over a relatively long time at low frequencies and peel strength as bond breaking process that occurs over a relatively short time at high frequencies [147-151].

Dynamic mechanical testing can be used to assess the bonding (tack) and peel properties of a pressure sensitive adhesive. To determine dynamic mechanical properties a sample is placed onto a disc that on a rheometer can be exposed to dynamic torsion using frequency sweep experiments. A Bohlin CVO Rheometer can be used for these types of experiments.

The complex modulus (G^*) is measured as a function of oscillation frequency (ω). The G^* can be divided into in-phase elastic modulus (G') and the out-of-phase viscous modulus (G''). The G' and G'' measured at low and high frequencies are relatable to tack and peel strength. A low G' at low frequencies is required for bonding and a high G' at high frequencies is required for bond breaking. The ratio G''/G' is known as tan δ (the loss tangent or phase angle) and shows how elastic or viscous the sample is, a tan δ below unity is required for skin adhesives. A plot of G' versus ω gives an indication of the tack and peel strength, the greater the slope the better the adhesive properties. See Appendix II - Rheology and Viscoelastic materials or the literature [168, 171-173].

8.2 Appendix II– Rheology and Viscoelastic materials

Introduction

Rheology is the study of the flow and deformation of matter. It describes the interrelation between force, material deformation and time. Rheology is principally concerned with extending the "classical" disciplines of elasticity and (Newtonian) fluid mechanics to materials whose mechanical behaviour cannot be described with the classical theories

One common factor between solids, liquids, and all materials whose behaviour is intermediate between solids and liquid is that if we apply a stress or load on any of them they will deform or strain. The deformation may be completely elastic and therefore temporary or it may be completely viscous and therefore permanent. Many materials exhibit elastic and viscous responses simultaneously and these materials are said to be viscoelastic. Polymers are an example of a viscoelastic material.

Two approaches are used to study polymers rheological behaviour - the continuum and the molecular. The following is based on the continuum approach.

Mechanical deformation

Figure 111 shows examples of types of deformations that may be felt in our example; these are tensile, compressive and shear. The state of stress in a body can be described using a stress tensor. The following is based on one dimensional model as two and three dimensional models would add to the mathematic intricacies without aiding explanation.

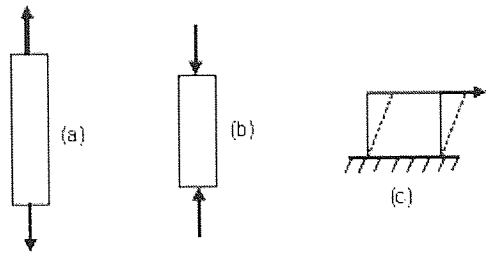

Figure 111. Examples of types of forces: (a) Tensile force. (b) Compressive force. (c) Shear force.

The shear (or shear stress, σ) involves the application of a lateral force (F) to a unit cube of material parallel to its top surface area (A). The σ is equal to F over A. It has units of Newtons per meter squared.

$$Shear\ Stress = \frac{Force}{Area} \quad Nm^{-2}$$

The strain (or shear strain, ε) is a measurement of the distance of material displacement (D) divided by the height (H) of the material sample. This has no units since as it is the ratio of two lengths.

$$Shear\ Strain = \frac{Displacement}{Height}$$

In the study of viscoelastic materials shear is the most important type of deformation but the same principles outlined above apply to the other types of forces illustrated in Figure 112.

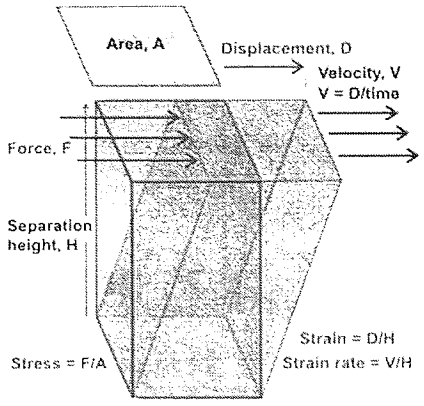

Figure 112. Shear strain

Simple rheological responses

The two simplest responses of the material are ideal elastic or purely viscous. The material response does not depend on the type of deformation applied and so the following example is based on shear deformations.

The ideal elastic response

Ideal elastic responses take place the instant that the stress is applied to the material and disappears upon removal of the stress. The stress is a function of the strain in ideal elastics. Hooke's law relates strain to stress via the material constant, the shear modulus (G). Stress is equal to the strain multiplied by the modulus ($\sigma = G \times \varepsilon$) or this can be transposed to give modulus equals stress over strain ($G = \sigma/\varepsilon$).

For ideal solids doubling the stress would double the stain and the material behaves in a linear fashion and the strain returns instantaneously to zero when the stress is removed. The deformation energy is stored and is released upon release of the stress. This is known as the Hookean response.

The purely viscous response

If we consider the material in the cube in Figure 112 as an ideal viscous fluid the application of the shear stress (force) will cause the cube to deform by the displacement (D) but the deformation will continually increase at a constant rate. The

rate of change is known as the shear rate (γ) and is the rate of change of strain as a function of time. Shear rate = change in strain / change in time ($\gamma = \delta \varepsilon / \delta t$). The units are reciprocal seconds.

$$Shear\ rate = \frac{change\ in\ strain}{change\ in\ time} \quad 1/s$$

The shear rate is dependent on a material's resistance to flow or viscosity (η). The viscosity is equal to the shear stress over the shear rate ($\eta = \sigma/\gamma$). It has units of Pascal seconds (PaS).

These materials are unable to store any deformation energy and are irreversibly deformed when subjected to stress, the material flows and the energy is dissipated as heat. If a material has a viscosity that is independent of shear stress then it is an ideal or a Newtonian fluid.

$$Viscosity = \frac{Shear\ stress}{Shear\ rate} \quad Nm^{-2}S\,(PaS)$$

Viscoelastic behaviour

Materials described by ideal elastic and purely viscous responses to stress are at ends of an entire spectrum of behaviours. Viscoelastic materials display both elastic and viscous responses to applied stresses. Various models have been designed that describe viscoelastic behaviour; examples are the Maxwell, Voight and the standard linear models [173-175]. These models use springs to represent the elastic element and dashpots to represent the viscous element as shown in Figure 113, where G is the elastic modulus and η is the viscosity modulus.

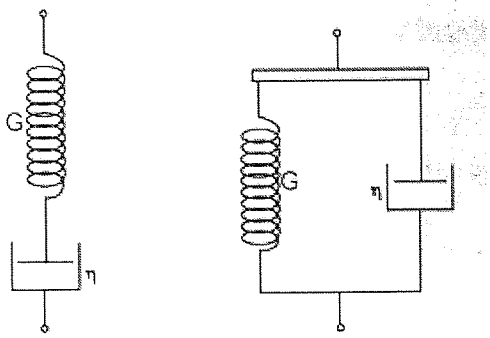

Figure 113. A Maxwell element (left) and a Voigt element (right)

Although these models can be used to represent the chief characteristics of viscoelastic behaviour of materials they are oversimplified. However, they will give the reader some idea of the possible complexities in modelling the time-dependent behaviour of polymeric materials

Dynamic mechanical analysis

Viscoelasticity can be studied using dynamic mechanical analysis. When we apply a small oscillatory strain and measure the resulting stress. Purely elastic materials have stress and strain in phase, so that the response of one caused by the other is immediate. In purely viscous materials, strain lags stress by a 90 degree phase lag (Figure 114). Viscoelastic materials exhibit behaviour somewhere in the middle of these two types of material, exhibiting some lag in strain.

where $\sigma 0$ and ε_0 are the amplitudes of stress and strain and δ is the phase shift between them.

G' is also called the storage modulus (since elastic energy is stored), while G" is often referred to as the loss modulus (since viscous energy is lost). The phase shift can be shown as G''/G' and is known as tan δ (or the damping factor)

Oscillatory frequency sweeps are well suited for characterizing the bonding and debonding behaviour of a PSA [147-151]. In this experiment constant sinusoidal amplitude is applied to a material, within the linear viscoelastic region, while varying the frequency of the oscillation. The range of frequencies (ω) is 1 to 10 Hz. The normal force is controlled to account for the thermal expansion of the sample throughout the test.

G', G'' and as tan δ can be plotted against frequency. The spectrum produced is fairly sensitive to small changes in molecular weight, degree of cure and copolymer composition.

Rheology and Pressure sensitive adhesives

The dynamic-mechanical properties of G' and G'' have been correlated to tack and peel [147-151]. The rationale behind the correlation is that peel adhesion or tack can be thought of as a combination of two processes:

- the bonding process, which occurs at relatively long times or small frequencies
- the de-bonding process, which occurs at relatively short times or high frequencies.

The G' and G'' when measured at low and high frequencies and should be able to be related to measured tack and peel. For the bonding process a low G' is required at low frequencies and the de-bonding process requires a high G' at a higher frequency, as both of these would lead to high tack and/or peel. The higher the slope of a G' versus ω plot, the better the adhesive properties

The requirements for the rheological performance of PSAs are described in the criteria reported by Chu and others [149, 150, 155]. The Chu criterion is:

(i) G' (ω = 0.1 rad/s) ~2 to 4×10^5 dynes/cm (0.2 - 4×10^4 Pa)

and

(ii) $5 < [G' (\omega = 100)/G'' (\omega = 0.1)] < 300$

Good cohesive properties can be expected from gels with a G' (1 rad/s) of between 1000– 10000 Pa and a G" (1 rad/s) of between 300 – 5000 Pa [147]. The tan δ plotted against ω an also be expected to have a positive gradient for good adhesive properties of gels [152-154]. For further reading on rheology [171-173]

8.3 Appendix III - Chromatography

Introduction to chromatography

Chromatography comes from the Greek (χρώμα:chroma) meaning colour. It is a collection of laboratory techniques used in the separation of mixtures. All types of chromatography involve passing a mixture through a stationary phase, which separates and isolates the molecules of interest (the analyte) from others in the mixture.

The separation is performed by exploiting the differences in partitioning of the analyte between the stationary and mobile phases. The differing components of the mixture interact with the two phases based on their charge, relative solubility or absorption. The plate and rate theories explain these interactions

The various types of chromatography (and their subdivisions) include

- Capillary-action chromatography
    - Paper Chromatography
    - Thin layer chromatography (TLC)
- Column chromatography
    - Fast performance liquid chromatography
    - High performance liquid chromatography (HPLC)
    - Ion exchange chromatography
    - Size exclusion chromatography
    - Affinity chromatography
- Gas-liquid chromatography (GC)
- Countercurrent chromatography

The retention is an important factor in chromatography and can be defined as "a measure of the speed at which a substance moves in a chromatographic system". In continuous development systems like HPLC or GC the retention is measured as the retention time (Rt or tR) of the analyte; this is the time between injection and detection. In interrupted development systems like TLC the retention is measured as

the retention factor (Rf), the run length of the compound divided by the run length of the eluent front.

Due to variables such as the eluent, the stationary phase, temperature, and the setup the retention of a compound can often differ between experiments and laboratories. It is therefore normal to use standard compounds under identical conditions to validate the experiments.

This work involves the use of High Performance Liquid Chromatography (HPLC) and Thin Layer Chromatography (TLC).

High Performance Liquid Chromatography (HPLC)

Introduction to HPLC

HPLC is a form of capillary chromatography and HPLC systems consist of a pump, an injection device (injector or autosampler), a column and a detector, as shown in Figure (Figure 115). There are many types of HPLC but this discussion will be limited to Partition HPLC. Partition HPLC is a system is composed of a stationary phase and a mobile phase. The stationary phase refers to the solid support contained within the column over which the mobile phase continuously flows. The mobile phase refers to the solvent that acts as a carrier for the sample solution.

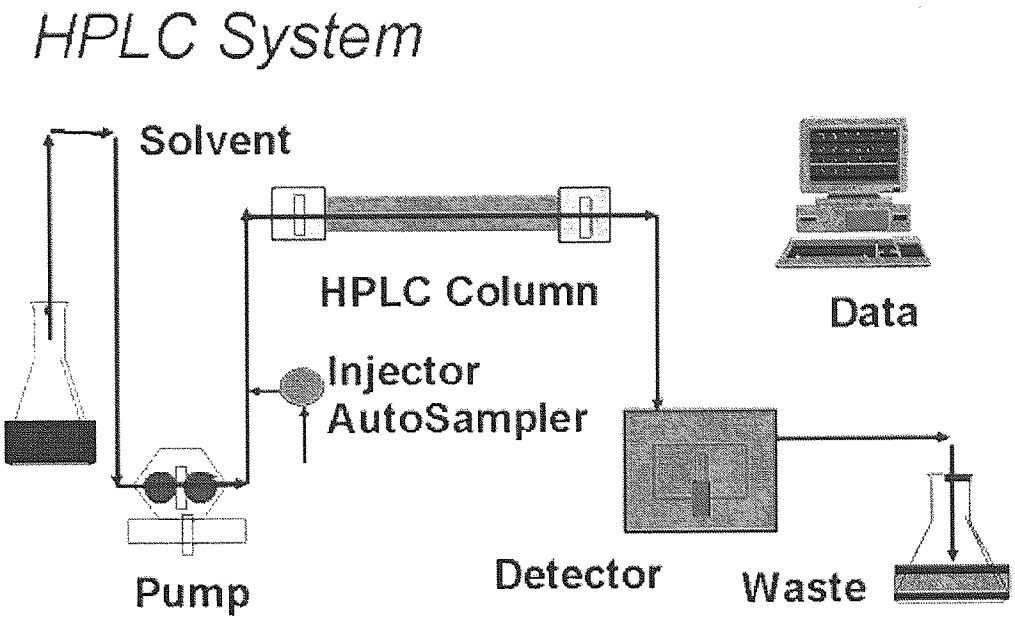

Figure 115. Components of an Isocratic Liquid Chromatography System

A sample solution is injected into the mobile phase through an injector port. As a sample solution flows through the column with the mobile phase, the components of that solution migrate according to the non-covalent interactions of the compound with the column. The chemical interactions of the mobile phase and sample, with the column, determine the degree of migration and separation of components contained in the sample. For example, those samples which have stronger interactions with the mobile phase than with the stationary phase will elute from the column faster, and thus have a shorter retention time, while the reverse is also true. The mobile phase can be altered in order to manipulate the interactions of the sample and the stationary phase.

Methods used in HPLC

There are many methods of HPLC and those of interest for this discussion are isocratic, gradient, normal and reverse phase chromatography.

In isocratic elution compounds are eluted using constant mobile phase composition. All compounds begin migration through the column at onset. However, each migrates at a different rate, resulting in faster or slower elution rate. This type of elution is both

simple and inexpensive, but resolution of some compounds is questionable and elution may not be obtained in a reasonable amount of time.

In gradient elution increasing the strength of the organic solvent elutes different compounds. The sample is injected while a weaker mobile phase is being applied to the system. The strength of the mobile phase is later increased in increments by raising the organic solvent fraction, which subsequently results in elution of retained components. This is usually done in a stepwise or linear fashion.

Normal phase operates on the basis of hydrophilicity and lipophilicity by using a polar stationary phase and a less polar mobile phase. Thus hydrophobic compounds elute more quickly than do hydrophilic compounds.

Reverse phase also operates on the basis of hydrophilicity and lipophilicity but this time the stationary phase consists of silica based packing with n-alkyl chains covalently bound. For example, C-8 signifies an octyl chain and C-18 an octadecyl ligand in the matrix. The more hydrophobic the matrix on each ligand, the greater is the tendency of the column to retain hydrophobic moieties. Thus hydrophilic compounds elute more quickly than do hydrophobic compounds.

Quantification

Quantification of compounds can be achieved in HPLC by internal or external standard methods. This work will use the external standard method that involves injecting a series of known concentrations of a standard compound solution onto the HPLC for detection. The chromatogram of these known concentrations will give a series of peaks that correlate to the concentration of the compound injected. The area under each peak is calculated and a set of data is generated to develop a calibration curve. This gives a line with the equation, $y = mx + c$, which is then used to find the concentration for x once the sample chromatograph has been read.

Thin Layer Chromatography (TLC)

Introduction to TLC

In TLC the stationary phase is a powdered adsorbent fixed to an aluminum, glass, or plastic plate. The mixture to be analyzed is loaded near the bottom of the plate. The plate is placed in a reservoir of solvent so that only the bottom of the plate is submerged. This solvent is the mobile phase; it moves up the plate causing the components of the mixture to distribute between the adsorbent on the plate and the moving solvent, thus separating the components of the mixture so that the components are separated into separate "spots" appearing from the bottom to the top of the plate (Figure 116).

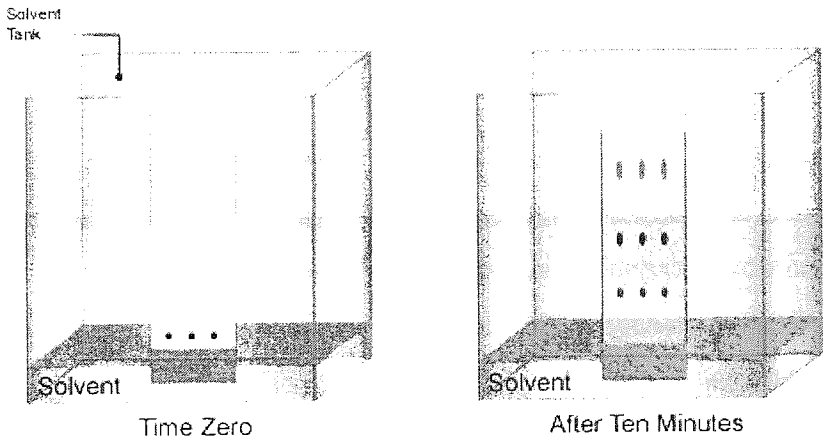

Figure 116. Thin Layer Chromatography (TLC)

Different species in the sample mixture migrate at different rates for reasons explained above and give each species a characteristic R_f. Variation in the solvent system used can vary the elution and R_f for example, if the solvent was a 90:10 mixture of hexane to ethyl acetate, then the solvent is more nonpolar than it is polar. In this case the nonpolar parts will move further up the plate. The polar compounds, in contrast, will not move as much. The reverse is true when using a solvent that is more polar than non-polar (10:90 hexane to ethyl acetate). With these solvents, the polar compounds will move higher up the plate, while the non-polar compounds will not move as much.

8.4 Appendix IV - Liquid Chromatography Mass Spectrometry (LCMS)

Introduction to LCMS

LCMS is a combinatorial technique of Liquid Chromatography (LC) which offers separation of complex mixtures of species and Mass Spectrometry (MS) which offers molecular structural information. Ardrey offers an excellent review of LCMS.

An LC system needs to be interfaced to the MS system for it to be considered an LCMS system, i.e. the LC flow needs to directly feed the MS. The direct introduction of a liquid flow into an MS is not a compatible format [176]. Early types on LCMS interfaces included moving belt, direct liquid introduction, thermospray and particle beam and while successful they were of limited sensitivity and non robust.

The advent of Atmospheric Pressure Ionisation (API), which is any process where the ions are formed at atmospheric pressure, overcame the sensitivity and ruggedness issues with earlier LCMS systems. API includes continuous flow Fast Atom Bombardment, Particle Beam, Electrospray Ionization (ESI), Atmospheric Pressure Photoionisation (APPI) and Atmospheric Pressure Chemical Ionisation (APCI) but it is the ESI, APCI and APPI that have seen widespread use, see R.E Ardrey and P Lemière for reviews of interfaces [177].

Figure 117 shows the API ionisation sources and their applicability with regard to sample polarity and molecular weight. ESI is best suited to molecules that are charged (polar).

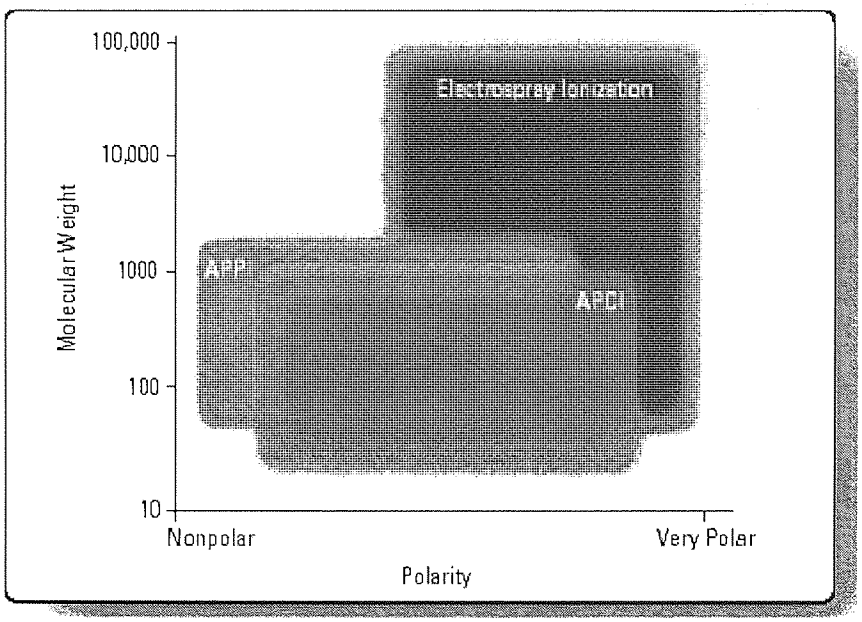

Figure 117. Different ionisation sources and their applicability with regard to sample polarity and molecular weight [70]

An LC-MS interface should provide uncompromised chromatography, no chemical modifications to analyte, high sample transfer, low background noise, ease of use and operationally compatible with LC and MS (this means that the interface should allow the LC to have flow rates from 2ml/min to 20nl/min without compromising the vacuum of the MS). ESI provides these properties and the Agilent 1100 Series LC/MSD (SL) LCMS used for this work has ESI capability.

Electrospray Ionisation (ESI)

Introduction to ESI

ESI is a relatively young technique for introducing ions to a MS which can be traced back to 1917 when John Zeleny described it. This work was followed by Malcolm Dole in 1968 describing the charged residue model of ESI. However it was in 1988 when John B. Fenn presented an identification of polypeptides and proteins of molecular weight 40kDa that ESI gained international recognition. John B. Fenn and Koichi Tanaka went on to win the 2002 Nobel Prize for their work in this field.

ESI can be divided into techniques which vary in how the spray is formed but all form ions from the droplets at atmospheric pressure using the same mechanism. The ions are then transported from the source to the vacuum of the MS analyser through one or

more differentially pumped stages separated by skimmers as shown in Figure 118. The ions are focused and guided through the skimmer openings into the MS by applying appropriate electric fields. The Agilent 1100 Series LC/MSD (SL) LCMS uses a pneumatic-assisted variety of spray formation.

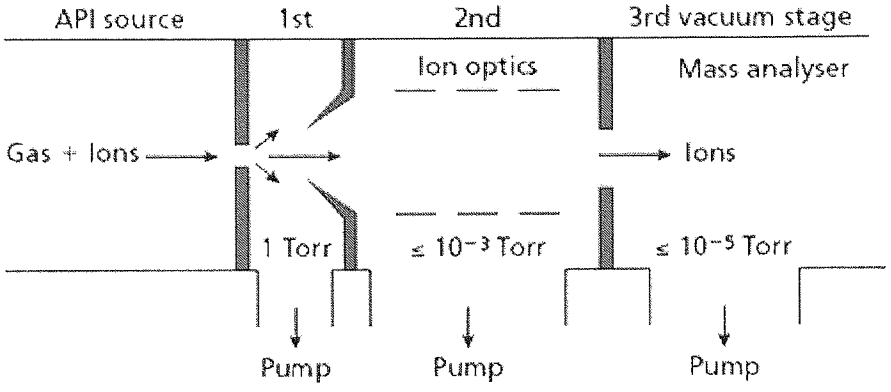

Figure 118. Overview of a differentially pumped API source coupled to a mass spectrometer [70]

The ESI interface

There have been several different configurations for the ESI interface and the Agilent orthogonal chamber was used for this work and is shown in Figure 119. The spray from the LC is introduced into the ESI chamber via a needle (the liquid inlet, shown in Figure 119) at a 90° angle to the capillary cap. The needle is held at a positive or negative potential (~ + 5kV or -5kV) to aid nebulisation and to charge the droplets formed.

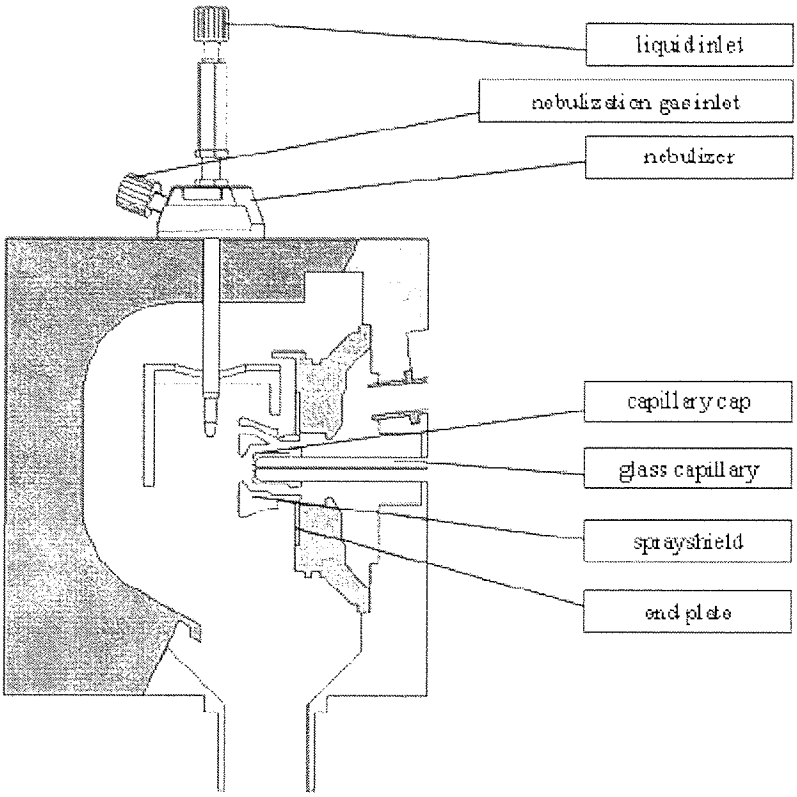

Figure 119. The Electrospay Ionisation Interface Chamber [70]

The nebulisation process is aided by a stream of nitrogen along the sides of the needle (the nebulisation gas inlet shown is in Figure 119).The capillary cap and glass capillary (Figure 119) are held at an opposite charge to the needle which enables the droplets formed to be drawn to the glass capillary and from there on into the MS chamber. The transferral of liquid inlet to charged droplets is explained in the ESI process.

ESI Process

The ESI process can be explained in terms of formation of ions, nebulisation, desolvation and ion evaporation.

i) Formation of Ions

The formation of ions can occur via solution chemistry or via nebulisation. In solution chemistry formation of ions we see the ions formed from the analyte (M^0) which

either becoming $[M-H]^-$ or $[M-H]^+$ depending upon the polarity of the electrospray chamber. Basic analytes use positive ionisation and sensitivity is promoted by slightly acidic conditions, <7pH. Acidic analytes use negative ionisation and sensitivity is promoted by slightly acidic conditions, >7pH. Solution chemistry is an important parameter in LCMS using ESI. Most significant is the alteration of the charge of the analyte (also suppression, chromatography, adduct formation). The formation of ions via nebulisation is explained in the nebulisation and desolvation stage of the ESI process.

ii) Nebulisation

The nebulisation stage is where a droplet can take on a charge (ion formation) and is also the stage where the liquid stream inlet is transformed into droplets (nebulised). Figure 120 shows the nebulisation or droplet formation which uses a coaxial flow of nitrogen used to enhance the spray formation.

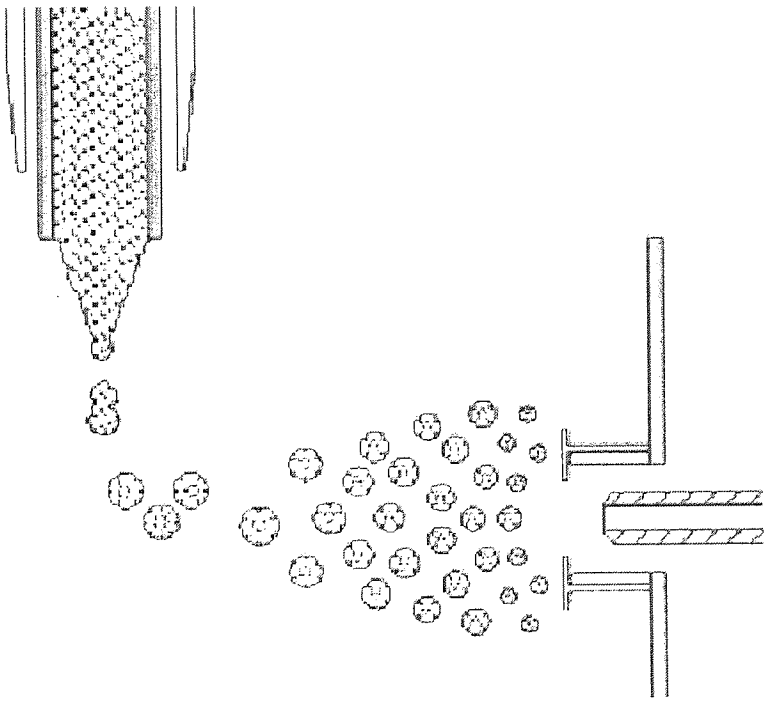

Figure 120. Nebulisation or droplet formation [70]

In addition to this nitrogen nebulisation there is a high electrical potential difference of about 3 kV between the capillary cap and glass capillary are and the needle (Figure

(Figure 119). Ions of the same polarity migrate toward the liquid at the capillary tip, where the liquid surface is drawn out of the capillary forming a 'Taylor cone', which is shown in Figure 121.

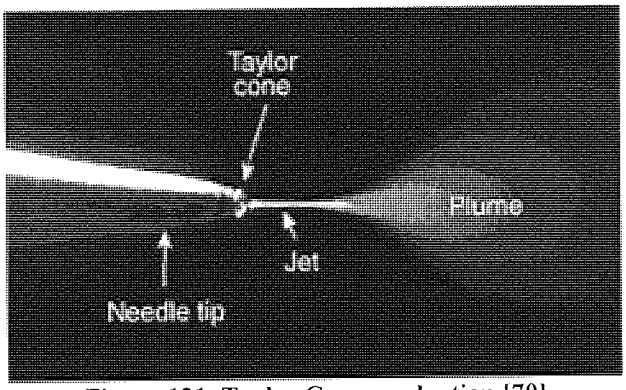

Figure 121. Taylor Cone production [70]

When the build-up of an excess of ions of one polarity at the surface of the liquid reaches the point that coulombic forces are sufficient to overcome the surface tension of the liquid, droplets (approximately 1 μm) enriched in one ion polarity are emitted from the capillary.

iii) Desolvation and iv) Evaporation

In the desolvation stage the droplets undergo sequential columbic explosions and evaporation steps to form ever decreasingly sized droplets and eventually single ions as shown in Figure 122. A counter flow of heated gas (nitrogen) aids desolvation. The process of ion evaporation occurs in a similar fashion to the desolvation process as shown in Figure 123.

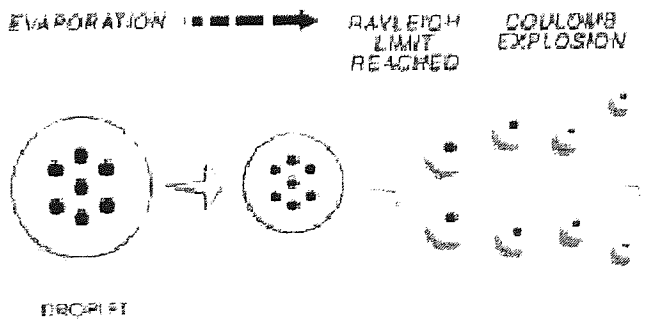

Figure 122. Desolvation process of ESI. The Rayleigh limit is where surface tension is overcome by the repulsion of the similar charges found within the dropets [70]

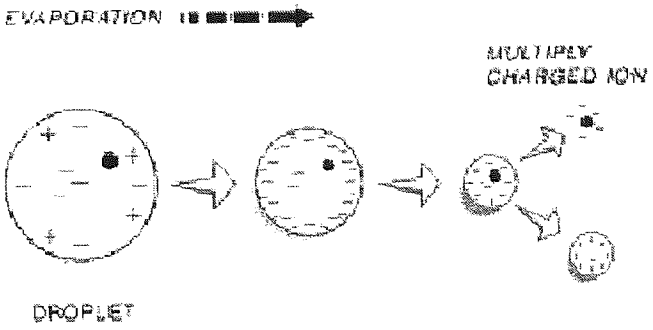

Figure 123. Evapouration process of ESI [70]

This leads to the production of very small droplets of 3-10 nanometers diameter which can lead to gas phase ions. How this process occurs is still under debate with theories by Irbarne and Thompson (desolvation process) and Dole (charged residue) [178] explaining many of the observations seen.

The ions are then drawn into the capillary via electrostatic charges and on into the MS chamber via vacuum. As explained in the formation of ions we can see that solution chemistry can provide us with ions of known charge whereas the nebulisation and desolvation process can leave ions that are multiple charged.

Detection Modes

The polarity of the ESI chamber can dictate which the ions are detected. If the MS is set up to detect negative ions then the end cap and capillary column of the interface will be positively charged to attract these species, and visa versa if we require detection of positively charged ions.

In positive polarity mode MS a small molecule species will have a hydrogen adduct and so be a $[M+H]^+$ species where M is the molecular mass of the species and H is a hydrogen, therefore the peak would be seen at one Th above the molecular weight of species. In negative polarity mode MS the molecule can lose a hydrogen and so we see $[M-H]^-$ with the peak appearing at one Th below the molecular weight of species. Charge transfer can also occur in the negative polarity mode. Other adduction is possible and typically we find sodium adducts $[M+Na]^+$ where the peak appears at twenty three Th above the molecular weight of species.

Multiple charged ions are typically seen with the larger molecules such as proteins which is another reason why ESI is a technique used for protein identification. The multiple charged ions allow large molecules to still be in the MS detection range.

8.5 Appendix V – Ion Trap Mass Spectrometer

Ion Trap Mass Spectrometer

An ion trap mass analyzer consists of a circular ring electrode plus two end caps that together form a chamber. Ions entering the chamber are "trapped" there by electromagnetic fields and another field can be applied to selectively eject ions from the trap, as shown in Figure 124 [70].

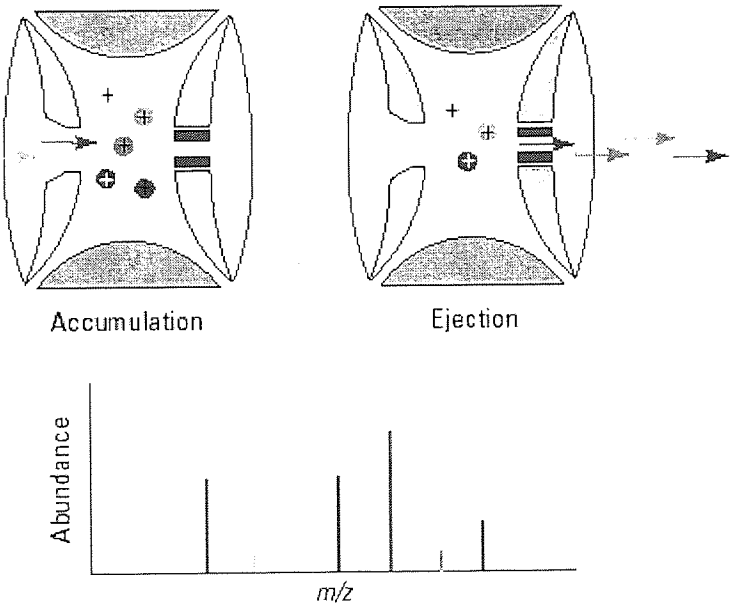

Figure 124. Ion trap accumulation and ejection of ions [70]

Ion traps have the advantage of being able to perform multiple stages of mass spectrometry without additional mass analyzers. In ion trap mass spectrometers all ions except the desired precursor ion are ejected from the trap (A in Figure 125 [70]). The precursor ion is then energized and collided to generate product ions (C in Figure 125). The product ions can be ejected to generate a mass spectrum, or a particular product ion can be retained and collided to obtain another set of product ions (D in Figure 125). This process can be sequentially automated so that the most abundant ion(s) from each stage of MS are retained and collided. This is a very powerful technique for determining the structure of molecules. It is also a powerful technique

for obtaining peptide mass information that relates to the sequence of amino acids in a peptide.

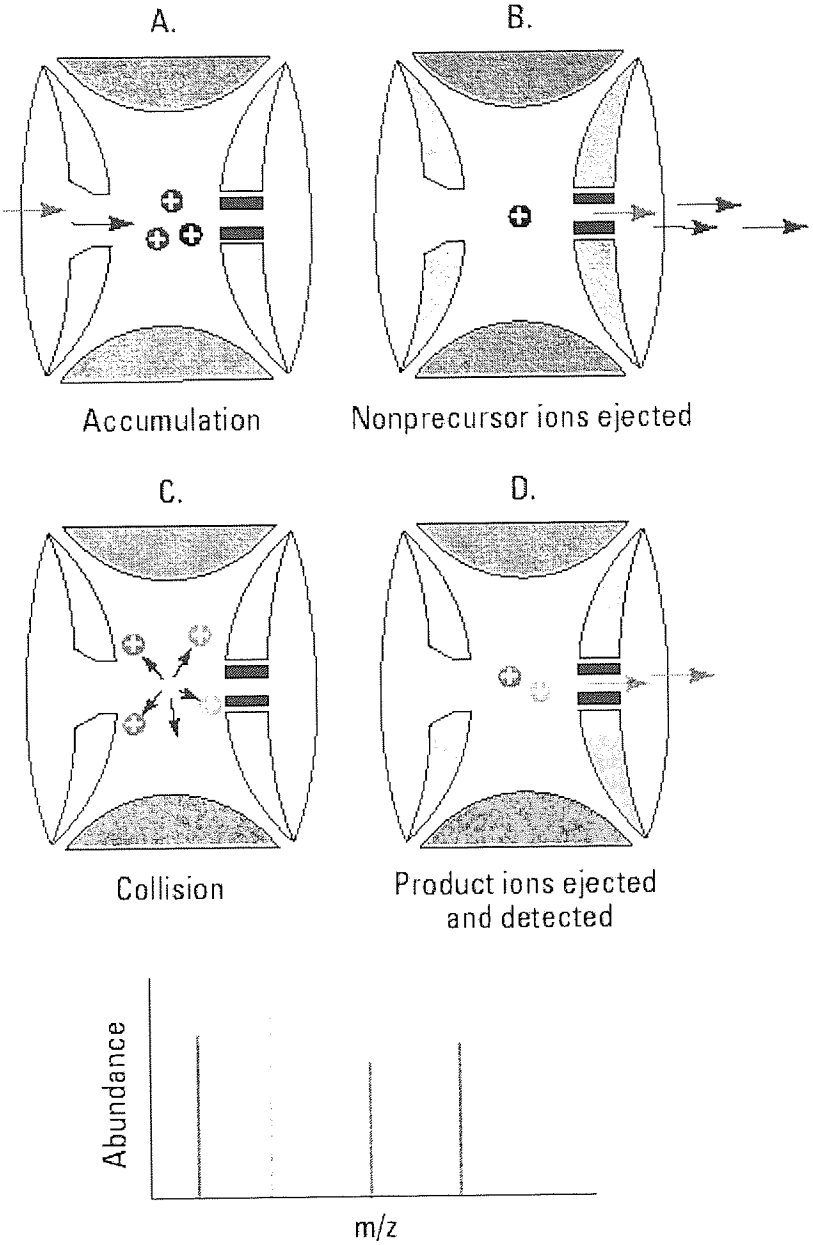

Figure 125. Figure showing how the ions are accumulated (A), ions are selected and the non precursor ions ejected (B), collision is induced (C) and the products ions are ejected and detected [70]

A major advantage of multiple-stage MS is its ability to use the first stage of MS to discard non analyte ions. Sample cleanup and chromatographic separation become much less critical. With relatively pure samples, it is quite common to do away with chromatographic separation altogether and infuse samples directly into the mass spectrometer to obtain product mass spectra for characterization or confirmation.

Reviews of Ion Trap MS can be found by R.E March, K.R Jonscher and J.R Yates and E de Hoffman and V Stroobant [179-181].

8.6 Appendix VI – Contact angle

Contact angle (θ) is a quantitative measure of the wetting of a solid by a liquid. It can be defined as the angle that a liquid forms at the three phase boundary where a liquid, gas and solid intersect as shown in Figure 126.

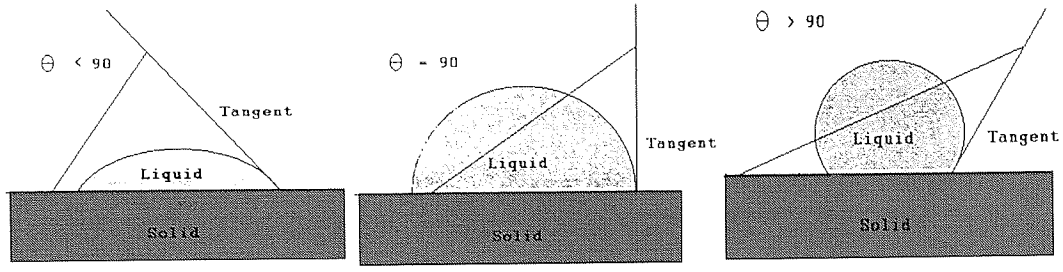

Figure 126. Examples of contact angle measurement

Figure (Figure 126) shows that a liquid spreads over a solid if it has low values of θ. The value of θ is an indication of its wetting ability, low values of θ have good wetting while high values of θ indicate poor wetting. If the angle θ is less than 90 the liquid is said to wet the solid. If it is greater than 90 it is said to be non-wetting. A zero contact angle represents complete wetting.

Young [182] considered contact angles of the materials involved in thermodynamics terms. This analysis involves the interfacial free energies between the three phases and is given by:

$$\gamma_{sv} = \gamma_{sl} + \gamma_{lv}\cos\theta$$

where γ_{lv} ,γ_{sv} and γ_{sl} refer to the interfacial energies of the liquid/vapor, solid/vapor and solid/liquid interfaces. Dupre [183] showed that the reversible work of adhesion of a liquid and solid, W_a, could be expressed as:

$$W_a = \gamma_s + \gamma_{lv} + \gamma_{sl}$$

These two equations may be combined to give the well-known Young-Dupre equation.

$$W_a = (\gamma_s - \gamma_{sv}) + \gamma_{lv}\,(1 + \cos\theta)$$

This equation is not adequate to deal with the action of polar forces across the interface. Owens and Wendt [184] determined the polar and dispersive forces to give an expression for the determination of the surface free energies of dehydrated polymer surfaces.

$$1 + \cos\theta = (2/\gamma_{lv})\,((\gamma_{lv}^{d}\gamma_s^{d})^{0.5} + (\gamma_{lv}^{p}\gamma_s^{p})^{0.5})$$

This equation is able to relate the contact angle (θ) to the polar (γ_s^p) and dispersive (γ_s^d) components of the solid. Where the γ_s^p and γ_s^d components for two wetting liquids are already known, the polar and dispersive components for the solid can be determined by solving the simultaneous equations. The total free surface energy (γ_s^t) can be found by adding the values of the polar and dispersive components [185].

$$\gamma_s^t = \gamma_s^d + \gamma_s^p$$

The most widely used wetting liquids are HPLC water and diiodomethane, due to their high total surface free energies and their balance of polar and dispersive components, shown in Table 32.

Table 32. Polar and dispersive components for water and diiodomethane

Liquid	γ_s^d (mN m^{-1})	γ_s^p (mN m^{-1})	γ_s^t (mN m^{-1})
Water	21.8	51.0	72.8
Diiodomethane	48.1	2.3	50.4